THE EFFECT OF AIR FLOW RATE AND FROTH THICKNESS ON BATCH AND CONTINUOUS FLOTATION KINETICS

by

MUAMMER KAYA

A Thesis Submitted To The
Faculty of Graduate Studies And Research
In Partial Fulfillment of The Requirements For
The Degree of Master of Engineering

Department of Mining and Metallurgical Engineering
McGill University
Montreal, Canada

© August 1985

ABSTRACT

A modified Denver 5 L flotation cell was used to investigate the effect of air flow rate (AFR) and froth thickness (FT) on the major transfer mechanisms in batch and continuous flotation.

The effect of AFR on the transfer of a deslimed sphalerite concentrate from the slurry to the froth was characterized. The maximum flotation rate constant (FRC), measured at an AFR, was in good agreement with that predicted from Anfruns and Kitchener's fundamental bubble-particle collision model (1976) using the AFR/bubble size relationship determined photographically.

The transfer from the froth into the concentrate stream (rate constant: FTC) and back to the slurry (rate constant: DBC), and the recovery in the froth, Rf, and overall recovery were determined for AFRs of 1.3 to 7.5 L/min and FTs of 0 to 5 cm. Overall recovery increased with increasing AFR and decreasing FT. The major effects were an increase in the FRC with increasing AFR and an increase in Rf with decreasing FT. AFR had little effect on Rf, because both the FTC and the DBC increased with increasing AFR.

Size-by-size rate constant were also determined. The FRC-size curves showed that the typical hump yielding a maximum FRC at a size of 23-30 μm, consistent with reported data. The FTC and DBC showed little dependence on particle size. Above 10 μm, presumably because bubble

coalescence and collapse and not hydraulic classification and particle-bubble detachment were the dominating drop-back mechanisms.

Hydraulic entrainment was examined as a function of AFR, FT and wash water addition. Significant reductions in hydraulic recovery were achieved by introducing the wash water just below the slurry-froth interface.

Liquid and solid residence time distributions were determined by using pulsed tracer techniques. The cell was found to behave as a perfect mixer for both liquid and solid phases.

RÉSUMÉ

Nous avons modifié une cellule de flottation Denver de 5-L pour étudier l'effet du débit d'air et de l'épaisseur de la couche de mousse sur les mécanismes de transferts les plus importants en flottation discontinue et continue.

Nous avons augmenté la hauteur de la cellule et installé des chicanes à mi-hauteur pour obtenir une interface pulpe-écume calme et diminuer l'entraînement hydraulique. Nous avons caractérisé l'effet du débit d'air et de la densité initiale de la pulpe sur le transfert du concentré de sphalérite déschlammée de la pulpe à l'écume. Nous avons utilisé une technique de récupération rapide de l'écume par débordement d'un film aqueux au-dessus de la lèvre de la cellule (essais en continu et en discontinu). Le débit d'air produisant le taux de flottation le plus rapide, 5.5 - 6.3 L/min, est en bon accord aved le débit prédit soit 5.6 L/min, à partir du modèle d'Anfruns et Kitchener (1976) et de la relation entre le débit d'air et le diamètre des bulles, mesuré photographiquement.

Nous avons déterminé les taux de transfert de la pulpe à l'écume (constante cinétique: FRC), de l'écume au concentré (constante cinétique: FTC), de l'écume à la pulpe (constante cinétique: DBC), la récupération dans l'écume, Rf, ainsi que la récupération totale, à des débits d'air de 1.3 à 7.5 L/min, et des épaisseurs d'écume de 0 à 5 cm. La récupération totale augmente lorsque le débit d'air augmente ou l'épaisseur d'écume

diminue. En particulier, la CTF augmente lorsque l'épaisseur d'écume diminue. Le débit d'air n'a que peu d'effet sur Rf, parce qu'en augmentant, la FTC et la DBC augmentent simultanément. On a classifié les produits de flottation à l'aide du 'cyclosizer' de Warman, afin de déterminer des constantes cinétiques des différentes classes granulométriques. La CTF maximale se retrouve à 23-30 µm, en accord avec d'autres résultats déjà publiés. La FTC et la DBC ne varient que très peu pour les classes granulométriques au-dessus de 10 µm, probablement parce que l'entraînement hydraulique et le bris des liens bulle-particule, tous deux fonctions de la granulométrie, ne sont pas des mécanismes importants de transferts dans notre système. Ceci nous permet de conclure que le mécanisme majeur de retour des particules à la pulpe est la coalescence et l'affaissement des bulles.

Nous avons étudié la récupération hydraulique de la silice et de la sphalérite en fonction du débit d'air, de l'épaissuer de l'écume et de l'addition d'eau de lavage. Nous avons réduit sensiblement la récupération de la silice en introduisant l'eau de lavage juste au-dessous de l'interface pulpe-écume.

Nous avons déterminé les distributions de temps de séjour dans la cellule des phases liquide et solide par essais de traçage. Toutes les distributions obtenues s'avèrent conformes au modèle d'un mélangeur parfait. En absence d'eau de lavage, les phases liquide et solide montrent le même temps de séjour moyen. L'addition d'eau de lavage et l'épaisseur de l'écume modifient toutefois le temps de séjour de la phase liquide.

ÖZET

Batch ve sürekli flotasyonda, pülpden köpüge, köpükten pülpe geri dönme ve pülpden konsantre olarak kazanılma transfer sabitleri hava miktarı ve köpük yüksekliginin (pülp seviyesi) bir fonksiyonu olarak özel yapılmış bir laboratuvar hücresinde incelenmiştir.

Pülpten köpüge olan transfer ara bir hava miktarında maksimuma ulaşmaktadır. Köpükten pülpe geri dönme hem hava miktarı hemde köpük yüksekligi artıkça artmaktadır. Pülpten konsantre olarak kazanılma ise hava miktarıyla artmakta ve köpük yüksekligiyle azalmaktadır.

İnce degersiz mineral parcaçıkların (gangue) hava kabarcıklarının ardından sürüklenerek köpüge girme ve oradanda istenmeden kazanılma mekanısması (hydraulic entrainment) hava miktarı, kopük yüksekligi, yıkama suyu ilavesi ve ilave seviyesinin bir fonksiyonu olarak incelenmiştir. Hava miktarı artıkça ve köpük yüksekligi azaldıkça, bu tür transfer mekanısmasının artıgı gorülmüştür. Köpük ile pülp arayüzeyinin altından su serpintisinin (spray) degersiz mineral parcaçıklarının kazanılmasını önemli bir ölçüde azaltıgı bulunmuştur.

Likid ve solid fazlarının Denver flotasyon hücresinde tamamen karıştıgı (perfectly mixed) radyoaktif iz metoduyla tespit edilmiştir.

ACKNOWLEDGEMENTS

The author wishes to thank his supervisor, Dr. A. R. Laplante for his supervision, keen interest and criticism throughout the research program.

The author is also indebted to other members of the Department, among whom Dr. J. A. Finch, Dr. S. R. Rao for their interesting lectures, Dr. Rene del Villar, C. Ercan for their computer help, M. Leroux for his kind of assistance during experiments, and my colleagues J. Yianatos and S. Yu for their discussions.

As well, I am sincerely grateful to the Scientific and Technical Research Council of Turkey for financial support from the NATO Science Fellowship, and Natural Sciences and Engineering Research Council of Canada.

TABLE OF CONTENTS

ABSTRACT i

RESUME iii

OZET v

ACKNOWLEDGEMENTS vi

TABLE OF CONTENTS vii

LIST OF FIGURES xii

LIST OF TABLES xvii

NOMENCLATURE xviii

Chapter 1 INTRODUCTION

1.1 Nature of the Problem 1

1.2 Methodology 3

Chapter 2 LITERATURE SURVEY

2.1 Introduction 5

2.2 Macroscobic Description of Flotation Kinetics 5

2.3 Theoretical and Experimental Work on Bubble-Particle Attachment 10

2.4 Froth Studies and Entrainment 18

2.5 Industrial Plant Process Stabilizing Control Practice Using Air Flow Rate and Froth thickness 21

Chapter 3 THE AIR-WATER SYSTEM

3.1 Introduction 30

3.2 Design of the Flotation Cell 31

3.3 Experimental Procedure and Data Analysis 33

3.4 Results and Discussion 37
3.4.1 Average Bubble diameter 40
3.4.2 Effect of Air Flow Rate on Gas Holdup

3.5 Summary 56

Chapter 4 SAMPLE AND REAGENT SELECTION, GENERAL EXPERIMENTAL PROCEDURE AND PRELIMINARY TESTING

4.1 Introduction 58

4.2 Sample and Reagent Selections
4.2.1 Sample 58
4.2.2 Activator 60
4.2.3 Collector 61
4.2.4 Frother 62
4.2.5 pH Modifier 64

4.3 General Experimental Procedure for Semi-Batch Flotation 64
4.3.1 Calculation of the Flotation Rate Constant 67

4.4 Preliminary Testing
4.4.1 Determination of the Optimum Wash Water Flow Rate 68
4.4.2 Collector Selection 72
4.4.3 Chemical Conditioning 72
4.4.4 Split Conditioning 73

4.5 Summary 74

Chapter 5 THE AIR-WATER-SPHALERITE SYSTEM

5.1 Introduction 75

5.2 Experimental Procedure 75

5.3 Results and Discussion
5.3.1 Calculation of the Size-by-Size FRC 76
5.3.2 Effect of Initial Pulp Density on Semi-Batch Flotation Kinetics 84
5.3.3 Representation of FRC as a Function of AFR 89
5.3.4 Comparison With Other Flotation System 92

5.4 Summary 94

Chapter 6 THE CONTINUOUS FLOTATION OF SPHALERITE

6.1 Introduction 95

6.2 Description of the Experimental System 96

6.3 Kinetics 99

6.4 The Effect of Froth Thickness on Kinetics 100

6.5 Experimental Procedure 102

6.6 Results and Discussion 103

6.7 Summary 122

Chapter 7 EFFECT OF PARTICLE SIZE ON DBC, FTC AND ORC IN CONTINUOUS FLOTATION

7.1 Introduction 124

7.2 Experimental Procedure 124

7.3 Results 125

7.4 Discussion 134

7.5 Summary 144

Chapter 8 ENTRAINMENT IN CONTINUOUS FLOTATION

8.1 Introduction 145

8.2 Experimental Procedure and Data Analysis 145

8.3 Results 146

8.4 Discussion 161

8.5 Summary 173

Chapter 9 RESIDENCE TIME DISTRIBUTION IN CONTINUOUS FLOTATION

9.1 Introduction 175

9.2 Experimental Procedure 175

9.2.1 Calculation Procedure

9.2.2 Determination of Liquid Residence Time Distribution 178

9.2.3 Determination of Solid Residence Time Distribution 179

9.3 Results 183

9.4 Discussion 191

9.5 Summary 193

Chapter 10 CONCLUSIONS

10.1 Effect of AFR on semi-batch flotation 195

10.2 Effect of AFR and FT on continuous flotation 196

10.3 Entrainment and residence time distributions 197

APPENDICES

Appendix 1 Bubble Size Distribution Results 199

Appendix 2 Effect of AFR on Gas Holdup 200

Appendix 3 Gas Holdup, BRV, BRT, GLIA. 202

Appendix 4.1 Calculation of the FRC in Semi-Batch Flotation 203

Appendix 4.2 Wash Water Flowmeter Calibration 205

Appendix 4.3 Gas Flowmeter Calibration 206

Appendix 5.1 Semi-Batch Flotation Results 207

Appendix 5.2 Air Flow Rate Versus Flotation Rate Constant Results (7% solids) 228

Appendix 5.3 Air Flow Rate Versus Flotation rate Constant Results (14% solids) 229

Appendix 5.4 Calculation of the FRC of Each Size Classes (Test 31) 230

Appendix 5.5 Calculation of the FRC of Each Size Classes (Test 33) 231

Appendix 6.1 Slurry Kinetics in Continous Flotation 232

Appendix 6.2 Slurry and Froth Kinetics in Continuous Flotation 240

Appendix 7.1 Size-by-Size Kinetics in Continuous Slurry-Froth Flotation 266

Appendix 8.1 Effect of AFR, FT, WWFR and WW level on Entrainment 269

Appendix 8.2 Effect of particle size on entrainment 275

Appendix 9.1 Liquid Residence Time Results 283

Appendix 9.2 Solid Residence Time Results 287

BIBLIOGRAPHY 291

LIST OF FIGURES

Fig. 2.1 Transfer mechanisms in a conventional flotation cell.

Fig. 2.2 Trajectories of particles on streamlines.

Fig. 2.3 Experimental and theoretical results presented in dimensionless form (from Anfruns and Kitchener, 1976).

Fig. 2.4 Typical grade-recovery curves.

Fig. 2.5 Flotation air control at MIM. (from McKee et al., 1976)

Fig. 2.6 Effect of FT on rougher and scavenger flotation (from McKee et al., 1976)

Fig. 2.7 Effect of AFR changes in rougher section on the performance of cleaner section. (from McKee et al., 1976)

Fig. 2.8 Measurements and control variables of zinc roughing and scavenging at Pyhasalmi (from Kallioinan, 1984).

Fig. 3.1 Plexiglass flotation cell designed for this work.

Fig. 3.2 Modified Denver Type D-1 Flotation Machine.

Fig. 3.3 Effect of AFR on bubble size distribution.

Fig. 3.4 Bubble size distribution at an AFR of 1.3 L/min.

Fig. 3.5 Effect of AFR and superficial gas velocity on bubble size.

Fig. 3.6 Effect of AFR and superficial gas velocity on specific bubble surface (mm^2/mm^3).

Fig. 3.7 Effect of AFR and superficial gas velocity on total bubble surface (cm /min).

Fig. 3.8 Effect of AFR and superficial gas velocity on gas holdup in the slurry phase.

Fig. 3.9 Effect of AFR and superficial gas velocity on average bubble residence time.

Fig. 3.10 Apparent bubble rise velocity as a function of AFR and superficial gas velocity.

Fig. 3.11 Apparent rise velocity versus average bubble radius.

Fig. 3.12 Effect of AFR on liquid-gas interfacial area in the slurry phase.

Fig. 3.13 Influence of liquid height on gas holdup in the slurry phase.

Fig. 3.14 Slurry phase in conventional cell.

Fig. 4.1. Crystal structure of ZnS.

Fig. 4.2. Influence of selected xanthates on recovery of ZnS.

Fig. 4.3. Flotation recovery of ZnS as a function of pH.

Fig. 4.4. Flowsheet of the experimental procedure of semi-batch flotation.

Fig. 4.5. Wash water flow rate versus flotation rate constant.

Fig. 5.1. Mass of sphalerite in the cell as a function of time.

Fig. 5.2. Flotation rate constant as a function of air flow rate.

Fig. 5.3. Flotation rate constant as a function of air flow rate.

Fig. 5.4. Classification curves of flotation products (split conditioned sample).

Fig. 5.5. Classification curves of flotation products.

Fig. 5.6. Flotation rate constant versus particle size (Test 31, AFR: 5 L/min).

Fig. 5.7. Flotation rate constant versus particle size (Test 33, AFR: 5 L/min).

Fig. 5.8. Effect of initial pulp density on semi-batch flotation.

Fig. 5.9. Inhibited and free flotation components of sphalerite.

Fig. 5.10 Bubble load versus air flow rate.

Fig. 6.1. The overall view of experimental set up.

Fig. 6.2. Continuous flotation flowsheet.

Fig. 6.3. Effect of AFR on recovery without froth phase.

Fig. 6.4. Effect of AFR on FRC.

Fig. 6.5. Effect of AFR and FT on overall recovery.

Fig. 6.6. AFR versus mass in the froth.

Fig. 6.7. Froth thickness versus froth transfer constant.

Fig. 6.8. Air flow rate versus froth transfer constant.

Fig. 6.9. Froth thickness versus drop-back constant.

Fig. 6.10 Air flow rate versus drop-back constant.

Fig. 6.11 Effect of FT and AFR on solid holdup in the froth phase.

Fig. 6.12 Schematic representation of two transport mechanisms in conventional flotation froths.

Fig. 6.13 Horizontal and vertical transfer velocities in conventional flotation froths (Moys, 1982).

Fig. 6.14 Probability of transfer of particles at froth surface to discharge (Cutting et al., 1982).

Fig. 6.15 Froth thickness versus overall rate constant.

Fig. 6.16 Air flow rate versus overall rate constant.

Fig. 7.1. Effect of particle size on DBC at different AFR and FT.

Fig. 7.2. Effect of particle size on FTC at different AFR and FT.

Fig. 7.3. Effect of particle size on ORC at different AFR and FT.

Fig. 7.4. DBC as a function of AFR at different particle size.

Fig. 7.5. FTC as a function of AFR at different particle size.

Fig. 7.6. ORC as a function of AFR at different particle size.

Fig. 7.7. Comparison between calculated and experimental ORC data.

Fig. 7.8 Schematic diagram of the elementary process taking place as a bubble enters the froth layer and possible particle motion (from Schulze, 1982).

Fig. 7.9 Different zones in the flotation cell.

Fig. 7.10 Mechanism of stabilization of a thin film by a close-packed monolayer of particles with low contact angels (from Dippenaar, 1978).

Fig. 7.11 Size-by-size recovery of galena and sphalerite (from Trahar, 1976).

Fig. 8.1 Effect of froth thickness on silica recovery.

Fig. 8.2 Effect of air flow rate on silica recovery.

Fig. 8.3 Effect of froth thickness on water recovery.

Fig. 8.4 Effect of air flow rate on water recovery.

Fig. 8.5 Effect of froth thickness on solid recovery.

Fig. 8.6 Effect of air flow rate on solid recovery.

Fig. 8.7 Relationship among water recovery, silica recovery and froth thickness in pure silica flotation.

Fig. 8.8 Effect of water recovery on silica recovery at different AFRs and FTs.

Fig. 8.9 Comparison of entrainment in conventional and column flotation.

Fig. 8.10 Wash water addition levels for entrainment tests.

Fig. 8.11 Effect of wash water addition flow rate and level on silica recovery for mixture and pure silica flotation (AFR: 7.5 L/min and FT: 3 cm).

Fig. 8.12 Effect of particle size on silica recovery.

Fig. 8.13 Effect of froth thickness on concentrate size distribution.

Fig. 8.14 Relationship between the recovery rates of silica and water at varying pulp densities in a pilot scale system (from Lynch et al, 1974).

Fig. 8.15 Correlation between the recovery of silica and the recovery of water for different sizes (from Engelbrecht-Woodburn, 1975).

Fig. 8.16 Water recoveries of mixture and pure silica flotation (AFR: 7.5 L/min, FT: 3 cm; A: above froth, B: below froth).

Fig. 8.17 Variation of froth profile with froth thickness (from Moys, 1976).

Fig. 8.18 Comparison between laboratory and plant scale flotation with respect to classification function.

Fig. 8.19 Effect of particle size on gangue recovery in plant scale (from Lynch, 1974).

Fig. 8.20 Effect of froth residence time on classification function (from Thorne et al, 1974).

Fig. 9.1 Decay scheme of radioactive Mn-56.

Fig. 9.2 Liquid RTD for tail and concentrate streams

Fig. 9.3 Effect of froth thickness on liquid RTD.

Fig. 9.4 Effect of WWFR on liquid RTD.

Fig. 9.5 Effect of tracer addition point on liquid RTD.

Fig. 9.6 Solid RTD of tail stream.

Fig. 9.7 Solid RTD of concentrate stream.

Fig. 9.8 Solid RTD of tail stream with wash water addition.

LIST OF TABLES

Table 2.1 Concentrators employing automatic flotation control using AFR and FT.

Table 2.2 Effect of varying AFR at scavenger section on retreatment and final tail.

Table 2.3 Outokumpu concentrators using automatic control.

Table 4.1a Particle size distribution of the original sample.

Table 4.1b Particle size distribution of the cyclone underflow product after three stage cycloning.

Table 4.2 Effect of WWFR on the FRC.

Table 4.3 Effect of collector type on FRC at different WWFRs.

Table 4.4 Influence of chemical conditioning on FRC.

Table 4.5 Influence of conditioning type on FRC.

Table 5.1 Experimental and predicted AFR yielding maximum FRC.

Table 5.2 Dimensionless air flow number and modified air flow number of different cells.

Table 7.1 Regression coefficients for FTC, DBC and CRC.

Table 8.1 Particle size distribution of silica.

Table 9.1 Solid and liquid RTD.

NOMENCLATURE

AFR(Q)	air flow rate, L/min
FT	froth thickness, cm
FRC(K)	flotation rate constant, 1/min
ORC	overall rate constant, 1/min
DBC(K_2)	drop-back constant, 1/min
FTC(K_1)	froth transfer constant, 1/min
C	concentration, g/cm^3
Co	initial concentration
C_∞	concentration after an infinite flotation time
y	rate of disapparence of floatable mineral by flotation
R	recovery, %
Rf	recovery in the froth, %
RTD	average residence time distribution
τ	mean residence time, min
Pc	probability of collision
Pa	probability of attachment
Ps	probabilty of formation of stable froth
Pd	probability of detachment
V	volume ,cm^3
F	stability factor
Ec	collision efficiency
Ek	collection efficiency
dp	particle diameter, μm or mm
db	bubble diameter, mm

Np	number of particles
ρp	particle specific gravity, g/cm^3
ρf	fluid specific gravity, g/cm^3
ρl	liquid specific gravity, g/cm^3
Ub	bubble rise velocity, cm/s
μ	pulp viscosity
S	total bubble surface
$\bar{S}$	specific bubble surface
K	scale factor
ni	number of bubbles measured in size class i
Ts	total bubble surface measured
Tv	total bubble volume measured
BRT	average bubble residence time, min
SGV(Vg)	superficial gas velocity, cm/s
BRV(Vr)	apparent bubble rise velocity, cm/s
LGIA	liquid-gas interfacial area
g	gravitational acceleration
σ	surface tension, dyn/s
Vt	terminal bubble velocity, cm/s
Vswarm	bubble swarm velocity, cm/s
Vs	bubble slip velocity, cm/s
ϵg	fractional gas holdup
NaAX	sodium amyl xanthate
NaEX	sodium ethyl xanthate
WWFR	wash water flow rate, L/min
A	cell cross-sectional area, cm^2
Qm	AFR at which FRC is maximum

C_1, C_2	constants
AFN	air flow number
MAFN	modified air flow number
N	impeller speed, rpm
D	impeller diameter, cm
a	constant
b,c	exponents
Ut	turbulent circulating flow
Qu	liquid entrapped in the froth structure
Qd	downward flow rate
ro	radius of curvature
CF_i	classification matrix values
R	counting rate
Y	counting efficiency
m	tracer amount, g
Mc	concentrate mass flow rate, cc/min
Mt	tail mass flow rate, cc/min
Vgas	gas volume in the slurry, cm^3
Vcell	cell volume, cm^3
c,t	subscripts for conc. and tail
MF	mass in the froth, g
A	activity, dps
Ao	remaining activity at time t
T	half-life, hours
W	weight
x,s	subscripts for unknown and standard samples.

CHAPTER 1

INTRODUCTION

1.1 NATURE OF THE PROBLEM

Pioneering automatic computer control for flotation took place in Pyhasalmi, Finland, Lake Dufault and Frood-Stobie, Canada in 1968. Flotation control systems are now operating (or are being installed in many countries, including Sweden, Australia, the United States, South Africa, Poland, Zambia, Brazil and Japan (Paakkinen and Cooper, 1980). On-stream analysers, such as Outokumpu's Courier, and several sensors, such as magnetic flow meters and density gauges, made possible the rapid determination of the performance of flotation circuits. Since 1960, the automatic control procedures for flotation circuits have progressed and significant metallurgical improvements, reagent savings and increased throughputs have been recorded (Smith, 1975). Control systems which include both stabilizing and optimizing control resulted in improved economics and rapid pay-back of the investments.

Air flow rate (AFR) and froth thickness (FT) are two outstanding stabilizing control parameters beside collecting, activating, depressing, frothing and pH modifying reagents.

Air offers attractive features as such, because of

its short residence time in both the slurry and the froth phases; as opposed to changes in collector addition rate, for which reaction times are in the order of 5 to 20 minutes. The effect of AFR is also reversible, as opposed to that of reagents.

FT is another attractive stabilizing control parameter. It significantly affects particle residence time in the froth and therefore gangue drainage. Flotation generally responds more rapidly to changes in AFR than FT. Consequently, AFR is often more effective than FT in maintaining stable circuit behavior. Another problem with FT control reported by Lynch et al. (1981, p. 194) is the difficulty in determination of the tailings or concentrate set point.

Despite important advantages of AFR and FT as control parameters, their effect on flotation kinetics are still incompletely understood, specifially for continuous flotation. The effect of AFR and FT on semi-batch flotation was extensively investigated by Laplante (1980). One of his conclusions was that continuous flotation systems were better suited to study froth-related kinetics.

The intent of this work is to provide a bridge between the simpler models of froth transfer for which a simple overall recovery is used (i.e. King et al, 1973-1974; Sutherland, 1977; and Harris, 1978) and the more complex one (Cooper, 1966, and Moys, 1978-1984).

1.2 METHODOLOGY

A plexiglass cell which is similar to 5 L Denver cell was designed and constructed to study flotation kinetics in both batch and continuous flotations. In order to obtain a quiescent slurry-froth interface, a buffer zone between the turbulent active zone and the froth zone was created by increasing the cell height. Specially designed Baffles were used to enhance the effect of buffer zone. To accomodate the increased cell height, both the standpipe and the rotor of the machine were extended.

Transfers were characterized using recovery data, slurry and froth solid inventories and tracer tests. Deslimed sphalerite was selected as a mineral phase. Excessive fines (-10 μm) were removed before floating, to provide a feed of relatively homogeneous behavior.

First, bubble size distributions were characterized as a function of AFR at constant frother concentration using a photographic technique. The gas holdup in the slurry phase was determined (Chapter 3).

Secondly, the effect of AFR and initial pulp density in semi-batch flotation was investigated. The experimental procedure and preliminary test work are presented in Chapter 4, and results are presented and discussed in Chapter 5.

Thirdly, the effect of AFR and FT on continuous flotation kinetics was characterized both in the slurry and froth phases (Chapter 6). Particle-size effect are presented in Chapter 7.

In chapter 8, the effect of AFR, FT and wash water addition on hydraulic entrainment are investigated. The final testing program consisted of determination of liquid and solid residence time distributions and mixing conditions of continuous flotation by using tracer techniques.

Finally, a summary of the experimental results and their significance in flotation practice are presented in conclusion (Chapter 10).

CHAPTER 2

LITERATURE SURVEY ON EXPERIMENTAL, THEORETICAL AND PLANT FLOTATION KINETICS

2.1 INTRODUCTION

This literature survey consists of four sections. The first part covers the basic macroscopic description of flotation kinetics. The second one reviews simple one bubble-one particle systems, the third one is related to froth studies and entrainment and lastly industrial plant process stabilizing control practice using AFR and FT are discussed.

2.2 MACROSCOPIC DESCRIPTION OF FLOTATION KINETICS

Flotation is a complex process in which a number of separate effects take place some competitively, some consecutively. It involves the interaction of three phases which are solid, liquid and air. In general, there are two distict zones within a flotation cell. The lower part is the active zone where particles are kept in suspension and particle-bubble contact is induced by the turbulent action of impeller. The froth phase is the upper zone where cleaning action takes place and sometimes froth removal is aided by use of paddles. A third zone between active and

froth zones can be developed in order to create a quiescent slurry-froth interface by increasing the cell height.

As a bubble rises through the pulp, it may collide with particles of ore or gangue. If they pass sufficiently close to each other, collision occurs over the front of the bubble, and the particles are then swept to the rear of the bubble until it reaches the surface. The results of these collisions might be either a) immediate detachment, b) rupture of the film separating bubble and particle and formation of a stable bubble-particle bond (for hydrophobic particles), and c) hydraulic entrainment of the particle in the wake of the bubble.

The major transfer mechanisms in flotation are the following (Fig. 2.1):

- transfer of hydrophobic particles from the slurry to froth ,
- drop-back of minerals from the froth to the slurry,
- transfer of minerals from the froth over the cell lip, and
- recovery of fine particles by hydraulic entrainment.

At constant AFR and cell volume, transfer of particles from the slurry to the froth can be compared to a first-order kinetics chemical reaction, as suggested by many researchers Jowett and Safvi (1960), Bushell (1962),

Imaizumi and Inoue (1963) and Cooper (1966).

The flotation rate can be expressed in the form:

$$y = dc/dt = -K.C \qquad 2.1$$

where C: concentration of certain species in the slurry at time t

K: flotation rate constant (1/min).

t: time (min)

y: rate of disappearance of floatable mineral by flotation.

Integration of Eq. 2.1 leads to:

$$C = C_0 * \exp(-K.t) \qquad 2.2$$

where Co is the initial concentration.

For graphical representation, this can be rewritten as:

$$Ln\ (C/C_0) = -K.t \qquad 2.3$$

It is likely that the reason for the departures from first-order kinetics reported in the literature is not that the exponent is different from unity, but that the rate constant is not identical for all the particles in the sample under test. The idea of defining a rate constant specific to each particle was first proposed by Imaizumi and Inoue (1963). The idea was extended by Woodburn and Loveday (1965) to semi-empirical models in which the flotation properties were continuously variable,

leading to the notation of the "distributed" rate constant, which has been found to be quite useful. For the time being, knowledge of many of the parameters required in the model is lacking and it is not possible to obtain useful solutions from it.

For batch or semi-batch systems, the concentration of mineral in the pulp decreases very rapidly at the beginning of flotation and then more and more slowly, eventually becoming asymptotic to the time axis. The height of the asymptote gives the concentration of the mineral of interest in the cell after an infinite flotation time. Then Eq. 2.2 may be represented (Bushell 1962):

$$(C - C_{\infty}) = (C_0 - C_{\infty}) * \exp(-K.t) \qquad 2.4$$

where C_{∞} is the value of C after prolonged flotation time.

In this case, recovery can be expressed:

$$R = R_{\infty} * (1-\exp(-Kt)) \qquad 2.5$$

Flotation kinetics depend on many variables such as particle composition, size and conditioning, cell geometry and AFR. Their effect can be conveniently quantified by measuring the flotation rate constant. Assuming first order rate and homogeneous froth phase, froth kinetics can be characterized. A similar approach has been used to describe continuous flotation as reported by Loveday and Marchant (1970). In this case, the recovery

of mineral of interest can be derived as:

$$R = \frac{\alpha * K * \tau}{1 + \alpha * K * \tau} \qquad 2.6$$

where τ: average residence time (min), equal to the cell slurry volume (cm^3) divided by the tail flow rate (cm/min).

$$\alpha = \frac{K_1}{K_1 + K_2} \qquad 2.7$$

where K_1: rate constant for the transfer of material from the froth to the concentrate (1/min), to be referred to from now on as FTC

K_2: rate constant for the transfer of material from the froth back to the slurry (1/min), to be referred to from now on as DBC

αK: rate constant for the overall transfer of material from the slurry to the concentrate, (1/min) to be referred to from now on as ORC.

All transfers occur simultaneously, and it is practically impossible to measure each separately. It is likely that all three rate constants K, K_1, K_2 are affected by AFR and FT although these particular relationships can not be derived theoretically. This can be attributed to the complexity of flotation systems,

which are very difficult to describe in terms of bubble and mineral particle motion and attachment.

2.3 THEORETICAL AND EXPERIMENTAL WORK ON BUBBLE-PARTICLE ATTACHMENT

Extensive theoretical work has been done on simple flotation systems, in which bubble-bubble or particle-particle interactions were not present, or could be neglected.

Theory and experiments indicate that the flotation process is first order with respect to particle concentration. The collision process appears to have some similarities with chemical reactions and some workers have described the rate of collection as the occurence of a series of events.

According to Schuhmann (1942), the rate of flotation (g/cm.s) of particles of average size x is given by:

$$dw/dt = P_c * P_a * C(x) * V * F \qquad 2.8$$

where Pc is the probability of collision between particles and bubbles. Pa represents the probability of adhesion after collision. C(x) denotes the concentration of particles of an average size x in the flotation cell. V expresses the volume of pulp in the cell, F is the froth stability factor.

Sutherland (1948) proposed that the overall rate of flotation was equal to the product of three factors: the rate of collision between particles and bubbles, the probability of adhesion after collision, and the probability that detachment would not take place subsequently. To find the rate of collision between a single particle and a single bubble in the cell, Sutherland assumed that the flow around the bubble was inviscid and could be computed from the potential theory. If the radius of partical is rp , a stream tube can be chosen that surrounds the bubble as it rises in the liquid. All particles within this stream tube ahead of the bubble are then potential candidates for capture, as shown Fig. 2.2. The radius of the stream tube at infinite distance from the bubble was defined as the " collision radius ". Sutherland (1948) showed that all particles lying within a distance R from the line of motion of the bubble will collide with it and defined the collision efficiency, Ec, as

$$E_c = 3 * (d_p / d_b) \qquad 2.9$$

where dp: particle diameter (cm),

db: bubble diameter (cm).

If the air volumetric flowrate is Q, the number of bubbles produced per second is $6Q/\pi db^3$, the rate of removal of particles from the cell is

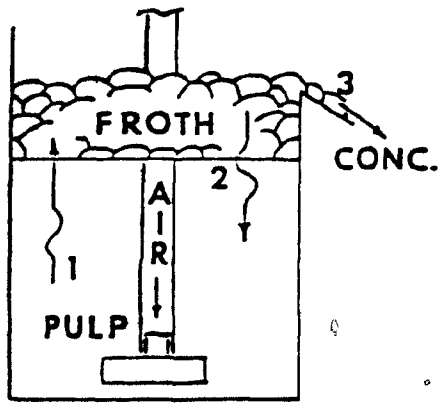

Fig. 2.1 Transfer mechanisms in a conventional flotation cell.

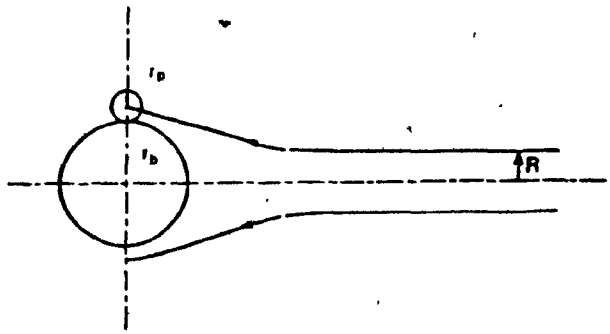

Fig. 2.2 Trajectories of particles on streamlines.

$$dN/dt = -\left(\frac{3 * Q * E_k * h}{2 * d_b * V_c}\right) N_p \qquad 2.10$$

therefore;

$$K = \frac{3 * Q * E_k * h}{2 * d_b * V_c} \qquad 2.11$$

Flint and Howarth (1971) found that there were two regions of particle behaviour characterized by a parameter K proposed by Fonde and Herne (1957):

$$K = \frac{2 * \rho_p * r_p * U_b}{9 * \mu * U_b} \qquad 2.12$$

where ρ_p : particle specific gravity,

μ : pulp viscosity.

When K is greater than 1 (large particles), the collision efficiency was strongly dependent on inertia forces, and the collision efficiency increased with increasing bubble size. For fine particles (K < 0.1), the collision efficiency was dependent on G, defined as

$$G = \frac{2 * (\rho_p - \rho_F) * r_p * g}{9 * \mu * U_b} \qquad 2.13$$

In this case, the collision efficiency increased with decreasing bubble size. For fine particles, the collision efficiency was independent of K, but strongly

dependent on G ; inertial effects can be neglected, as would be expected. In this regime the collection efficiency defined by Flint and Howarth (1971) was simply

$$E_k = G/(1 + G) \qquad 2.14$$

The assumption that a particle would be captured if the trajectories of the centre of the particle made grazing contact with the surface of the bubble is one of the drawbacks in Flint and Howarth's work. They obtained:

$$E_c \propto (d_p / d_b)^2 \qquad 2.15$$

Reay and Ratcliff (1975) made the alternative hypothesis that collision would occur if the surface of the particle and bubble made grazing contact with each other. A particle not touching the bubble at any stage would not be collected. But, they were particularly interested in effluent treatment and flotation of very fine particles (<20 μm) with small bubbles (<100 μm). Reay and Ratcliff (1975) have found the collision efficiency, i.e. the fraction of particles in the path of the bubble that actually collide with it, was given

$$E_c \propto (d_p / d_b)^N \qquad 2.16$$

where the exponent N was 1.9 for particles with $\rho_p/\rho_F = 1.0$ and 2.05 for $\rho_p/\rho_F = 2.5$. This is essentially the same as Flint and Howarth (1971) differing because of the

definitions of the collision efficiency referred to above.

They made a number of important assumptions, namely that the flow around the front of the bubble was that of a Stokes flow around a rigid sphere; that electrical interactions between bubble and particle have a negligible effect on trajectories; that particles which are collected at the front of the bubble are immediately swept to the rear, so that the full frontal surface is always clear; that the motion of the bubble is not affected by the pressure of the particles.

Anfruns and Kitchener (1976) reported on experimental and theoretical work performed in a flotation column using strongly surface methylated quartz. The collision efficiency was evaluated from the integration of the following equation, which describes the motion of the particle in dimensionless variables.

$$Stk(dv_p^*/dt^*) = v_{sp}^* - (v_p^* - v_f^*) \qquad 2.17$$

where $v_p^* = v_p/U_b$; $v_f^* = v_f/U_b$; $t^* = U_b t/R_b$

$$v_{sp}^* = \frac{2g\,(\rho_p - \rho_f)\,r_p^2}{9\ \eta\ U_b}$$ (a dimensionless settling velocity of the particle)

$$Stk = \frac{Re.a^2}{9}\left(\frac{\rho_p}{\rho_f}\right)$$ (Stokes number)

$$Re = 2\rho_f R_b U_b/\eta$$ (Reynolds number of the bubble)

$a = r_p/R_b$: (The $\underline{v}$ terms are understood to be vectors)

<u>Symbols:</u> v_p = velocity of particle relative to bubble : v_f = velocity of fluid relative to bubble : U_b = rising velocity of bubble : R_b = radius of bubble : r_p = radius of particle : ρ_p = density of particle : ρ_f = density of fluid : η = viscosity of fluid : g = acceleration due to gravity.

The results are summarized in Fig. 2.3 (from Anfruns and Kitchener, 1976). The experimental collection efficiencies are in good agreement with the theoretical curves. It was shown that theoretical collision efficiencies derived from either a potential flow solution (Re_b >1000) or a Stokes flow solution (Re_b <1) are seriously in error. Nevertheless, these two solutions predict approximately correctly the relationship between the particle-to-bubble size ratio. Lately, Jameson and coworker (1971) summarized Anfruns and Kitchener's work:

for 10<dp<50 μm; 600<db<1000 μm

$$E_c \propto (d_b^2 / d_p^{1.69}) \qquad 2.18$$

the measured exponent (1.69) is seen to be between the values given by the viscous theory of the Reay and Ratcliff (1975), and the inviscid theory of Sutherland (1948).

The probability that the particle will be captured by a bubble is the product of collision efficiency, and attachment efficiency. The collision efficiency is the sum of the gravitational, and interceptional collision efficiencies (Weber, 1981). The probability of adhesion is connected with induction time, i.e. the time required for thinning the disjoining film to such a thickness that

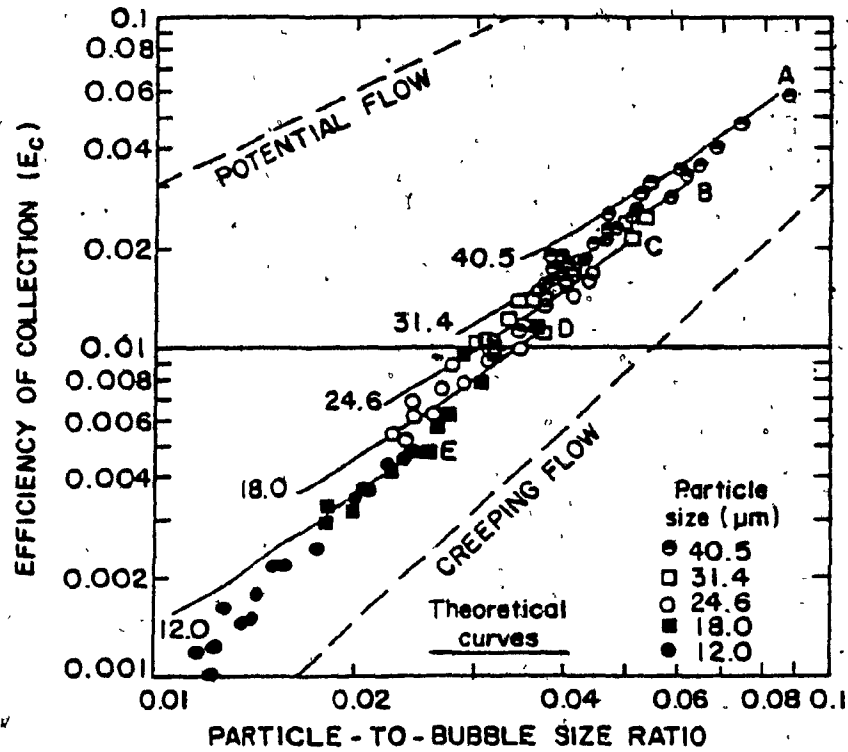

Fig. 2.3 Experimental and theoretical results presented in dimensionless form (from Anfruns and Kitchener, 1976).

rupture can take place. It means that a collision is fruitful, only when the time of contact between bubble and particle is longer than the induction time.

Dobby (1984) recently proposed a model without detachment mechanism for column flotation. He considers that particle collection by a gas bubble occurs via particle-bubble collision followed by attachment during the period that the particle is sliding over the bubble surface. He pointed out that the contact time of a particle on the surface of a gas bubble decreases as particle size increases. This is a result of the significant tangential velocity gradient that exists at the bubble surface. He also showed that the induction time decreases with increasing particle diameter.

Derjaguin and Dukhin (1960) analysed theoretically the various stages in the flotation process and showed that when the thickness of the liquid film between a bubble and a particle become very thin, the effects of adsorbed ions of the same charge on the two opposite surfaces would tend to keep particle and bubble apart. Other workers have found that the maximum rate of flotation occured when the zeta potential of the particles was zero.

2.4 FROTH STUDIES AND ENTRAINMENT

Despite the importance of the physical processes

which take place in the froth, little detailed experimentation has been done until recently. The two phase model of Arbiter and Harris (1962) has formed the basis of much of the work done. They proposed a perfectly mixed froth phase, which was challenged by Cooper (1966). He proposed a plug flow model of the froth which was little used for design and control applications.

The work of Watson and Grainger-Allen (1977) using their "equilibrium cell" revealed the importance of froth stability as affected by various control parameters and slurry properties (e.g. slurry density and concentration of gangue). They assumed that both pulp and froth phases were perfectly mixed. Cutting and Devenish (1975) using a similar experimental method took the non-homogeneity of the froth phase into account, and measured mineral concentration gradients as a function of height above the froth base. These studies were limited to batch experiments which do not take into account the fact that, in continuous operations, the time taken to establish the final steady-state froth may be different from the residence time of the pulp phase, resulting in froth-phase properties different from those obtained in batch tests.

Cutting et al. (1982) using a multipoint sampling lance investigated the grade enrichment mechanisms and froth mobility in a continuous flotation cell. He found that the grade of the concentrate increased markedly within the froth. Much work has been done which highlights

the need for a deeper understanding of process in the froth phase (Mika and Fuerstenau, 1969; King et al, 1973). Recently, a model based on counter-current plug-flow assumptios was described and advanced by Moys (1978, 1984).

In early work of flotation modelling, most attention was paid to the behavior of valuable particles which were recovered predominantly by the bubble collision mechanism.

After conducting experiments on a continuous laboratory cell with an artificial mixture quartz and fluorspar and with a coal-shale mixture, Jowett (1966) recognized the importance of the entrainment mechanism and suggested that the concentration of free gangue in the concentrate is proportional to the concentration of free gangue in the pulp volume.

Further evidence concerning the entrainment mechanism, in the modelling of industrial machines was reported by Johnson et al, (1972) who proposed a classification matrix to describe the entrainment mechanism. Further detailed studies of entrainment mechanism by Bisshop and White (1976) showed that the classification function is dependent on the residence time of particles in the froth.

Alteration of other variables (collector, frother, modifier additions, AFR, FT and impeller speed) cause movement along a particular relationship (Johnson et al,

1972; Engelbrecht and Woodburn, 1975; and Bisshop and White, 1976). Most of the authors reported a convex relationship between water and gangue recoveries.

2.5 INDUSTRIAL PLANT PROCESS STABILIZING CONTROL PRACTICE USING AIR FLOW RATE AND FROTH THICKNESS

Circuit grade-recovery curves may be used to explain control objectives in flotation in more detail. One result of flotation control should be to move from an operating curve represented by A in Fig. 2.4 to the more efficient regions represented by B and ultimately by C, representing the best metallurgical performance possible. The required operating point on curve C, for instance point P, can then ideally be attained by change in variables as necessary.

An important aspect of obtaining improved metallurgical performance is to achieve circuit stability. Measurements of concentrate grades and recoveries are made as early as possible in the rougher bank so that a change in the ore entering the plant can be readily detected by sensing instruments.

Improvements in overall plant metallurgical performance are possible by introducing FT and air control loops into the flotation circuits. Although, these are relatively simple parameters to monitor and control, very little laboratory and plant results have been published. A

list of flotation control installations employing FT, i.e cell slurry level, and AFR as control is given in Table 2.1.

The most instructive study on the effect of AFR and FT is reported by McKee and coworkers (1976). They described the automatic control system of the Mount Isa Mines, MIM, chalcopyrite flotation circuit (Fig. 2.5).

FT can be used to control either concentrate or tail grade. Increasing the FT increases the particle residence time in the froth phase and therefore increases gangue drainage. This produces a higher concentrate grade, but often at the expense of a slight loss of recovery,

The grade-recovery curves from rougher and scavenger banks obtained by varying the FT is shown in Fig. 2.6. Three distinct curves existed for the rougher bank with the 30 cm (12 in) FT curve indicating the best operation. At this FT, a grade gain of 3.4% was achieved over a 10 cm (4 in) FT with no recovery loss.

In the case of the scavenger bank, the improved grades at the higher FTs were obtained at the expense of some recovery, but a small decrease in recovery is not necessarily detrimental to total circuit recovery.

Air is an important input to the flotation process as it affects the recovery rate of both valuable and gangue minerals. An increase in AFR increases the probability of collision between particles and bubbles and increases the rate of transfer of particles into the

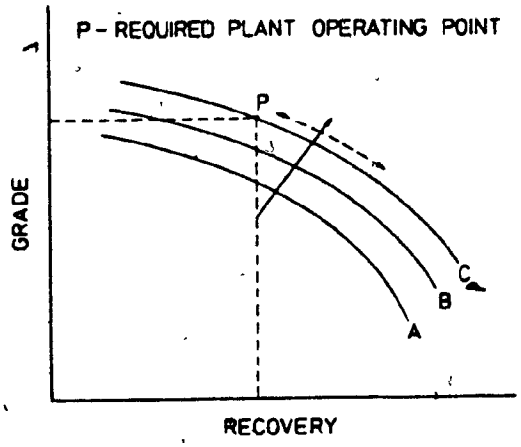

Fig. 2.4 Typical grade-recovery curves.

Fig. 2.5 Flotation air control at MIM.
(from McKee et al., 1976)

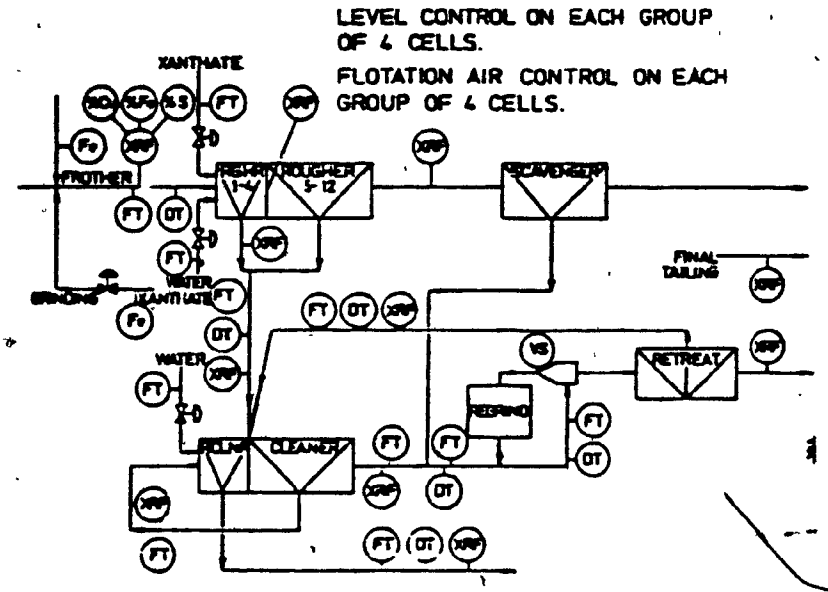

- No. 4 Concentrator flotation circuit.

Concentrator	Location	Year	Tpd * throughput	Concentrate products	Mode of control: Reagents	Cell level	Aeration
Frood Stobie	Canada	1968	24,000	Cu, Ni, S	x	x	
Lake Dufault	Canada	1968	1,400	Cu, Zn	x		
Pyhasalmi	Finland	1968	2,600	Cu, Zn	x	x	x
Ecstall	Canada	1970	10,000	Cu, Zn	x	x	
Kamioka	Japan	1970	4,342	Pb, Zn	x		
Strathcona	Canada	1971	7,000	Ni, Cu	x		
New Broken Hill	Australia	1971	6,000	Pb, Zn	x		
Clarabelle	Canada	1972	7,500	Ni	x	x	
Opemiska	Canada	1972	3,000	Cu, Au, Ag			
Vuonos	Finland	1972	8,000	Cu, Ni	x	x	x
Morenci	U.S.A.	1973	60,000	Cu	x	x	
Kristienberg	Sweden	1973	1,035	Cu, Zn, S	x		
Mattagami	Canada	1973	3,850	Zn, Cu, S	x	x	
Mount Isa No. 4	Australia	1973	16,000	Cu, Pb, Ag, Zn	x	x	x
Kotalahti	Finland	1973	1,400	Ni, Cu	x	x	x
Manibridge	Canada	1973	1,000	Ni, Cu			
Vihanti	Finland	1974	2,400	Zn, Cu	x	x	x
Broken Hill (Zinc Corp.)	Australia	1974	2,900	Zn, Pb	x		
Flin Flon	Canada	1974	4,600	Cu, Zn	x		
Keretti	Finland	1975	2,000	Cu, Co	x	x	
Heath Steele	Canada	1975	3,000	Zn, Pb, Cu	x	x	
Sullivan	Canada	1975	11,000	Cu	x	x	x
Frank (Rustenberg)	South Africa	1976	10,000	Pt, Cu, Ni		x	
South Broken Hill	Australia	1977	5,000	Pb, Zn	x		
Laisvall	Sweden	1977	5,000	Cu, Zn	x		
Samarco	Brazil	1977	30,000	Fe	x	x	x
Mount Isa No. 2	Australia	1978	12,000	Cu, Pb, Zn	x		
Brunswick	Canada	1978	2,850	Pb, Zn	x	x	x
Reserve	U.S.A.	1979	60,000	Fe	x	x	
Baluba	Zambia	1979	10,000	Cu			
Hayden	U.S.A.	1979	25,000	Cu, Mo			
Snow Lake	Canada	1979	900	Cu, Zn			
Amax Lead	U.S.A.	1979	4,850	Pb, Zn			
Black Mountain	South Africa	1979	6,000	Cu, Zn, Pb			

* Metric equivalent: 1 st × 0.907 184 7 = t.

Table 2.1 Concentrators employing automatic flotation control using AFR and FT.

Table 2.2 Effect of varying AFR at scavenger section on retreatment and final tail (from McKee, 1976)

Operation	Retreat Flows (TPH) Feed	Conc.	Tail	Retreat Tail	Final Tail	Calculated Scav. Tail
Normal	110-120	45-50	70-75	0.33	0.120	0.09
Increased air to Scavs	180-190	60-65	120-130	0.45	0.135	0.08

froth. It also increases the rate of transfer of water into the froth with a consequent increase in the recovery of valuable and gangue minerals.

AFR can be used to control concentrate grade, tail grade or mass flow of concentrate from a particular bank, depending on the control objective. For MIM rougher circuit, an AFR decrease is beneficial to the circuit provided the xanthate control loop is operating, i.e. xanthate addition rate is increased.

Control of the retreater and cleaning flotation may not be as sophisticated as control of roughing and scavenging. The aim is often to stabilize the circulation loads and flotation results (Kallioinen, 1984).

Improved gains from rougher and scavenger should be translated into total circuit gains. The effect of the changes in AFR at the rougher section on the performance of the cleaner-recleaner section is shown in Fig. 2.7 (from Lynch et al, 1981). It is possible to obtain improved grade-recovery curves from cleaning by manipulating both AFR and FT in roughers. Thus, the curve obtained in roughing determines the total circuit performance.

An AFR decrease in the scavenger section results in a scavenger concentrate flow rate drop. This decreased feed flow rate is the reason for a much lower retreater, and final tail grade, even though the scavenger tail grade is itself increased (Table 2.2).

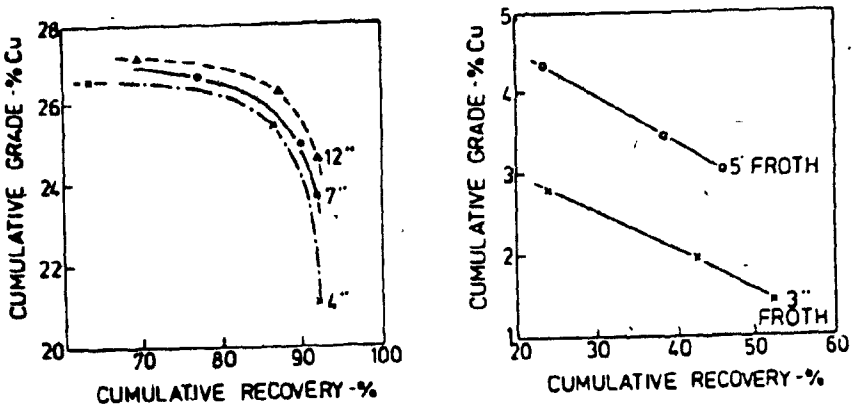

- A. Rougher grade/recovery curves at varying froth depths.
B. Scavenger grade/recovery curves at varying pulp levels.

Fig. 2.6 Effect of FT on rougher and scavenger flotation (from McKee et al., 1976)

Fig. 2.7 Effect of AFR changes in rougher section on the performance of cleaner section. (from McKee et al., 1976)

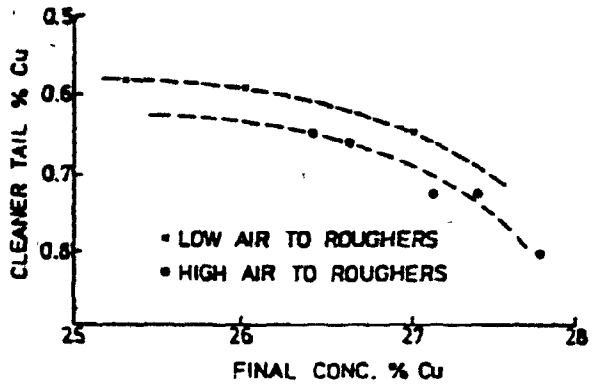

- The effect of changes in air addition rate at the rougher section on the performance of the cleaner-recleaner section.

However, variation of AFR in cleaning will only move the operating point along the curve, and will not cause movement to a higher or more efficient curve. The operating and control philosophy should be to achieve the best possible grade-recovery curve in roughing and then operate at the optimum point on cleaners grade-recovery curve (Lynch et al, 1981).

AFR is also used at the Kotalahti concentrator at the scavenger stage to maintain the circulating load flow rate constant. As the circulating load is made of the scavenger concentrate and the cleaner tails, AFR control is used to compensate for fluctuations in the cleaner tails flow rate (Laplante, 1980).

The control system at Pyhasalmi includes both stabilizing and optimizing control (Fig. 2.8). Both rougher and scavenger control are accomplished by using AFR and FT as stabilizing and $CuSO_4$ as optimizing control variables. The circulating load is controlled by AFR in three cleaning steps.

Stabilizing and optimizing control at Outokumpu concentrators, Finland, increased total metallurgical values or productivity by 2 % at only slight decrease in copper recovery (Table 2.3 from Paakkinen-Cooper, 1980).

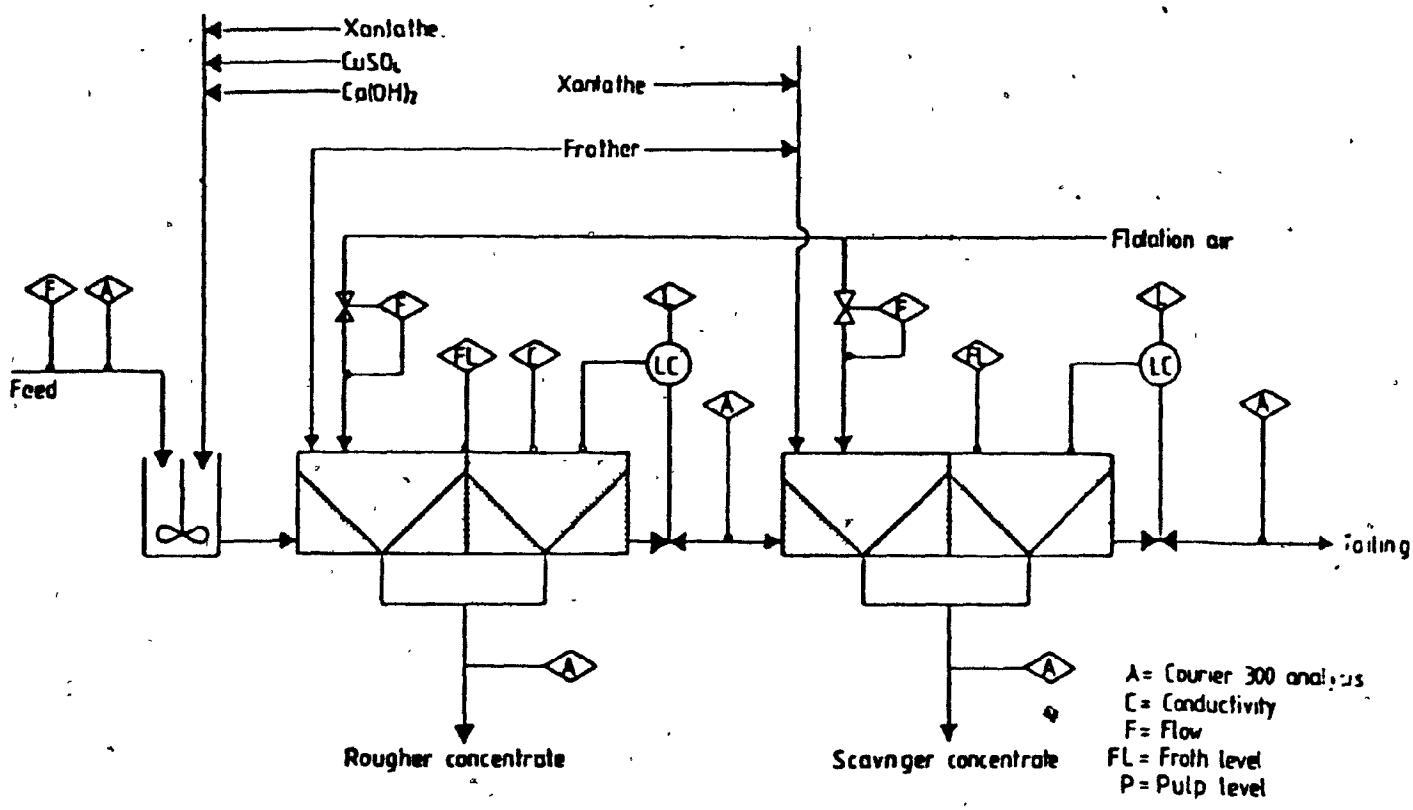

Fig. 2.8 Measurements and control variables of zinc roughing and scavenging at Pyhasalmi (from Kallioinan, 1984).

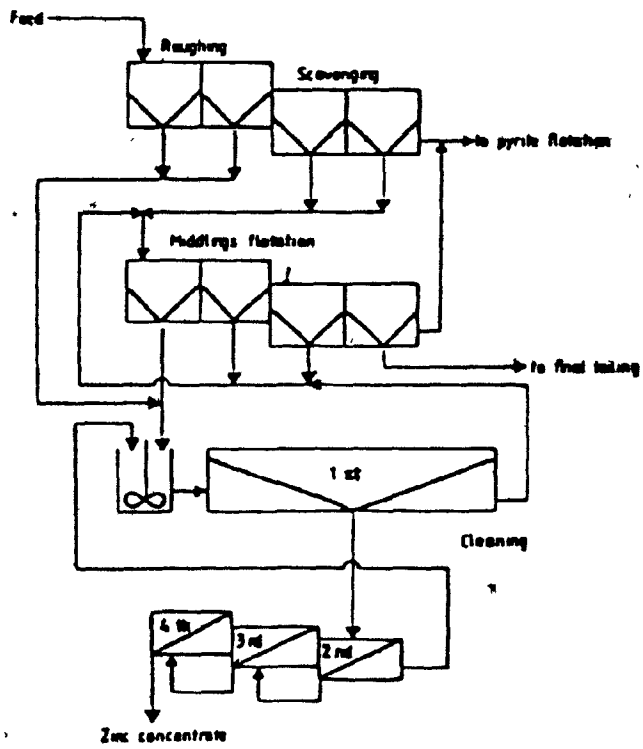

	Capacity	Concentrates	Mode of controls	Results
Pyhasalmi	2500 tpd*	Cu, Zn, Fe	Stabilizing control 1969 and optimizing control 1972	2.5% increase metallurgical values from optimized control ($450,000 annual gain)
Vuonos	1500 tpd copper circuit; 4500 tpd nickel circuit	Cu, Ni	Direct digital control in 1972 for operation of crushing and materials handling; stabilization control in 1974	1.5% increased cooper recovery
Kotalahti	2200 tpd	Ni, Cu	Proscon 103 stabilizing control in 1975	2% increased nickel and copper recovery
Vihanti	2500 tpd	Zn, Pb, Cu	Proscon 103 stabilizing control in 1974	2% increased zinc recovery
Keretti	1500 tpd new feed; 3000 tpd reclaimed tails feed	Cu, Zn, Co	Proscon 103 stabilizing control in 1975	About $200,000 net annual gain in reagents savings, improved recovery

* Metric equivalent: 1 st × 0.907 184 7 = t.

Table 2.3 Outokumpu concentrators using automatic control. (From Paakkinen and Cooper)

CHAPTER 3

THE AIR-WATER SYSTEM

3.1 INTRODUCTION

The main objective of this experimental section was to determine the effect of AFR on bubble size distributions and gas holdup. The mean bubble size is extremely important when correlating flotation kinetics with AFR.

Gas holdup is one of the important parameters characterizing the hydrodynamics of flotation cells. In two phase systems, it gives the volume fraction of the phases present in the cell, and hence their residence time. From the gas holdup, AFR and cell geometry bubble rise velocity and gas-liquid interfacial area can be determined (Shah et al. 1982).

This work was done in the absence of any mineral phase, to facilitate observation of the air-water phase. As the mineral phase, when present, does not affect the bubble formation mechanism (Grainger-Allen, 1970), results from this section can be used to analyze the flotation kinetics of transfer from the slurry to the froth.

3.2 DESIGN OF THE FLOTATION CELL

A plexiglass flotation cell with the following features was designed and constructed in order to investigate flotation kinetics:

a) similarity to existing industrial machines, i.e. Denver subaeration type.

b) high cell height to froth surface ratio, to create a quiescent slurry surface, which in turn facilitates froth thickness control and increases froth stability.

c) both batch and continuous operation, i.e. the feed can be pumped in and out.

d) ease of bubble photography, i.e. the cell is made of flat transparent plexiglass.

The plexiglass cell was cemented with epoxy glue. Its height up to the cell lip is 32 cm and up to the top 40 cm. It has a square cross-section with a 15 cm inside length. Except for its height, the cell is similar to one of the standard Denver 5 L cells.

In continuous operation, slurry is fed from the left side, 10 cm above the cell bottom, while tails are discharged from the right side, at the bottom (Fig. 3.1).

A Denver subaeration (D-1) type 1-5 L laboratory flotation machine was modified to accommodate the additional cell height. The rotor shaft and stand pipe

COLOURED PICTURES
Images en couleur

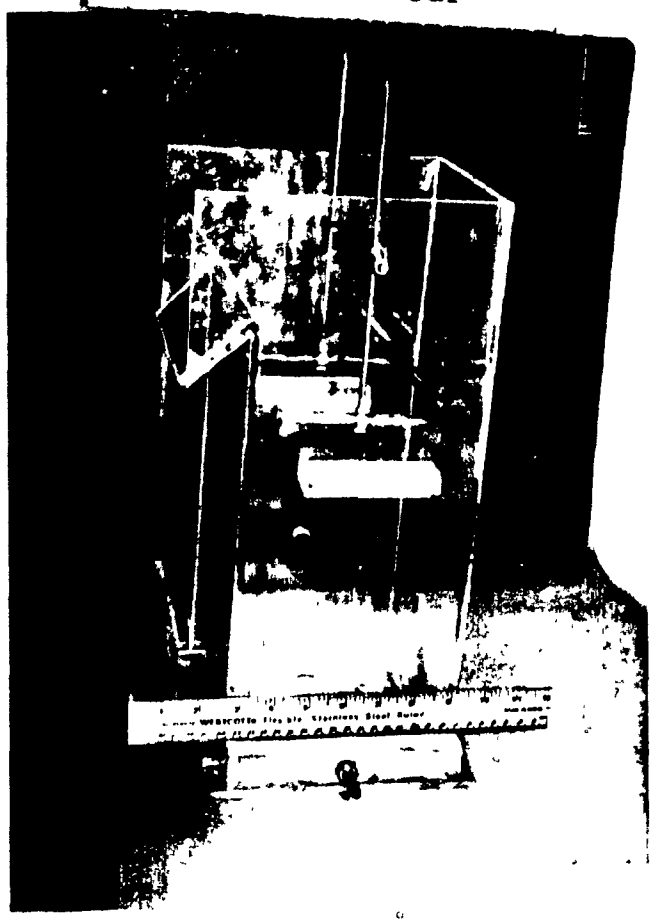

Fig. 3.1 Plexiglass flotation cell designed for this work.

were extended 20 cm. The machine body was also raised 33 cm by means of four iron pipes, to facilitate cell removal (Fig. 3.2). A wooden block was designed to fit tightly between the cell and the machine platform, to prevent vibration of the cell and raise it to the impeller level.

Wash water can be sprayed horizontally towards the back and lateral sides of the cell, through a copper pipe 1 cm in diameter. Small holes at 1 cm intervals evenly distribute wash water supplied from an elevated water tank. The pipe is fixed to the cell by a screw mechanism, and can be adjusted at the desired level. Flow is monitored using a rotameter.

3.3 EXPERIMENTAL PROCEDURE AND DATA ANALYSIS

Bubble size distribution was determined as a function of AFR, 1.3 to 6.25 L/min, at a Dowfroth 250C concentration of 10 ppm.

To measure bubble size, photographs were taken of the front middle of flotation cell using a piece of black plexiglass as background. This plate limited the thickness of the cell volume under investigation and provided a contrasting background for bubbles. A Canon camera with a wide angle lens, mounted on a stand and positioned facing the cell, was used. The distance between background plate and the cell front side was 2 cm, while the focal distance

COLOURED PICTURES
Images en couleur

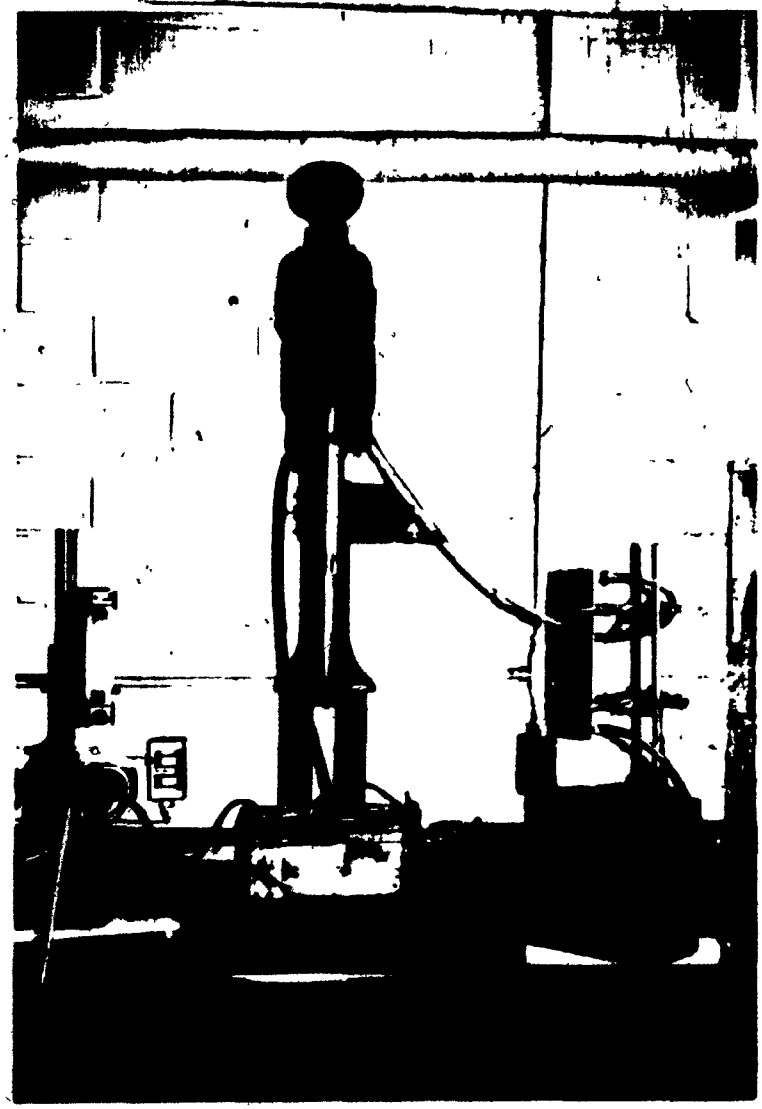

Fig. 3.2 Modified Denver Type D-1 Flotation Machine

was 30 cm. A high contrast scale was printed on the background plate. Two flashes were installed on both sides of the cell, at a 45° angle to the front of the cell, to avoid direct reflection at the camera. Bubble diameters were measured under microscope using a micrometric scale.

This photographic technique provides a representative description of the bubble population if the following assumptions are valid (Laplante, 1980):

a) the bubble sample photographed is representative of the whole bubble population;

b) the rising speed of a bubble is independent of its diameter;

c) the metallic plate used as a background does not effect bubble size;

d) bubbles do not coalesce during ascent;

e) the bubble distribution is even within in the photographed volume.

To simplify the characterization of the bubble population, each bubble was arbitrarily ascribed the surface to volume ratio of a sphere of diameter equal to its largest dimension. The most useful information to describe the behavior of the system can be easily obtained from the measured bubble size distributions in the following way.

$$T_s = \sum_{i=1}^{n} n_i \pi K^2 * d_i^2 \qquad 3.1$$

$$T_v = \sum_{i=1}^{n} n_i \pi K^3 * d_i^3 \qquad 3.2$$

where

di: average diameter of bubble size class i (mm)

ni: number of bubbles measured in size class i

K : scale factor relating the measured diameter to the actual one

Ts: total surface of the measured bubbles (mm^2)

Tv: total volume of the measured bubbles (mm^3)

Q : AFR (L/min)

The specific bubble surface, and total bubble surface produced per unit time can be expressed as;

$$\bar{S}\ (mm^{-1}) = T_v / T_s = (6/K) * \left(\sum n_i * d_i^2 \ / \sum n_i * d_i^3 \right) \qquad 3.3$$

$$S\ (cm^2/min) = 10^4 * \bar{S} * Q \qquad 3.4$$

In the two phase system, an additional series of experiments was also conducted to determine how gas holdup, average bubble residence time (BRT), superficial gas velocity (SGV), apparent bubble rise velocity (BRV) and liquid-gas interfacial area (LGIA) in the slurry phase vary with AFR. Since the water surface is quiescent under normal operation, it was possible to measure the gas holdup in the cell by filling it completely with water and

measuring how much was displaced as a function of AFR. Gas holdup in the slurry phase at different liquid height was determined by measuring the water level change in the cell at different AFRs. All relevant results and calculations are provided in Appendix 2.

3.4 RESULTS AND DISCUSSION

3.4.1 Average Bubble Diameter

The bubble population was represented by an "average" bubble diameter, dav, defined as the diameter of a bubble of specific surface $\bar{S}$, i.e. the size that would yield the same bubble surface if all bubbles were of equal diameter (dav = 6ds where ds is the Sauter mean diameter).

Fig. 3.3 shows two photographs of bubble populations at 1.3 and 7.5 L/min. As expected, an increase in AFR yields larger bubbles. Large bubbles produced at high AFRs are often highly non-spherical. Attention was, therefore, restricted to low AFRs which generate small and spherical bubbles and correspond to normal flotation practice (1.3-6.25 L/min). Fig. 3.4 shows a typical bubble size distribution at an AFR of 1.3 L/min and a Dowfroth 250C dosage of 10 ppm. The most frequent observation is around 2 mm, which is typical of conventional flotation systems.

The effect of AFR, Q, on the average bubble

COLOURED PICTURES
Images en couleur

AFR: 7.5 L/min

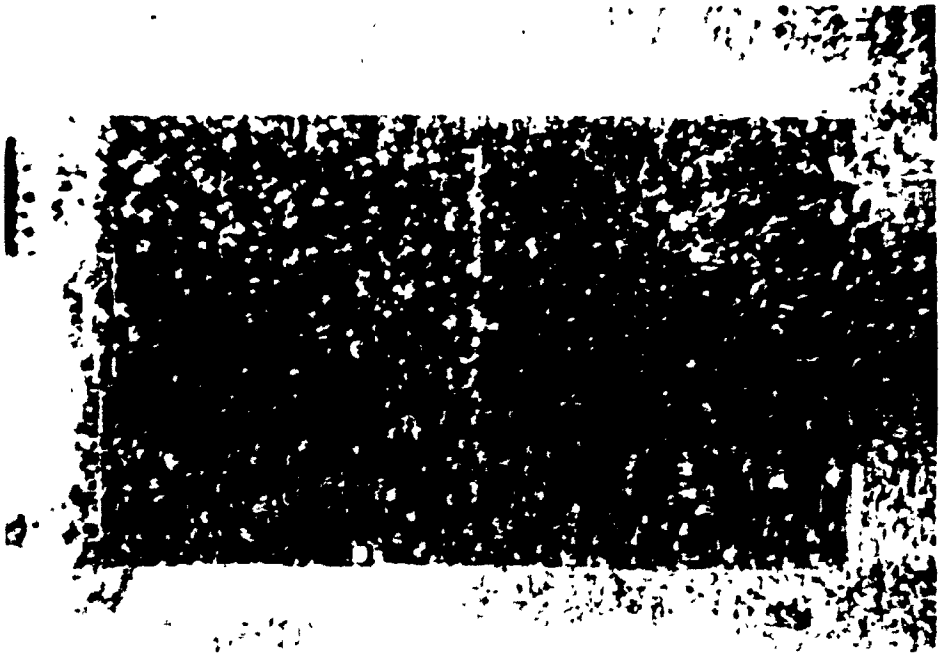

AFR: 1.3 L/min

Fig. 3.3 Effect of AFR on bubble size distribution.

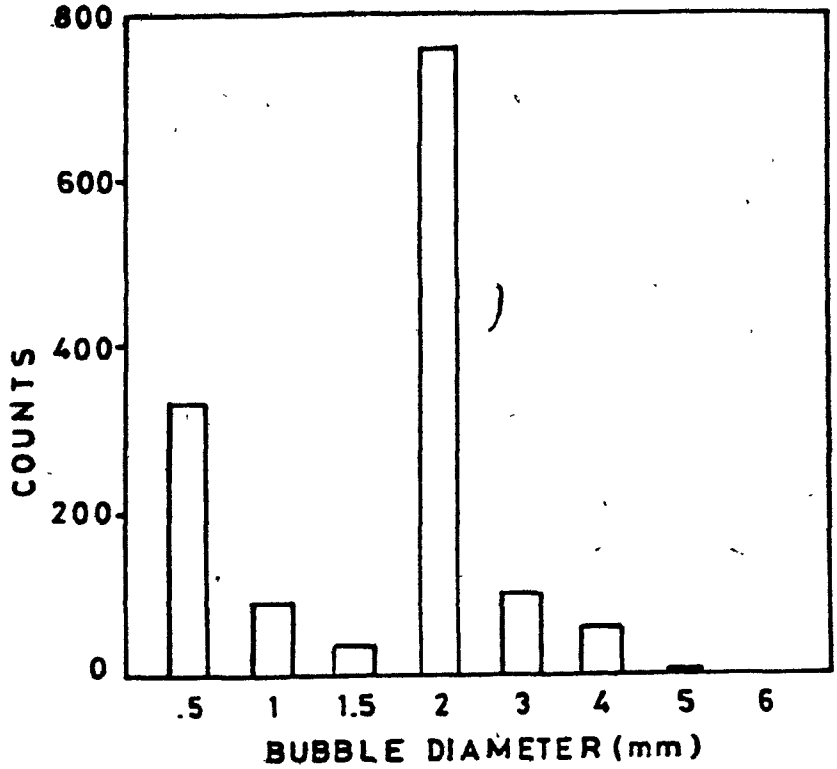

Fig. 3.4 Bubble size distribution at an AFR of 1.3 L/min.

diameter, dav, is summarized in the following relationship obtained by linear regression.

$$Ln\ (d_b) = (0.067 \mp 0.003) * Q + 0.897 \qquad 3.5$$

(correlation coefficient: 0.94)

where Q is in litres per minute and d_b in mm (Appendix 1).

The relationship between AFR, superficial gas velocity, Vg, and bubble size is shown in Fig. 3.5. Specific bubble surface decreases slightly as AFR or Vg increases (Fig. 3.6). The relationship between AFR and the production rate of total bubble surface is shown in Fig. 3.7. Total bubble surface significantly increases with increasing AFR.

3.4.2. Effect of Air Flow Rate on Gas Holdup

The effect of AFR on gas holdup in the slurry phase is given in Fig. 3.8. A very good linear relationship between AFR and gas holdup was found in the operating range of AFR (1.3-7.5 L/min). Above 7.5 L/min, the curve reaches a plateau. This corresponds to the transition from the bubbly zone, which has homogeneous bubbles, to churn turbulent flow, which yields heterogeneous bubbles and is inappropriate for efficient

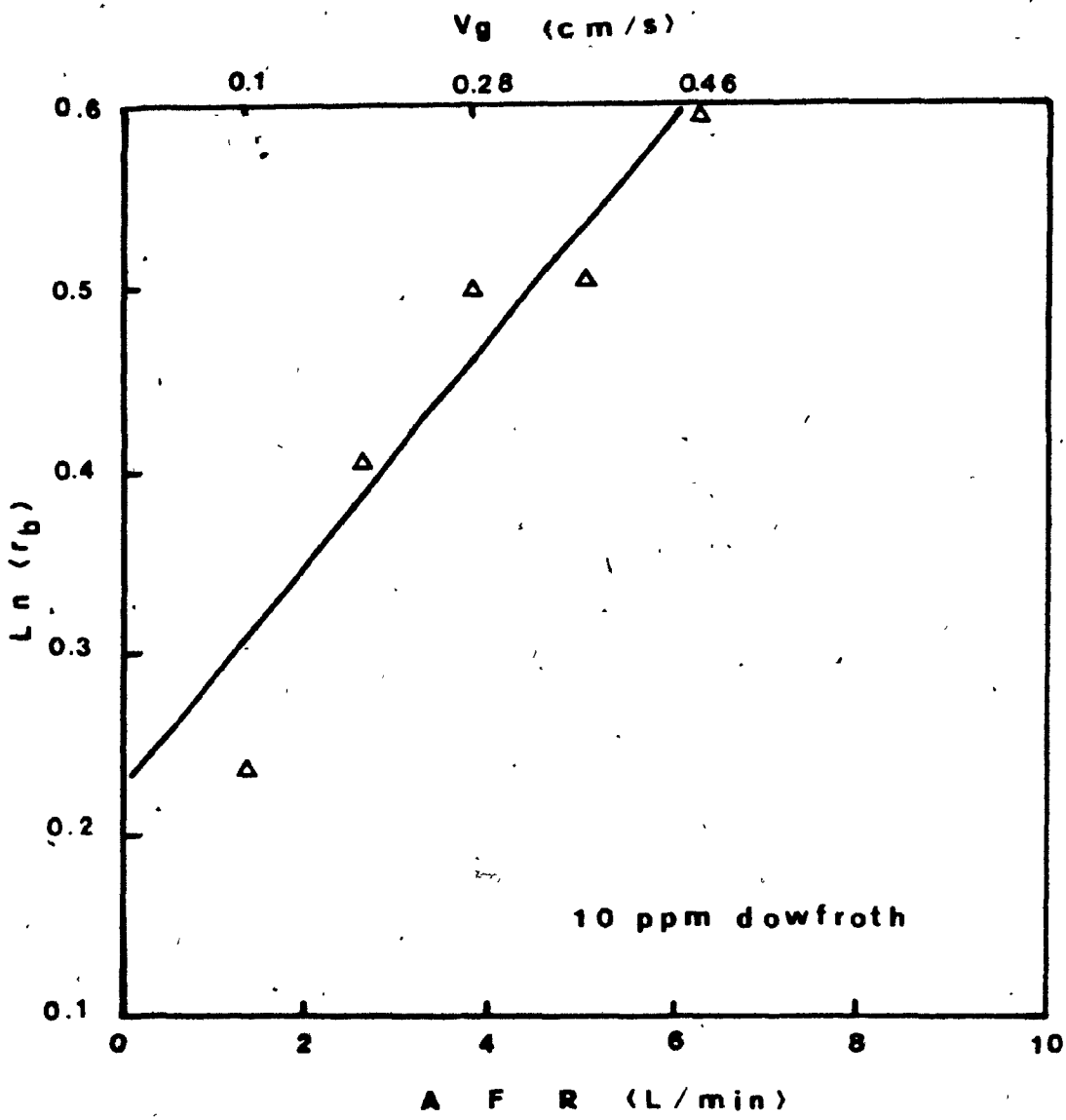

Fig. 3.5 Effect of AFR and superficial gas velocity on bubble size.

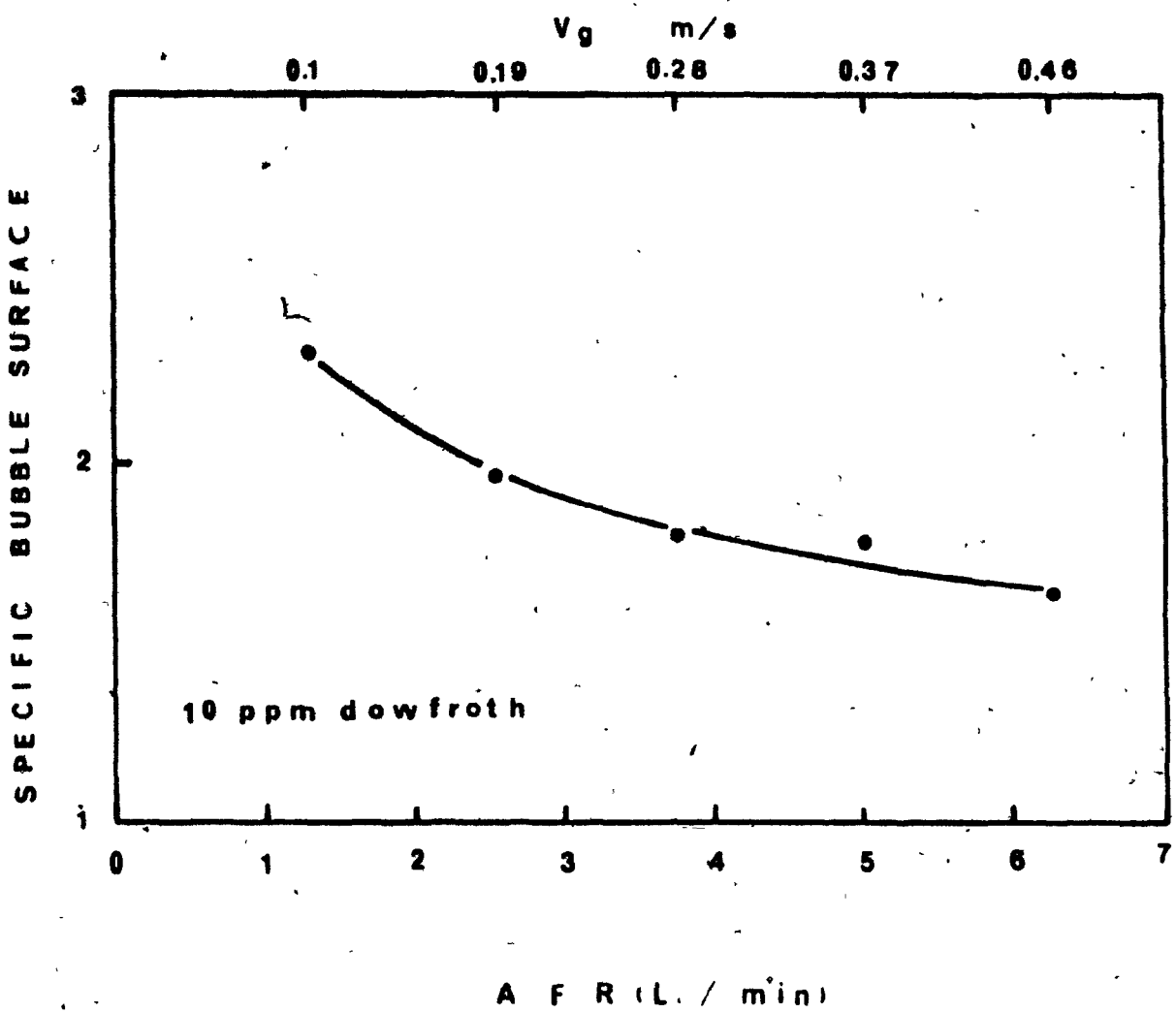

Fig. 3.6 Effect of AFR and superficial gas velocity on specific bubble surface (mm^2/mm^3).

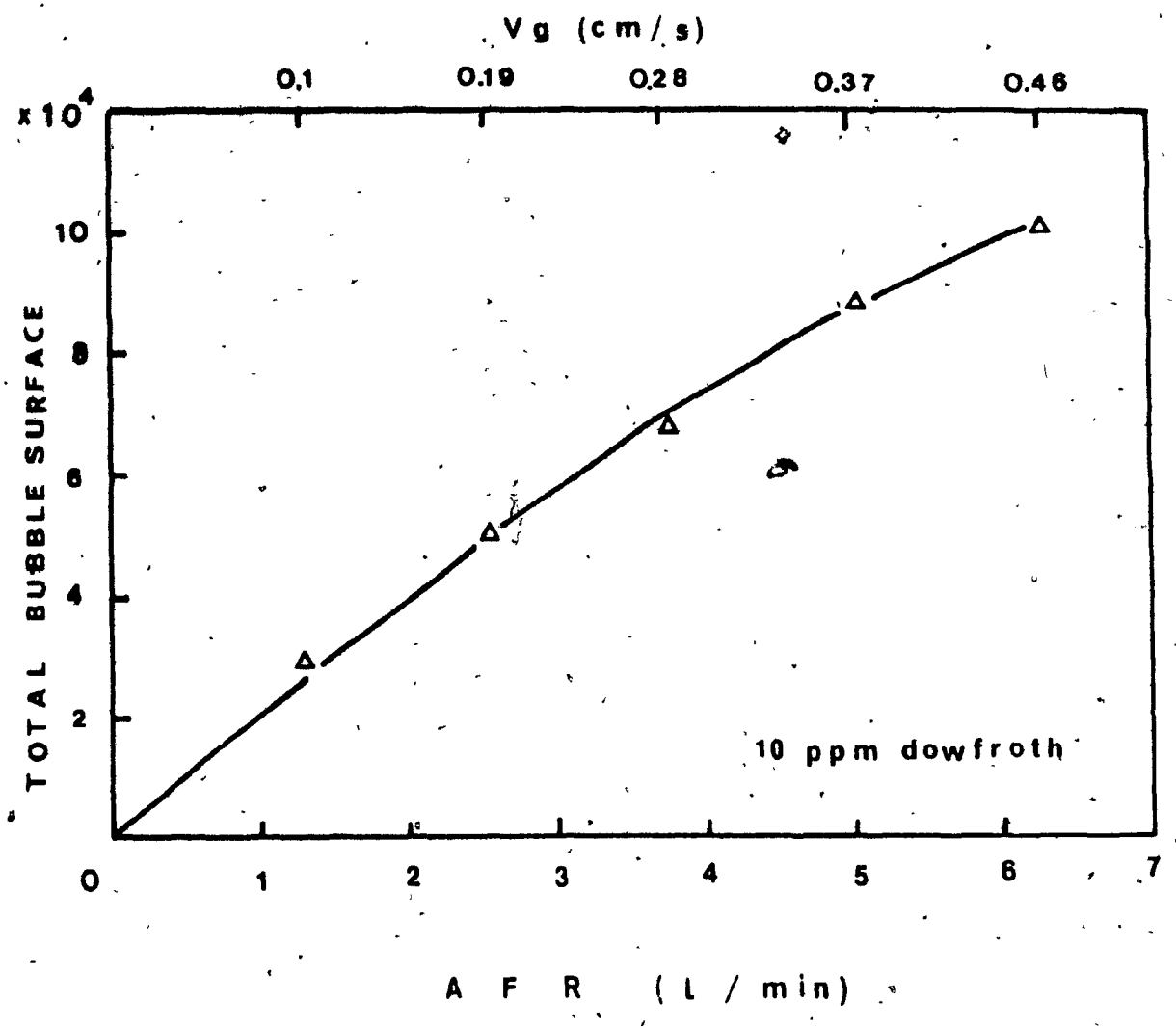

Fig. 3.7 Effect of AFR and superficial gas velocity on total bubble surface (cm /min).

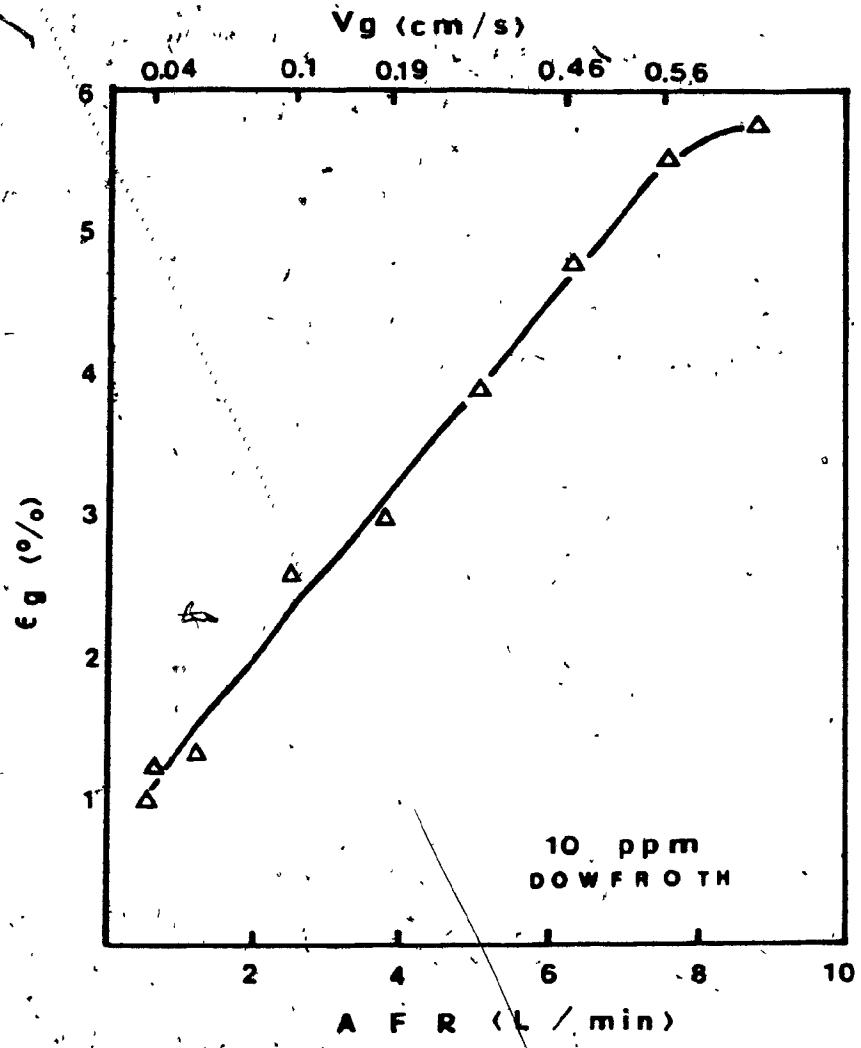

Fig. 3.8 Effect of AFR and superficial gas velocity on gas holdup in the slurry phase.

flotation (Shah et al., 1982).

The average BRT in the slurry phase is equal to the gas volumetric holdup divided by the AFR. Fig. 3.9 shows that average BRT decreases only slightly as AFR increases, except at very low AFRs. The residence time of a bubble in the slurry phase of conventional flotation machines was found to be 5-10 times shorter than in a flotation column (Dobby, 1984). Thus, the possibility of a bubble becoming fully loaded is considerably smaller than in a column.

As AFR increases both gas holdup and bubble diameter in the slurry phase increase. The increase in bubble diameter is modest (from 2.5 to 3.75 mm as AFR increases from 1.3 to 6.25 L/min). Its effect on the BRV is partially offset by the increased gas holdup, which lowers rise velocity by 13% when gas holdup increases from 1 to 5.5% (Richardson and Zaki, 1954). The net result is only a slight increase in BRV and decrease in BRT with increasing AFR. This is shown in Fig. 3.10, where the apparent rise velocity is plotted as a function of AFR and the superficial gas velocity. As AFR increases, the apparent BRV increases by only 20% from 2-8 L/min. The rise velocity increases very sharply below 2 L/min, but this is below the normal operating range, as discussed in section 5.3.4.

Fig. 3.11 shows that the apparent BRV increases as average bubble size increases. The convex relationship

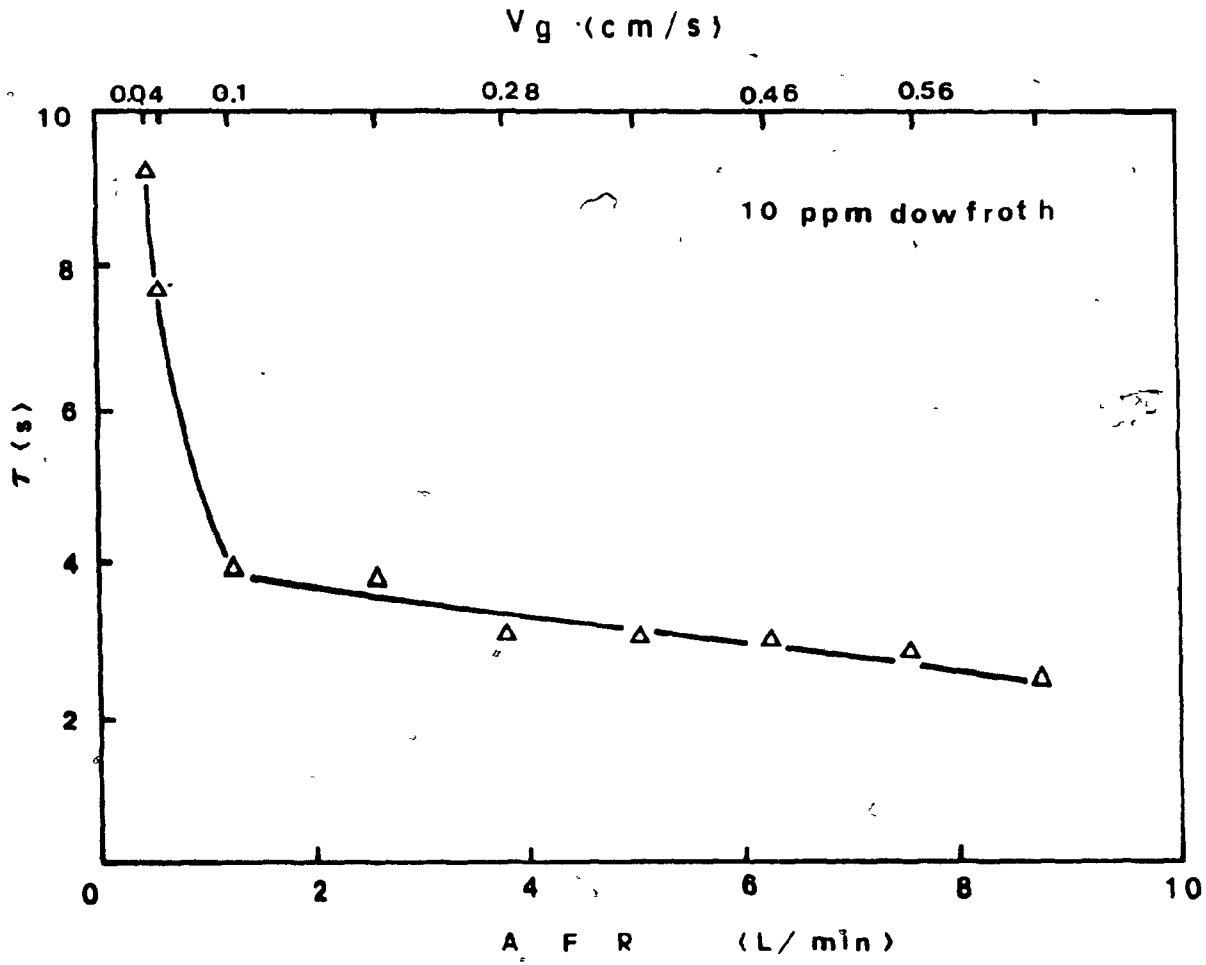

Fig. 3.9 Effect of AFR and superficial gas velocity on average bubble residence time.

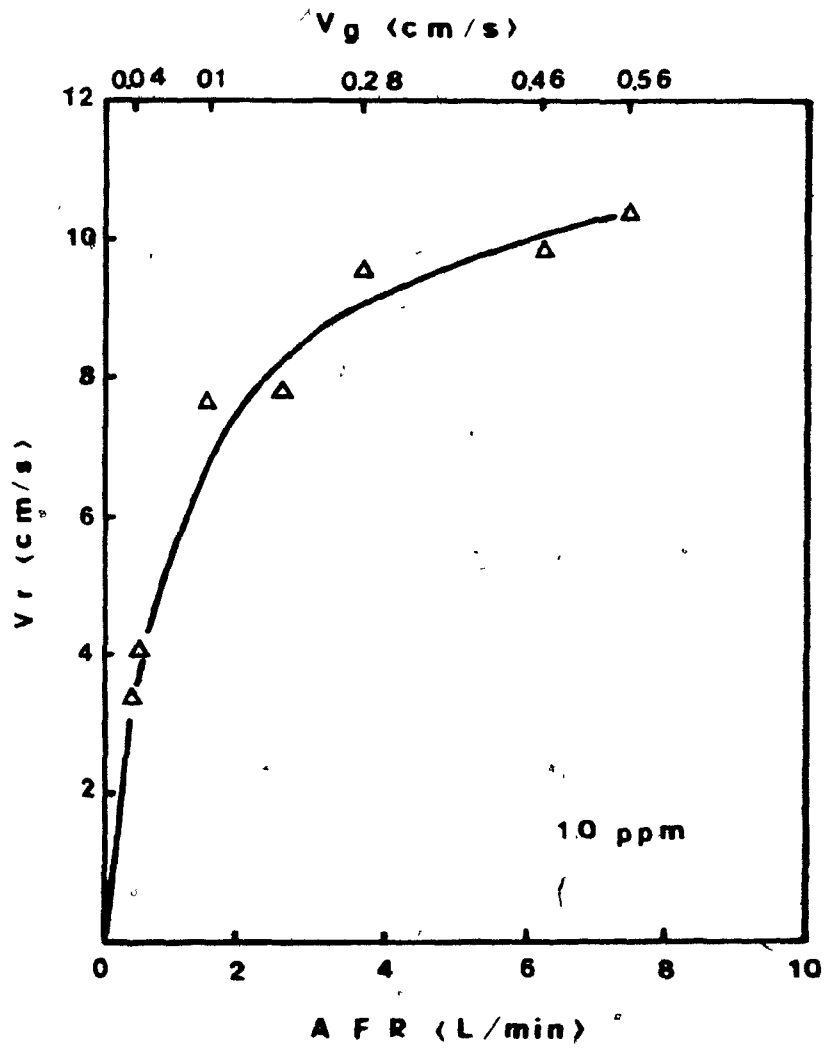

Fig. 3.10 Apparent bubble rise velocity as a function of AFR and superficial gas velocity.

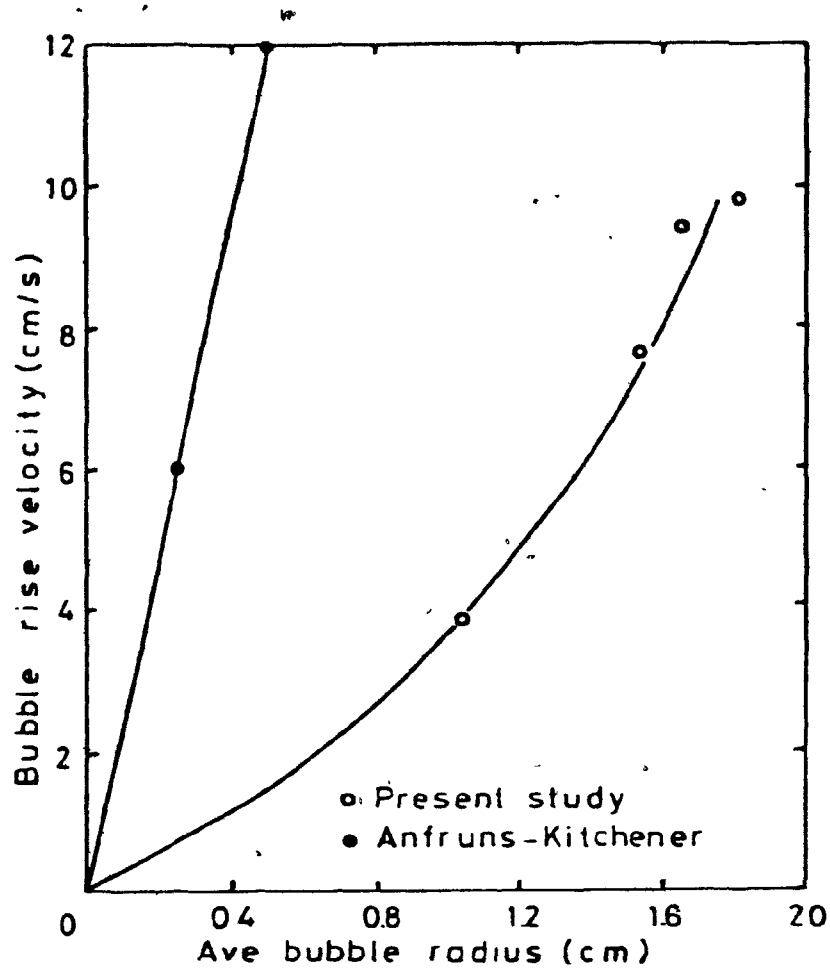

Fig. 3.11 Apparent rise velocity versus average bubble radius.

expresses the importance of bubble swarms and hydrodynamic conditions in a conventional flotation cell. For the sake of qualitative comparison Anfruns and Kitchener's data (1976) were also plotted on the same graph. It is obvious that there is a significant difference between bubble rise velocities in single and multiple bubble systems because of vigorous turbulence and dense bubble population.

The effect of bubble swarms can be better understood using the concept of collision efficiency. While single bubble-particle models provide a convenient basis for assessing the effect of bubble size on collision efficiency for a particular size and type of particle, the relatively high bubble voidages encountered in flotation machines raise the question of how closely these predicted collision efficiencies represent the actual situation.

Flint and Howarth (1971) found that the collision efficiency of particles with bubbles in a swarm can be several times as large as those calculated from a single bubble model. Dobby (1984) reported that collection efficiency goes down with increasing AFR, and is generally much lower that the collection efficiency reported by Anfruns and Kitchener (1976).

The collision efficiency of a particle with a bubble in a bubble swarm will differ from that of a particle with a single bubble for at least three reasons.

a) As can be seen before, the bubble rise velocity relative to liquid will be reduced due to hindered effects

of the neighboring bubbles, for a particular bubble and particle. For fine particles and bubbles, this reduction in rise velocity leads to an increased collision efficiency.

b) The shape of the liquid streamlines around each bubble is different. In a bubble swarm, the divergence of the streamlines is limited. In this way, the presence of a bubble swarm again tends to increase collision efficiency.

c) The motion of particles at large distances upstream from the target bubble is no longer parallel to the direction of bubble motion but is influenced by layers of bubbles ahead of it.

The liquid-gas interfacial area is an important design variable which depends on the geometry of the apparatus, the operating conditions and the physical properties of liquid media. Mass transfer rates can be easily influenced by varying interfacial area. Fig. 3.12 shows that the liquid-gas interfacial area increases as AFR increases.

The effect of superficial gas velocity, which is defined as the air flow rate divided by surface area of the cell, and bubble size on flotation kinetics ,more specifically flotation rate constant, can be expressed (Jameson and coworkers, 1977):

$$K = (1.5 * V_g * E_k / d_b) \qquad 3.6$$

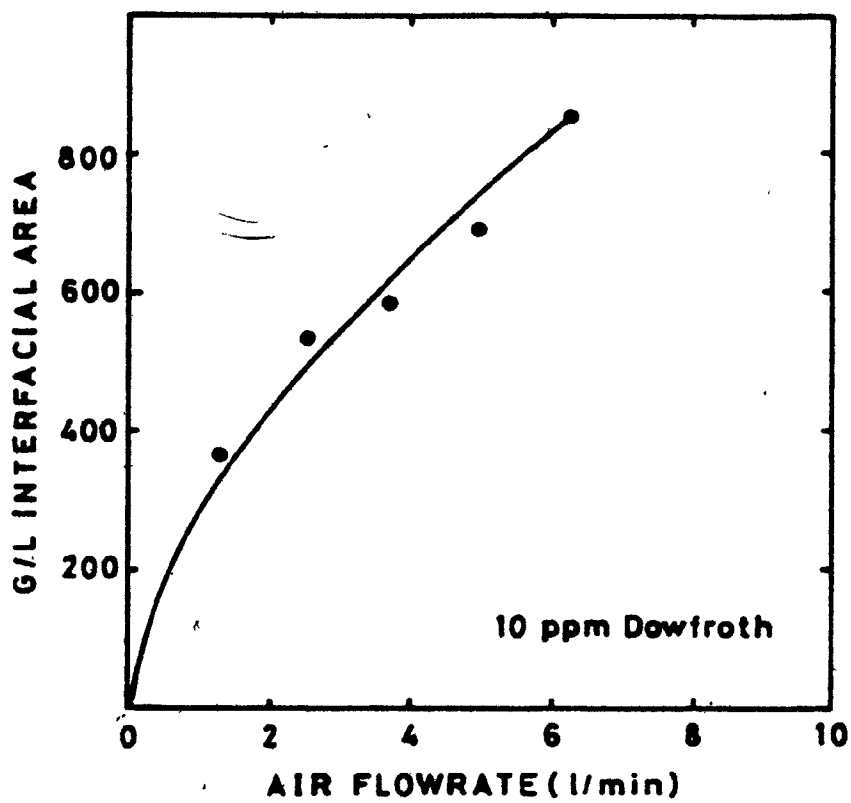

Fig. 3.12 Effect of AFR on liquid-gas interfacial area in the slurry phase.

where K: FRC (1/min)

Vg: Superficial gas velocity (cm/s)

Ek: Collection efficiency

db : Bubble diameter (cm)

and

$$E_k \propto d_p/d_b^{2.69} \qquad 3.7$$

where dp: particle diameter (mm).

The higher the AFR which produces larger bubbles, the higher will be the superficial gas velocity. Thus, an increase in superficial gas velocity increases the FRC while an increase in bubble size decreases the FRC. It was found that superficial gas velocity of flotation columns are much higher, 1-4 cm/s, than conventional flotation machines, 0.2-0.5 cm/s.

Peebles and Garber (1953) have defined the factors affecting the rise velocity of single bubbles in stagnant liquids under turbulent conditions. They found that the following relationship for the rise of bubbles in the constant velocity region in which db varies from 1 cm to 2 mm (Bhaga, 1970).

$$V_t = 1.18\left(\frac{g\,\sigma\,(\rho_l - \rho_g)}{\rho_l^2}\right)^{1/4} \qquad 3.8$$

where ρ_l, ρ_g: densities of liquid and gas respectively (g/cm)

g : gravitational acceleration (cm/s)

σ : surface tension (dyn/s)

Vt: terminal bubble velocity (cm/s)

It can be seen from the literature that the velocity of rise of the swarm, which is generally equal to the slip velocity, is expressed in general by

$$V_{swarm} = V_s = V_t * f(\epsilon_g) \qquad 3.9$$

where Vswarm: bubble swarm velocity, cm/s

Vs: bubble slip velocity (cm/s)

ϵg: gas holdup in the slurry (%)

$f(\epsilon g)$ is only slightly below unity for gas holdups in studied range.

For an AFR of 6.25 L/min, Vt was calculated at about 18 cm/s (Eq.3.8) however, the experimentally calculated average rise velocity is 9.72 cm/s. To explain this difference, it was decided to investigate the gas holdup in the slurry phase with respect to liquid height in the cell. At constant AFR and without frother addition, the change in water level was measured at different liquid height. Results shown in Fig. 3.13 interestingly indicate that there are two distinct zones within the flotation cell. The lower part of the cell from 5 to 15 cm shows constant gas holdup. However, the gas holdup drastically

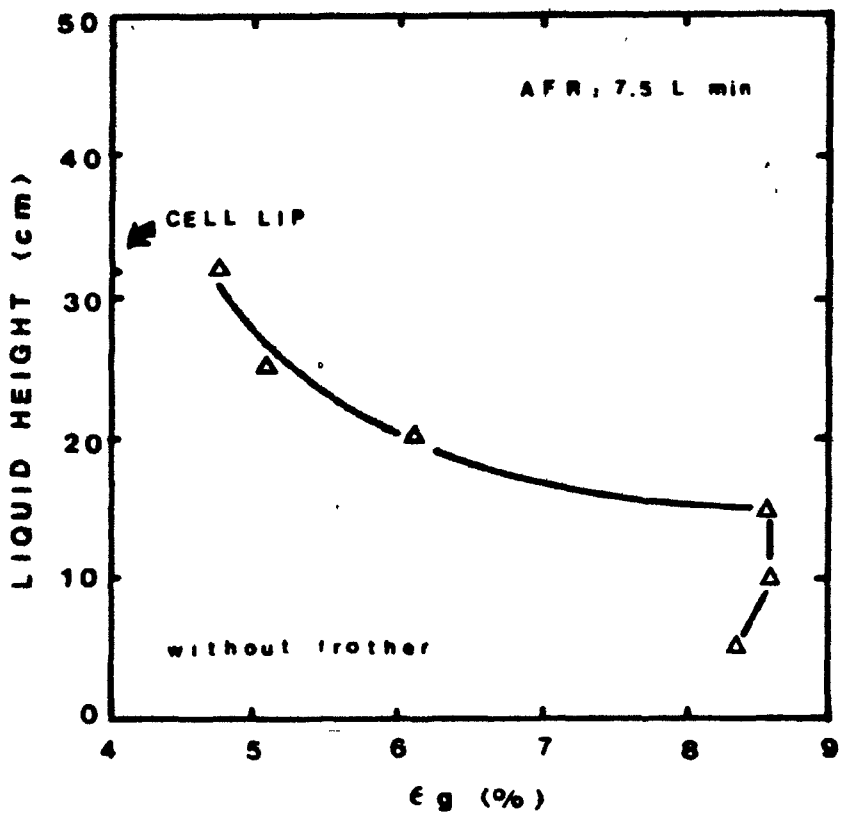

Fig. 3.13 Influence of liquid height on gas holdup in the slurry phase.

decreases between 15 cm and the cell lip. The small decrease in gas holdup at 5 cm may be explained by the presence of the impeller and dead spaces at the bottom corners of the cell, shown in Fig. 3.14.

It is possible to divide the slurry phase of stirred cell into two zones according to the apparent BRV. The lower part is the active zone where the particles are kept in suspension and particle bubble contact is induced by the turbulent action of impeller. In this zone, the apparent BRV is slow due to higher gas holdup, significant bubble swarm effects, and strong agitation. However, the upper part which is called the buffer zone is relatively quiescent. The apparent BRV in buffer zone is significantly higher than the active zone because of the lesser gas holdup, bubble swarm and agitation.

By assuming that the bottom third of the cell height is the perfectly mixed active zone, the apparent BRV and BRT in the active zone were calculated as 5.37 cm/s, and 1.86 s respectively at 6.25 L/min. In the buffer zone, the apparent BRV reaches 17.5 cm/s, close to the predicted Vt and the average BRT is about 1.14 s.

This analsis shows that bubbles will stay for a longer time in the active zone which is desirable for increased collision efficiency. The presence of a buffer zone, in the conventional flotation cell can be useful. On the one hand, it provides a quiescent slurry-froth interface; on the other hand, it works as a cleaning or

COLOURED PICTURES
Images en couleur

Fig. 3.14 Slurry phase in conventional cell.
(Notice the absence of bubbles in the lower cell corners)

filtering zone. Since BRV is high in this intermediate zone, some of the entrained gangue particles in the wake of bubbles may drop back to the active zone. This may be further promoted by addition of wash water, as will be presented in Chap. 8.

3.5 SUMMARY

In this chapter, a description of the basic flotation cell used throughout this research program was provided. The first part of this research, the air-water system, was also covered.

Firstly, it was found that the total bubble surface produced per unit time increases as AFR increases, whereas the specific bubble surface, inversely proportional to the average bubble size, decreases slightly.

Secondly, the effect of AFR on gas holdup were characterized. Holdup, the fraction of air in the air/slurry mixture, increases with increasing AFR and decreasing bubble size (smaller bubbles rise more slowly giving larger residence time and increased holdup).

Then, the effect of AFR on apparent BRV, BRT and LGIA was determined. Those are important design parameters and also can be used for scale up purposes.

Two distinct zones with respect to the apparent bubble rise velocity were observed in the slurry phase of

the present system: a lower zone, active zone, similar to the mechanically agitated flotation cells, and a buffer zone, between the active and froth zones, where agitation is less important, bubble rise velocities higher and gas holdup lower than in the active zone.

It is believed that the lower zone is more conducive to bubble-particle collection and attachment. Consequently, capture models such as that of Anfruns and Kitchener (1976), derived in environment similar to the buffer zone, are unlikely to represent precisely flotation phenomena taking place in a different hydrodynamic environment.

CHAPTER 4

SAMPLE AND REAGENT SELECTIONS, GENERAL EXPERIMENTAL PROCEDURE AND PRELIMINARY TESTS

4.1 INTRODUCTION

The best known example of sulphide mineral that generally does not respond well to flotation with thiol collectors is sphalerite. For example, with short chain xanthates at moderate concentrations, sphalerite does not float and this behavior can be used to separate it from other sulphide minerals. However with addition of copper sulphide to the system, sphalerite responds readily to flotation. This is the classical example of activation in flotation technology.

In this chapter, first the surface active reagent selection for sphalerite flotation will be discussed and then the general aspects of semi-batch experimental procedure will be given. Finally, results of the preliminary tests to determine the best operating conditions will be presented.

4.2 SAMPLE AND REAGENT SELECTIONS

4.2.1 Sample

The sample used was wet final zinc concentrate from Brunswick Mining and Smelting Corporation, Canada. Its size distribution as received is shown in Table 4.1a. To obtain a

more homogeneous flotation behavior, dried samples were deslimed to 10 μm by means of three-stage cycloning. The size distribution of the redried cyclone underflow product is given in Table 4.1b. Removing all -8 μm material is impossible; thus the decrease from 23 to 7% -8 μm, as shown in Table 4.1b, is an acceptable compromise.

Particle size (μm)	Mass (%)
- 74	100
-30 + 23	83
-23 + 16	68
-16 + 10	49
-10 + 8	33
-8	23

Table 4.1a Particle size distribution of the original sample.

Particle size (μm)	Mass (%)
- 74	100
-30 + 23	74
-23 + 16	53
-16 + 10	29
-10 + 8	14
-8	7

Table 4.1b Particle size distribution of the cyclone underflow product after three stage cycloning.

4.2.2 Activator

The most commonly used and economical activator for sphalerite is copper sulfate, which is added to the pulp during conditioning. Required conditioning time will depend upon the characteristics of the ore, but is generally less than 10 minutes. Adsorption of copper will take place on sphalerite surface and coated sphalerite particles will behave as the corresponding copper mineral.

The chemical reaction between sphalerite and xanthate is reversible and slow.

$$ZnS + 2X^{-} \longrightarrow ZnX + S^{=} \qquad 4.1$$

After activation with copper sulfate, the sphalerite surface is covered by Cu++ , cupric ions.

$$CuSO_4 \longrightarrow Cu^{++} + SO_4^{=} \qquad 4.2$$

$$ZnS(s) + Cu^{++} \longrightarrow CuS(s) + Zn^{++} \qquad 4.3$$

Experiments with radioisotopic Cu^{++} 64 indicate sphalerite activation to be a chemical exchange of Cu++ for Zn++ in the sphalerite lattice. The uptake of copper is rapid, being a slight function of the copper concentration in solution and controlled by solution diffusion. In this system

Cu abstraction is approximately one monolayer of the ZnS crystal structure, shown in Fig. 4.1. However, it can proceed beyond the monolayer and once the uptake exceeds three monolayers, the process is controlled by the parabolic rate law for diffusion in the solid state (Gaudin et al., 1959).

A typical industrial copper sulfate dosage of 500 g/t, and a 15 minute conditioning time were selected to activate sphalerite.

4.2.3 Collector

Sphalerite does not float with ethyl xanthate in the absence of activation (Fig. 4.2, from Sutherland and Wark, 1955). It responds, however, quite readily to flotation at higher concentrations of larger chain xanthates, such as n-heptyl. Amyl xanthate clearly fails to yield good recoveries, although some degree of hydrophobicity is achieved.

After activation, ethyl xanthate (Aero-325), isopropyl xanthate (Aero-343), and amyl xanthate (Aero-350) may be used as a collector. Sodium ethyl xanthate has the shortest carbon chain, and can be used if good selectivity is desired. Sodium isopropyl xanthate is the most widely used xanthate in the flotation of sulphide minerals, primarily due to its low cost. In many instances the more powerful members of xanthate family are preferred, for improved recovery (Cyanamid Manual, 1982).

Sodium amyl xanthate (NaAX) is the longest-chain

xanthate commercially available. It is useful in operating where a powerful and non-selective sulphide promoter is desired, as in the present study, where sphalerite is the only sulfate used.

It was decided to use NaAX at a dosage of 100 g/t, to achieve strong hydrophobicity and short induction times.

4.2.4 Frother

A dilute aqueous solution of Dowfroth 250C at a concentration of 75 g/t was used throughout the experiments as frother. Dowfroth 250C is mainly made of polypropyle glycol methyl ethers and can be used on both alkaline and acid pulps. It is claimed that Dowfroth 250C is usually effective in considerably smaller amounts than other frothers. It produces a froth of high selectivity yielding concentrates of maximum grade consistent with high mineral recovery as well (Dowfroth Manual, 1984). Frother was added both to the cell initially and to the wash water tank to maintain its concentration in the system.

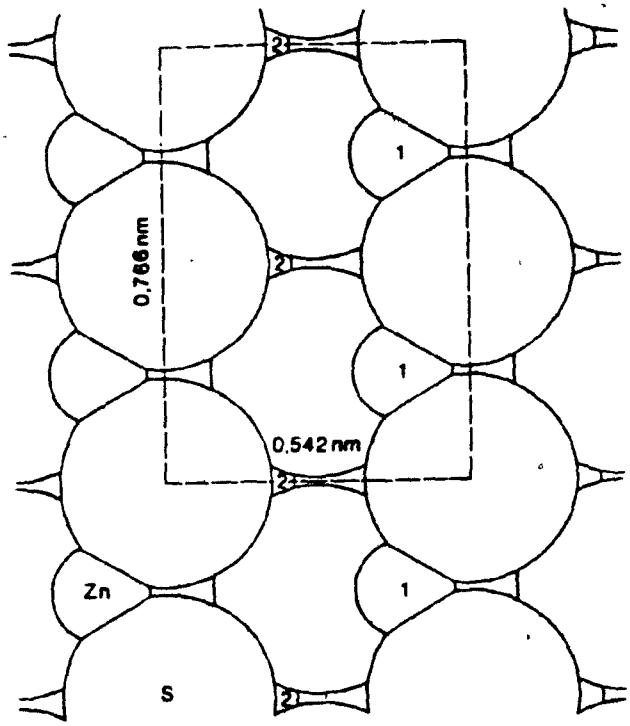

Figure 4.1 The (110) plane of sphalerite. Unit area, 0.419 nm². Zinc ions in the surface are designated by numeral 1 and zinc ions in the next lower layer by numeral 2 (Gaudin, Fuerstenau and Mao, 1959)

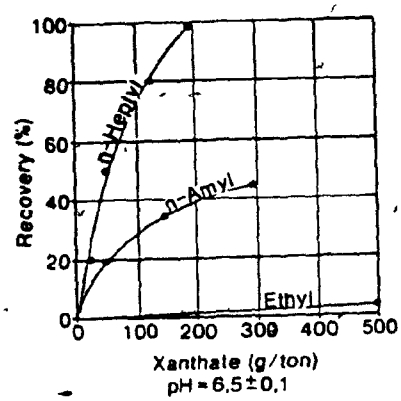

Figure 4.2 Influence of selected xanthates on recovery of zinc blende (Sutherland and Wark, 1955)

4.2.5 pH Modifier

If a copper salt such as copper sulfate is added to an alkaline or neutral sphalerite pulp and conditioned for a few minutes, the mineral behavior toward the collector is changed. The influence of pH on sphalerite flotation is shown in Fig. 4.3. It is obvious that maximum flotation recovery can be achieved between pH 5 and 8.5. Therefore, it was decided to maintain a pH 7.5-8 by adding small amount of lime.

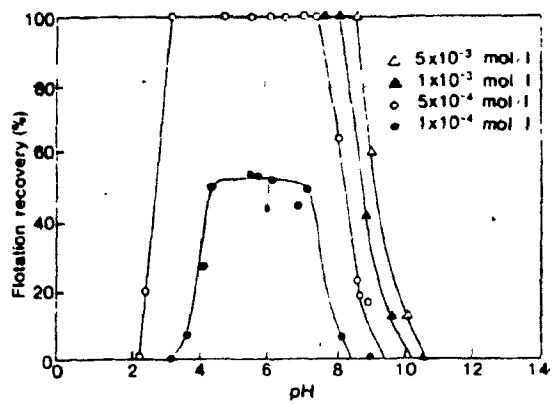

Figure 4.3 Flotation recovery of sphalerite as a function of pH in the presence of various concentrations of amyl xanthate (Fuerstenau, M. C, Clifford and Kuhn, 1974)

4.3 GENERAL EXPERIMENTAL PROCEDURE FOR SEMI-BATCH FLOTATION

Rapid removal of the froth was one of the criteria used in the design of the flotation cell. The feature used to achieve this purpose is the high cell height-to-depth ratio which creates two distinct zones within the liquid phase. The lower part is the active zone where the particle are kept in

suspension and particle bubble contact is induced by the turbulent action of impeller. The second zone which is the upper part is weakly agitated to provide a quiescent slurry-froth interface.

Consequently, it was possible to remove the froth quickly, by addition of a continuous flow of washing water, sufficient to create a film of liquid flowing over the cell lip. Firstly, the samples were activated with copper sulfate for 10 min and then conditioned with collector. After frother addition, froth was permitted to build up for 10 seconds before any concentrate was removed. The mineral laden froth was then collected in pans periodically replaced at time intervals varying from 10 to 30 s. This procedure was carried out until there was no material being floated. The last concentrate product was collected for several minutes to ensure the recovery of all hydrophobic material. The products were then filtered, dried, weighed, and saved for size analysis by cyclosizer. The semi-batch flotation flowsheet is summarized in Fig. 4.4.

Prior to the flotation tests, the air and water Cole Palmer rotameters were calibrated using a dry-gas meter and graduated cylinder, respectively. Calibration curves are given in Appendices 4.2 and 4.3. Compressed air supplied from a compressor was introduced to the cell through the stand pipe. The amount of gas was controlled by a manometer and pressure reducer.

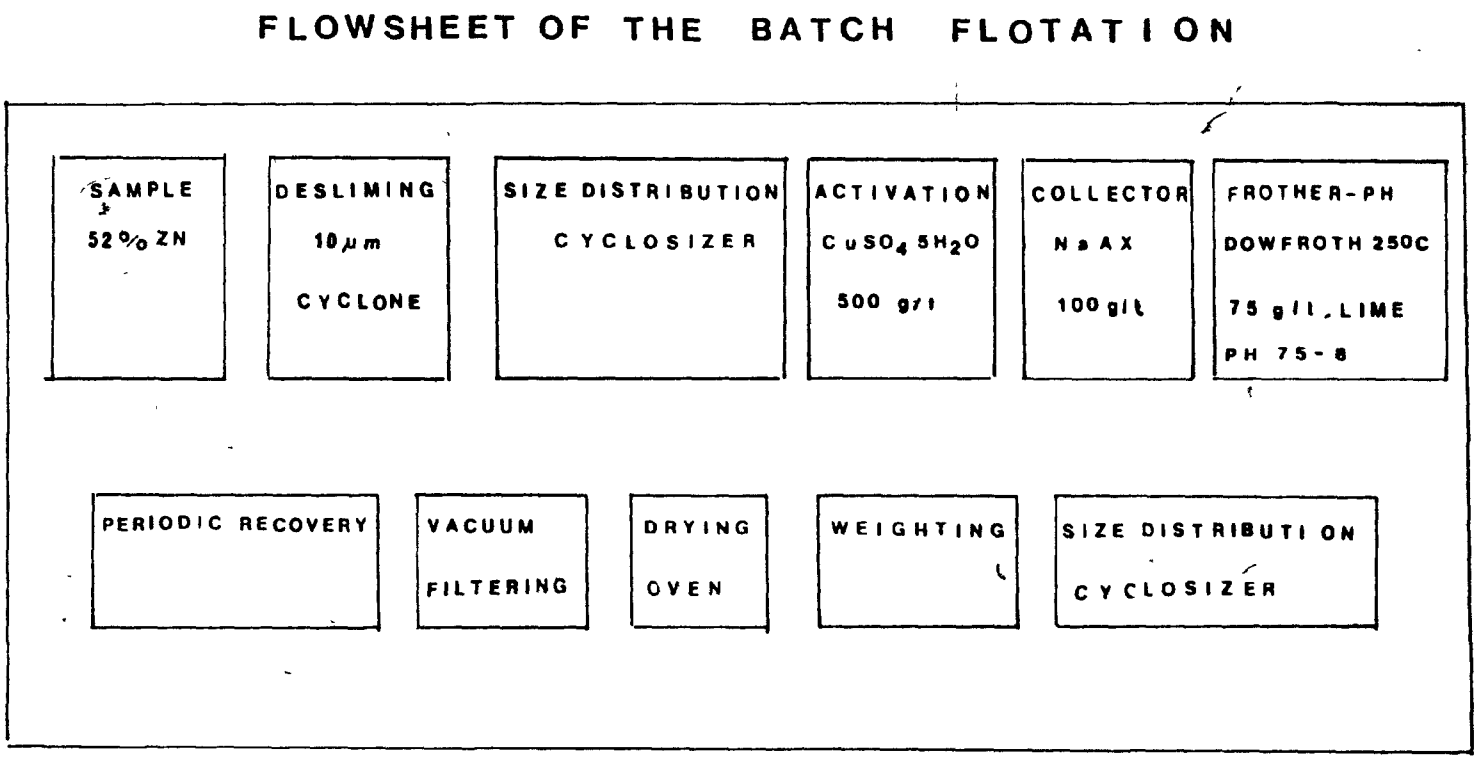

Fig. 4.4 Flow sheet of the experimental procedure of semi-batch flotation.

4.3.1 Calculation of the Flotation Rate Constant

The transfer of material from the slurry to the froth was assumed to follow first order kinetics with respect to the mass in the slurry phase, as suggested by many researchers (Jowett and Safvi, 1960; Imaizumi and Inoue, 1963; and Cooper, 1966). Then the FRC is the slope of the linear section of the plot of the natural logarithm of the mass of hydrophobic sphalerite remaining in the cell as a function of time.

Detailed calculation of the FRC in the semi batch flotation is provided in Appendix 4.1. In general, mass vs. time data were analyzed by computer and lines were obtained by least squares fit. They were plotted using the Energraphics computer program as mass in the cell versus time (on a semilogarithmic vertical scale). Curves are practically linear for most tests, confirming the assumption of first order kinetics. It should be noted that when most material is floated, the slope of the curves decreases slightly with increasing time, because slow floating fine material is preferentially left in the flotation cell.

For most experiments, the point corresponding to the first sample was not taken into account, because of the timing error, i.e. the start-up error associated with the exact time at which wash water and air are turned on, and when the water film begins to overflow the entire cell lip.

Flotation time varied between 3.5 and 4 minutes, yielding recoveries of 65 to 95 %. This indicates that not all

sphalerite particles were sufficiently hydrophobic. Therefore, the rate constant determining plot was based on solely the recovered sphalerite, as advocated by many authors (Jameson and coworkers, 1977; and Bushell, 1962). In this particular case, where the total recovery is not exactly known, the largest errors in the rate constant plot are found for high flotation times, as the mass of material remaining in the cell is very small. The last points of each plot are therefore more susceptible to large deviations from linearity. These were also discarded for the calculation of the FRC.

The spillage of the material while the pans were changed was negligible. Froth cohesiveness and adherence to the cell wall were minimised by addition of wash water and use of low frother dosage.

4.4 PRELIMINARY TESTING

Tabulated results of all preliminary flotation tests are provided in Appendix 5.1.

4.4.1 Determination of the Optimum Wash Water Flow Rate

A series of experiments using 200 g sphalerite samples at an AFR of 6.25 L/min were done to determine the best wash water flow rate (WWFR), within a range of 2.35 to 3.2 L/min. Experimental results are summarized in Table 4.2.

A plot of WWFR versus flotation rate constant, FRC, is

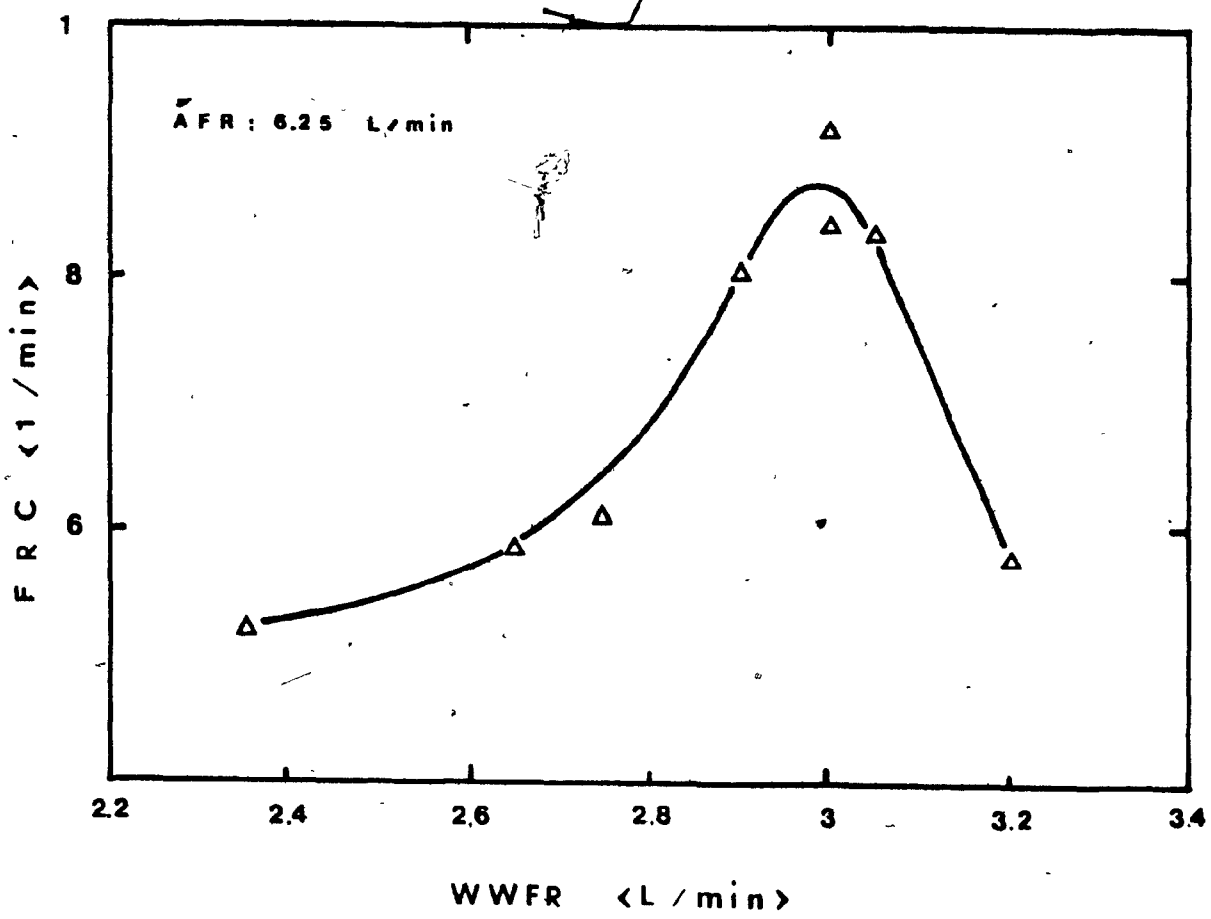

Fig. 4.5 Wash water flow rate versus flotation rate constant.

given in Fig. 4.5. It is apparent that the maximum FRC is obtained at the WWFR of 3 L/min., which was selected for all semi-batch flotation tests.

4.4.2 Collector selection

Both NaAX and sodium ethyl xanthate (NaEX) were tested at an AFR of 6.25 L/min. Results are shown in Table 4.3. and confirm that NaAX, which yielded higher FRCs, is a more powerful collector.

4.4.3 Chemical Conditioning

Two experiments were also conducted at an AFR of 5 L/min. and a WWFR of 3 L/min., to determine the effect of activator and surfactant concentration. Experimental conditions and results are given in Table 4.4. Flotation without activator yields a low FRC (FRC: 0.52 min.; test 34), and confirms the need for activator addition. Tests 29 and 32 show that flotation kinetics are affected by collector and activator dosages, but not exceedingly so, as dosage increases of 300% and 100%, respectively, produced an 20% increase in the FRC. Finally, test 6 clearly shows the need for frother addition.

TABLE 4-2

TEST NUMBER	WWFR (L/min)	FRC (1/min)
5	2.35	0.52
7	2.65	0.59
3	2.75	0.61
1	2.90	0.81
2	3.00	0.84
29	3.00	0.92
13	3.05	0.83
4	3.20	0.58

AFR: 6.25 L/min, SAMPLE: 200 g

TABLE 4-3

TEST NUMBER	WWFR (L/min)	COLLECTOR	FRC (1/min)
1	2.90	NaAX	0.81
20	2.90	NaEX	0.63
2	3.00	NaAX	0.84
29	3.00	NaAX	0.92
19	3.00	NaEX	0.70
13	3.05	NaAX	0.83
21	3.05	NaEX	0.69

AFR: 6.25 L/min , SAMPLE: 200 g

Table 4.2 Effect of WWFR on the flotation rate constant.

Table 4.3 Effect of collector type on flotation rate constant at different WWFRs.

4.4.4 Split conditioning

Evidence that adequate activation of coarse sphalerite by copper sulfate may not achieved during conditioning has been reported by Rey (1968). It was suggested that it is related to a copper sulfate deficiency caused by excessive adsorption onto ultrafines during conditioning. This might account in part for the apparent quantitative inefficiency of copper sulfate as an activator occasionally observed in practice.

On the basis of these observations, a test was conducted at an AFR of 5 L/min, WWFR of 3 L/min by using a split conditioned sample. The sample was divided into two fractions on a 38 μm stainless steel sieve. The coarse fraction was conditioned for 20 minutes with 65% of the total collector addition, at 70% solids. The fine fraction was conditioned with the remainder of the collector at 20% solids, for the same time. The two fractions were then combined and conditioned for a further 10 minutes before flotation.

Results are reported in Table 4.5. The use of split conditioning did not result in any significant change of the FRC, and will not be used in the present work. Similar results had been reported by Anthony et al. (1975) who concluded that fine particles did not appear to consume greatly disproportionate amounts of copper sulfate during conditioning.

TABLE 4-4

TEST NUMBER	NaAX (g/t)	CuSO 5H O (g/t)	FROTHER (g/t)	FRC (1/min)
34	100	0	75	0.52
29	100	500	75	0.92
32	400	1000	75	1.11
6	100	500	0	0.37

AFR: 6.25 L/min , SAMPLE: 200 g

TABLE 4-5

TEST NUMBER	NaAX (G/T)	CuSO 5H O (G/T)	FROTHER (g/t)	CONDITIONING	FRC (1/min)
33	100	500	75	SPLIT	0.78
31	100	500	75	NORMAL	0.80
24	100	500	75	NORMAL	0.81

AFR:5 L/min WWFR: 3 L/min SAMPLE: 500 g

TABLE 4.4 Influence of chemical conditioning on flotation rate constant.

TABLE 4.5 Influence of conditioning type on flotation rate constant.

4.5 SUMMARY

In this chapter, an overall view of sample and reagent selection strategies was presented. General aspects of the semi-batch experimental procedure were then introduced. Lastly, preliminary test results were discussed.

Preliminary semi-batch flotation tests confirmed the need for activator and frother addition. Copper sulfate, 500 g/t, NaAX, 100 g/t, Dowfroth 250C, 75 g/t, and lime were selected as activator, collector, frother, and pH regulator, respectively. The dosages and conditioning times were chosen from typical industrial applications.

The results of preliminary tests been conducted to determine the best operating conditions showed that a wash water addition flow rate of 3 L/min was optimal. In addition, split conditioning and increased reagent dosages did not increase the FRC significantly.

CHAPTER 5

THE AIR-WATER-SPHALERITE SYSTEM

5.1 INTRODUCTION

In chapter 3, the effect of AFR on bubble populations was characterized. In the present chapter, the effect of AFR and initial pulp density on the FRC of sphalerite in semi-batch flotation will be investigated. The effect of particle size on flotation kinetics in semi-batch flotation will be discussed.

The approach used was to remove the froth phase as soon as formed, so that the recovery rate limiting step is mineral flotation in the slurry phase, that is, particle-bubble collision and attachment.

5.2 EXPERIMENTAL PROCEDURE

The experimental procedure is similar to that described in chapter 4. Two different sets of experiments without froth phase were completed using 500, 7 % solids, and 1000 g, 14 % solids samples at 1100 rpm.

The particle size distribution of the products of some of the tests was measured to characterize size-by-size kinetics. The Sedigraph 5000D did not yield reproducible particle size analyses for some strongly

hydrophobic samples, possibly because of dispersion problems. The Warman cyclosizer gave good reproducibility, and was used for all sphalerite size analyses. As some samples did not disperse well in water, methanol was used to wet the cyclosizer feed.

5.3 RESULTS AND DISCUSSION

The results of each experiment are given in detail in Appendix 5.1. Typical results are shown in Fig. 5.1, where the logarithm of mass of hydrophobic material remaining in the cell is plotted as a function of time.

Semi-batch flotation test results are tabulated in Appendices 5.2 and 5.3 for 7% and 14% solids feeds, respectively. The correlation between AFR and FRC is given in Figs. 5.2 and 5.3. The FRC increases as AFR increases to reach a maximum at an intermediate AFR, after which further increases in AFR affect flotation kinetics adversely. Maximum FRCs were obtained at an AFR of 5.46 L/min for 7% solids and 6.33 L/min for 14% solids.

5.3.1 Calculation of the Size-By-Size FRC

Some of the concentrate products were cyclosized in order to investigate size-by-size flotation kinetics. When individual concentrate products were too small to insure good size analysis, successive samples were

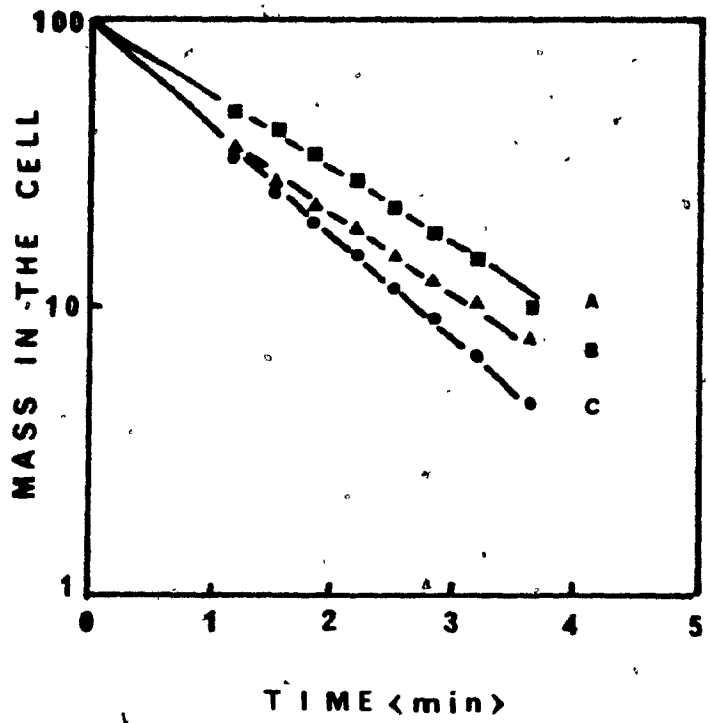

Fig. 5.1 Mass of sphalerite in the cell as a function of time.

(a, AFR: 3.75, b; AFR. 6.25, c, AFR: 5 L/min).

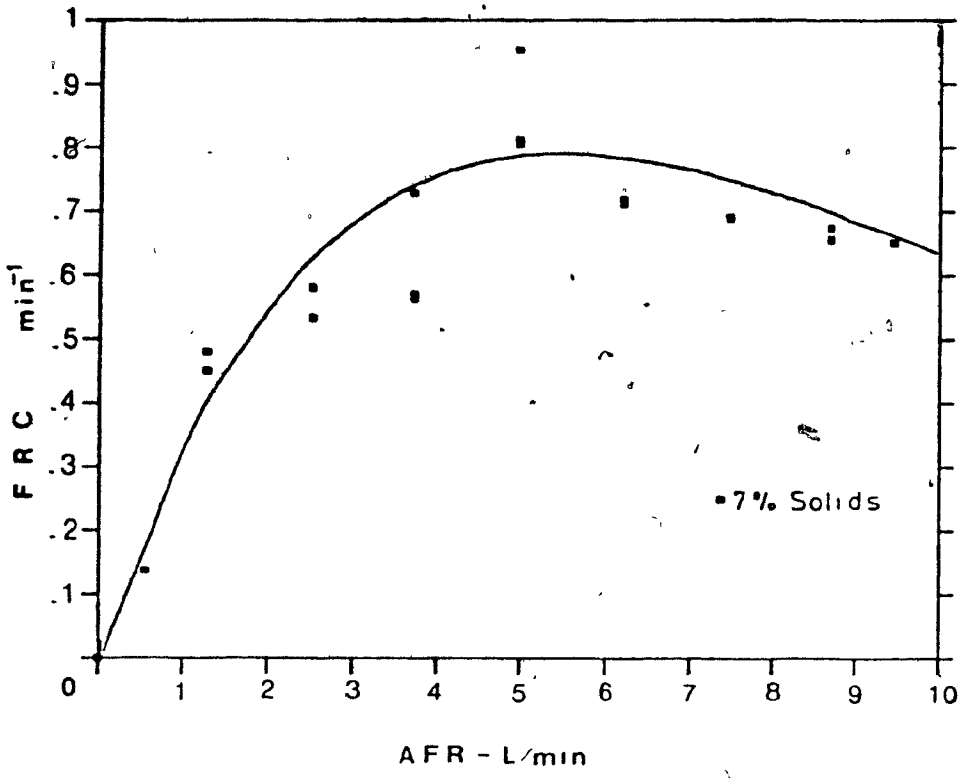

Fig. 5.2 Flotation rate constant as a function of air flow rate.

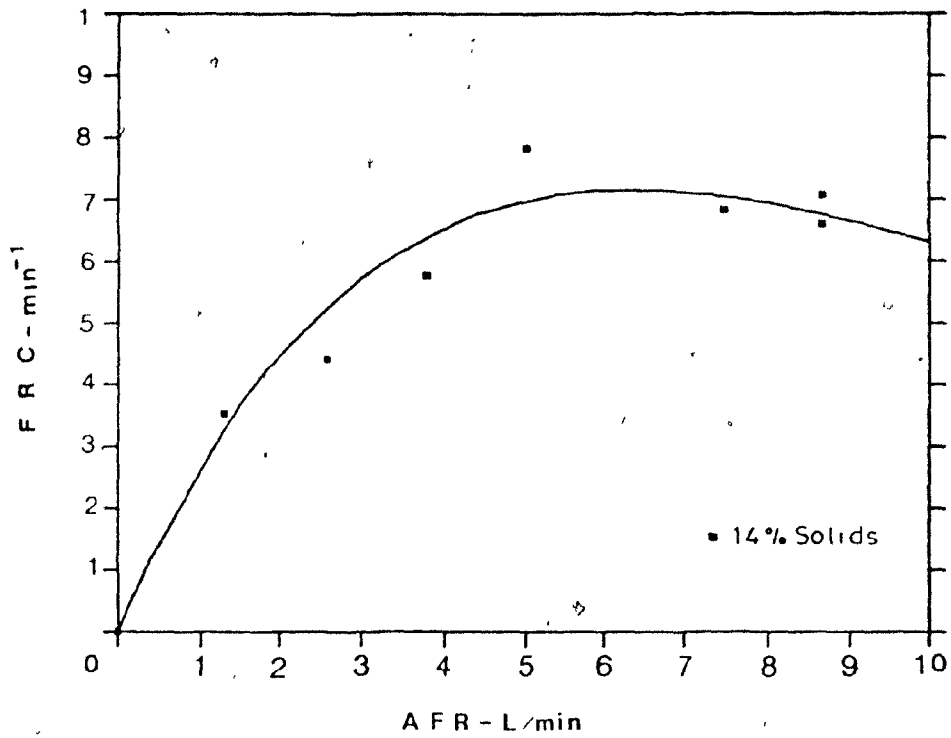

Fig..5.3 Flotation rate constant as a function of air flow rate.

combined to get enough material, 40 g, for cyclosizing.

Classification curves of tests 31 and 33, shown in Figs. 5.4 and 5.5, indicate that the particle size distribution of floated products becomes finer as time progresses. The FRC of each size classes was calculated, using the size analysis of each product and cumulative weight recoveries, to plot the natural logarithm of percentage weight of each size classes remaining in the flotation cell, as a function of time. The data were plotted on a semi-logarithmic paper and the slope of linear part of each curve was obtained by linear regression. All results are included in Appendices 5.4 and 5.5. Figs. 5.6 and 5.7 show typical results at an AFR of 5 L/min. The FRC increases with increasing particle size up to the 23-30 μm size class. After reaching a maximum, the FRC drops slightly. This finding agrees with those previously reported (King, 1976; Trahar, 1976). The high FRC of ~8 μm size fraction, which is less than 10% of the floated products, could be explained by hydraulic entrainment into froth phase, compounded by rapid froth removal.

Particle size plays an important role in each of the collection subprocesses. Anfruns and Kitchener (1976) and Weber (1981) showed that collision efficiency, Ec, increases with increasing particle size. Dobby (1984) proposed that attachment efficiency decreases with increasing particle size. He showed that fine particles

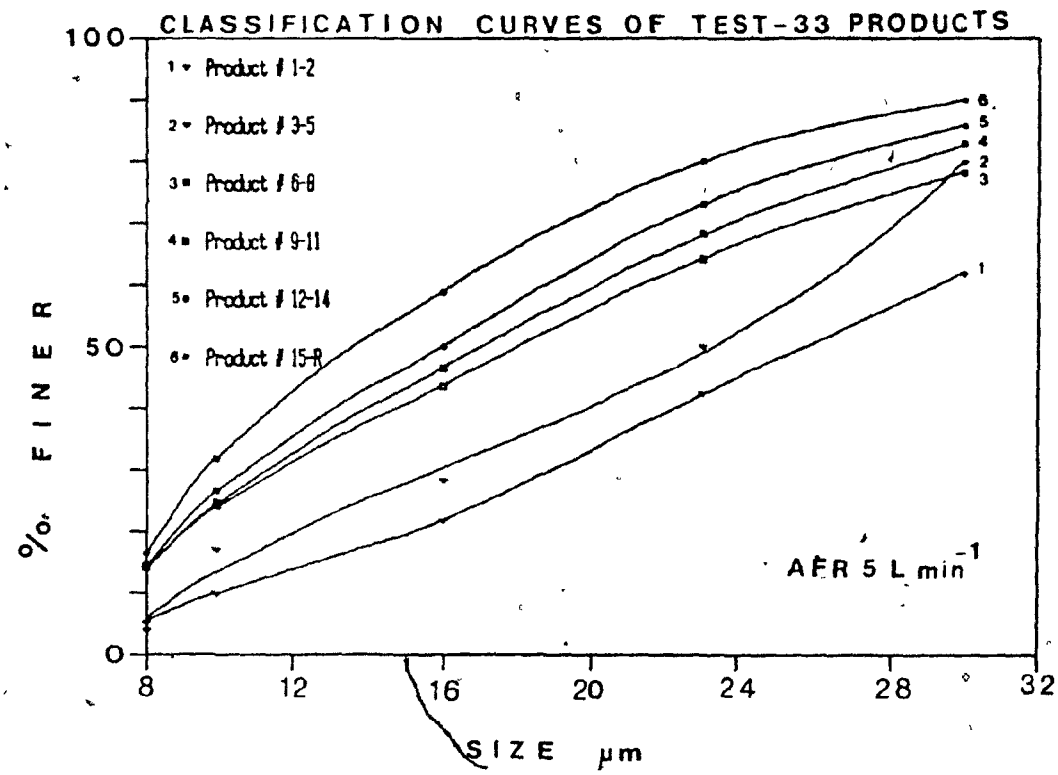

Fig. 5.4 Classification curves of flotation products (split conditioned sample).

Product #	Flotation time (min)
1 - 2	0 - 0.3
3 - 5	0.3 - 0.8
6 - 8	0.8 - 1.5
9 - 11	1.5 - 2.5
12 - 14	2.5 - 3.6
15 - Rem.	3.6 - 4.2

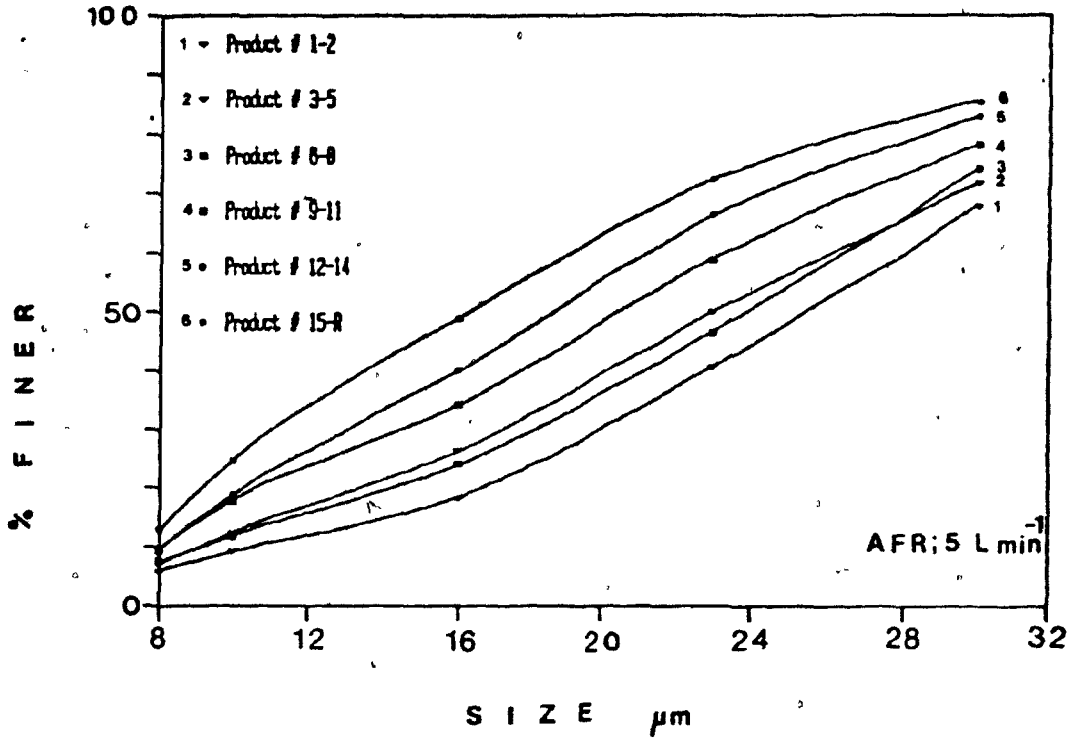

Fig. 5.5 Classification curves of flotation products.

Product #	Flotation time (min)
1 - 2	0 - 0.3
3 - 5	0.3 - 0.8
6 - 8	0.8 - 1.5
9 - 11	1.5 - 2.5
12 - 14	2.5 - 3.6
15 - Rem.	3.6 - 4.2

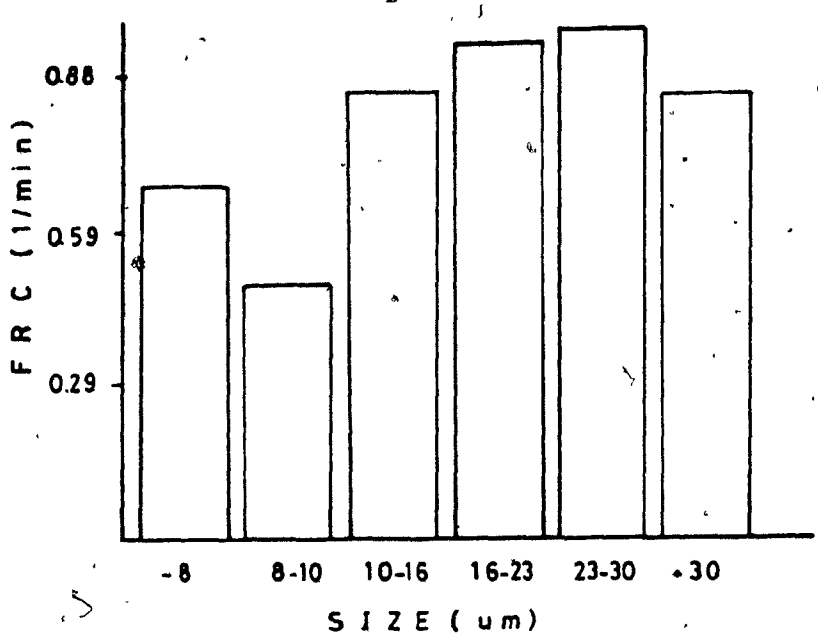

Fig. 5.6 Flotation rate constant versus particle size (Test 31, AFR: 5 L/min).

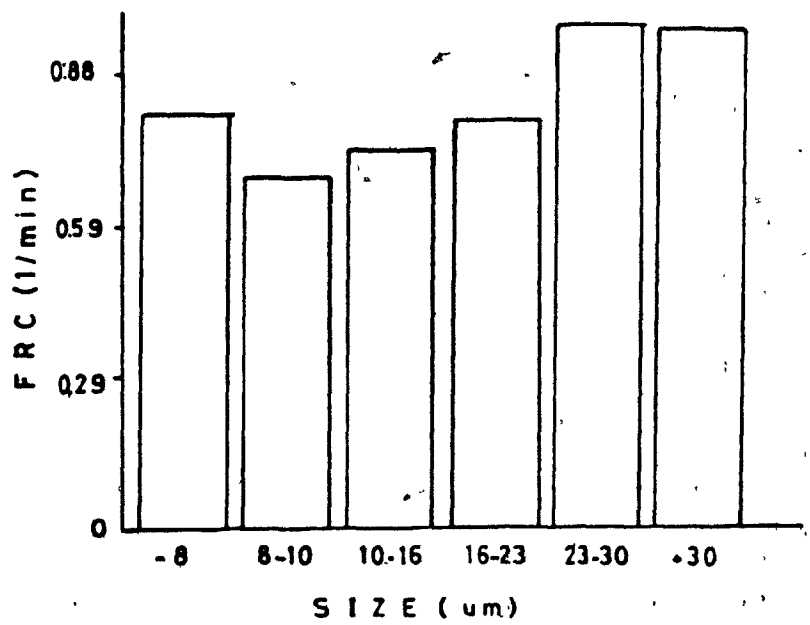

Fig. 5.7 Flotation rate constant versus particle size (Test 33, AFR. 5 L/min).

would remain in contact with bubbles for much longer time periods than coarse particles, and that induction times decrease with increasing particle size. Therefore, the net effect is an increasing attachment efficiency with decreasing particle size. King (1972) and Bascur and Herbst (1982) pointed out that the probability of detachment in the slurry phase increases as particle size increases.

Accordingly, the reason for the peak is the opposing effect of particle size upon collision and attachment efficiencies; as dp increases Ec increases and Ea decreases. Probability of detachment also increasses with particle size.

5.3.2 Effect of Initial Pulp Density on Semi-Batch Flotation Kinetics

Hydrophobic particle concentration is highest at the beginning of the batch test, which might lead to hindered flotation. This generally occurs when air bubbles are so saturated with hydrophobic particles that flotation kinetics no longer follow first order kinetics. Hindered or inhibited flotation is more common for lower AFRs, because the total bubble surface is smaller and more readily saturated with floated particles.

Rate plots at different initial pulp densities yielded lines that are parallel within experimental errors, in the range of free flotation (Fig. 5.8). Curve 1

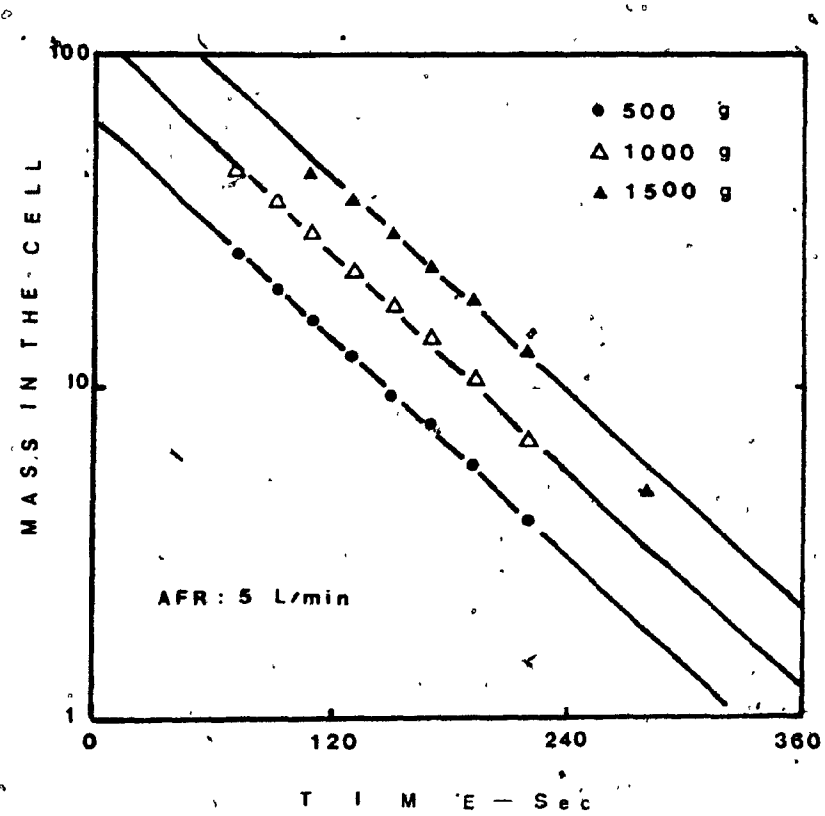

Fig. 5.8 Effect of initial pulp density on semi-batch flotation.

500 g	7 % solids	Test-31
1000 g	14 % solids	Test-35
1500 g	21 % solids	Test-43

clearly shows that the highest initial concentration, hindered flotation takes place for approximately 120 s. At constant AFR, the total hindered flotation time will increase with increasing initial concentration. The proper FRC can be extracted from each curve using the section corresponding to free flotation. This FRC shows no or little dependence on initial pulp density. When the vertical logarithmic plot does not identify readily the transition from the hindered to free flotation, the same relationship should be plotted on a vertical linear scale (Fig. 5.9). A linear relationship at the beginning of the test will then clearly identify the extent of hindered flotation i.e. zero order removal of material. This parallelism indicates that the transfer of material from the slurry to the froth follows first order kinetics (Imaizumi and Inoue, 1962).

The specific bubble load in g/cm was calculated by dividing the zero order production rate of concentrate measured under hindered flotation (in g/min) by the total bubble surface production rate (in cm^2/min). All solids were assumed recovered by bubble attachment, and bubbles were assumed fully loaded. Fig. 5.10 shows that the specific bubble load decreases with increasing AFR. It is believed that the smaller bubbles produced at lower AFR have a lower rise velocity because of their size and much reduced buoyancy when fully loaded. Thus, attached particles are not shed as easily, by the vortices behind

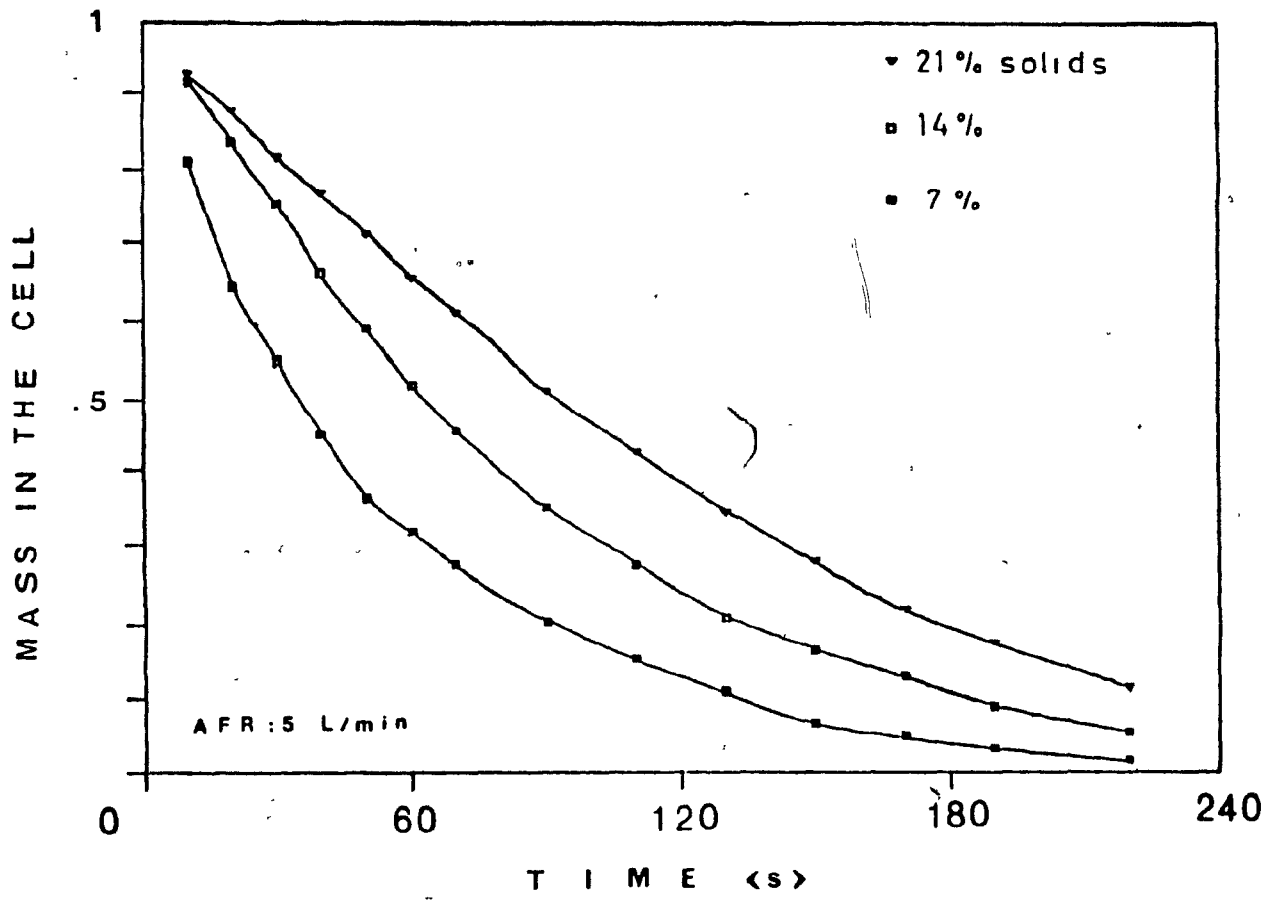

Fig. 5.9 Inhibited and free flotation components of sphalerite

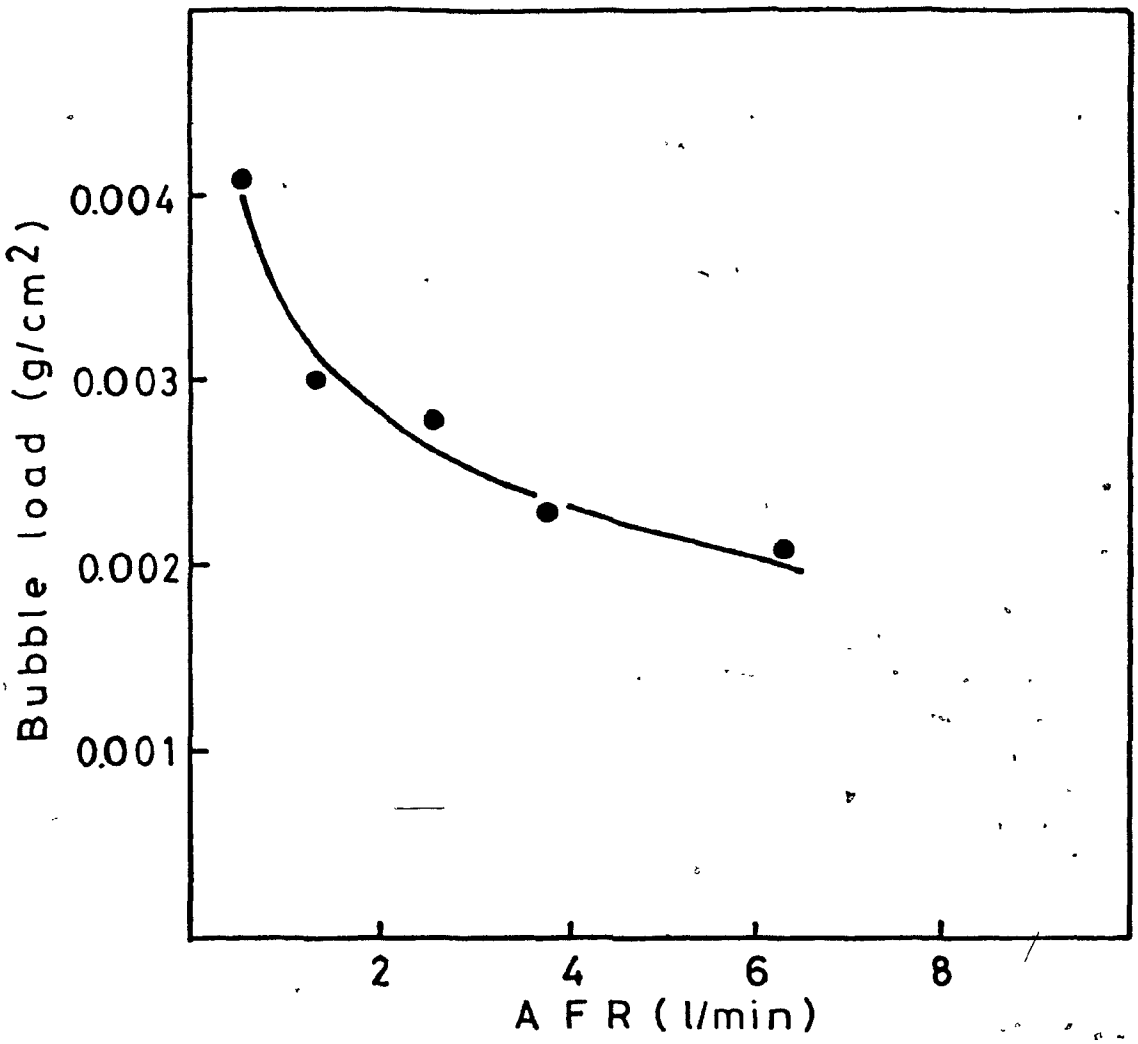

Fig. 5.10 Bubble load versus air flow rate.

rising bubbles or the shearing action of the fluid along their surface. Additionally, if the maximum bubble specific load is determined by a dynamic equlibrium between the capture and detachment rates the increased collision efficiency of smaller bubbles should favour the capture rate and further increase the specific bubble load. The higher collision efficiency of the smaller bubbles produced at low AFR and their increased retention time in the slurry may explain why hindered flotation takes place at low AFRs. The smaller bubbles produced at lower AFR also have an increased load capacity per unit surface (Fig. 5.10), presumably because of their lower rise velocity.

5.3.3 Representation of FRC as a Function of AFR

Experimental data given in Appendix 5.1 were fitted by the eq: (Laplante, 1980)

$$FRC = C_2 * Q * \exp(C_1 * Q) \qquad 5.1$$

C_1 and C_2 are constants determined by regression on a linearized form of Eq. 5.1:

$$Ln\,(FRC/Q) = Ln(C_2) + C_1 * Q \qquad 5.2$$

For 7% solids, the relationship between AFR and FRC is given by;

$$FRC = 0.3229 * Q * \exp(-0.183 + 0.017 * Q) \quad 5.3$$

A similar relation is also obtained for 14% solids:

$$FRC = 0.3069 * Q * \exp(-0.158 + 0.012 * Q) \quad 5.4$$

The first term indicates that more air means more bubble and more bubble surface and therefore, an increased FRC. The second term accounts for the fact that increased AFR implies larger i.e. less efficient bubbles and hence air is not as efficiently used per unit volume. Laplante (1983b) suggested a model to estimate the AFR at which FRC is maximum based on the work of Anfruns and Kitchener (1976), as analyzed by Jameson et al. (1977):

$$K = \beta \; Q/d_b^{2.69} \quad 5.5$$

where K: FRC (1/min)

Q: AFR (L/min)

db: average bubble diameter (mm)

β : 1.5 (Ek/A)

Ek: collection efficiency

A: cell surface area (cm^2)

In the air-water system of the present study, db

was characterized as a function of AFR.

$$Ln(d_b) = \theta(0.067 \mp 0.003) + 0.897 \qquad 3.5$$

where db is millimeters and Q is litres per minute. Substituting in eq. 3.5,

$$FRC = Q * \exp((0.1802 \mp 0.0054) * Q) \qquad 5.6$$

This last equation is similar to the more general expression used in eq. 5.1.

By differentiating eq.5.1, it can be shown that maximum FRC occurs at an AFR given by:

$$Q = 1/C_1 \qquad 5.7$$

Experimentally observed values of Qm from eq. 5.3 and 5.4 are in good agreement with predicted values from eq. 5.6 (Table 5.1).

% SOLIDS	Observed Qm	Predicted Qm
7	5.46∓0.5	5.63∓0.5
14	6.33∓0.6	5.63∓0.5

Table 5.1 Experimental and predicted AFR yielding maximum FRC.

This suggests that the relationship between AFR and average bubble size can be used to predict the AFR at which FRC is maximum.

5.3.4 Comparison With Other Flotation System

It is convenient to use the dimensionless air flow number, AFN, or more accurately the modified air flow number, MAFN, to compare flotation machines of different sizes (Harris, 1974). The dimensionless AFN, and MAFN are given by:

$$AFN = Q * (N * D^3) \qquad 5.8$$

where Q: AFR (cm /min)

N: impeller speed (rpm)

D: impeller diameter (cm)

$$MAFN = AFN * (D^2 / A) \qquad 5.9$$

where A: cell cross-section (cm^2)

As expected, the AFN and MAFN of the present work are similar to those suggested for Denver flotation cells of similar design (Table 5.2). This indicates that the range of AFRs under investigation in the present study is comparable to those used in other types and sizes of flotation cells.

	AIR FLOW NUMBER	MODIFIED AIR FLOW NUMBER
DENVER (STANDARD)	$1\text{-}2*10^{-2}$	$2.5\text{-}5 * 10^{-3}$
FAGERGEN (I-I)	$4\text{-}7*10^{-2}$	$2.0\text{-}5.6 * 10^{-3}$
LAPLANTE'S CELL		
all scale	$0\text{-}3.4*10^{-2}$	$0\text{-}7.3 * 10^{-3}$
optimum range	$1\text{-}2*10^{-2}$	$2.2\text{-}4.4 * 10^{-3}$
THIS WORK		
all scale	$0.3\text{-}2*10^{-2}$	$0.6\text{-}4.1 * 10^{-3}$
optimum range	$1.0\text{-}1.7*10^{-2}$	$2\text{-}3.5 * 10^{-3}$

TABLE 5.2 Dimensionless air flow number and modified air flow number of different cells.

5.4 SUMMARY

In this chapter, a technique which allows for quick froth removal was used to investigate the effects of AFR on flotation kinetics of flotation in the slurry phase.

For sphalerite, the FRC was found to increase to maximum at an intermediate AFR, and then to decrease as the AFR was further increased. As AFR increases total bubble surface increases, and the average bubble diameter decreases; the first effect favours an increased FRC, whereas the second has the opposite effect. A maximum FRC is obtained at an intermediate AFR, when these two effects are equal in magnitude.

A size-by-size analysis of flotation kinetics confirms previous results of an intermediate particle size at which maximum flotability is observed, in this system 23-30 μm. The unusual high FRC of the slimes, -8 μm, is attributed to hydraulic entrainment.

The effect of initial pulp density on the kinetics of transfer from the slurry to the froth is small, provided that the bubble surface is not saturated with captured particles. At low AFR or high particle concentration, zero order kinetics are observed as the rate limiting step is the limited capacity of the bubbles to carry captured particles into the froth.

CHAPTER 6

THE CONTINUOUS FLOTATION OF SPHALERITE

6.1 INTRODUCTION

In the preceeding chapter, the effect of AFR on the kinetics of semi-batch flotation was investigated, in a system for which froth removal was performed as quickly as possible, quite unlike industrial practice. This procedure was followed in order to measure bubble-particle collision and attachment rates in the slurry phase i.e. the effect of AFR on the transfer from the slurry to the froth.

The results of these experiments have to be interpreted in the light of the fact that they were obtained in a small-scale batch system. Industrial flotation, using larger scale continuous cells and complex unliberated ores, can present dissimilar mineral behavior in the slurry and froth phases.

In this chapter, the small scale continuous flotation of a zinc ore will be investigated, under controlled FTs varied at three different AFRs, in order to bridge at least partially the gap between batch work and large scale continuous flotation as used in industrial flotation plants.

6.2 DESCRIPTION OF THE EXPERIMENTAL SYSTEM

One of the design criteria of the cell used was to operate either batch or continuous. The same cell was used after two major modifications were introduced. Firstly, the feed was pumped in and the tailing was pumped out by Masterflex peristaltic pumps. As mentioned earlier, the presence of buffer zone provides a quiescent slurry-froth interface. This action was enhanced by using eight specially designed interconnected pyramidal baffles made of plexiglass, mounted into the cell, close to the active and buffer zone interface, to minimize turbulent circulation of the cell content and limit hydraulic entrainment to the concentrate.

The overall view of the experimental set up can be seen in Fig. 6.1. It consists of a modified Denver flotation machine, a plexiglass cell, two variable speed pumps, a 60 litre feed tank with stirrer, a continuous frother addition pump and an electronic liquid level controller. Slurry conditioned in the feed tank was pumped into the cell, while the concentrate was collected over the cell lip and tails were discharged from the bottom by another pump.

Fig. 6.2 provides a detailed flowsheet of the various operations. Deslimed zinc concentrate was conditioned prior to the flotation tests using copper sulfate and NaAX at 10% solids by weight. Natural pH was

COLOURED PICTURES
Images en couleur

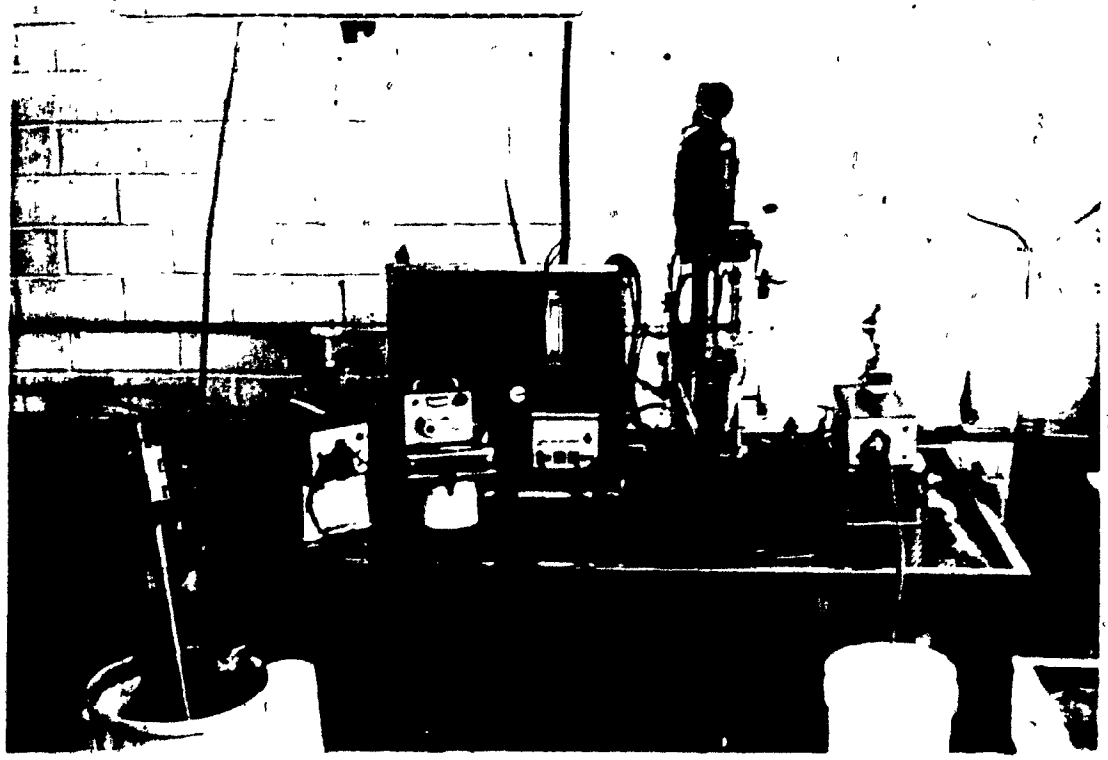

Fig..6.1 The overall view of experimental set up.

CONTINUOUS FLOTATION FLOWSHEET

DESLIMING	CONDITIONING	FLOTATION
52 % Zn 10 - 74 µm	Activator : $CuSO_4$ (500 g/t) Collector : NaAX (100 g/t) Frother : Dowfroth(75 g/t) pH : 7.5-8 (Lime) RPM : 1500 , Solid: 10 %	Samples: Feed Tails Conc.

PRODUCT EVALUATION	SIZE DISTRIBUTION
Weighing Filtering Drying Weighing	Cyclosizer Sedigraph

Fig. 6.2 Continuous Flotation Flowsheet.

maintained, while the frother was continuously added to the feed stream.

The feed, concentrate and tailing streams were all easily accessible for sampling. Flotation products were weighed, filtered, dried, and weighed again. For some tests, the particle size distribution of the tail and concentrate streams were determined by using the cyclosizer.

6.3 KINETICS

The transfer of hydrophobic particles from the slurry to the froth was investigated in a system having no froth phase.

The following assumptions were made to calculate the FRC;

a) the transfer of material from the slurry to the froth follows first order kinetics (previously confirmed in semi-batch tests) and

b) there is no drop-back from the froth to the slurry i.e all sphalerite transferred to the froth phase will also be transferred over the cell lip. Any such drop-back, if present, should be minimal since all sphalerite particles in the slurry were hydrophobic and the froth-slurry interface was very quiescent.

c) all the sphalerite are hydrophobic.

FRC can be calculated by using the following well-known equation assuming perfectly mixed slurry phase (Loveday-Marchant, 1970):

$$R = K * \tau / K * \tau + 1 \qquad 6.1$$

where R: fractional recovery

K: FRC, 1/min

τ: average solids residence time, min.

and

τ = Mass in the slurry/mass in the tails streams

The results of each experiment are given in detail in Appendix 6.1.

6.4 THE EFFECT OF FROTH THICKNESS ON KINETICS

The transfer of material from the froth over the cell lip and drop-back of material from the froth to the slurry can be characterized in a system having a froth phase.

The following assumptions were made (Laplante, 1980):

a) the froth phase is homogeneous; this can be acceptable for very thin froths.

b) the transfer of material from the froth over the cell lip follows first order kinetics with respect to the

mass of material in the froth phase (FTC).

c) the transfer of material from the froth back to the slurry follows first order kinetics with respect to the mass of material in the froth (DBC)

d) the transfer of mineral from the slurry to the froth follows first order kinetics with respect to the mass of mineral in the slurry.

Both transfer rates from the froth back to the slurry and to the concentrate stream have been modelled as first order reaction rates, in which case the recovery ,R, becomes:

$$R \quad \frac{\alpha * K * \tau}{1 + \alpha * K * \tau} \qquad 6.2$$

$$\alpha = \frac{K_1}{K_1 + K_2} \qquad 6.3$$

where K : FTC (1/min)

K_1: DBC (1/min)

K_2: ORC (1/min)

Derivation of equations 6.1, 6.2 and 6.3 and calculation procedures are given in Appendix 6.2. The FRC has already been calculated (section 6.3). Therefore, it is possible to calculate FTC from the concentrate rate and

froth mass. Then, the DBC can be calculated from α and the FTC, using Eq. 6.3.

6.5 EXPERIMENTAL PROCEDURE

To determine the FRC, the cell was operated continuously at 1500 rpm. Wash water supplied from a head tank was added continuously to the cell, 1.2 L/min, to remove the froth phase. The slurry level was always kept at the cell lip, as the sum of feed (1.5 L/min) and wash water flow rate were greater than the tail flow rate (1350 L/min). Two Masterflex pumps yielded constant feed and tail flow rates.

After conditioning with copper sulfate and collector in the feed tank, the system was turned on. Samples from the feed were taken. The system was then allowed to reach steady-state. Four timed samples of the concentrate and five of the tails were collected at steady state. The AFR was then changed for another sampling cycle similar to the first. AFR was varied from 1.3 to 8.7 L/min in random order. After the last sampling cycle, feed, tailings, air and water valves were turned off simultaneously. The material in the cell was discharged and weighed to determine the solids residence time. All samples were weighed, filtered, dried, weighed again and cyclosized.

A different experimental technique was used to

determine FTC and DBC at a non-zero FT. AFR was varied from 1.3 to 7.5 L/min and FT varied from 1 to 5 cm. Froth thickness, which is generally defined as the vertical distance between slurry level and flotation cell lip, was varied by changing tails flowrate while keeping the feed flow rate constant at low FTs. For higher FTs ,i.e. 5 cm, the electronic liquid level controller was used in conjunction with tails flow rate to keep slurry level constant.

After taking timed samples from feed, concentrate, and tailings streams at steady-state, feed and tails pumps and air flow were turned off simultaneously. Then the slurry-froth interface was immediately raised to the cell lip level to recover all particles trapped in the froth by adding wash water under the froth phase. The froth content was collected in a separate container.

6.6 RESULTS AND DISCUSSION

The relationship between AFR and recovery in absence of froth phase is given in Fig. 6.3. Recovery increases with increasing AFR. After reaching a maximum, it drops slightly. As can be seen from Fig. 6.4, the maximum FRC calculated using Eq. 6.1 was obtained again at an intermediate AFR. Similar results were obtained in semi-batch flotation. The peak was only shifted towards a

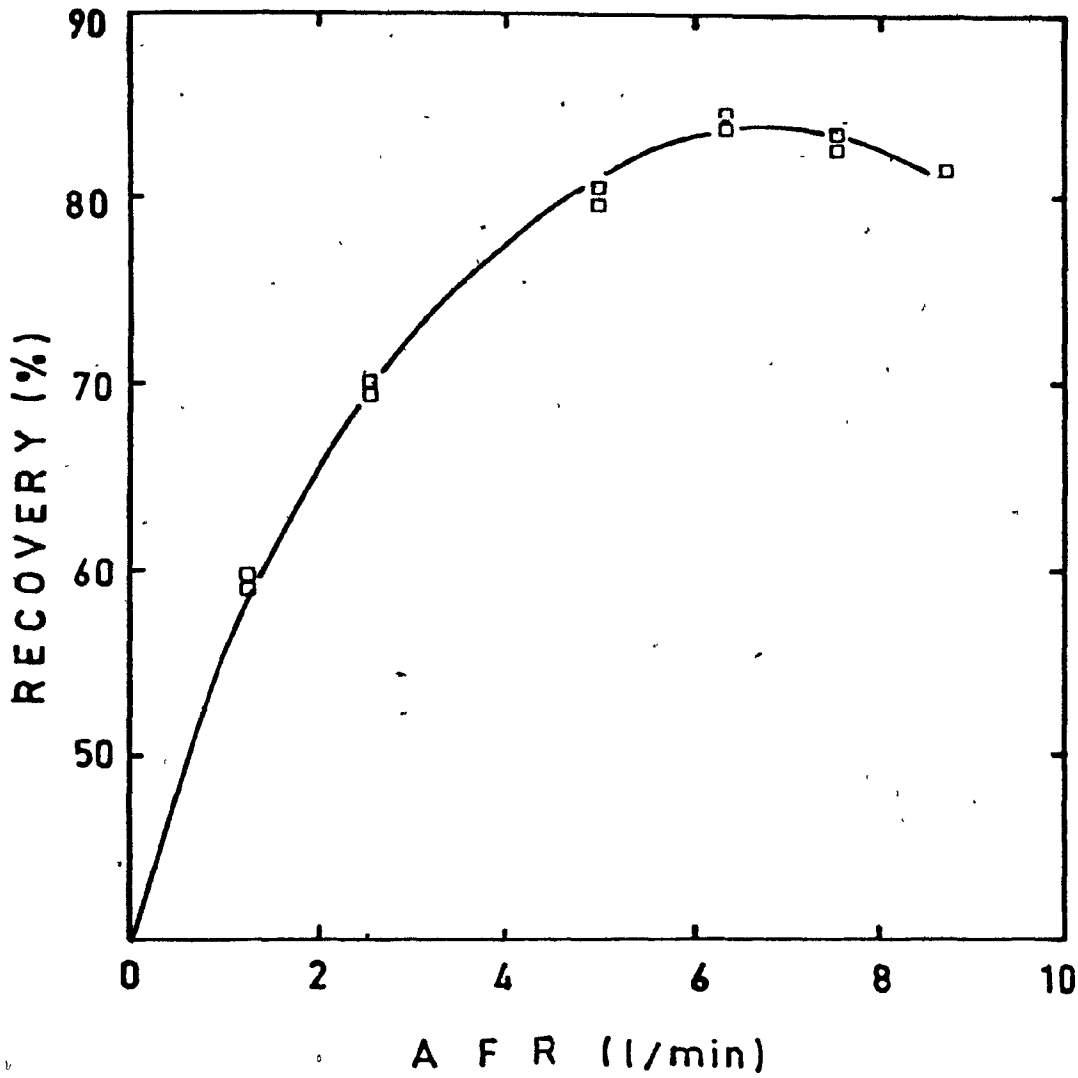

Fig. 6.3 Effect of AFR on recovery without froth phase.

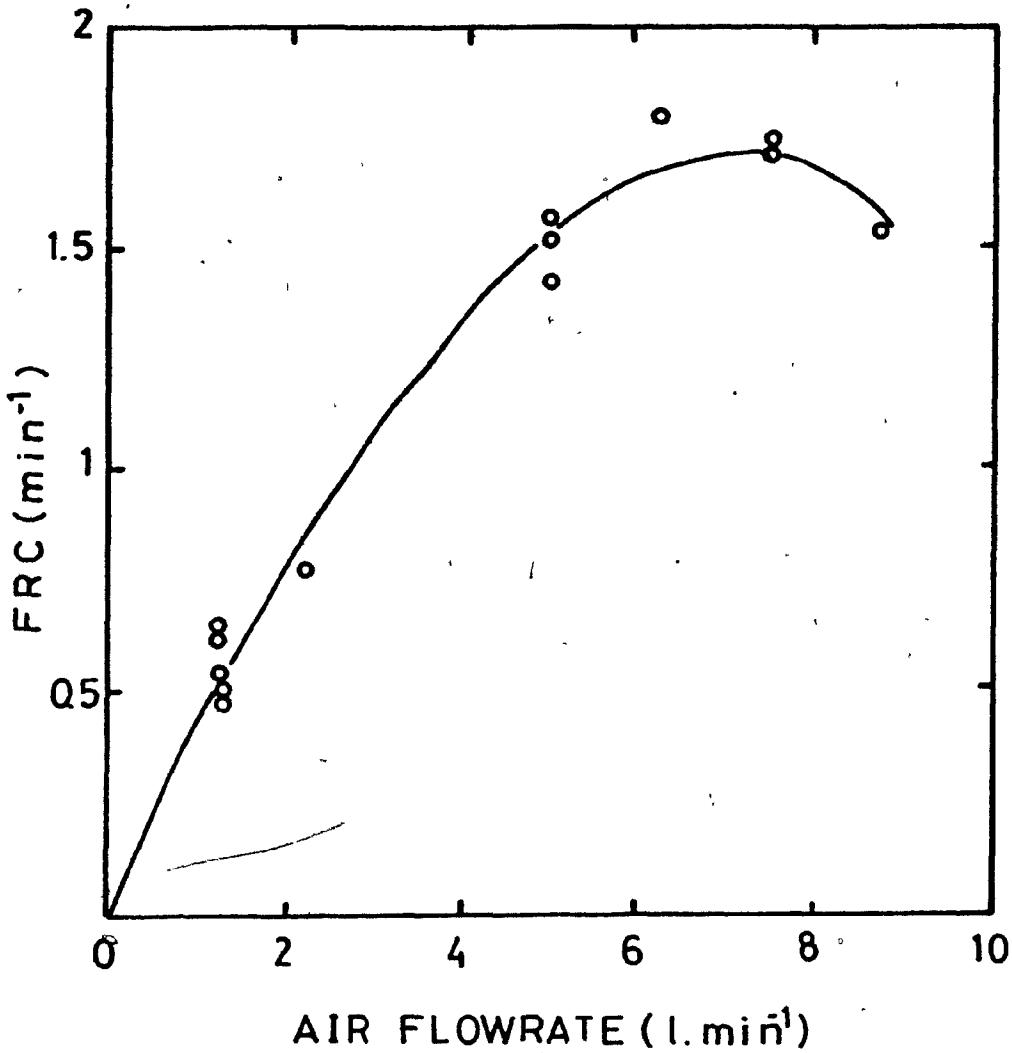

Fig. 6.4 Effect of AFR on FRC.

higher AFR, probably due to the slightly increased impeller speed.

A plot of AFR against recovery at different FTs is shown in Fig. 6.5. As either AFR increases or FT decreases, overall recovery increases. The relationship between AFR and mass in the froth phase again at different FTs is given in Fig. 6.6. The mass in the froth decreases with increasing AFR. This decrease is more significant at higher FTs.

The results of each experiment are given in detail in Appendix 6.3. The effect of FT on the FTC at four different AFRs is shown in Fig. 6.7. As FT increases, the FTC significantly decreases due to an increase in the particle residence time in the froth phase.

A plot of AFR versus FTC is given in Fig. 6.8 at different FTs. There is an increase in FTC with increasing AFR from 1.3 to 5 L/min. Above 5 L/min, the FTC increases with AFR at a FT of 5 cm, and decreases at lower FTs. Generally speaking, the FTC increases as the AFR increases i.e froth removal into the concentrate stream becomes more effective as AFR increases.

The relationship between FT and DBC is summarized in Fig. 6.9. Results indicate that DBC slightly increases with increasing FT. Fig. 6.10 shows the correlation between AFR and DBC at different FTs. At low AFRs, DBC increases significantly with increasing AFR; then a

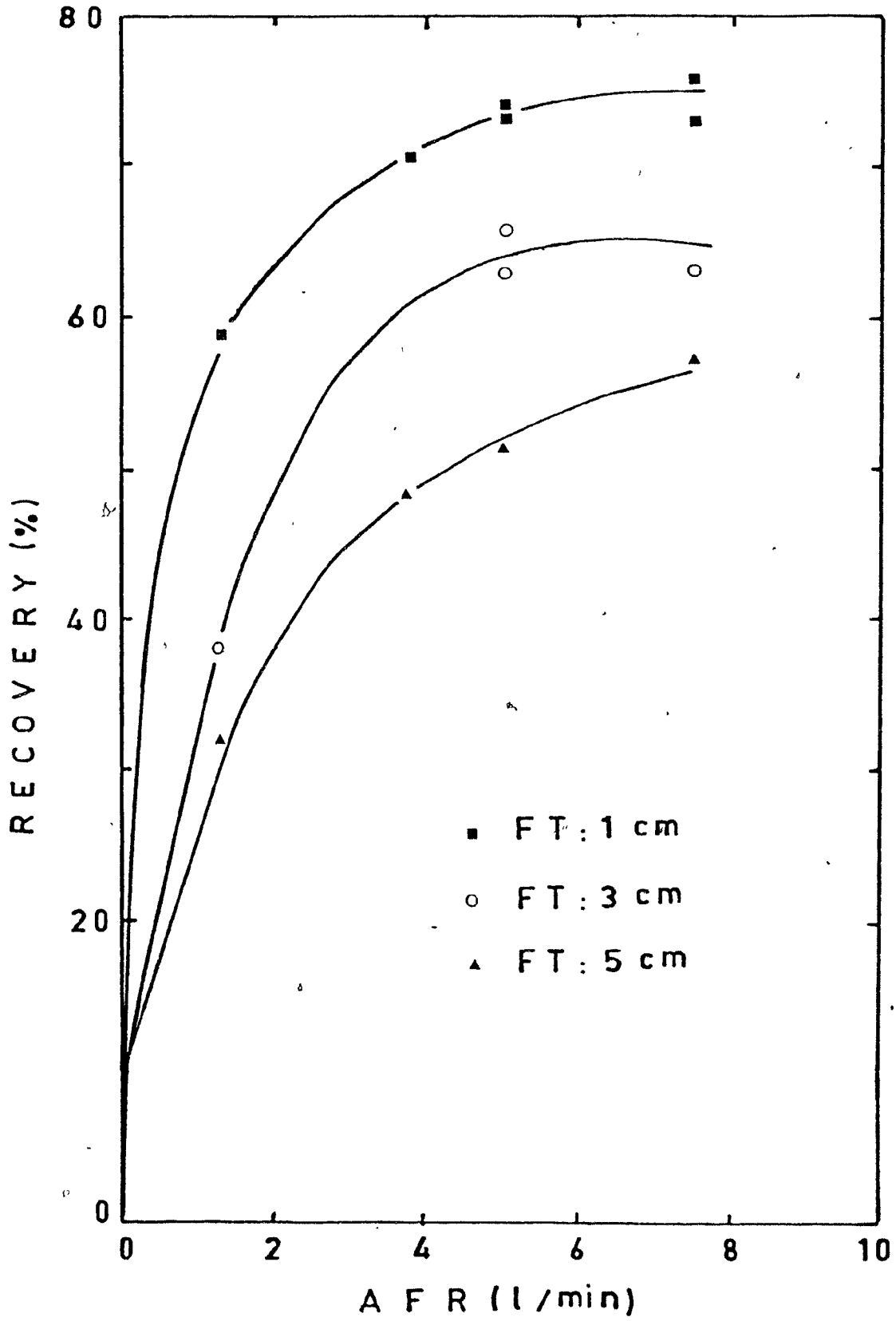

Fig. 6.5 Effect of AFR and FT on overall recovery.

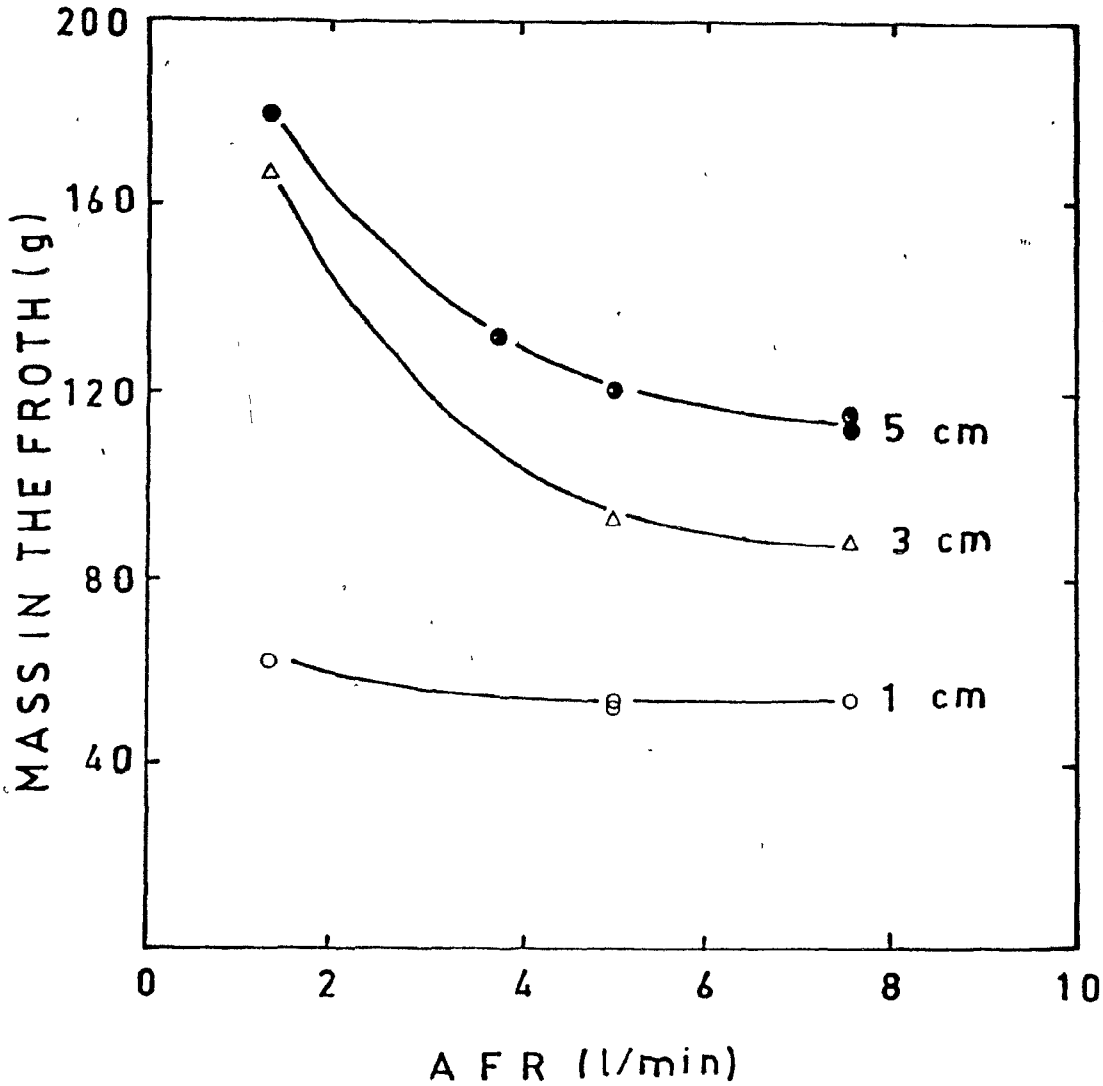

Fig. 6.6 AFR versus mass in the froth.

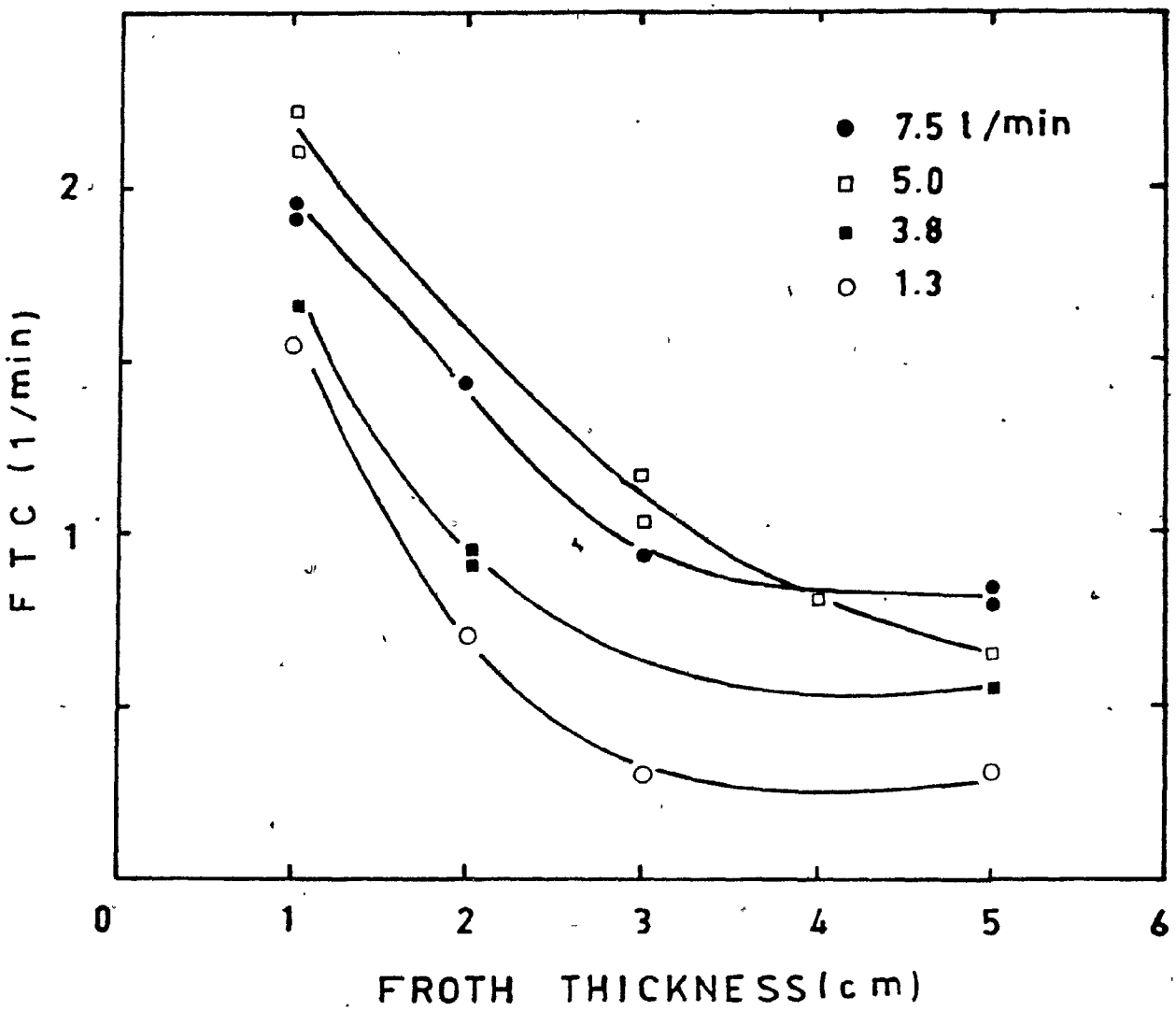

Fig. 6.7 Froth thickness versus froth transfer constant.

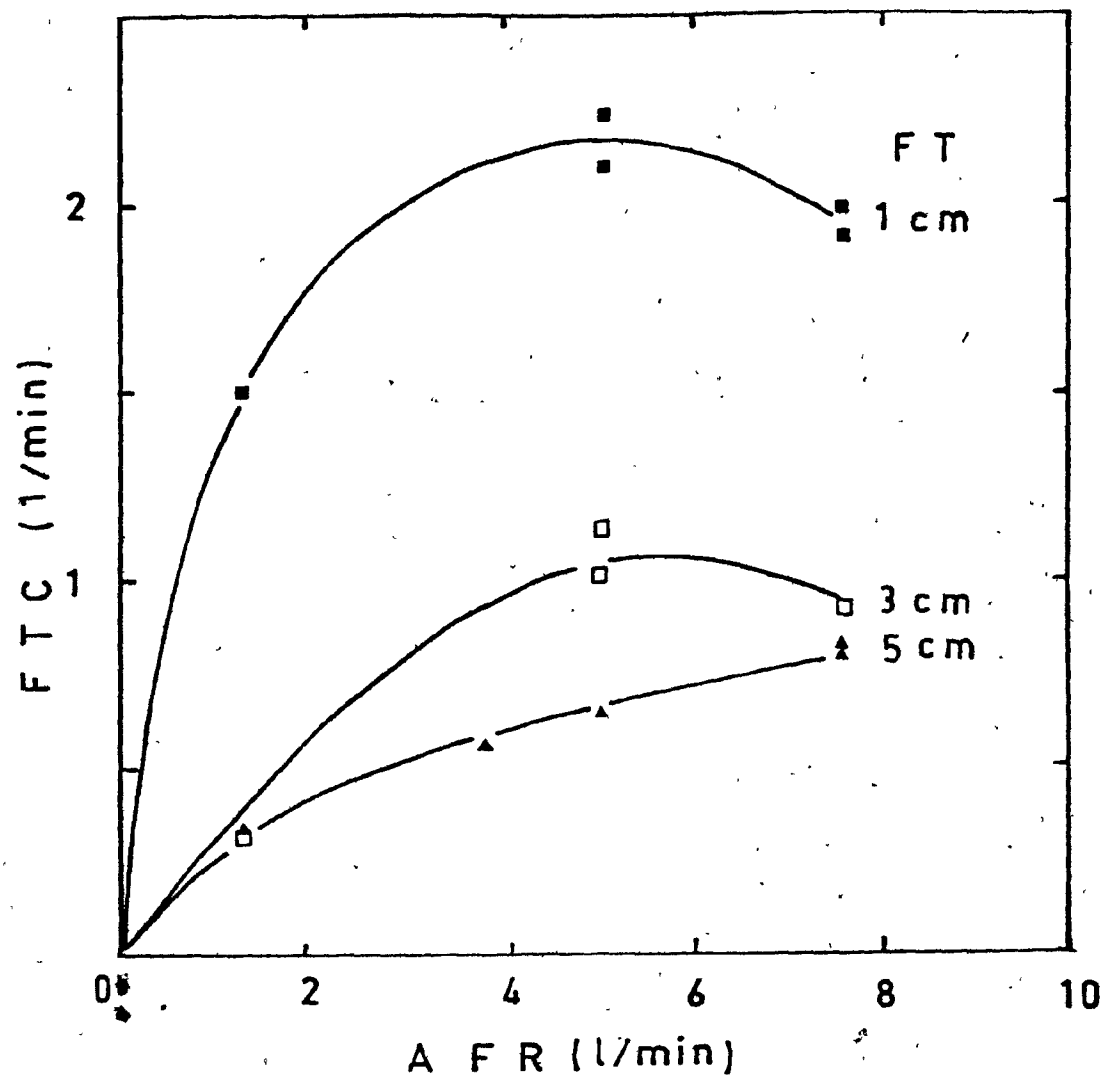

Fig. 6.8 Air flow rate versus froth transfer constant.

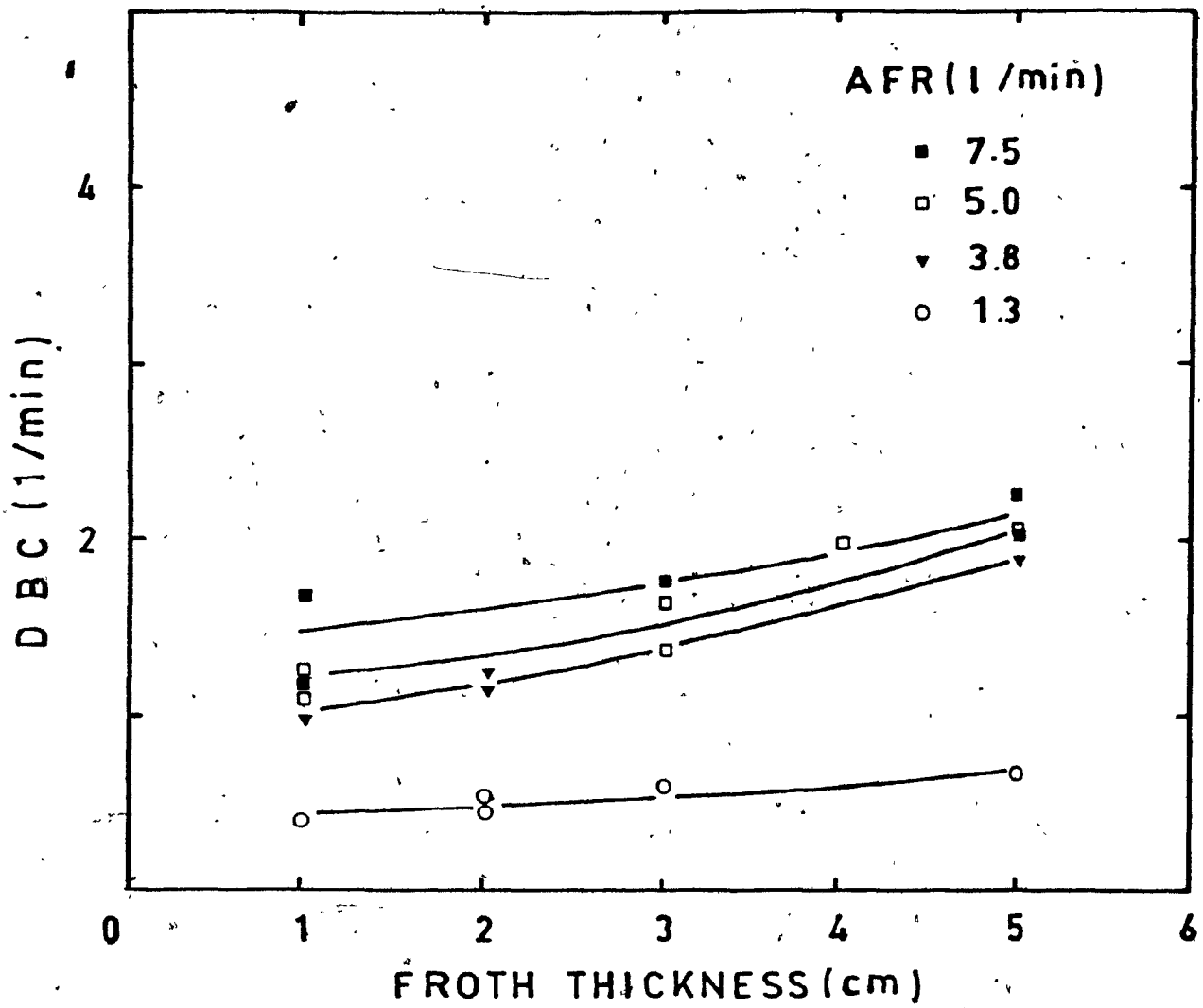

Fig. 6.9 Froth thickness versus drop-back constant.

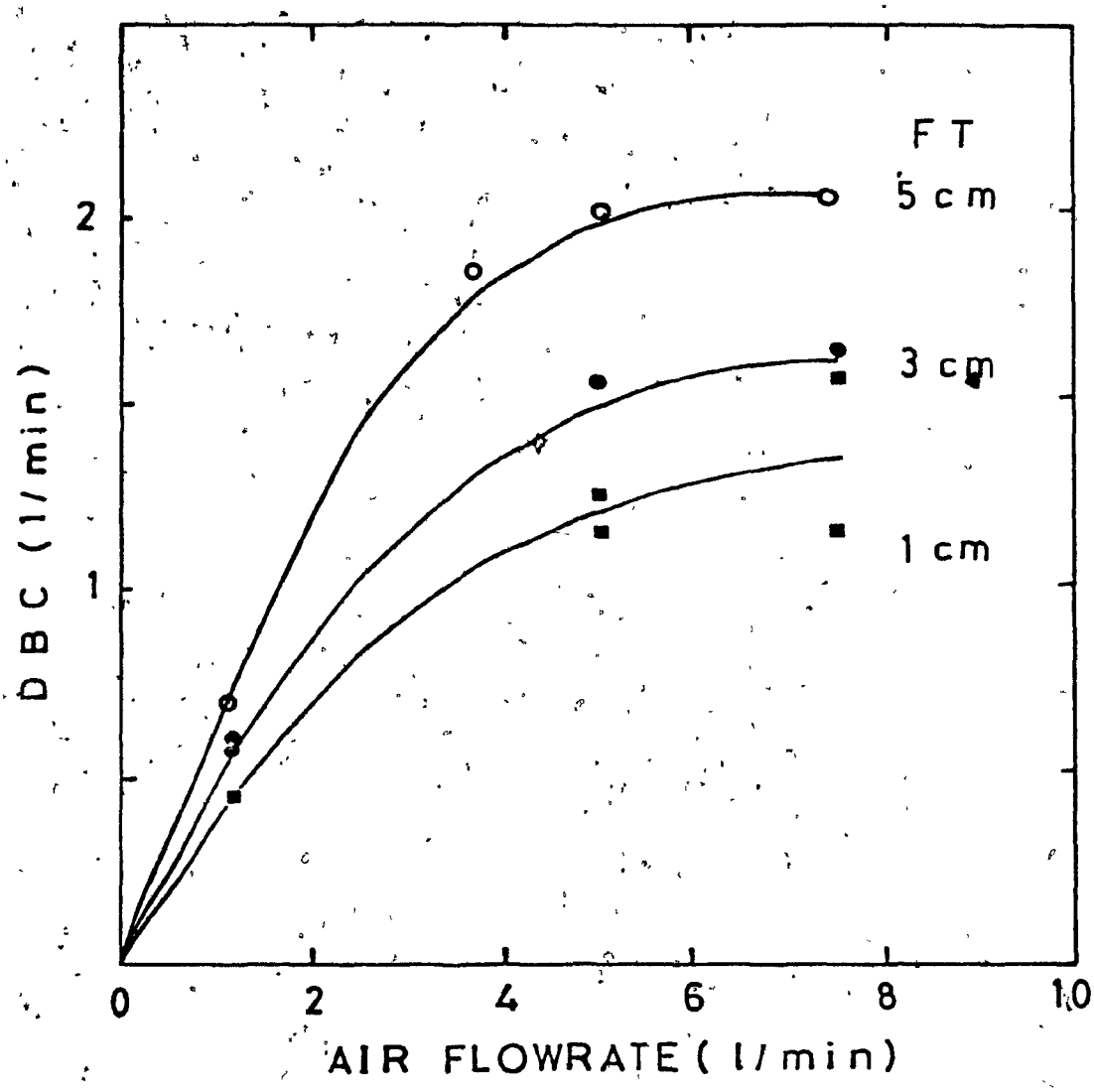

Fig..6.10 Air flow rate versus drop-back constant.

plateau is reached at intermediate to high AFRs.

The relationship between AFR, FT and DBC can be summarized by:

$$DBC = 0.5862 * Q^{0.7020} * FT^{0.3038} \qquad 6.4$$

(correlation coefficient: 0.97)

The slight increase in DBC as FT increases could be explained by a number of mechanisms. Firstly, the particle residence time in the froth increases with increasing FT. This leads to a higher probability of detachment in the froth phase. Secondly, as FT increases, liquid recovery into the concentrate is decreased. As the same liquid flow rate is entrained into the froth by air, water drainage must increase. The froth is drier, and the probability of bubble coalescence increased.

The DBC is lowest at an AFR of 1.3 L/min. This is a direct consequence of the hindered flotation caused by saturation of bubble surface with hydrophobic particles. The existence of hindered flotation was confirmed by comparing the solid holdup in the cell in continuous operation with batch work under similar conditions. These highly loaded bubbles reduce coalescence showed by Dippenaar (1978) who stated that the froth then highly flocculated becomes stabilized by solids when they adhere to the air water interface so closely together that liquid drainage is restricted. The high bubble load at low AFR is

confirming by Fig. 6.11 which gives the solid holdup in the froth as a function of FT for AFRs of 1.3, 5 and 7.5 L/min.

In general, factors that reduce the rate of drainage of the froth film will increase the stability of froth. Thus, the smaller the bubbles forming the froth, in this case, at low AFRs, the greater the stability of froth, i.e. less drop-back.

From Fig. 6.9, it will be noted that the DBC does not converge to zero as the FT approaches zero. This might be explained by the fact that even though the FT is assumed to be zero, at least one or two froth layers flow horizontally on the froth surface (Fig. 6.12). It is interesting that the magnitude of DBC at zero FT is about 60 % of DBC for 5 cm FT . This is no way invalidates the technique used to determine the FRC, for which the froth is removed on a film of wash water. This in fact increases the FTC yielding alpha values close to unity.

Moys (1982) has presented a comprehensive mathematical model for the behavior of froth phase mobility. He showed that there were two transfer mechanisms in the froth. Velocity in the horizontal direction is lower than in the vertical direction at the back of the cell (Fig. 6.13). Cutting et al. (1982) investigated the froth phase by measuring the probability of transfer of particles at the top of the froth phase

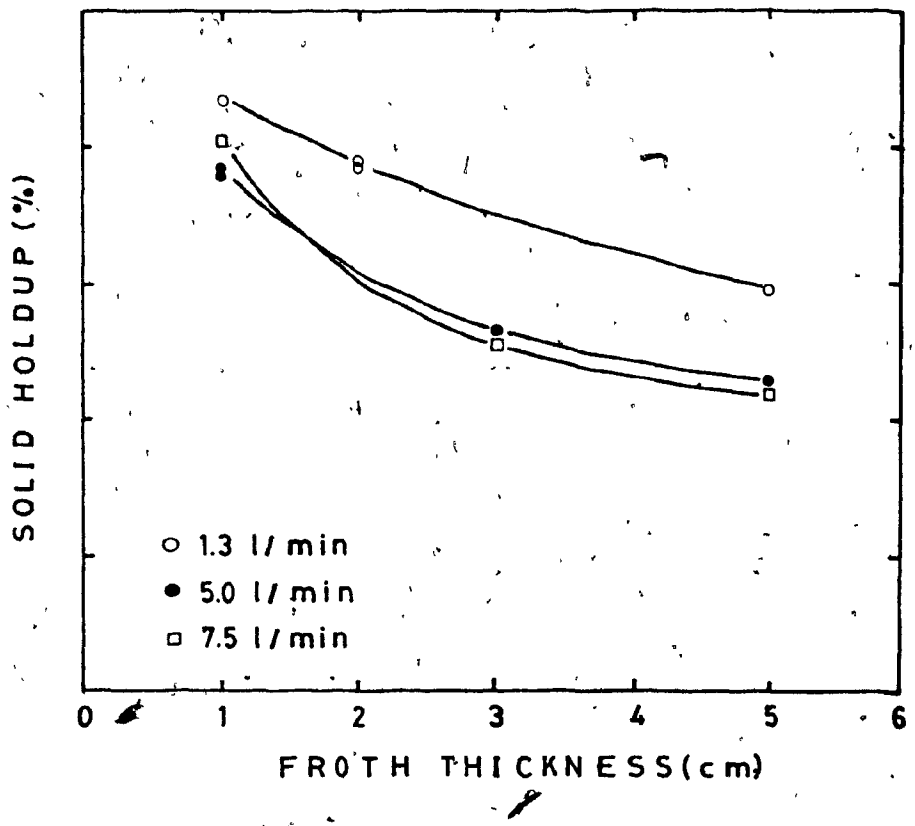

Fig. 6.11 Effect of FT and AFR on solid holdup in the froth phase.

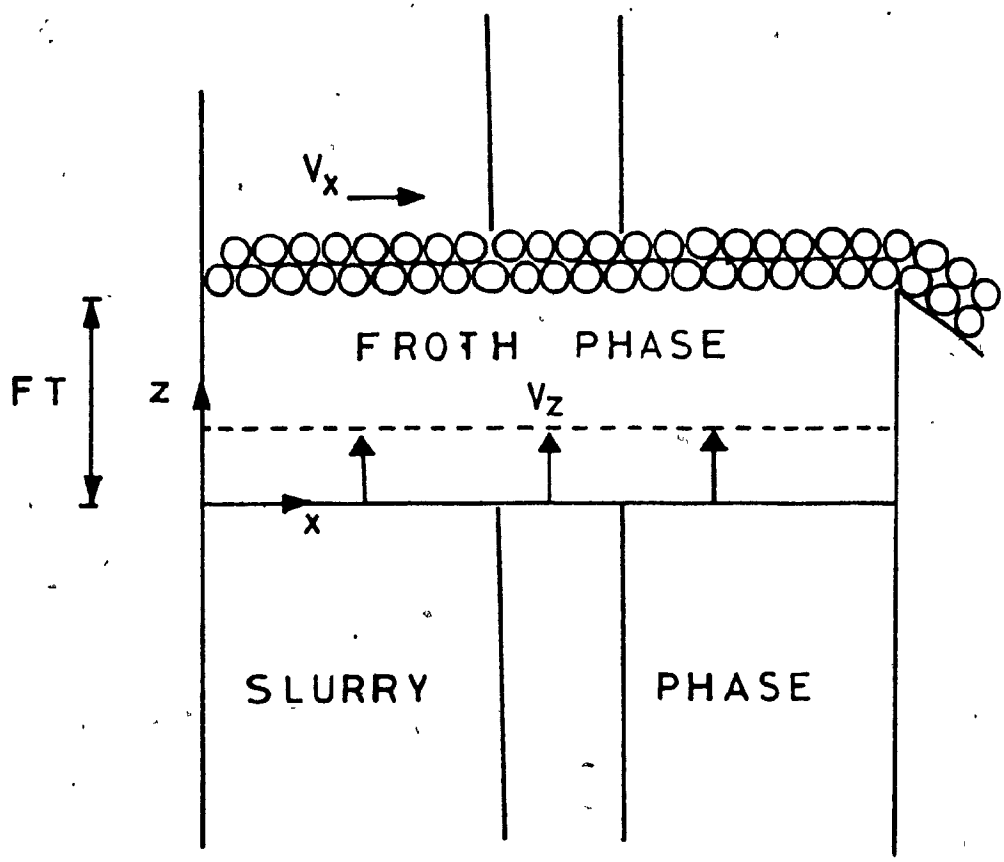

Fig. 6.12 Schematic representation of two transport mechanisms in conventional flotation froths.
(Vz: vertical transport velocity,
Vx: horizontal transport velocity,
FT: froth thickness).

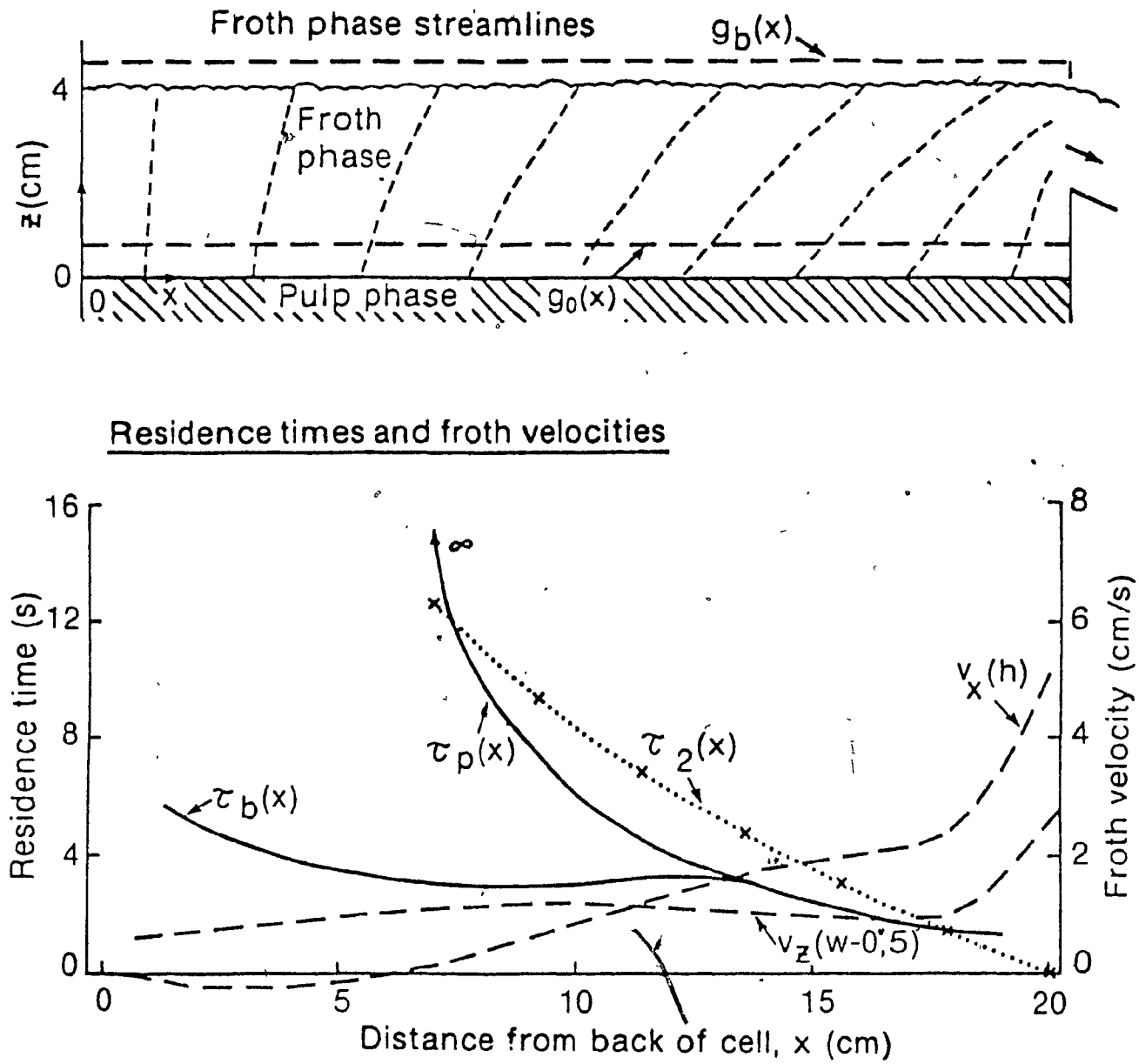

($g_b(x)$: flux of air through the froth surface; V_x: froth velocity in x direction; V_z: froth velocity in z direction; τ: residence time; b, p: subscripts for bubble, particle)

Fig. 6.13 Horizontal and vertical transfer velocities in conventional flotation froths (Moys, 1982).

(Fig. 6.14). Detachment of hydrophobic particles during horizontal transport results mainly from coalescence and a subsequent decrease in the surface area holding the minerals in the upper part of the froth owing to high gas holdup. If a bubble reaches the top of the froth and bursts, the probability that the detached particles will reattach to bubbles in the thin conventional flotation froth and reach the cell lip is low.

In individual flotation cells, all transfers occur simultaneously and it is practically impossible to measure each separately. Thus, flotation kinetics are usually characterized by an overall transfer rate which can be easily measured, and includes the effect of all transfer rates. It is characterized by its rate constant, the overall rate constant (ORC), which is the product of the FRC and α. A significant decrease in ORC which was plotted as a function of FT at four AFRs, was obtained as FT increases or AFR increases(Fig.6.15). The effect of AFR on ORC is clearly seen in Fig. 6.16.

The correlation between AFR, FT and the ORC is

$$ORC = 0.3990 * Q^{0.5392} * FT^{0.5586} \qquad 6.5$$

(correlation coefficient: 0.97)

Data points for FT of 1 to 5 cm were

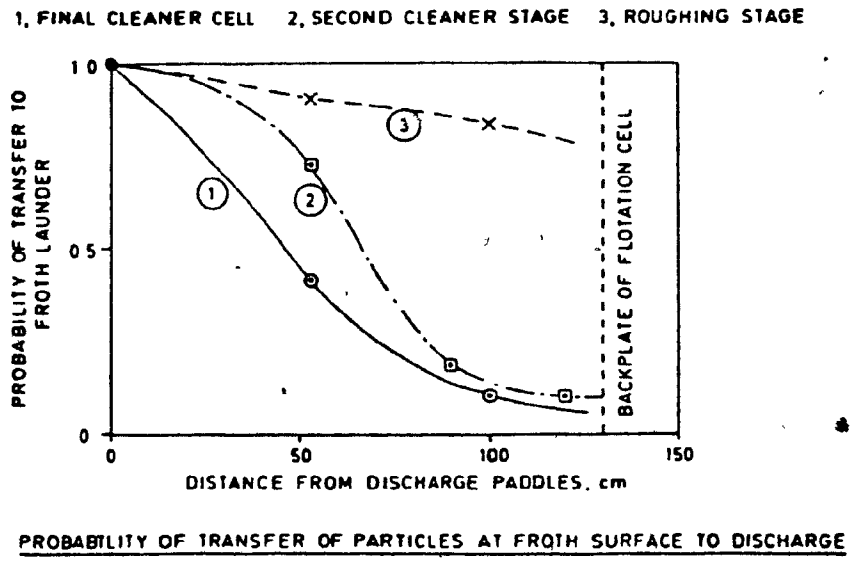

Fig. 6.14 Probability of transfer of particles at froth surface to discharge (Cutting et al., 1982).

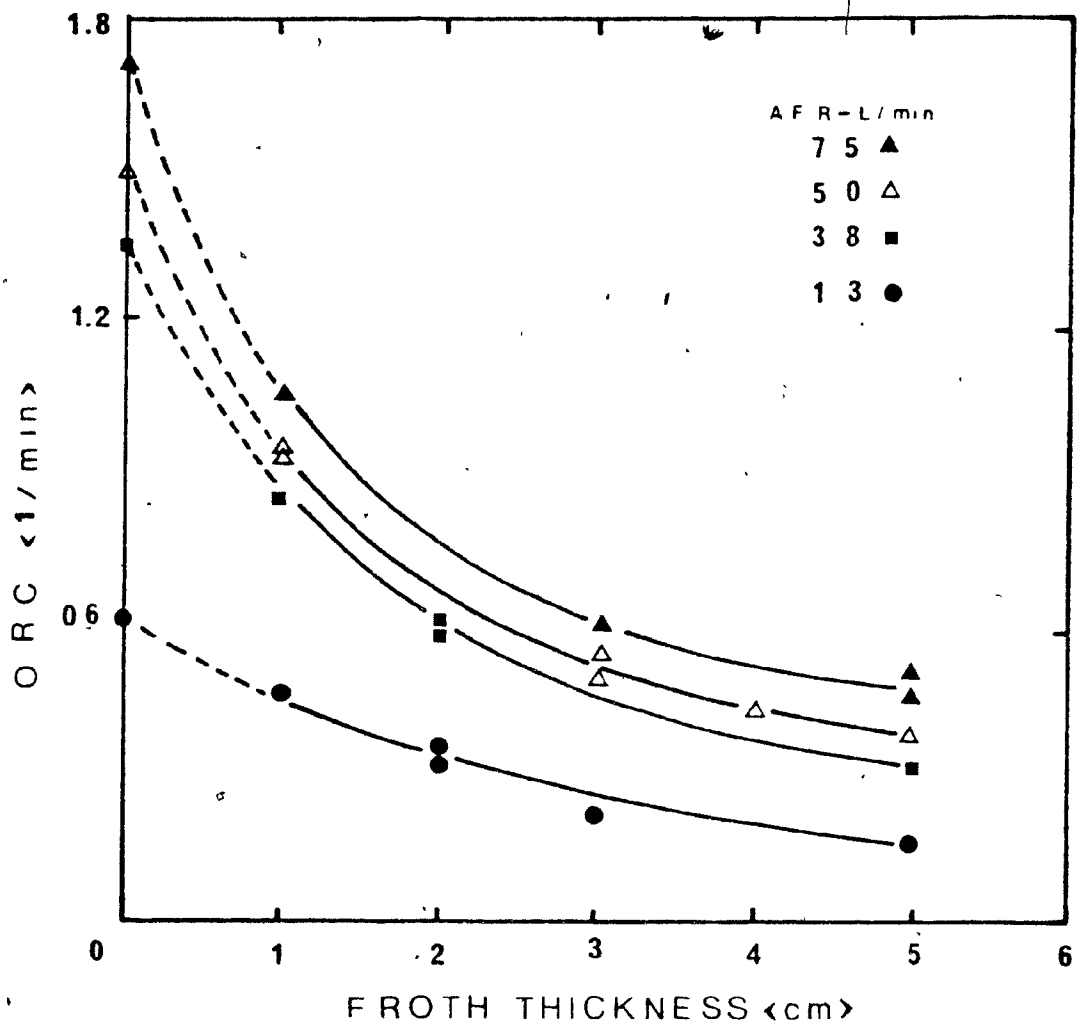

Fig. 6.15 Froth thickness versus overall rate constant.

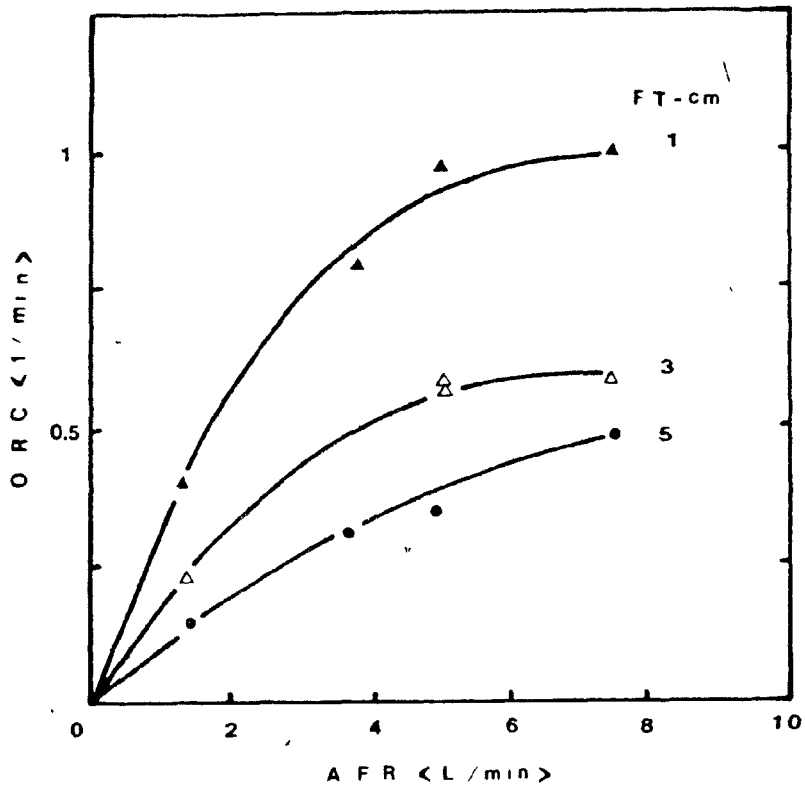

Fig. 6.16 Air flow rate versus overall rate constant.

experimentally found from the slurry-froth kinetics study. Extrapolation of these curves to zero FT is in good agreement with the experimental FRC , i.e the data points on the y axis, taken from Fig. 6.4. The agreement between the ORC at zero FT and the FRC suggests that there is a possibility to determine FRC in the presence of froth phase, by extrapolation of the ORC to a zero FT.

Both the DBC and the FTC increase with increasing AFR; the overall effect on α is small. The effect of FT on α is far more significant, because the FTC increases and DBC decreases with increasing FT, the result is a marked increase in α. Thus in this system, froth kinetics are more effectively controlled by FT. The effect of AFR is to increase the FRC. Eq. 6.6 shows that both FT and AFR affect overall kinetics about equally, within the range of experimentation (FT: 1 to 5 cm; AFR: 1.3 to 7.5 L/min).

6.7 SUMMARY

In this chapter, the combined effects of AFR and FT on flotation kinetics of sphalerite were investigated in continuous flotation.

The FRC was characterized firstly as a function of AFR. Results show that a maximum FRC is obtained at an intermediate AFR and the FRC decreases on either side of this AFR. However, most of the experimental range was on

the ascending side of the curve.

The FTC and DBC of the system were also determined, assuming a homogeneous froth and first-order kinetics for the transfer of material from the froth to the concentrate and from the froth over the cell lip. It was found that the FTC decreases as FT increases or AFR decreases. The DBC increases as FT or AFR increases. The net result is a relatively small effect of AFR on the froth recovery, R_F, whereas α clearly increases with decreasing FT.

The ORC was found to increase as AFR increased, and FT decreased, mostly as a result of the effect of AFR on the FRC and FT on α.

In the next chapter, the effect of particle size on each transfer mechanisms will be investigated as a function of AFR and FT.

CHAPTER 7

EFFECT OF PARTICLE SIZE ON THE DBC, FTC, AND ORC IN CONTINUOUS FLOTATION

7.1 INTRODUCTION

In this chapter, the effect of particle size on the DBC, FTC, and ORC will be investigated as a function of AFR and FT. Particle size has a paramount importance in flotation kinetics, and rate constants are the best method of comparing the flotation behavior of particles of different sizes.

7.2 EXPERIMENTAL PROCEDURE

Usually all samples collected from tails and concentrate streams were combined to give a large enough sample (30 or 40 g) for size analysis by Warman cyclosizer. From the size analyses of the concentrate, tail and froth holdup, the rate constants of each size class were calculated.

In all graphs where the transfer rate constants were plotted as a function of particle size, the values for the finest fraction (-8 μm) were omitted, as the behavior of slimes was not of prime interest in this chapter, and is difficult to characterize in the present

system because of hydraulic entrainment.

7.3 RESULTS

Experimental results are provided in Appendix 7.1. In order to explain the effect of particle size on each transfer mechanism, first, bar graphs at different AFRs and FTs were plotted. In Fig. 7.1, a common horizontal axis indicates the particle size range and the vertical axis shows the DBC. For each size range three bars were plotted, for FTs of 1, 3 and 5 cm, respectively. The DBC increases as FT and AFR increase. These results are in good agreement with the behavior of unclassified feed repeated in chapter 6.

The high drop-back of the 9-13 μm fraction is, presumably because a significant fraction is hydraulicly entrained in the froth phase, and is not attached to bubbles. It is thus easily washed back to the slurry by liquid drainage. The high drop-back of the plus 37 μm at FTs of 3 and 5 cm is probably caused by an increased probability of detachment, reported by King (1973).

It can be noticed that a high AFR appears to favour entrainment of fine particles. The DBC of the -13+9 m size classes is high. The DBC of intermediate classes is the lowest. A higher DBC of the coarsest size classes at an AFR of 5 L/min than 7.5 L/min can be explained by an increase in water drainage. Increasing the

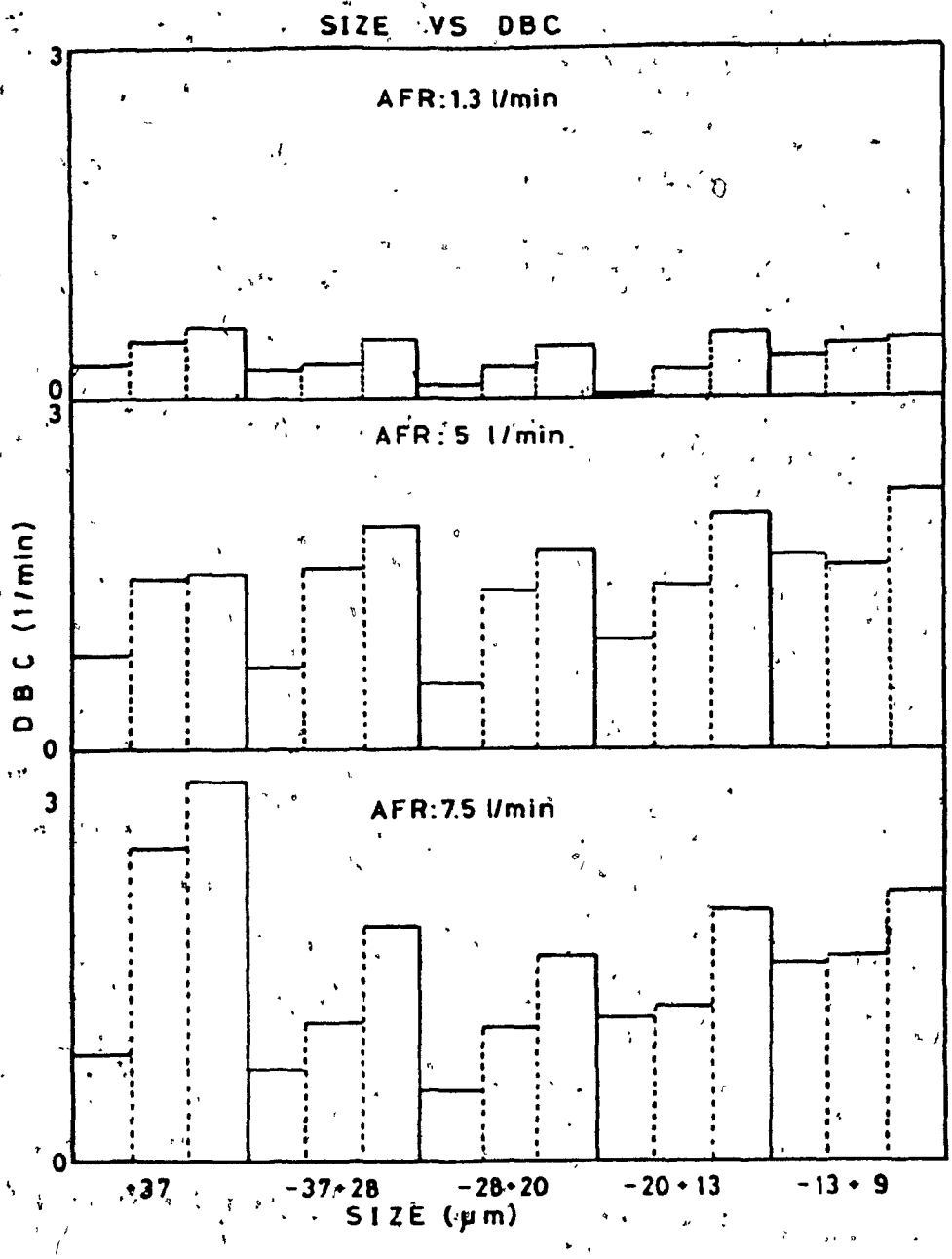

Fig. 7.1 Effect of particle size on DBC at different AFR and FT.

(For each AFR and size classes, values of DBC are given for FT= 1, 3 and 5 cm).

AFR increases the wetness of the froth.

There could not be found a maximum ORC at an intermediate AFR even for very thin froths. This implies that, at higher AFRs, even if the transfer rate of material from the slurry to the froth decreases with increasing AFR, the transfer rate from the froth to the concentrate increases sufficiently to produce an increase in the overall transfer rate. This illustrates that, in the present system, the transfer of material from the froth to the concentrate, as opposed to the transfer from the slurry to the froth, is rate limiting step. This behavior would be even more pronounced in industrial flotation cells, where both horizontal and vertical travel distances in the froth are greater.

However, it is difficult to determine the precise effect of particle size on detachment of hydrophobic particles. This may be attributed to the complexity of mineralized flotation froths in structure and behavior.

The effect of particle size on the FTC at different AFRs and FTs is given in Fig. 7.2. Generally speaking, as FT decreases or AFR increases the FTC increases. It will be noted that the FTC is seen to be independent of particle size at the lowest AFR. As AFR increases, to intermediate and high levels, size effects appear. Most tests show that the maximum FTC is obtained at an intermediate size range and that it decreases on

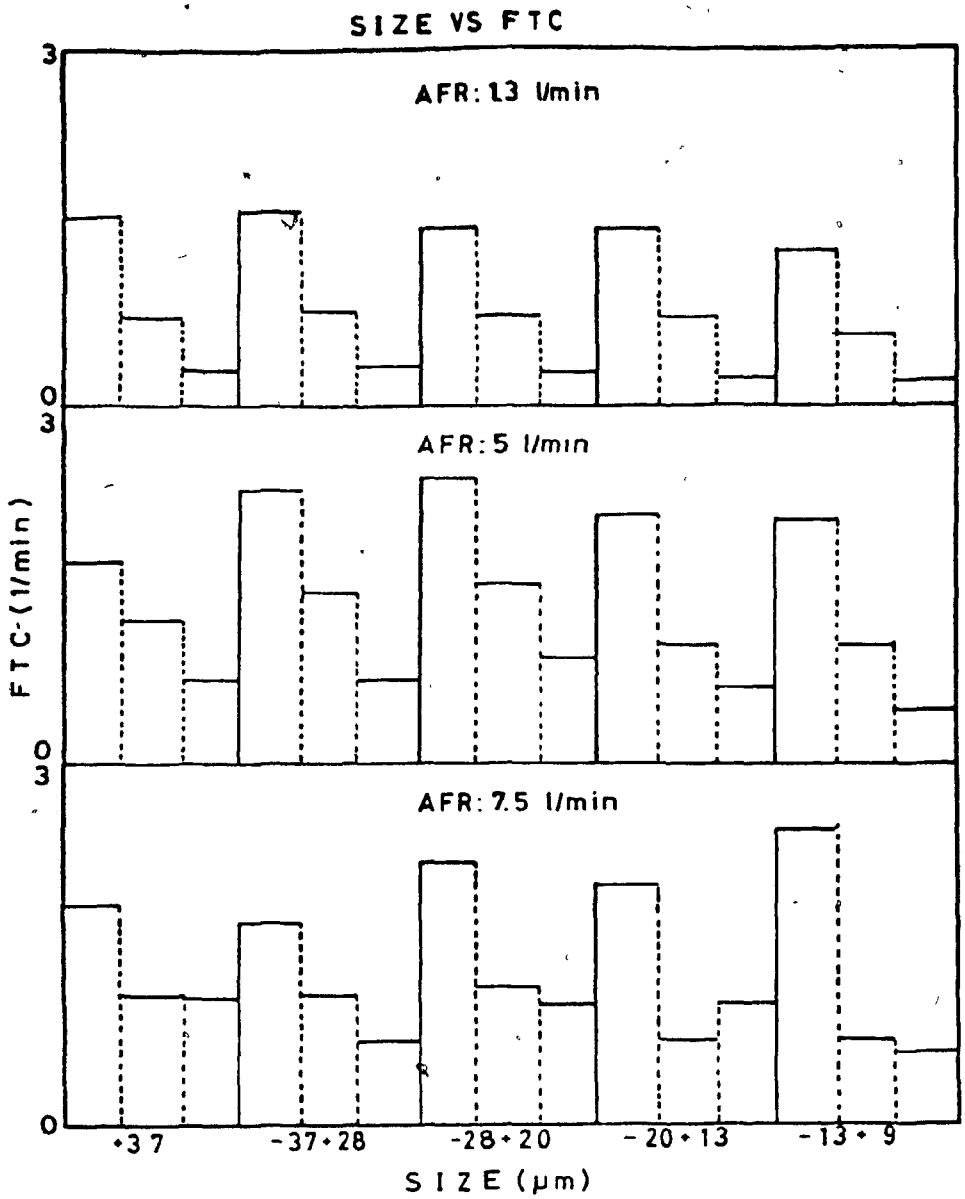

Fig. 7.2 Effect of particle size on FTC at different AFR and FT.

(for each AFR and size classes, values of FTC are given for FT= 1, 3 and 5 cm).

either side of this maximum.

Fig. 7.3 shows the relationship between the ORC and particle size in bar graphs again. As either AFR decreases or FT increases, the ORC decreases. The ORC is at an intermediate size range, 20-28 μm. Maximum FRC was found for the -37+28 μm particle size class. The shift of peak for the ORC is related to the low and high DBC.

The relationship between the DBC and AFR at different particle sizes is given in Fig. 7.4, for the 5 cyclosizer products. As observed in Fig. 6.10 for unclassified sphalerite the DBC increases with increasing AFR and FT.

The correlation between the FTC and AFR is given in Fig. 7.5 at different particle sizes and FTs. At a FT of 5 cm, as AFR increases, FTC also increases, whereas at a FT of 1 cm, some particle sizes show a maximum at intermediate AFR. There is not detectable size effect.

Fig. 7.6 shows the effect of AFR on the ORC for the same size classes and FTs. The 20-28 μm class clearly outperforms all others. The 9-13 μm class shows the slowest recovery kinetics.

The size-by-size data were fitted to the following general equation:

$$K = a * Q^{b} * FT^{c} \qquad 7.1$$

where K : FTC, DBC, or ORC (1/min)

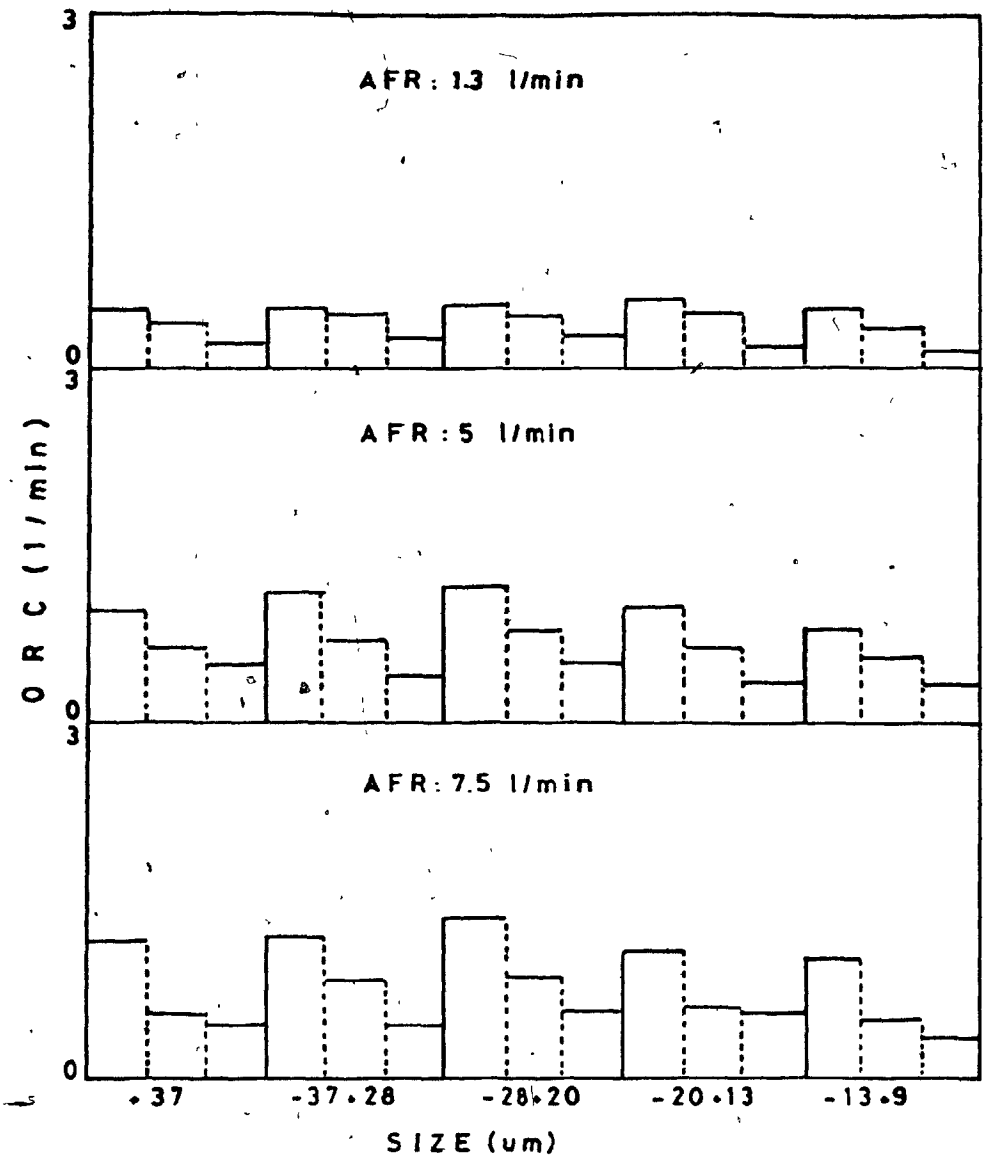

Fig. 7.3 Effect of particle size on ORC at different AFR and FI.

(for each AFR and size classes, values of ORC are given for FI= 1, 3 and 5 cm).

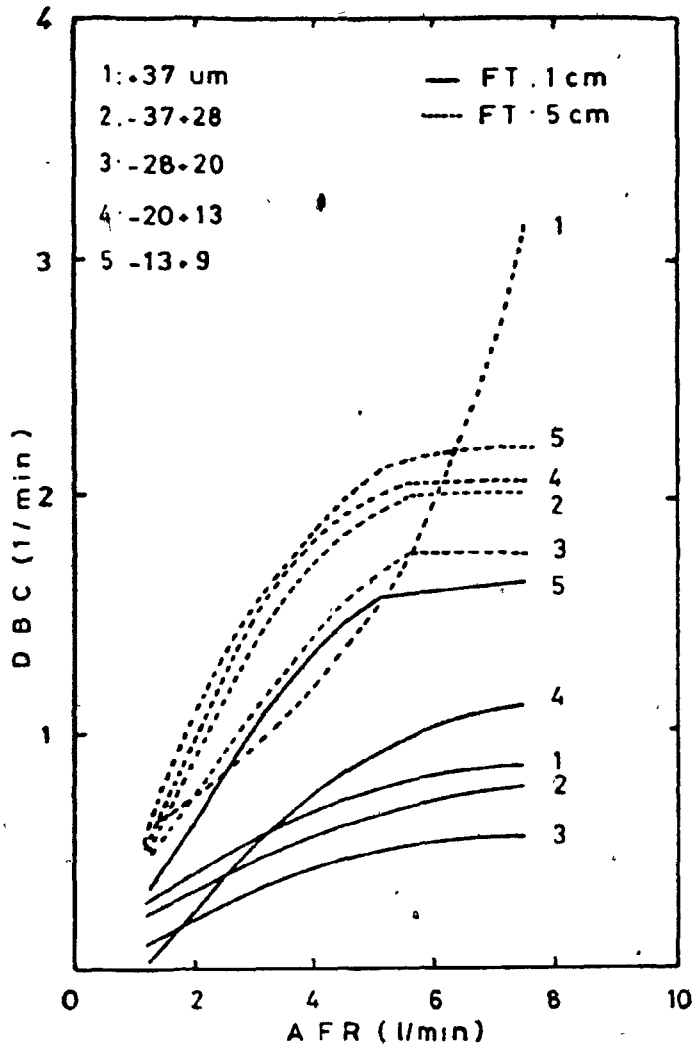

Fig. 7.4 DBC as a function of AFR at different particle size.

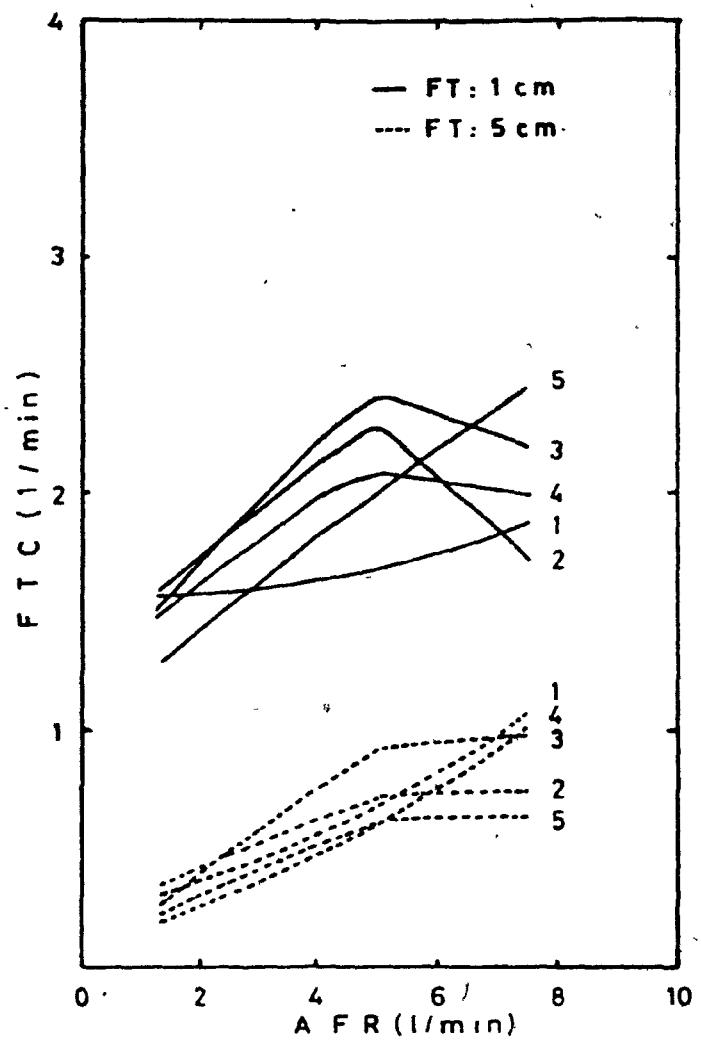

Fig. 7.5 FTC as a function of AFR at different particle size.

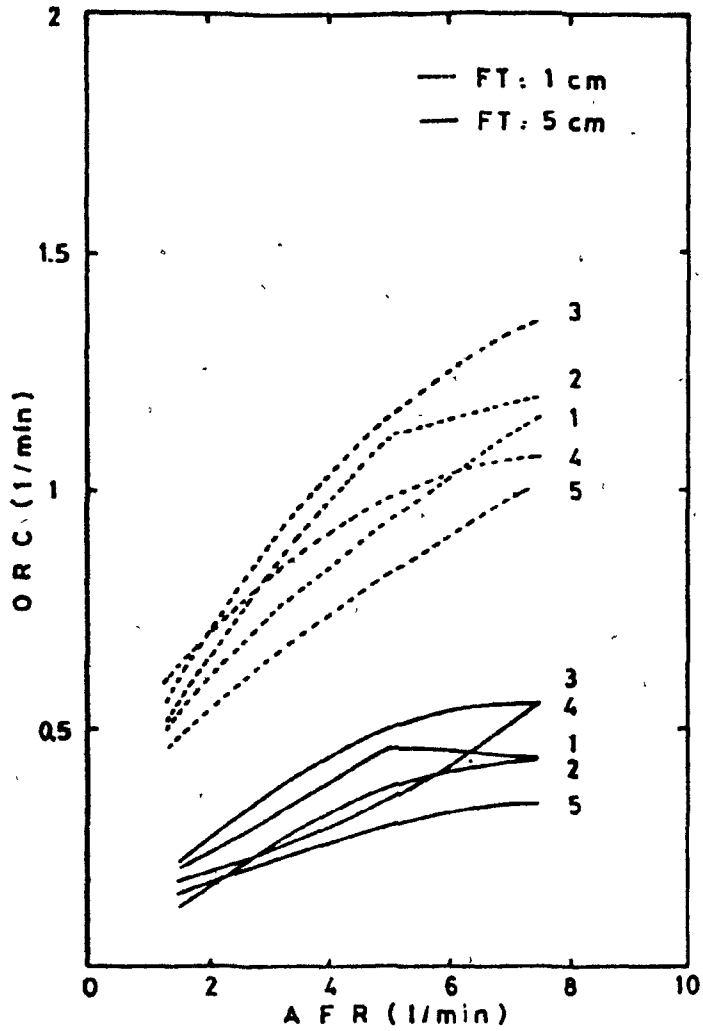

Fig. 7.6 ORC as a function of AFR at different particle size.

a : constant

Q : AFR (L/min)

FT: Froth thickness (cm)

a,b: exponents

The regression coefficients and correlation coefficients for each rate constant are summarized in Table 7.1. It is obvious that the particle size effect on each rate constant is very complex. The experimental data fit the calculated data from Eq. 7.1 well (Fig. 7.7). From the table, it can be said that the effect of FT on the FTC is more deleterious with decreasing particle size. The effect of AFR and FT on the ORC is remarkably size-independent, as both a and b are inconsistent over the full size range. It is clear that -9 μm size class results are inconsistent. Comparison of Fig. 7.7 and Fig. 6.15 shows a similar tendency for classified and unclassified sample.

7.4 DISCUSSION

Test results seem to indicate that particle size does not play very significant role in the transfer mechanisms. As sphalerite particles are strongly hydrophobic, they are not easily detached from the bubbles and most drop-back is due to bubble coalescence which yields a size-independent DBC. The 9-13 μm size class,

SIZE (μ)	Q(L/min) a	b	FT(cm)	CORRELATION COEFFICIENT
REGRESSION COEFFICIENTS FOR FTC				
+37	1.04	.3874	.6099	.92
-37+28	1.24	.3273	-.7159	.93
-28+20	1.06	.5017	-.7157	.94
-20+13	1.07	.4095	-.7919	.92
-13+9	0.97	.5001	-.9605	.97
-9	0.85	.5163	-1.009	.91
REGRESSION COEFFICIENTS FOR DBC				
+37	0.21	.8187	.5674	.98
-37+28	0.17	.7979	.5548	.97
-28+20	0.10	.9304	.7754	.97
-20+13	0.05	1.3935	.9167	.91
-13+9	0.30	.8732	.1432	.95
-9	0.97	.9548	-.9271	.78
REGRESSION COEFFICIENTS FOR ORC				
+37	0.47	.4408	-.5261	.97
-37+28	0.52	.4435	-.5411	.97
-28+20	0.49	.5434	-.5149	.99
-20+13	0.49	.4335	-.5706	.94
-13+9	0.42	.4364	-.6163	.98
-9	0.14	.8506	-.5419	.82

TABLE 7.1

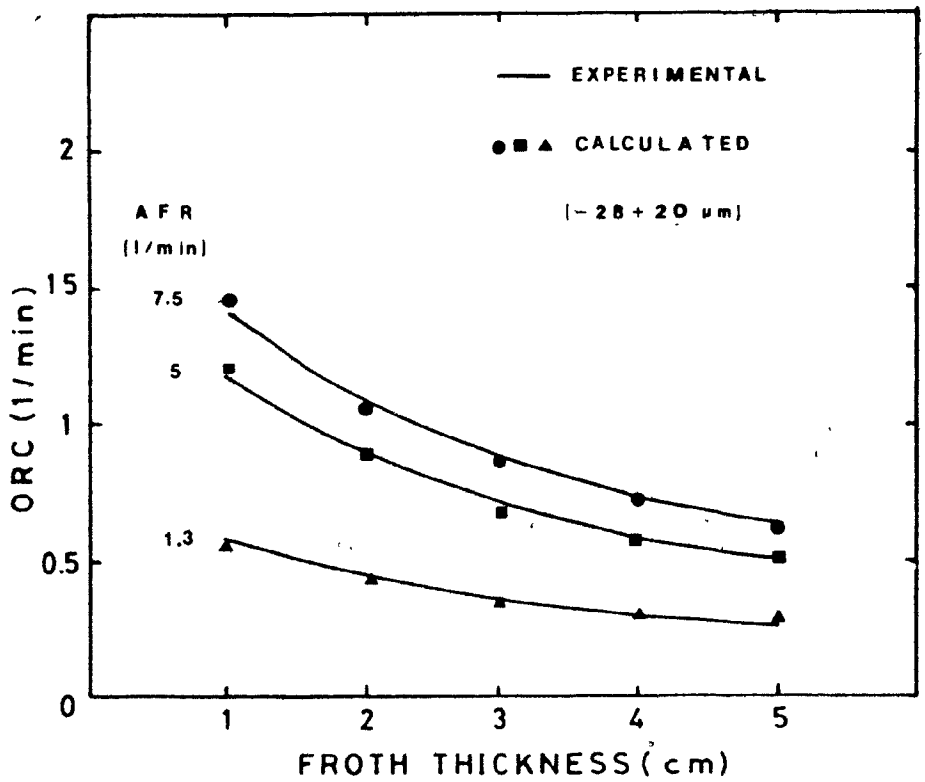

Fig. 7.7 Comparison between calculated and experimental **ORC data.**

(calculated values from Eq.7.1 and Table 7.1).

which exhibits the most dropback, presumably because of its significant hydraulic entrainment, is the exception.

According to Wollmann's model (1981) the re-entry of particles into the pulp is explained by disturbances in the coupling of the first froth layer or in the dewatering of the channels. Considering that turbulent circulating flow, u_T, at the fictitious lower froth boundary will affect especially the first layer, the re-entry into the pulp appears to be mainly due to hindered coupling to the first layer. That is, most of the re-entering particles come from the fictitious boundary between the froth and pulp and not from Gibbs channels (Fig. 7.8 from Schulze, 1982).

In order to prevent the direct effect of turbulent circulating flow at the active zone, a buffer zone was created between the froth and active zone (Fig. 7.9). Nevertheless, fast rising bubbles should have some effect on the fictitious boundary of the froth layer as in a conventional cell.

It seems that the hydrophobic particles are rejected randomly from the froth by bubble coalescence and collapse. The results indicate that the froth phase behaves as a filter for detached particles. Coarse particles can easily block the Gibbs channels since those are strongly hydrophobic, and the fines easily pass through the dewatering channels, and return to the slurry

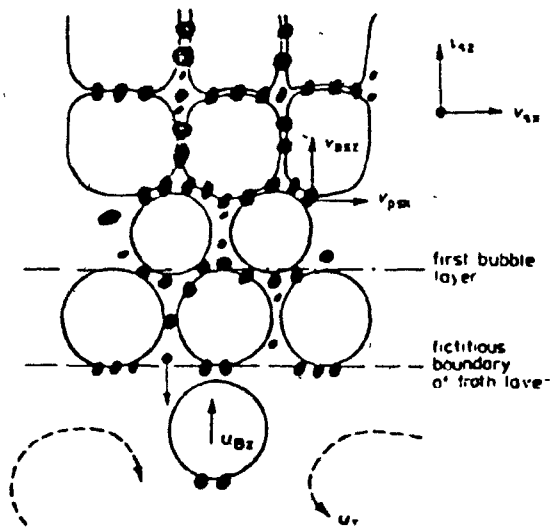

Fig. 7.8 Schematic diagram of the elementary process taking place as a bubble enters the froth layer and possible particle motion (from Schulze, 1982).

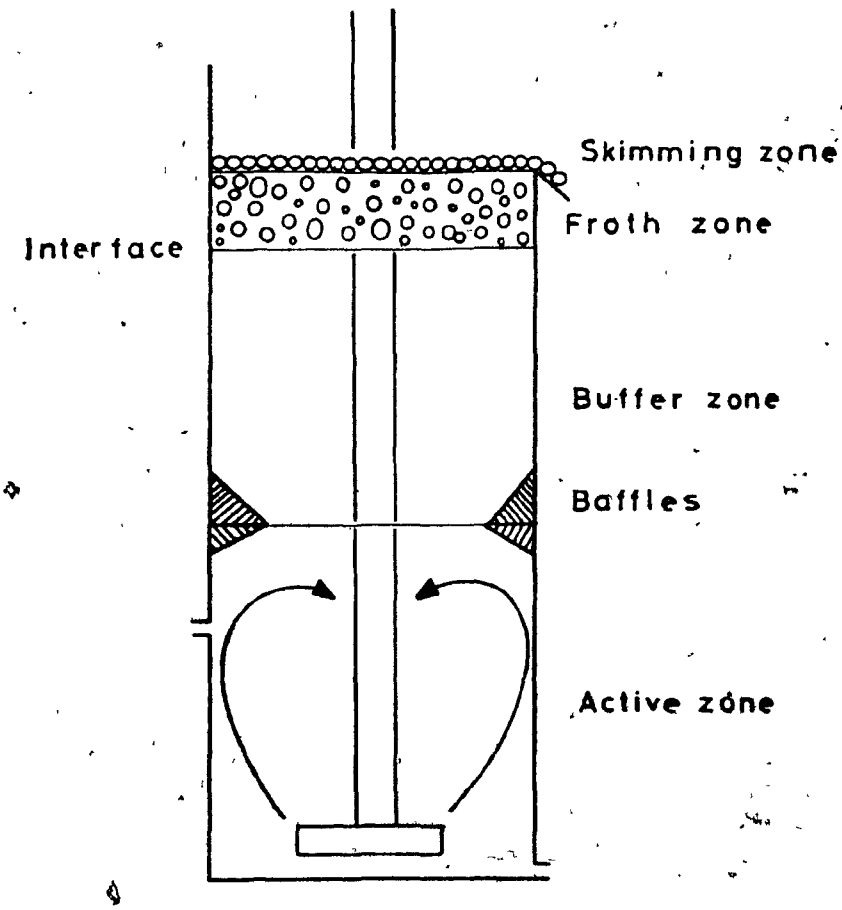

Fig. 7.9 Different zones in the flotation cell.

phase. (Fig. 7.10).

Fig. 7.10 Mechanism of stabilization of a thin film by a close-packed monolayer of particles with low contact angles (from Dippenaar 1978)

The presence of solid particles incorporated within the froth structure has a profound effect on the characteristics of the froth stability (Leja, 1982). Hemmings (1981) has pointed out that particles of diameter greater than the lamellea thickness would bridge two bubbles and be more strongly retained. This may in part explain the higher drop-back of fines to the slurry phase.

Bubbles experience a shear force exerted by the fluid draining in the downward direction. Therefore, the larger the particles, the larger the force for disruption. The other effect considered is that due to gravity (Bascur and Herbst, 1982). But, it was found that these forces do not affect the hydrophobic particles significantly in the froth phase, except at an AFR of 7.5 L/min, FIs of 3 and 5 cm, for the 37 μm.

In general, the probability of flotation is related to particle-bubble collision, adherence, and detachment. (Dobby, 1984).

$$P_F \alpha P_c * P_a * (1-P_d) \qquad 7.2$$

where Pf, Pc, Pa, and Pd refer to the probabilities of flotation, collision, adherence, and detachment. For present purposes, it is simpler to replace (1-Pd) by Ps, where Ps is the probability that the particle-bubble combination, once formed, will be stable enough to enter the concentrate.

The effect of particle size on each mechanism was investigated by many researchers. The probability of particle-bubble collision has attracted much attention (Sutherland, 1948; Flint and Howarth, 1971; Reay and Ratcliff, 1973) whose work has been summarized by Jameson and coworkers (1977). Although the exact form of the relation between collision frequency and other variables has not been established beyond dispute, there is no real doubt that Pc is related to physical variables, i.e. particle and bubble diameters, particle and liquid densities, liquid viscosity, relative particle-bubble velocity, etc, and in particular, to particle diameter, dp.

The variables which influence the probability of adherence, Pa, are less well understood. Dobby, (1984) recently suggested that the induction times and contact times decrease with increasing particle size. As the contact time decreases even more rapidly, the net effect is a decrease of the attachment efficiency with increasing

particle size.

The third term Ps is dependent on the force of adhesion between particle and bubble which in turn is related to particle size. Morris (1950) considers that coarser particles are affected more than fines, because the contact angle required for static equilibrium is smaller for fine particles than for coarse particles for a given bubble size. He pointed out that the greater the degree of flexibility, the greater is the chance for a bubble-particle system to withstand rupture.

The decrease in the recovery of particles beyond a certain size was explained by Schulze (1977). The concept on which Schulze's theory is based is that work must be done in order to rupture a particle-bubble couplet, against the restoring force of the surface tension. Thus, if the kinetic energy of the particle exceeds the work of rupture, the particle will detach.

In summary, Pc is directly related to a function of dp while Pa and Ps are inversely related to a function of the hydrophobicities. Therefore, there is a maximum at an intermediate particle size, 20-28 μm in this system. This result agrees very well with previously reported studies on sphalerite flotation (Fig. 7.11 from Trahar, 1976).

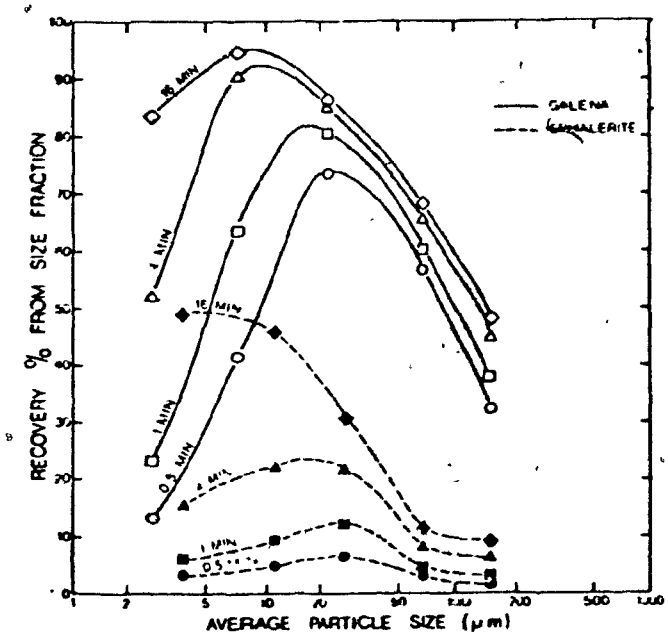

Fig. 7.11 Size-by-size recovery of galena and sphalerite (from Trahar, 1976).

7.5 SUMMARY

The relationship between flotation rates and particle size for the continuous flotation of sphalerite was investigated for different AFRs and FTs.

There is a little evidence to suggest that there is a substantial return of values from the froth. Presumably, the major drop-back mechanism of values from the froth is generally related to bubble coalescence and collapse. While some particles randomly return to the slurry zone, some are retained in the froth phase by bridging. Lower water and solid holdups destabilize the froth and facilitates the bubble coalescence.

The suggested equation ($K = a.*Q^{b}.*.FT^{c}$) experimental data fits well within experimental error. The size-by-size flotation behavior of sphalerite indicates that the ORC peaks at an intermediate particle size range (20-28 μm).

CHAPTER 8

ENTRAINMENT IN CONTINUOUS FLOTATION

8.1 INTRODUCTION

In this chapter, the importance of hydraulic recovery mechanisms for free gangue, hydrophilic silica, and hydrophobic sphalerite will be discussed. The effect of AFR, FT and wash water addition flow rate and level on entrainment will be investigated.

A new technique which can reduce the entrainment of silica about 30 to 50 % will be introduced.

8.2 EXPERIMENTAL PROCEDURE AND DATA ANALYSIS

An extensive entrainment study was carried out using an artificial sphalerite-silica mixture containing 33 % silica by weight and pure silica samples. The size distribution of silica obtained from Industmin Ltd, Canada, is given in Table 8.1.

Particle size (μm)	Mass (%)
-80	100
-60	95
-30	77
-20	60
-10	35
-8	30

Table 8.1 Particle size distribution of silica.

Frother was the only reagent added (75 g/t) to the pulp for mixture and pure silica systems. All flotation feeds averaged a density of 10% solids by weight. Firstly, the effect of AFR and FT was characterized in the sphalerite-silica system. The recovery rates of sphalerite, silica and water were determined from timed samples of the concentrate and tailing. As all silica was free and unconditioned, it was recovered by hydraulic entrainment. Another series of tests were conducted to investigate the effect of wash water addition both in mixture and pure silica systems. Three different wash water addition flow rates and two different addition levels were used to reduce the entrainment of gangue particles.

Silica content was determined by aqua regia dissolution of sphalerite at high temparature, followed by filtration and weighing of the solid residue.

A sedigraph 5000D was used to determine the size distribution of some of the flotation products, in the pure silica system, to analyze size-by-size entrainment.

8.3 RESULTS

The results of each test are given in Appendix 8.1. The effect of FT on silica recovery due to

entrainment in the mixture system is given at different AFRs in Fig. 8.1. (95 % confidence intervals are shown). Entrainment of gangue particles decreases as froth thickness increases. Fig. 8.2 shows the relationship between AFR and silica recovery at different FTs in the mixture system. In this case, entrainment slightly increases with increasing AFR. Figs. 8.3 to 8.6 show that both solids and water recoveries increase with increasing AFR and decreasing FT.

It is well known that hydrophilic particle recovery caused by entrainment is related to water recovery. Typical results are shown in Fig. 8.7, where the effect of FT on silica recovery at an AFR of 7.5 L/min is shown for pure silica flotation. There is a convex relationship between silica and water recovery for pure silica flotation. The sensitivity of entrainment to FT can also be seen from the same graph. For example, if there is no froth phase, silica recovery due to entrainment is more than 50% but a FT of 4.5 cm decreases the entrainment to less than 4%.

The combined effect of AFR and FT on gangue entrainment is shown in Fig. 8.8 where silica recovery was plotted as a function of water recovery. While there is a concave relationship between water and silica recoveries at constant FT, a convex relationship was obtained at constant AFR. Fig. 8.8 also shows that increasing FT and AFR at a constant water recovery will achieve a reduction

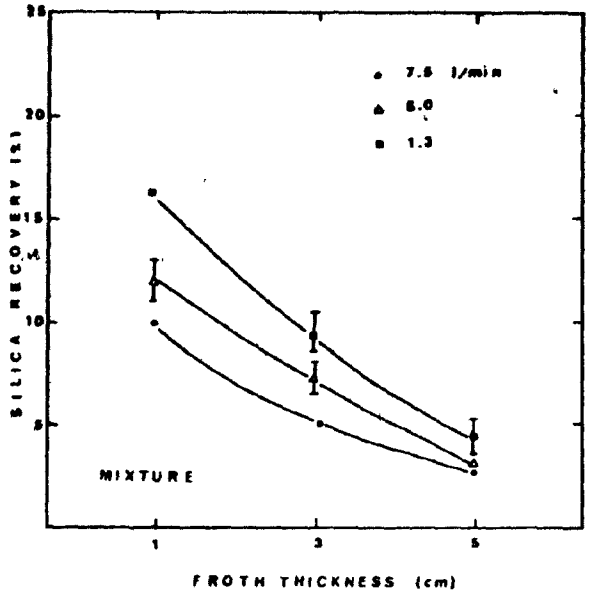

Fig.8.1 Effect of froth thickness on silica recovery.

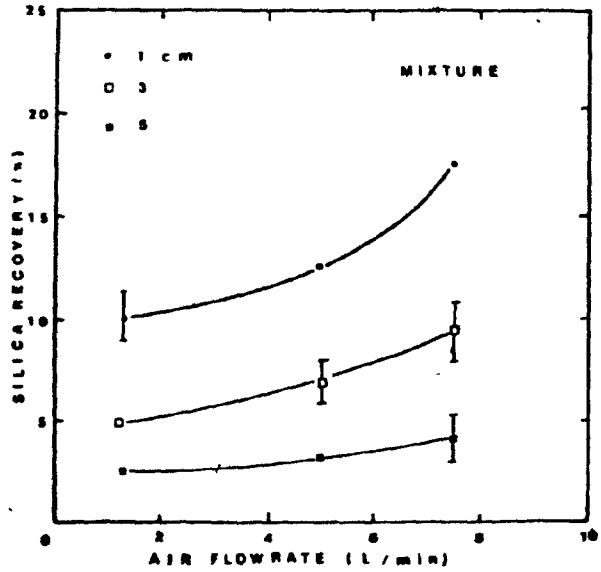

Fig.8.2 Effect of air flow rate on silica recovery.

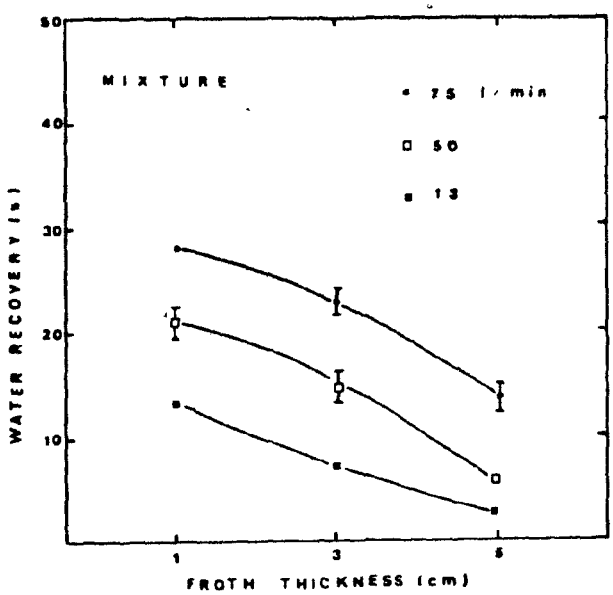

Fig.8.3 Effect of froth thickness on water recovery.

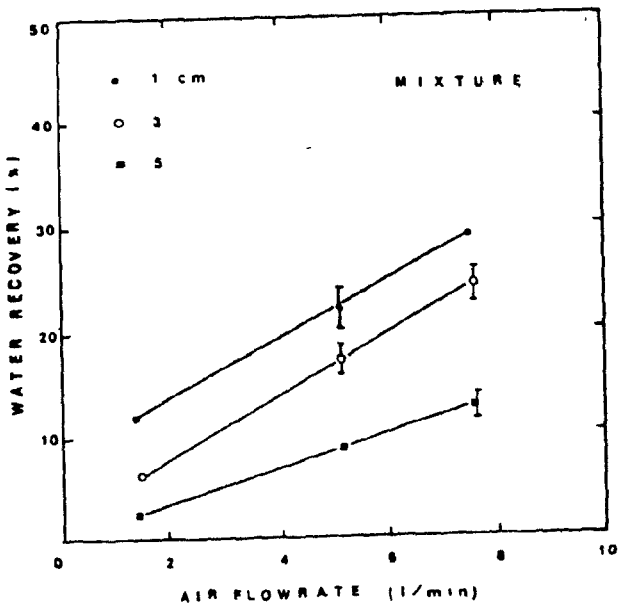

Fig.8.4 Effect of air flow rate on water recovery.

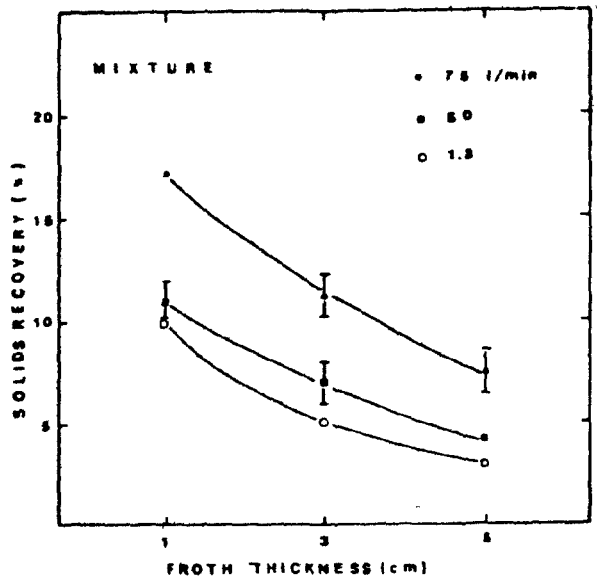

Fig.8.5 Effect of froth thickness on solid recovery.

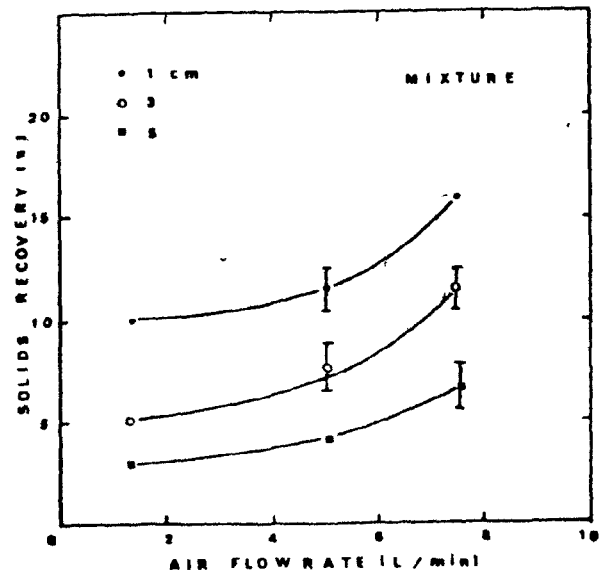

Fig.8.6 Effect of air flow rate on solid recovery.

in entrainment (point 1 to point 2). It is apparent that increasing FT at constant AFR will decrease water recovery and consequently silica recovery by hydraulic entrainment.

As AFR increases, water recovery to the concentrate increases. At the same time water drainage in the froth also increases. This water drainage is the cause of comparatively lower entrainment at higher AFRs at constant water recovery. At lower AFRs, the amount of water draining through plateau borders is considerably less, therefore the probability of drop-back of gangue to slurry phase is small.

In contrast to column flotation, entrainment of fine particles into the froth is a very serious and inevitable problem for conventional flotation. A qualitative comparison between conventional flotation and column flotation (from Yu, 1985) with respect to entrainment is shown in Fig. 8.9. It is obvious that recovery due to hydraulic entrainment in conventional flotation is much higher than in column flotation. However, conventional flotation results were obtained without wash water addition. Thus, it was decided to investigate the use of wash water to reduce entrainment in the present system.

Firstly, the effect of wash water addition, 1 cm below the slurry-froth interface and 1 cm above the froth surface, was investigated by using both mixture and pure silica feeds (Fig. 8.10).

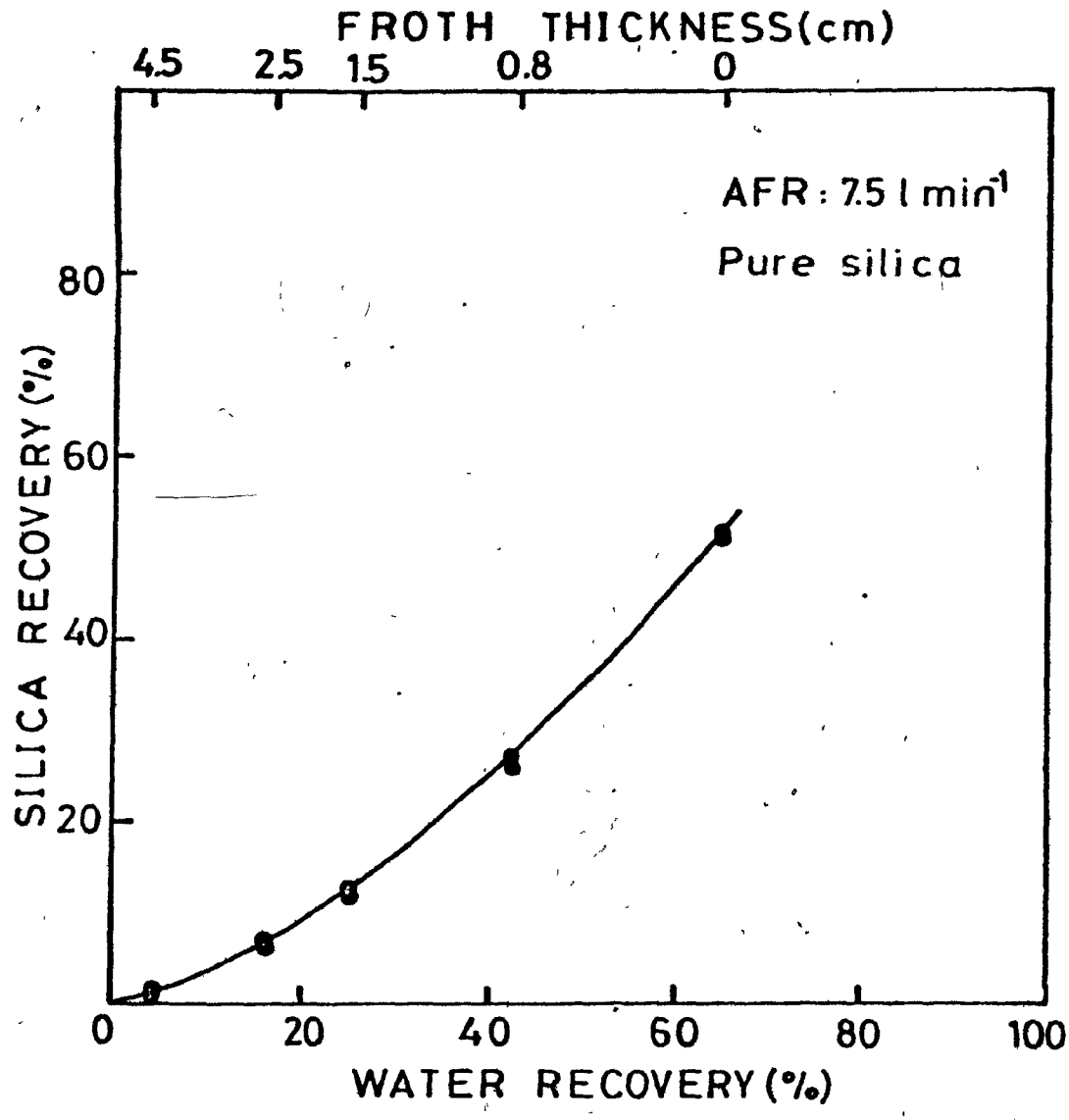

Fig.8.7 Relationship among water recovery, silica recovery and froth thickness in pure silica flotation.

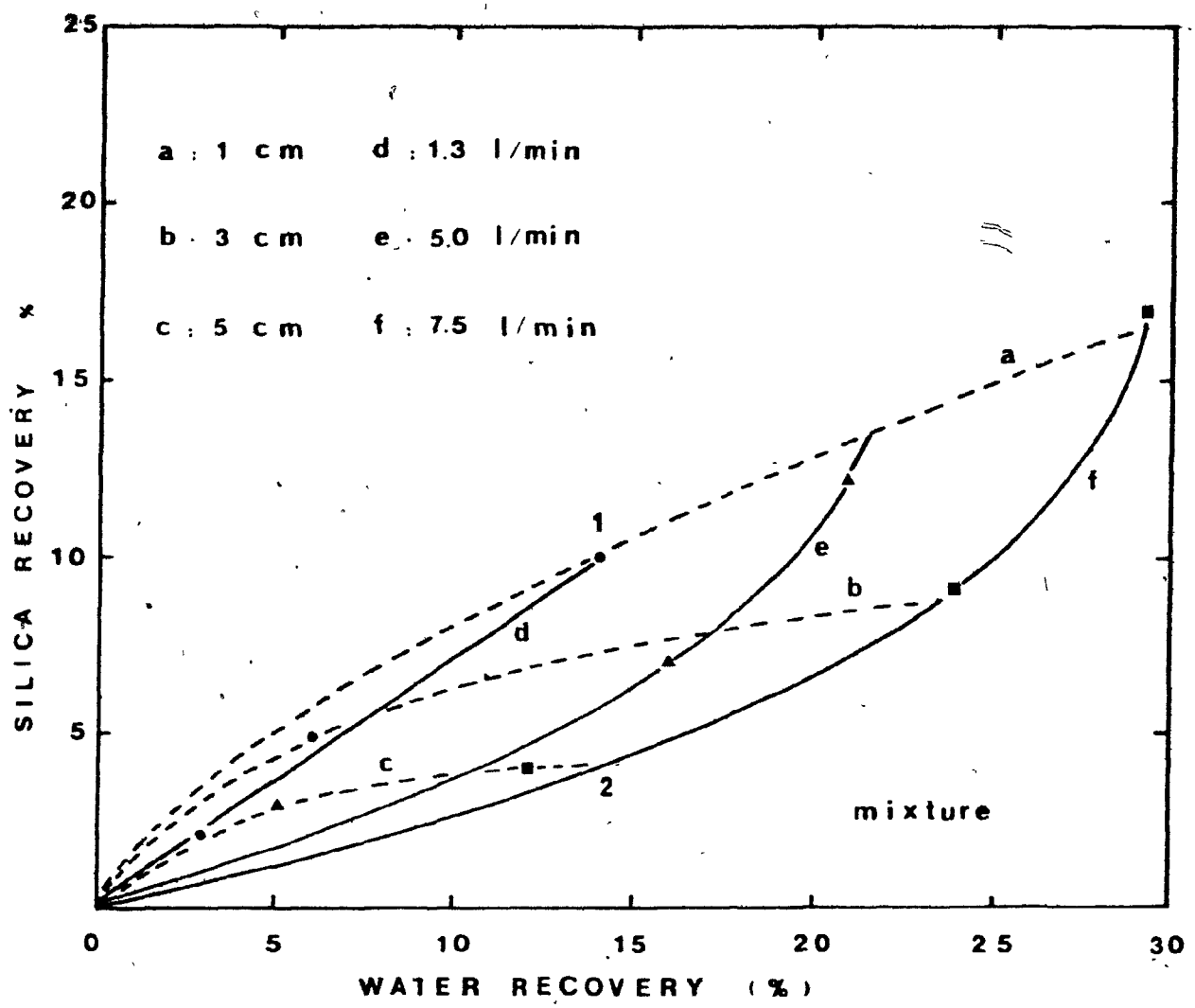

Fig. 8.8 Effect of water recovery on silica recovery at different AFR and FT.

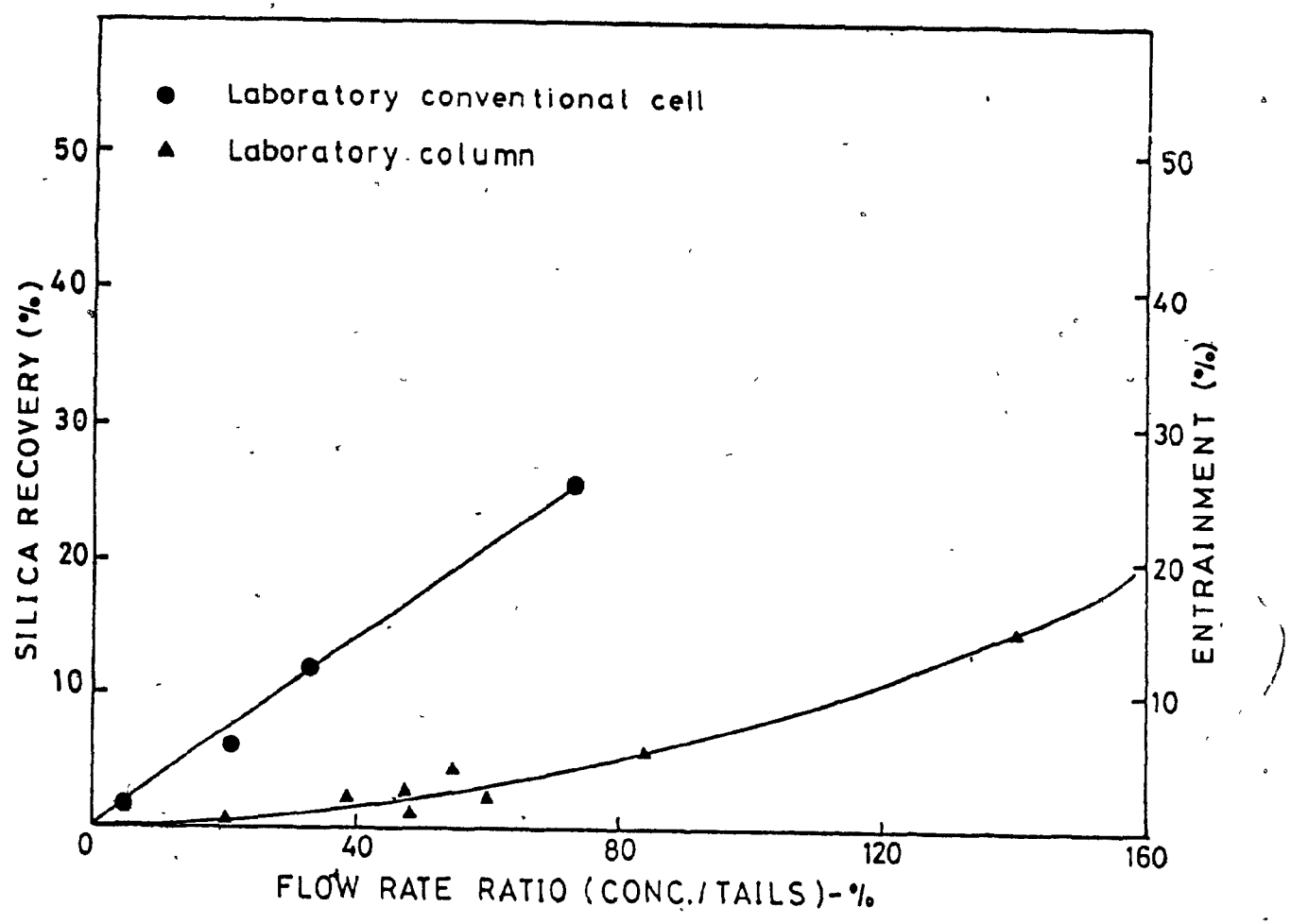

Fig.8.9 Comparison of entrainment in conventional and column flotation.

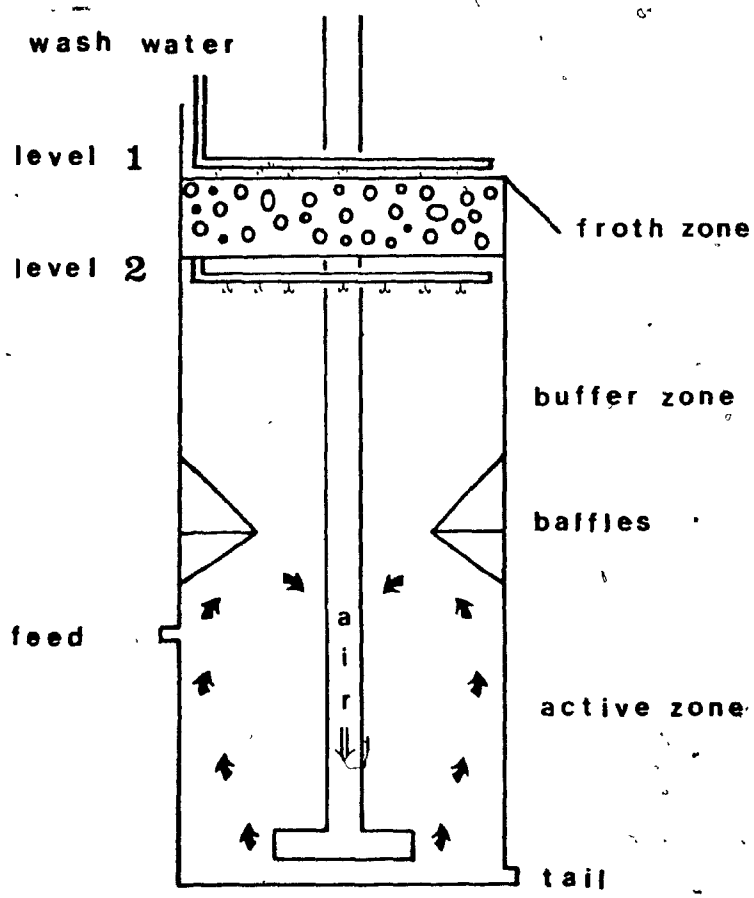

Fig. 8.10 Wash water addition levels for entrainment tests.

Fig. 8.11 shows the effect of wash water flow rate in mixture and pure silica flotation. Mixture flotation showed about 4% higher entrainment than pure silica. The higher recovery of hydrophilic particles in mixture flotation could be attributed mainly to entrapment in sphalerite particles. Jowett (1966) recognized that fine particles can be recovered also from physical associations with other particles e.g., from the existence of slime coatings on the large particles.

It was found that entrainment of gangue particles could be reduced by wash water addition. A 3% reduction in entrainment out of 5.5% for pure silica flotation was achieved by adding wash water. As wash water addition flow rate, either above or below the froth, increases from 0 to 0.6 L/min, silica recovery decreases. The superficial liquid velocities for these additions were between 0.9 and 2.7 cm/min, much lower than those used in columns (1-4cm/s). Interestingly, further improvements were obtained by washing the upper part of the flotation pulp i.e. addition of wash water 1 cm below the froth-slurry interface showed less entrainment than addition of wash water 1 cm above the froth, presumably because fewer gangue particles enter the froth phase. Wash water addition in the froth also stabilizes the froth and enhances recovery.

If silica is recovered by hydraulic entrainment, and if there is a weak or zero adherence between particles and bubbles, coarse silica particles should be

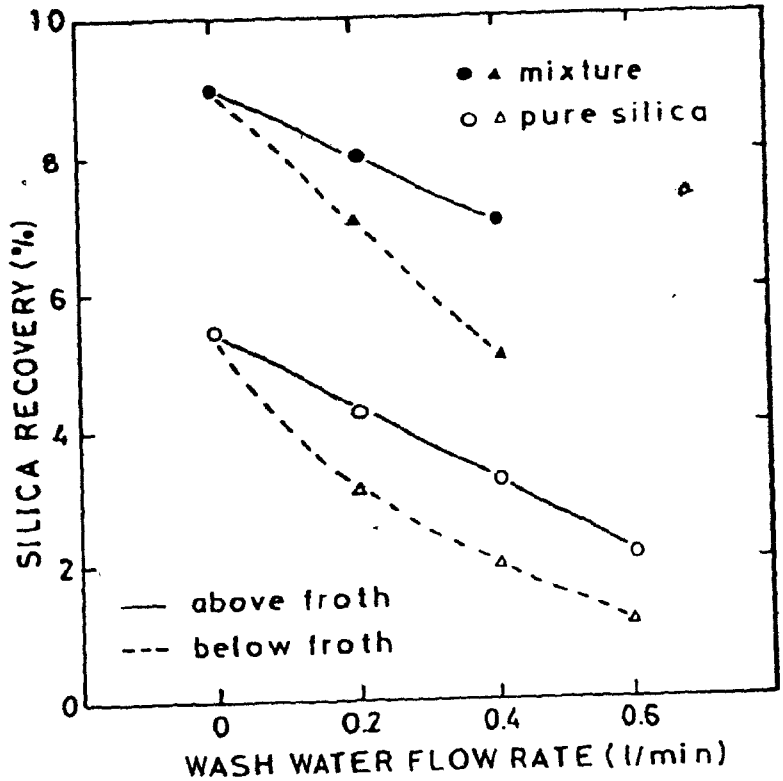

Fig.8.11 Effect of wash water addition flow rate and level on silica recovery for mixture and pure silica flotation (AFR: 7.5 L/min and FT: 3 cm).

preferentially drained from the froth. Hence, silica recovery should be highest for fine particles. These considerations introduce the concept of hydraulic classification of silica particles in the froth on the basis of size.

A typical results for pure silica flotation is shown in Fig. 8.12 where silica recovery was plotted as a function of particle size at an AFR of 7.5 L/min. It is evident that the fine gangue particles have a greater tendency to be entrained by water than coarse gangue particles. Thus, there is a classification in the froth with respect to particle size.

The effect of particle size on silica recovery at different FTs, wash water addition flow rate, and level is summarized in Appendix 8.2. Size distribution of concentrate and tail products for pure silica flotation showed that the concentrate product is much finer than the tail product. The influence of particle size on pure silica entrainment at different FTs indicates that concentrate product size distribution gets finer with an increase in FT (Fig. 8.13). These findings confirm the increasing classification action in the froth phase as FT increases. Coarse silica particles return to the slurry phase due to drainage of water through plateau borders. The effect of particle size on entrainment of pure silica at different WWFR and addition level showed that fine particles are more entrained to the froth at low wash

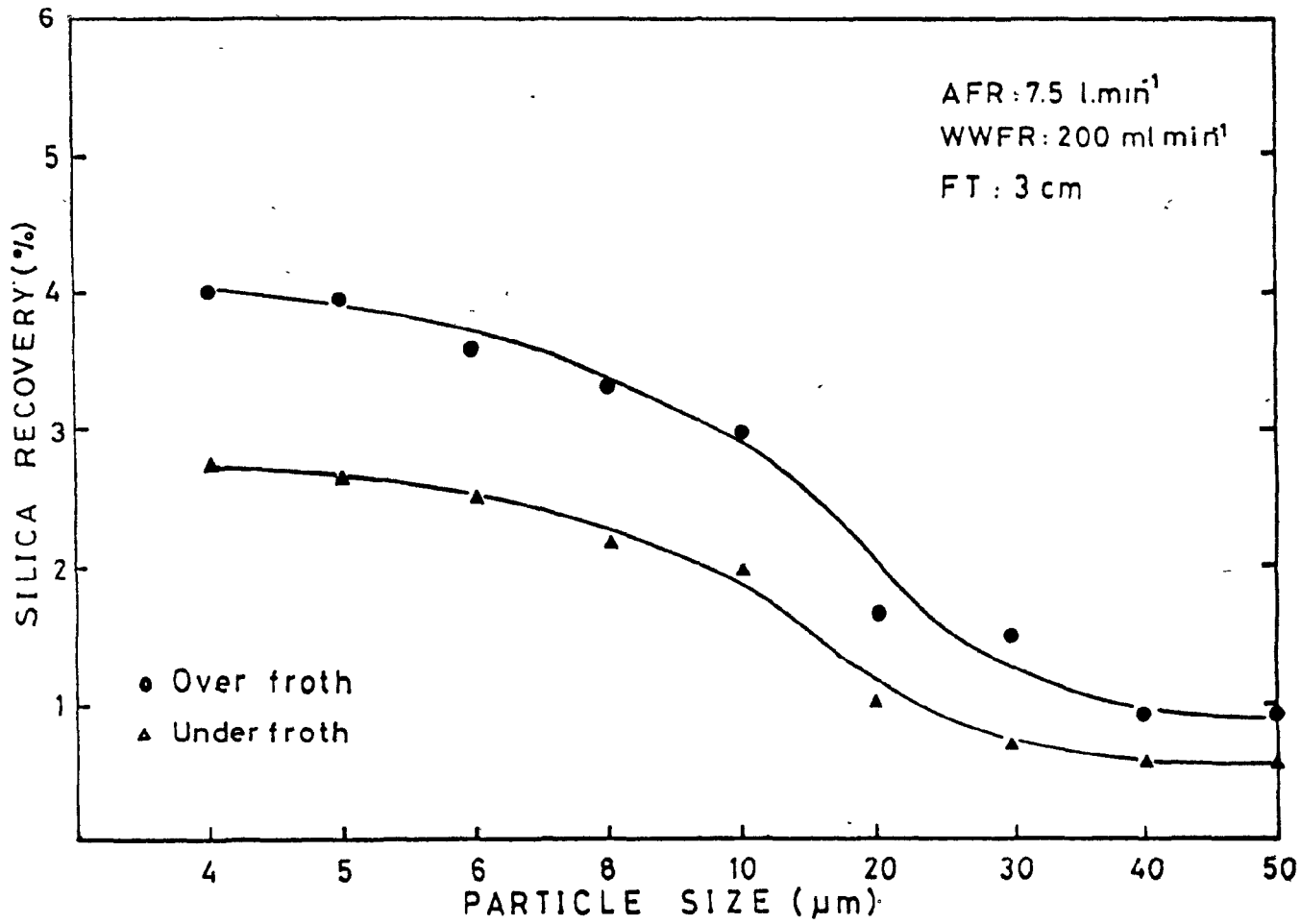

Fig.8.12 Effect of particle size on silica recovery.

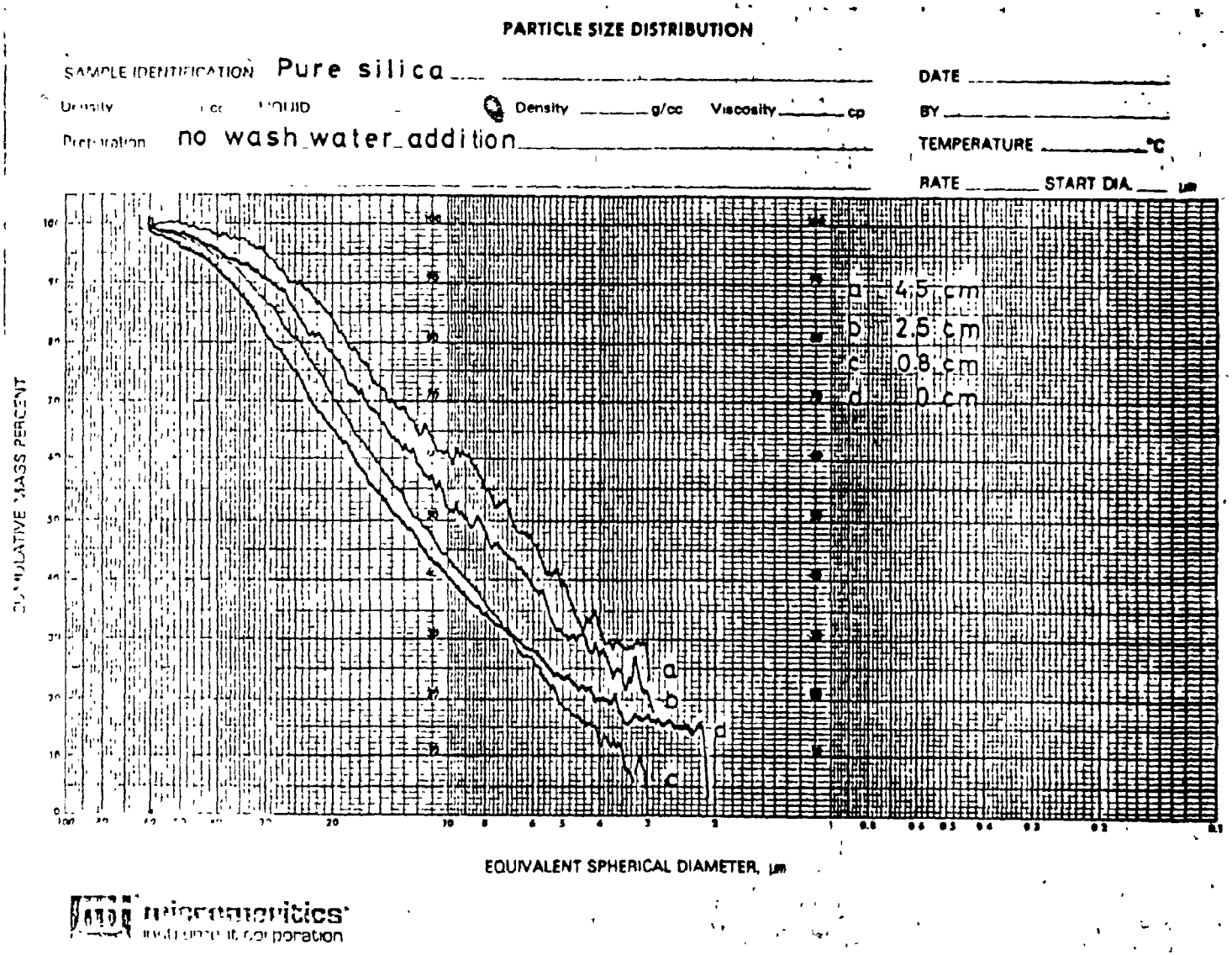

Fig. 8.13 Effect of froth thickness on concentrate size distribution.

water addition flow rates.

8.4 DISCUSSION

Mika and Fuerstenau (1969), and more recently Moys (1978) and Herbst (1982) used the concept that a major proportion of water and nonfloatable fines cross into the froth entrapped in a "boundary layer" of water around the bubble. In flotation the magnitude of this boundary layer is apparently controlled by hydration effects at the air-water interface and by the turbulence levels in the pulp (Herbst, 1982).

Steiner et al (1977) found that a model in which the upward movement of the froth structure as a whole is balanced by the downward in both the plateau borders and the films gives the best agreement with experimental data.

$$Q_u = V_g * (1-\epsilon)/\epsilon \qquad 8.1$$

where Qu is the liquid entrapped in the froth structure and ϵ is the gas holdup.

However, drainage of water from the froth is a complex phenomenon which has received very little attention in flotation and is more difficult to quantify. Steiner et al (1977), and more recently Herbst (1982) calculated the froth drainage for mineralized froth, using the relationship.

$$Q_d = \frac{K * \epsilon^2 * g * r_o^4}{\mu * d_b} \rho \qquad 8.2$$

where Qd is downward flowrate, ϵ the is air holdup, ρ is pulp density, ro is the radius of curvature in the plateau borders, μ is the pulp viscosity, db is the bubble diameter, K is a constant and g is gravity acceleration.

There are two main mechanisms by which silica particles enters the concentrate, natural flotation and entrainment in the water which passes through the froth. The former mechanism is negligible unless surface active reagents are present in the system. A small amount of silica was tested and it was found that the natural flotation contribution, if present, was negligible. Thus, all silica particles are recovered by the latter mechanism.

The findings between silica recovery and FT of the present study can be explained by the particle residence time in the froth phase. As FT increases, residence times of particles increase, and water recovery to the concentrate decreases. Accordingly, particles have a longer residence time and a relatively higher liquid flowrate returns to the slurry phase. Thorne et al (1977) report similar results for galena in the New Broken Hill Consolidated rougher banks.

There is a linear relationship between AFR and water recovery. When AFR increases, superficial gas velocity increases (see Eq. 8.1). Hence, water recovery in

the concentrate also increases. However, the downward water flowrate through the plateau borders (see Eq. 8.2) also increases, and this limits the increase of silica entrainment. The effect of AFR is much more significant at low FTs.

There is a strong correlation between water recovery to the concentrate and hydrophilic particle recovery. This finding agrees very well with Engelbrecht-Woodburn (1975) and Lynch et al (1974), whose results for different pulp densities are shown in (Fig. 8.14).

Bisshop and White (1976) showed that very fine particles remain in the suspension and follow the movement of the water so closely that a linear relationship exists between the recovery rates of water and fine gangue particles. Coarser particles, because of their higher settling velocity, are rejected more readily. The slightly parabolic relationship between the overall rates of recovery of gangue and water is due to the increase in both water recovery and CF with increasing FT. (Fig..8.15).

In most entrainment studies, only the recovery of hydrophilic particles is taken into account. However, hydrophobic particles can also be entrained into the froth. In mixture flotation, it was found that sphalerite recovery is slightly higher than silica recovery without collector addition. The lower sphalerite recovery was attributed to the weak hydrophobicity of sample. The

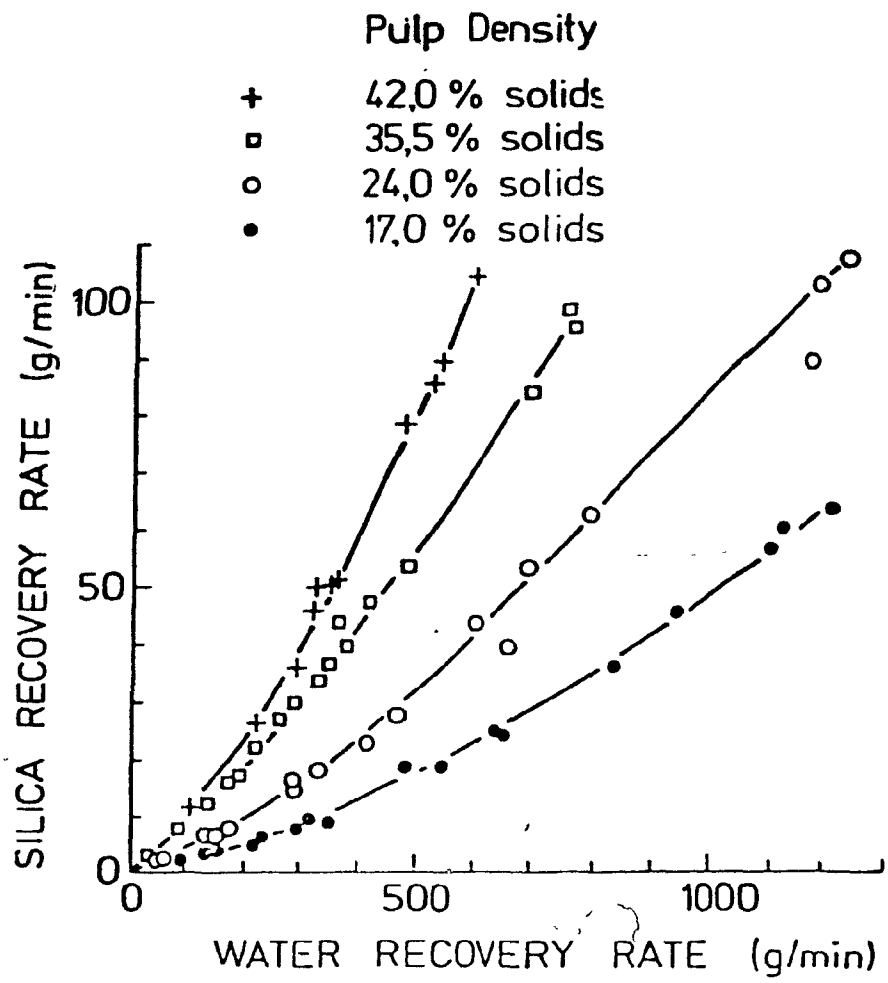

Fig.B.14 Relationship between the recovery rates of silica and water at varying pulp densities in a pilot scale work (from Lynch et al, 1974).

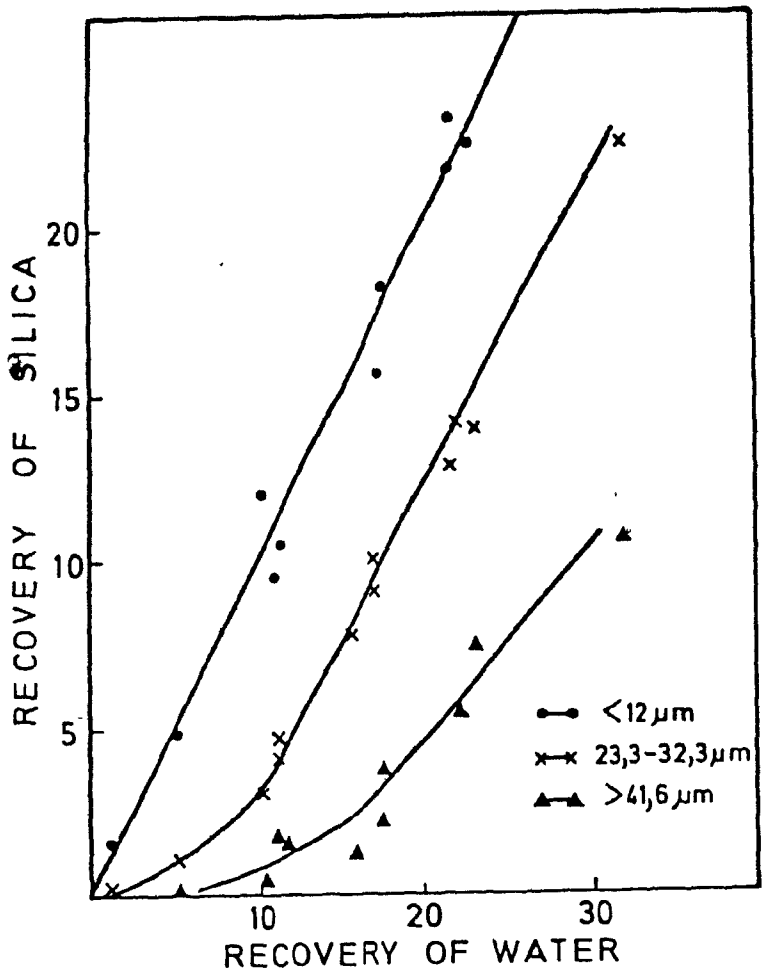

Fig.8.15 Correlation between the recovery of silica and the recovery of water for different sizes (from Engelbrecht-Woodburn, 1975).

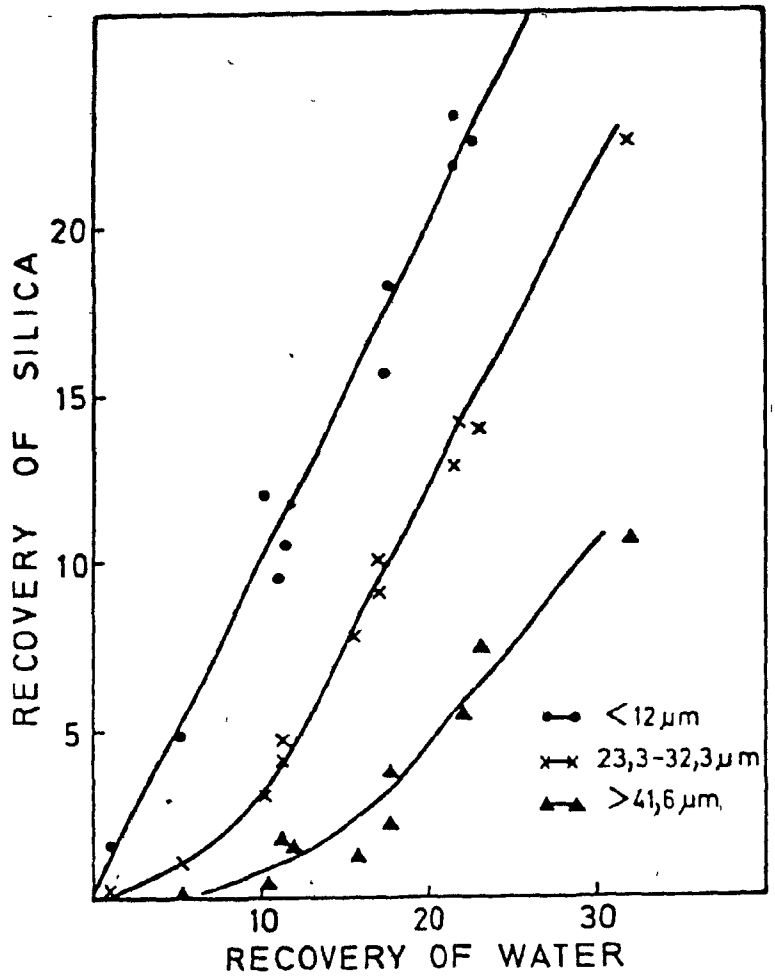

Fig.8.15 Correlation between the recovery of silica and the recovery of water for different sizes (from Engelbrecht-Woodburn, 1975).

higher silica recovery during mixture flotation can be explained by.

a) entrapment in which silica particles are thought to be held in the froth by bridging across floatable particles held by adjoining bubbles.

b) sphalerite stabilisation of the froth and decrease of water drainage, water recovery is therefore greater in the mixture flotation.

c) slime coating is another likely source of gangue associated with mineral mass transfer to the concentrate (Jowett, 1966).

d) presence of locked-silica in sphalerite concentrate.

After realizing the significance of entrainment in conventional flotation, the effect of wash water addition was investigated in mixture and pure silica flotation. Wash water addition was found to be very effective to reduce the entrainment by about 3% out of 9% and 5.5% for the mixture and pure silica systems respectively. A decrease in silica recovery as WWFR increases could be explained by the higher liquid drainage in the froth phase as WWFR increases. Then, different water addition levels were considered. Wash water addition below the froth was more effective in reducing entrainment than addition above the froth. Water recoveries of mixture and pure silica flotation are given in Fig. 8.16. It is obvious that water recovery in the concentrate stream is lower when wash

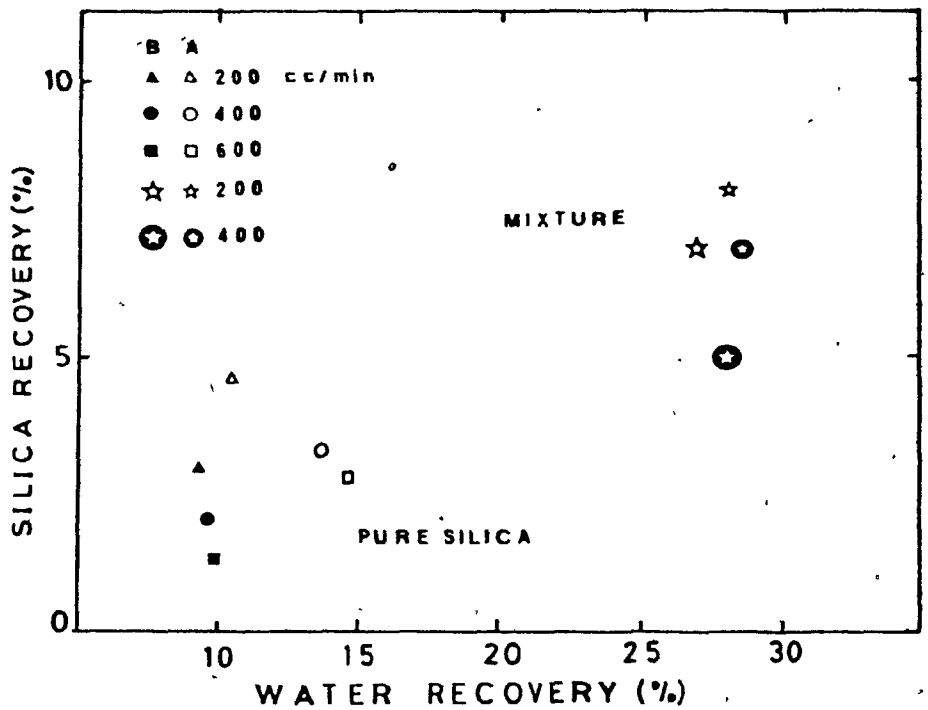

Fig. B.16 Water recoveries of mixture and pure silica flotation (AFR: 7.5 L/min, FI: 3 cm; A: above froth, B: below froth).

water is added below the froth phase close to the slurry-froth interface, especially in the silica system.

Froth grade profiles were investigated by Moys (1977). A typical result is shown in Fig. 8.17 where grades are plotted as a function of distance from the slurry-froth interface. In the slurry phase and close to interface the gangue grade is more than 50%, and that of sphalerite below 5%. If washing water is introduced horizontally close to the interface, some of the gangue particles can be rejected by local dilution of the slurry, without significantly affecting sphalerite recovery. When wash water is added above the froth, the cleaning action takes place in the froth, where silica rejection may be hindered by entrapment. As mentioned earlier, the rise velocity of bubbles in buffer zone is very high, close to the terminal velocity. Sudden wash water spray at the top of buffer zone detaches some of hydrophilic particles from the bubble wakes and then, the possibility that gangue particles reattach to the rising bubbles in this intermediate zone is low. Therefore, they return to the active zone.

A classification matrix CF, was proposed to describe the behavior of gangue in the froth (Johnson et al, 1974). It can be readily included in a mathematical model of the process to describe the behavior of hydrophilic particles:

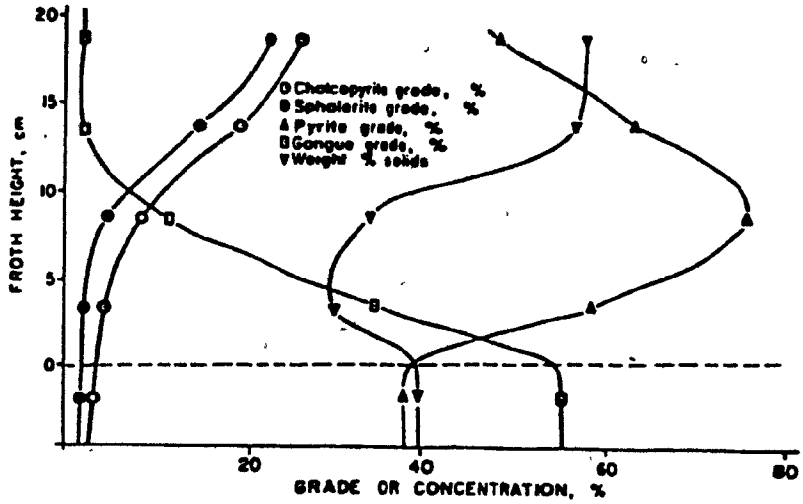

Fig..8.17 Variation of froth profile with froth thickness (from Moys, 1976).

$$CF_i = \frac{\text{weight of gangue per unit weight of water in the conc.}}{\text{weight of gangue per unit weight of water in the pulp}} \quad 8.3$$

Classification matrix values for pure silica flotation at AFR: 7.5 L/min and FT: 3 cm were calculated, and compared with plant results in Fig. 8.18. It is obvious that CF_i decreases slightly with increasing particle size, both for the data of Johnson and the present work. However, it decreases more sharply for plant tests. This difference in CF_i at coarse particle sizes could be related to the different particle residence time in the froth phase, usually much higher in industrial cells.

Similar results related to particle size were also reported by Lynch et. al. (1974) (Fig. 8.19). This size classification of gangue particles in the froth phase suggests that the major drop-back mechanism for gangue particles is liquid drainage between bubbles into the slurry phase which is aided by their settling velocity.

The amount of drainage from the froth is strongly dependent upon the froth residence time. The effect is shown in Fig. 8.20 where the classification function is plotted against particle size at increasing nominal froth residence time. Thus the recovery of gangue mineral can be minimized by controling the variables that affect the residence time in the froth.

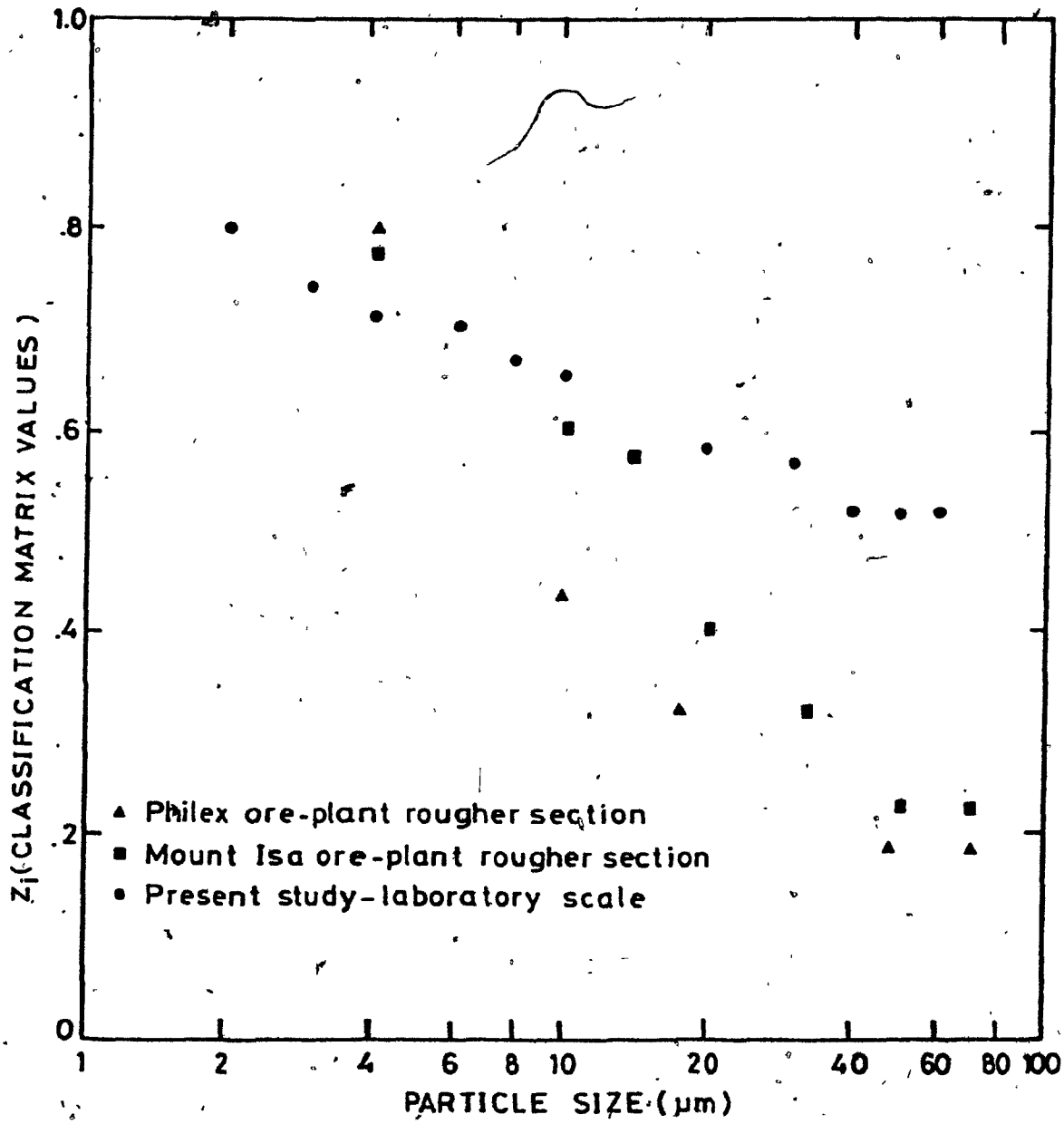

Fig. 8.1B Comparison between laboratory and plant scale flotations with respect to classification function.

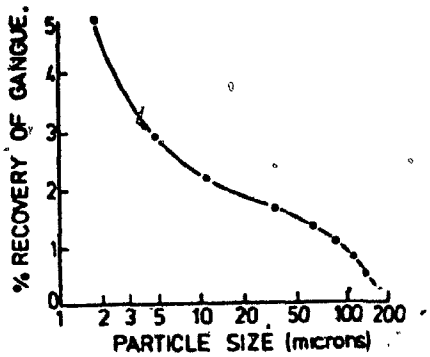

Fig. 8.19 Effect of particle size on gangue recovery in plant scale (from Lynch, 1974).

Fig. 8.20 Effect of froth residence time on classification function (from Thorne et al, 1974).

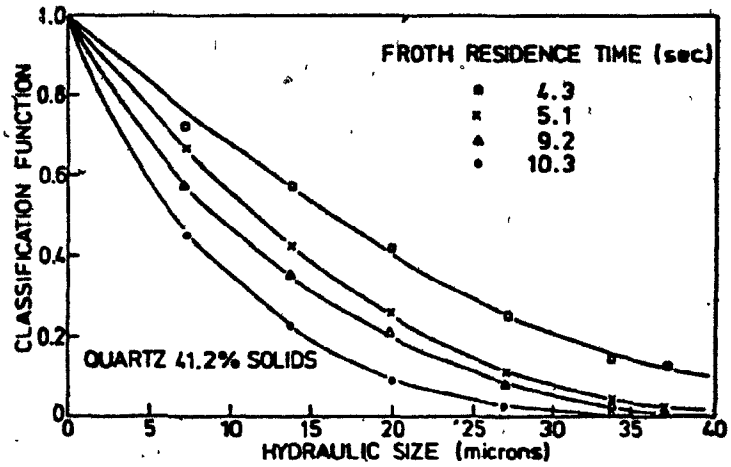

8.5 SUMMARY

The behavior of sphalerite and silica in continuous flotation without collector addition was investigated. A parabolic relationship between the recovery rates of silica and water was observed.

The effect of AFRs, FIs, and wash water additions on water recovery was examined. Results showed that entrainment of hydrophilic silica particles could be reduced by reducing the flow rate of water into the concentrate. Selective drainage of gangue particles from the froth can be achieved in deeper froths or lower AFRs i.e at high froth residence times.

Significant reduction in silica entrainment was also achieved by washing the flotation pulp with a spray of water. Better results were achieved when this spray was located below the slurry-froth interface, rather than above.

There is evidence that silica transported from the pulp to the froth in the water is subjected to hydraulic classification in the froth phase. It was postulated that the major detachment mechanism is a combination of liquid drainage between bubbles in the froth and the particles own settling velocity.

The results of the present work agree very well with previous plant studies. It must be noted that particle entrainment can not be eliminated, but its effect

on concentrate grade can be significantly reduced if proper attention is paid to entrainment and drainage mechanisms.

CHAPTER 9

RESIDENCE TIME DISTRIBUTIONS IN CONTINUOUS FLOTATION

9.1 INTRODUCTION

The last part of the present study will be characterization of mixing conditions and average residence times of the system by tracer techniques.

Pulsed tracer tests were performed with both liquid and solid tracers. Since radioactive tracers provide the most sensitive and the least cumbersome means of measuring the residence time distribution (RTD) in flotation cells. The development and use of a short-lived radioactive tracer method to measure the RTD of continuous flotation process will be described.

9.2 EXPERIMENTAL PROCEDURE

9.2.1 Calculation Procedure

The tracer method is a technique for obtaining information about a system or some part of a system by observing the behavior of a specific substance called tracer that has been added to the system.

An important parameter in many continuous process is the residence time of phases within the system. The

average residence time, τ, is defined as the average time spent by a given phase or material in a reactor. RTDs are experimentally determined using tracer methods. Typically, an impulse amount tracer is added to the feed, and its concentration is measured at tail stream, either by periodical sampling or continuous monitoring at the discharge. When periodical sampling is used, the sampling interval should be kept below 5% of the total sampling time. The RTD is equal to:

$$E(t) = \frac{C(t)}{\int_0^\infty C(t) * dt} \qquad 9.1$$

where E(t): RTD

C(t): tracer concentration

t : time

The mean residence time, τ, is determined from the first moment of the tracer concentration or residence time distribution.

$$\tau = \frac{\int_0^\infty t * C(t) * dt}{\int_0^\infty C(t) * dt} \qquad 9.2$$

If a radiotracer is used to label the material or

phase of interest, then the usual substitution of counting rate for concentration can be made.

$$\tau = \frac{\int_0^\infty t * R * dt}{\int_0^\infty R * dt} \qquad 9.3$$

where R is the counting rate at time t at the tail, or concentrate, stream. The counting rates are related to the radiotracer amount of each samples.

$$R = Y * m \qquad 9.4$$

where R is the counting rate (cps), m is the tracer amount (g) and Y is the counting efficiency.

The RTD of a perfectly mixed system can be expressed by:

$$E(t) = (1/\tau) * \exp(t/\tau) \qquad 9.5$$

and mean residence times

$$\tau = \int_0^\infty t * E(t) * dt \qquad 9.6$$

The amount of radiotracer, A, injected into the

feed stream at time zero can be calculated from:

$$A = \int_0^\infty M_c * C_c * dt + \int_0^\infty M_t * C_t * dt \qquad 9.7$$

where Mc and Mt are concentrate and tail mass flow rates respectively, (cc/min), Cc and Ct are concentrate and tail concentrations respectively, (g/cc) and t is time (min).

9.2.2 Determination of Liquid Residence Time Distribution

Liquid RTDs were detemined using LiCl as a tracer. A problem that is often encountered when using a tracer in a mineral system is adsorption of tracer onto the solids. Prior to the RTD experiments, laboratory adsorption tests were performed with dissolved MnO_2 and LiCl under similar flotation conditions. A reasonably small fraction (<3 %) of LiCl was adsorbed on sphalerite at the end of 2 hrs. However, 24% of dissolved MnO_2 was adsorped during the same time.

LiCl was selected as the liquid tracer because it best satisfied the following requirements:

a) almost inert to the system
b) easily dissolved in water
c) ease of analysis with atomic absorption
d) reasonable cost

Liquid RTDs were measured with a method of tracer impulse injection to the feed stream using a syringe followed by sampling of the tail and concentrate streams over a fixed time period and subsequent tracer analysis of the samples using atomic absorption.

As the time of injection of the tracer material, 1 g, was very short, 10 sec., in comparison to the residence time in the cell, the observed concentration-time curve in the tail stream could reasonably be considered that of a response to a perfect impulse.

Liquid RTDs were investigated at two different AFRs, FTs and wash water addition flowrates. All data were analysed by using the Visicalc computer program and are summarized in Appendix 9.1.

9.2.3 Determination of Solid Residence Time Distribution

In conventional flotation, it is the RTD of solids, not liquid, that is prime of importance. RTDs of solid particles were determined by radioactive tracing. An irradiated $^{56}_{25}Mn$ isotope which emits gamma-rays was chosen as a solid tracer for the following reasons:

a) Safety;

-because the half-life is only 2.58 hours, special disposal procedures are unnecessary.

b) Accuracy of signal;

- detection limitation by the instrument, type and energy of radiation emitted.
- ease of differenciation from background noise.

c) Convenience;

- naturally hydrophilic.
- inert, no adsoption on solids.
- similar specific density to floated product.
- easily produced by neutron bombardment.
- similar size distribution to floated product.

d) Reasonable cost.

The amount of radioactivity used should be small enough to prevent any health hazards but large enough to sufficiently minimize fluctuations in the detector response due to normal counting statistics. Manganese-56 (half-live: 2.58 hrs and gamma-ray energy: 0.85 MeV) is a very commonly used short-lived radioactive tracer produced upon transmutation by neutrons.

The samples, 1 g of MnO_2, were irradiated in the Slowpoke Nuclear Reactor of Ecole Polytechnique, Montreal, for 17 seconds in a thermal neutron flux of 10^{11} neutrons

per square centimeter per second. The decay scheme of $^{56}_{25}Mn$ is shown in Fig. 9.1.

After injection of the activated tracer into the feed stream, discrete samples from the tail and concentrate streams were collected at fixed time intervals. Timing was commenced when the tracer was added. Then, the tracer activity of each sample was determined using a Tennelec Single Channel Scintillation Counter-Detector. For gamma-ray detection, a 7.5 cm dia. by 7.5 cm thick NaI(Tl) scintillation detector set to count all gamma-ray energies greater than some minimum threshold which is dictated by the noise level in the detector system and by the energies at the natural background radiation was used.

The count rate of any sample is directly proportional to the mass of radiotracer. To establish the average concentration of the tracer over the sampling time, t, a simple procedure was used. Constant volume of samples using standard type of containers were collected at constant time intervals.

Sampling was continued over a time that insures the complete passage of the tracer. A blank sample from the cell before tracer addition was collected and analysed for background determination. One tenth of the irradiated tracer was kept as a standard reference counted regularly during the experiment. For the solid RTD tests, the collected samples were weighed, counted, dried and

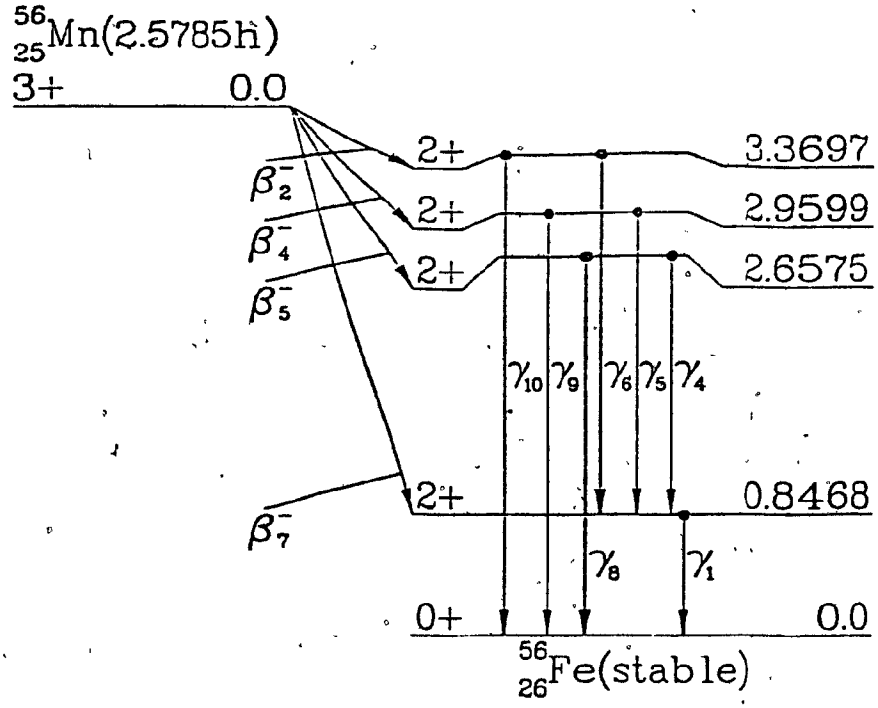

25-MANGANESE-56

HALFLIFE = 2.5785 HOURS 04-MAR-77
DECAY MODE(S): β

RADIATION	y(i) (Bq-s)⁻¹	E(i) (MeV)	y(i)×E(i)
β 2	1.16E-02	9.681E-02*	1.15E-03
β 4	1.46E-01	2.548E-01*	3.72E-02
β 5	2.78E-01	3.815E-01*	1.06E-01
β 7	5.63E-01	1.216E 00*	6.85E-01
γ 1	9.89E-01	8.468E-01	8.37E-01
γ 4	2.72E-01	1.811E 00	4.92E-01
γ 5	1.43E-01	2.113E 00	3.03E-01
γ 6	9.89E-03	2.523E 00	2.49E-02
γ 8	6.53E-03	2.657E 00	1.73E-02
γ 9	3.06E-03	2.960E 00	9.07E-03
γ 10	1.68E-03	3.370E 00	5.66E-03

LISTED X, γ AND γ± RADIATIONS	1.69E 00
OMITTED X, γ AND γ± RADIATIONS**	2.12E-03
LISTED d, ce AND Auger RADIATIONS	8.29E-01
OMITTED d, ce AND Auger RADIATIONS**	7.56E-04
LISTED RADIATIONS	2.52E 00
OMITTED RADIATIONS**	2.88E-03

* AVERAGE ENERGY (MeV)
** EACH OMITTED TRANSITION CONTRIBUTES <0.100% TO Σ(i)×E(i) IN ITS CATEGORY.
IRON 56 DAUGHTER IS STABLE

Fig. 9.1 Decay scheme of radioactive Mn-56.

reweighed.

Occupational hazard during the experiment was controlled by careful tracer handling, experimental design and monitoring techniques.

9.3 RESULTS

The effect of AFR, WWFR and tracer addition point on liquid residence time was characterized. In tracer tests, raw results are usually a plot of Li concentration (ppm) as a function of time. The first step is analyzing these data is the determination of the mean residence time. The RTD of any component is defined as the mass fraction of this component in the tail or concentrate stream which has spent a time between T and T+dt in the system before being removed.

Liquid and solid tracer test results are summarized in Table 9.1. Mean residence time determined from tracer sampling of the tailing, concentrate and dividing the slurry volume by the tailing flow rate. A typical result where Li concentration was plotted as a function of time (test 4) is shown in Fig. 9.2. Perfect mixing is clearly exhibited. Table 9.1 shows that mean residence time calculated from the tail stream is slightly smaller than the mean residence time calculated from concentrate stream. The mean residence time calculated from the tailing flowrate is between that of tail and

	TEST 1	TEST 2	TEST 3
	AFR: 5 L/min WWFR: 0 L/min FT: 3 cm	AFR: 7.5 L/min WWFR: 0 L/min FT: 3 cm	AFR: 5 L/min WWFR: 1200 L/min FT:3 cm
TAIL	3.83	4.06	3.47
CONC.	4.04		
T.F.R.	3.95	4.09	3.51

	TEST 4	TEST 5
	AFR: 7.5 L/min WWFR: 400 L/min FT: 3 cm Feed	AFR: 7.5 L/min WWFR: 400 L/min FT: 3 cm W.Water
TAIL	3.88	3.85
CONC.	4.04	3.89
T.F.R.	3.88	3.88

	TEST 6	TEST 7
	AFR: 5 L/min WWFR: 0 L/min FT: 3 cm	AFR: 5 L/min WWFR: 1200 L/min FT: 0 cm
TAIL	3.76	2.97
CONC.		2.95
T.F.R.		2.95

AVERAGE RESIDENCE TIME DETERMINED FROM TRACER SAMPLING OF THE CONCENTRATE (CONC.), TAILING (TAIL), OR DIVIDING THE SLURRY VOLUME BY TAILING FLOWRATE (T.R.F.).

TEST 1 TO 5 LIQUID RTD TESTS

TEST 6 AND 7 SOLID RTD TESTS

TABLE 9.1

Solid and liquid RTD results

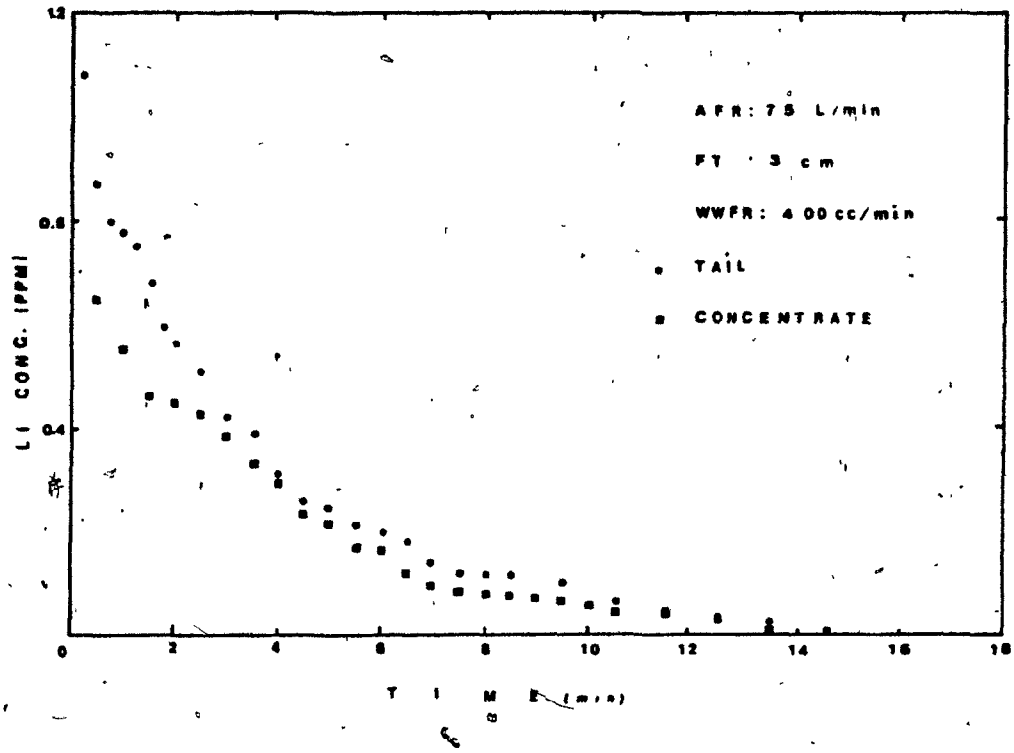

Fig. 9.2 Liquid RTD for tail and concentrate streams.

Fig. 9.3 Effect of froth thickness on liquid RTD.

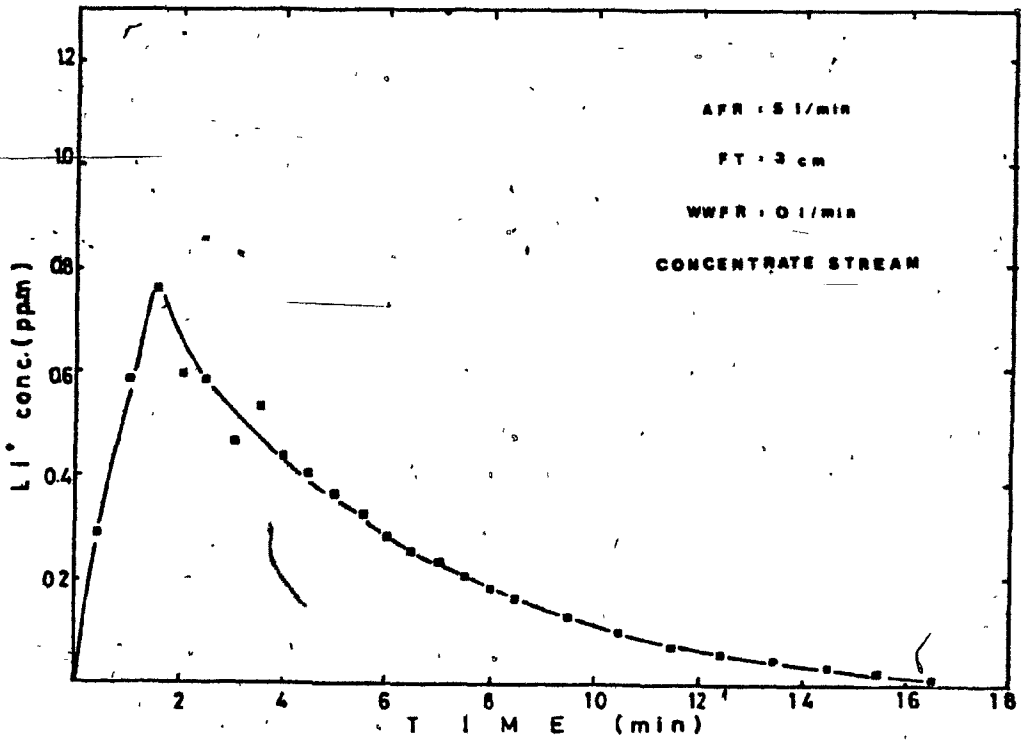

concentrate streams. The slightly higher mean residence time for the concentrate stream can be attributed to the presence of a froth phase. Since part of the liquid tracer drains back to the slurry between bubbles, the residence time of the liquid also increases slightly. A slightly lower concentration for the concentrate stream can be explained by a high wash water addition flowrate which provides a negative bias.

As can be seen from Fig. 9.3, there is some deviation from the perfectly mixed system at a froth thickness of 3 cm. During this experiment wash water was not added, therefore the transport of liquid from the froth into the concentrate stream was not very fast. This may be the main reason for the shift in count peak.

It was found that the liquid residence time slightly increases with increasing AFR (test 1 and test 2). The relationship between Li concentration against time at two different wash water addition flow rates (test 1 and 3; test 2,4 and 5) is shown in Fig. 9.4. The liquid residence time decreases with increasing wash water addition flow rate due to dilution of the tracer. Thus the higher the WWFR, the less the liquid residence time in the system.

Lastly, the effect of tracer addition level was also investigated. Tracer was firstly injected to the feed stream, then to the wash water stream added below the froth phase. In both cases similar mean residence times

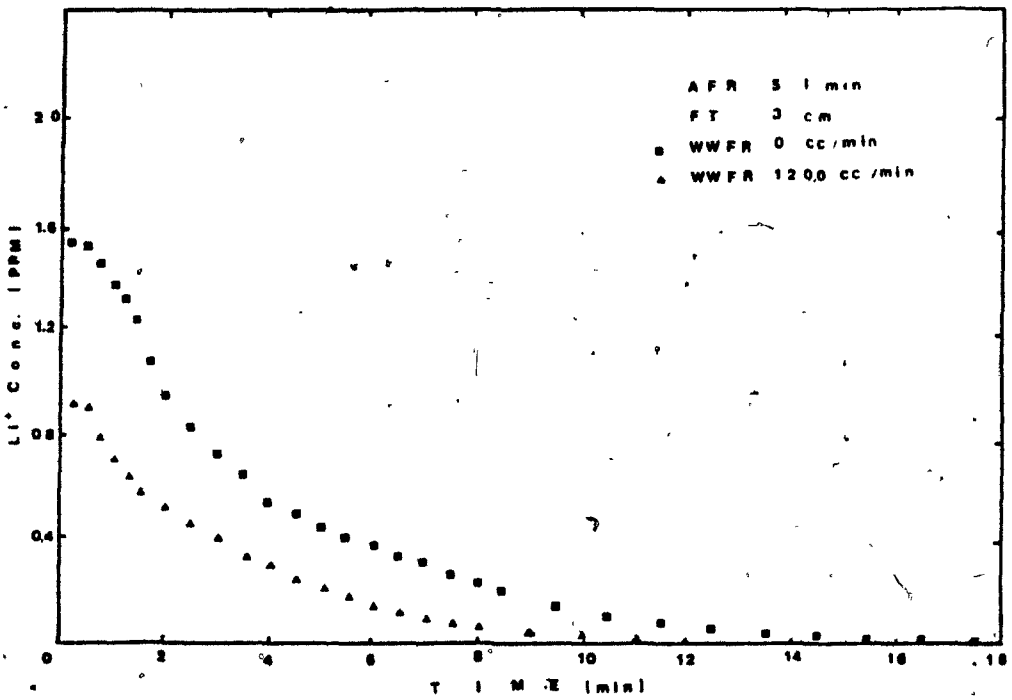

Fig. 9.4 Effect of WWFR on liquid RTD.

Fig. 9.5 Effect of tracer addition point on liquid RTD.

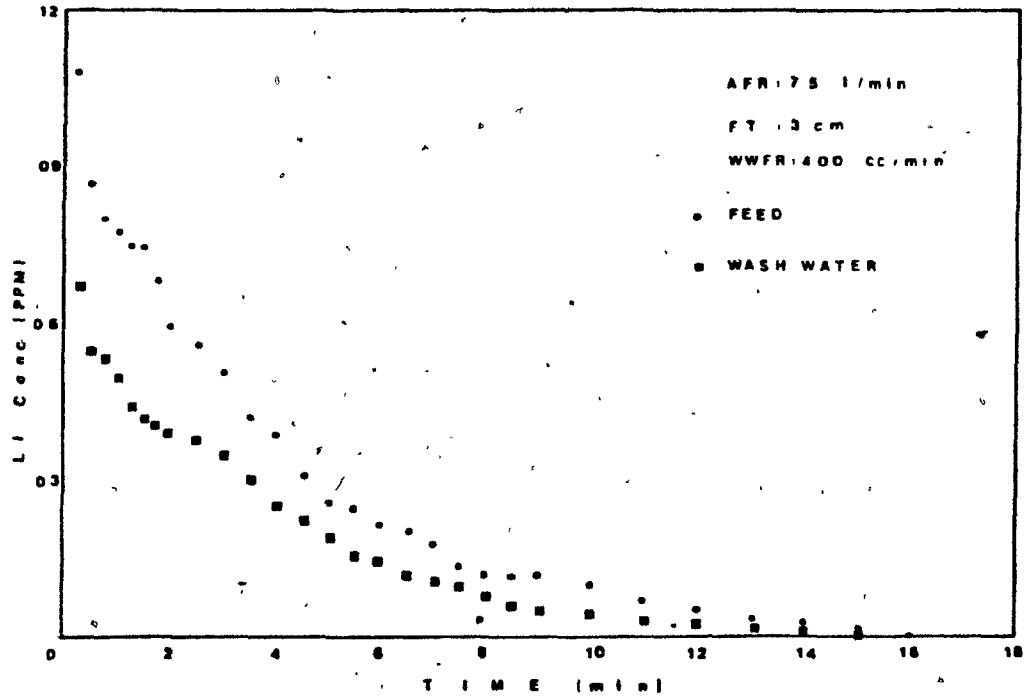

were obtained. This indicates that wash water added below the froth does not short circuit to the concentrate stream, and mixes perfectly with the cell content (Fig. 9.5). Wash water and feed water split 53% and 33% to the concentrate stream and 47% and 67% to the tail stream respectively.

The result and calculation procedures of solid residence time are given in Appendix 9.2. It was found that the FRC of manganese was very low, 0.009 1/min. Therefore, it was neglected for all calculations.

Similar mean residence times were found for tail and concentrate streams. A slightly lower solid residence time (test 1 and 6) can be attributed to the density difference between liquid and solid phases which facilitates solid recovery in the tail stream. Presence of a froth phase without wash water addition showed a higher solid residence time than without froth phase and wash water addition (test 6 and 7). In the presence of wash water addition, very close mean solid residence times were obtained from tail and concentrate streams. Figs. 9.6 to 9.8 show the linearized counting rates for solid RTD tests. Tail streams fit very well to a straight line. For concentrate stream, the fit is not as good as tail stream.

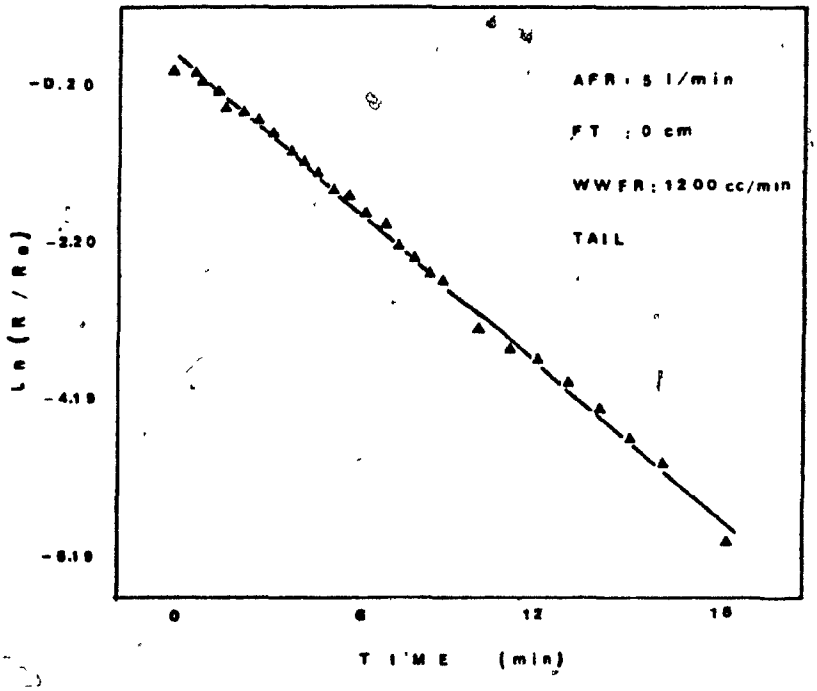

Fig. 9.6 Solid RTD of tail stream.

Fig. 9.7 Solid RTD of concentrate stream.

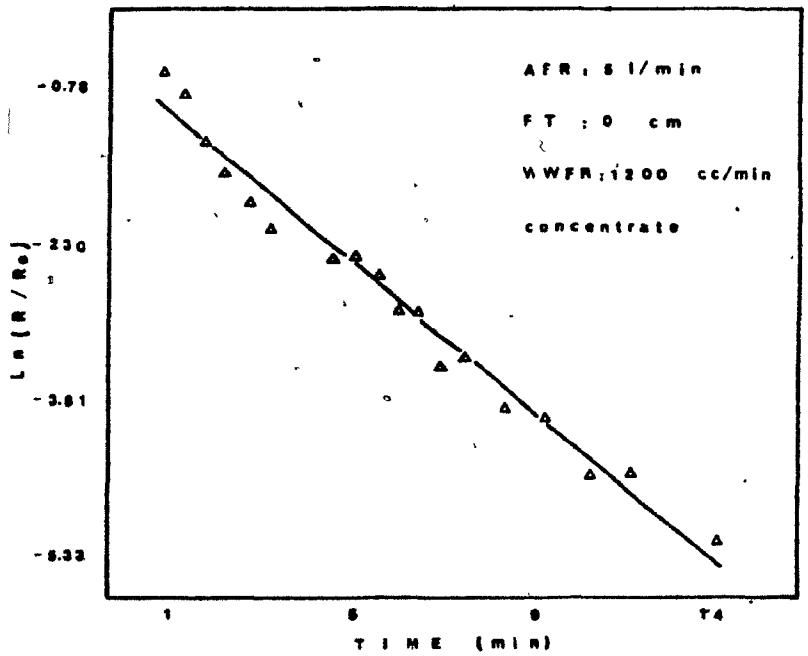

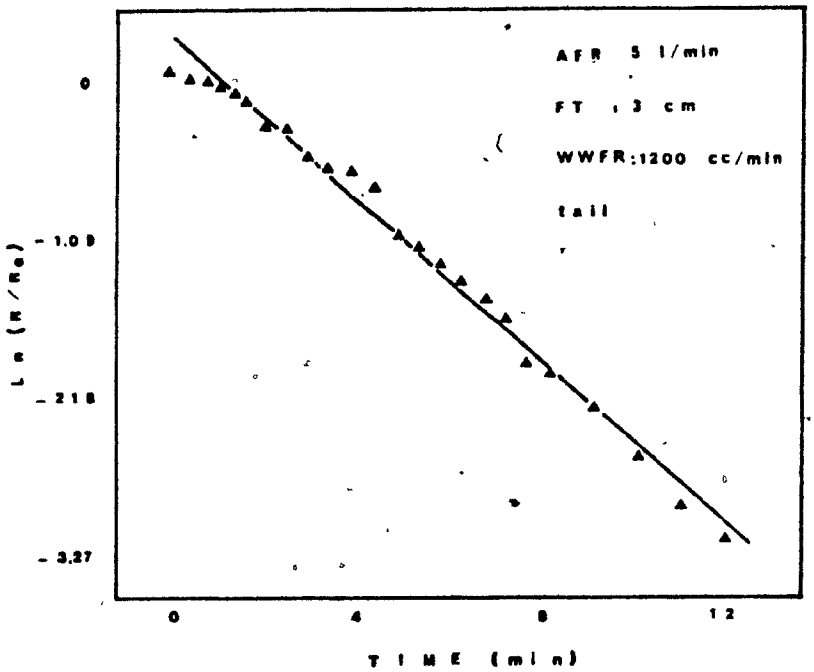

Fig. 9.8 Solid RTD of tail stream with wash water addition.

9.4 DISCUSSION

An ideal mixer may be defined as a stirred cell in which an increment of slurry feed is immediately dispersed uniformly throughout the cell; it follows that the tail stream must have the same composition as the pulp in the cell.

It is apparent from the results presented that the cell behaves very close to an ideal mixer as far as liquid and solid phases are concerned.

Mean liquid residence time calculated from the tail, concentrate streams or tail flow rate are in very close agreement. A slightly higher mean residence time calcutated from concentrate stream is caused by presence of a froth phase which has its own residence time. Wash water addition below the slurry-froth interface decreases the mean RTD.

The effect of AFR on the liquid residence time is mainly related to liquid drainage. As AFR increases the amount of water carried to the froth increases, but the amount of water drainage to the slurry phase also increases. Therefore, a slightly higher liquid residence time is obtained at higher AFRs.

Experiments done with and without a froth phase showed that liquid residence times are significantly affected by the presence of a froth phase due to water drainage effect. Liquid residence time also decreases with

increasing wash water addition flow rate.

Addition of tracer either from the feed or wash water stream showed that the system was perfectly mixed. This implies that wash water added below the froth is not short circuited to the concentrate stream.

One of the main assumptions in the slurry-froth kinetics study of chapter 6 was the slurry phase behaved as a perfectly mixed system with respect to the solid phase. Radioactive tracer tests confirmed this assumption. Mean solid residence time calculated from tail and concentrate streams are similar when there is no froth phase and wash water addition. The mean residence time calculated from the tail flow rate and mass of solid in the pulp in chapter 6 is very close to the mean residence time found from radiotracer tests. Therefore, it is reasonable to use the tail flow rate for calculating solid residence time in perfectly mixed flotation systems.

A slightly lower mean solid residence time than liquid can be attributed to the wash water addition. It is interesting to point out the fact that specific density does not play a very significant role. Since the tracer addition point to the cell is 10 cm above the tail discharge outlet. Therefore, the distance from feed inlet to the tail discharge outlet is not long enough to enhance the settling velocity effect. But, in an industrial flotation column, a very significant particle size effect was reported by Dobby (1984). He found that when particle

size increased from 20 to 100 μm particle residence time dropped from 12 to 6 minutes.

The recovery and flotation rate constant of solid tracer are about 2.5% and 0.009 1/min respectively. The experimental conditions were AFR: 5 L/min, FT: 0 cm and WWFR: 1200 cc/min. An experiment done with only pure silica at similar conditions except for WWFR of 600 cc/min showed 2.1 % silica recovery. As discussed previously, the presence of sphalerite increases silica recovery in mixture flotation. The recovery of Mn in radioactive tracer tests is very close to the silica recovery in mixture flotation, indicating a similar behavior.

9.5 SUMMARY

The mixing behavior and average residence time of the flotation cell has been experimentally investigated by using the conventional stimulus-response technique.

Continuous flotation done in the designed cell with modified Denver flotation machine behaves as a perfectly mixed system as far as liquid and solid phases are concerned.

The RTDs of liquid and solids have been found identical if there is no wash water addition under similar operating conditions. Addition of wash water decreases liquid residence time more significantly than solid residence time. The liquid residence time can be also

significantly altered by charging the froth thickness.

Different tracer addition points revealed that the system was perfectly mixed and there was no short circuiting of the material either to concentrate or tail stream

CHAPTER 10

CONCLUSIONS

10.1 EFFECT OF AIR FLOW RATE ON SEMI-BATCH FLOTATION

The particular design of the flotation cell used for this work made it possible to remove the froth as soon as it was formed, therefore directly measuring the material removal rate from the slurry. To characterize the effect of AFR on the kinetics of flotation in the slurry phase, the FRC was measured at different AFRs. In all initial pulp densities, the FRC first increased as AFR increased, Reaching a maximum after which further increases of AFR caused the FRC to decrease. The existence of the maximum FRC in semi-batch flotation had been previously recognized by Laplante (1980).

Harris (1974) reported the existence of an optimum AFR range above which recovery decreases. He attributed this phenomenon to a decrease in agitation efficiency, which caused coarser particles to settle to the bottom of the cell. From the present study no evidence of sedimented coarse particles was found at high AFR. In this work, the calculation of the FRC excluded unfloated, i.e. settled, material.

From the present study, it can be concluded that the effect of AFR on the FRC can be attributed to the increased average bubble size resulting from an increase

in AFR. This increase in average size decreases collection efficiency, as theoretically derived and experimentally verified by other researchers.

It was found that the representation of actual flotation conditions by using single bubble-particle system which did not take into account the hindered effect of bubbles and hydrodynamic conditions of perfectly mixed conventional flotation cells was difficult.

The effect of initial pulp density on the transfer of material from the slurry to the froth is small if the bubble surface is not saturated with hydrophobic particles.

10.2 EFFECT OF AIR FLOW RATE AND FROTH THICKNESS ON CONTINUOUS FLOTATION

The combined effect of AFR and FT on continuous flotation of sphalerite showed that the DBC increased as FT or AFR increased. However the contribution of the cell design and froth removal efficiency from the top of the froth were found to be more significant than AFR or FT. It was confirmed that the major drop-back mechanism was caused by bubble coalescence and collapse reducing the total bubble surface, and was essentially particle-size independent.

It was found that FTC increased as FT decreased or AFR increased. The ORC was also found to increase as AFR increased whereas it decreased as FT increased.

The result of present study indicated that particle size did not play very significant role in the froth transfer. There is little or no hydraulic classification of hydrophobic particles in the froth. The size-by-size flotation behavior of sphalerite indicated that there was a peak in flotability at an intermediate particle size (20-28 μm), reported in other studies.

10.3 ENTRAINMENT AND RESIDENCE TIME DISTRIBUTIONS

An extensive entrainment study showed that entrainment of hydrophilic silica could be reduced by reducing the water flow into the concentrate stream. A definite FT has to be maintained to allow "cleaning" of the floated material to take place. Hydraulically entrained gangue particles will tend to escape with the draining liquid. It was found that an increasing AFR did not result in significant increase in entrainment as expected, because of the increase in liquid drainage back to the slurry. It was postulated that the major drop-back mechanism for gangue particles is the liquid drainage in the froth phase aided by the particle own settling velocity.

An additional reduction in entrainment was achieved by washing the flotation pulp with a spray of water. Better results were obtained when this spray was located below the froth phase.

Both liquid and solid RTD studies showed that the continous flotation could be modelled as perfecly mixed system. The presence of FT and wash water addition significantly affects the liquid residence time. The RTDs of liquids and solids were similar if there was no wash water addition.

APPENDIX 1

BUBBLE DIAMETER (mm)	COUNTS AT DIFFERENT AIR FLOW RATES (L/min) 1.3	2.55	3.75	5	6.25
.5	329	18	3	1	0
1	88	300	78	26	34
1.5	36	22	25	0	12
2	759	481	190	320	185
3	99	306	239	452	360
4	60	183	120	256	390
5	2	1	11	11	20
6	0	1	4	3	6
TOTAL	1373	1312	670	1069	1007
S.B.S. (1/mm)	2.38	1.96	1.79	1.78	1.65
T.B.S. (cm/min)	30925.81	50009.70	67108.38	89043.10	103018.3
Rb (mm)	1.26	1.53	1.67	1.68	1.82
Ln(Rb)	0.23	0.43	0.51	0.52	0.60

S.B.S.: Specific bubble surface, (1/min)

T.B.S.: Total bubble surface produced per unit time, (cm/min)

K: Correction factor, 1

Rb: Average bubble radius (mm)

Bubble size distribution results

APPENDIX 2

a) Measurement of gas holdup in the slurry phase;

These measurements were performed by bubbling gas through the flotation cell, originally completely filled with water. The gas holdup equals the quantity of water overflow that could be easily gathered and measured. Since the displaced amount is equal to the gas volume in the slurry phase, gas holdup can be calculated by;

$$\epsilon g = Vgas/Vcell \qquad (1)$$

where ϵg: gas holdup in the slurry phase (dimensionless)

Vgas: volume of gas in the slurry phase (cm^3)

Vcell: cell/slurry volume (cm^3).

b) Calculation of superficial gas velocity;

$$Vg = Q/Acell \qquad (2)$$

where Vg: superficial gas velocity (cm/s)

Q: AFR (cm^3/s)

Acell: Cell surface area (cm^2)

c) Calculation of average bubble residence time;

$$\tau = Vgas/Q \qquad (3)$$

where τ: average bubble residence time.

d) Calculation of average bubble rise velocity;

The mean rise velocity of the bubbles in a bubble swarm is equivalent to the interstitial gas velocity which follows from the superficial gas velocity (Shah et al., 1982).

$$Vr = Vg/\varepsilon g \qquad (4)$$

where Vr: average bubble rise velocity.

e) Calculation of average liquid-gas interfacial area;

From the gas holdup in the slurry and average bubble diameter, the specific interfacial area can be calculated as; (Shah et al., 1982)

$$a = Vgas/dav \qquad (5)$$

where a: liquid-gas interfacial area (cm^2)

Vgas: gas volume in the slurry phase, (cc)

dav: mean bubble diameter, (cm)

APPENDIX 3

AFR (L/min)	Vg (cm/s)	Vgas (cm^3)	εg (%)	τ (s)	Vr (cm/s)	Rb (mm)	a (cm^2)
0.50	0.04	77.00	1.17	9.24	3.16		
0.61	0.05	78.20	1.19	7.69	3.79		
1.30	0.10	85.00	1.30	3.90	7.43	1.16	366.38
2.55	0.19	163.20	2.49	3.84	7.59	1.53	533.33
3.75	0.28	195.00	2.97	3.12	9.34	1.67	583.83
5.00	0.37	225.00	3.43	3.06	10.80	1.68	669.64
6.25	0.46	312.50	4.76	3.00	9.72	1.82	858.52
7.50	0.56	360.00	5.49	2.88	10.12		

Vg: Superficial gas velocity

Vr: Bubble rise velocity

Vgas: Gas volume in the slurry phase

εg: Gas holdup in the slurry phase

τ: Gas residence time in the slurry phase

Rb: Bubble radius

a: Gas-liquid interfacial area

Cell volume: 6560 cm^3

Cell cross section: 225 cm^2

APPENDIX 4.1

CALCULATION OF THE FRC IN SEMI-BATCH FLOTATION:

At constant AFR and cell volume, flotation can be compared to a first-order kinetics chemical reaction. The rate constant can be expressed in the form :

$$y = -dc/dt = K * C \qquad 1$$

where C: concentration of certain species in the slurry at time t.

K: FRC (1/min)

n: order of the reaction (in this case 1)

y: rate of disappearence of flotable mineral by flotation.

Integration of eq.1 leads to

$$C = C_0 * \exp(-Kt) \qquad 2$$

where Co is the initial charge. For graphical representation, this can be rewritten as;

$$Ln(C/C_0) = -Kt \qquad 3$$

where C= M/V, M is mass and V is volume. Since V is

constant throughout the experiments, this formulation can be simplified by using only the weight of floatable solid. Therefore,

$$y = W_{cl} / W_o = \exp(-Kt) \qquad 4$$

where Wo is initial charge, Wcl is the mass of floatable mineral in the cell at time t.

Taking into account only floatable mineral after prolonged flotation time,

$$(W_{cl} - W_{\infty}) \quad (W_o - W_{\infty})\exp(-Kt) \qquad 5$$

where W_{∞} contains both the remaining material mass in the pulp and experimental losses after an infinite flotation time.

A plot of $Ln((Wcl-W_{\infty})/(Wo-W_{\infty}))$ versus time in second on a semilog paper will result in a straight line with a slope of $-K/(2.303*60)$, if first order equation applies. The FRC in 1/min is given by;

$$-(\text{slope}) * (60 * 2.303) \quad 1/\text{min} \qquad 6$$

In this case recovery can be calculated by using the following equation.

$$R = R_{\infty} (1-\exp(-Kt)) \qquad 7$$

APPENDIX 4.2

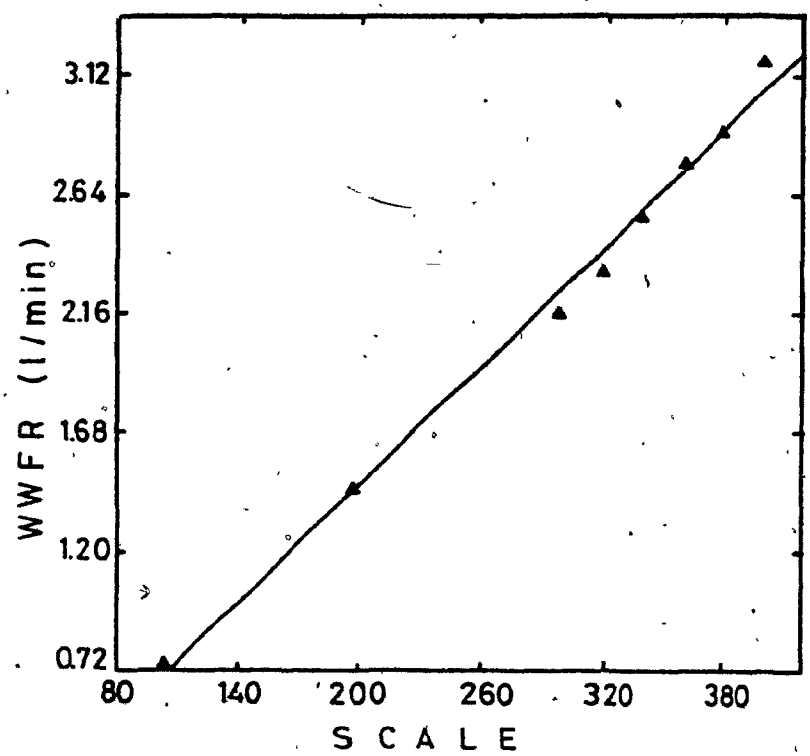

Wash water flowmeter calibration (Temp. 20° C)

APPENDIX 4.3

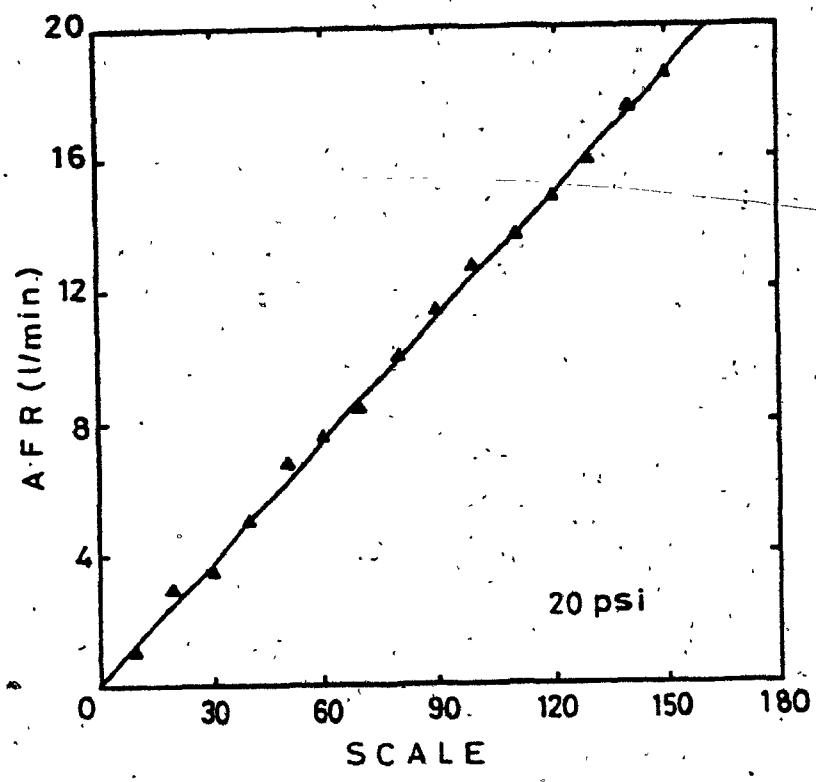

Gas flowmeter calibration

TEST NO: 1 AFR: 6.25L/min WWFR: 3 L/min

TIME (s)	Wc (g)	Wcl (g)	Wcl-Woo	Wcl-Woo / Wo-Woo	Ln(Wcl-Woo) / (Wo-Woo)
10	53.72	146.28	135.05	0.72	-0.33
20	22.17	124.11	112.88	0.60	-0.51
30	19.36	104.75	93.52	0.50	-0.70
40	13.07	91.68	80.45	0.43	-0.85
50	10.05	81.63	70.40	0.37	-0.99
60	10.81	70.82	59.59	0.32	-1.15
70	6.38	64.44	53.21	0.28	-1.27
90	13.46	50.98	39.75	0.21	-1.56
110	9.25	41.73	30.50	0.16	-1.82
130	7.60	34.13	22.90	0.12	-2.11
150	4.97	29.16	17.93	0.09	-2.35
170	4.54	24.62	13.39	0.07	-2.65
200	2.78	21.84	10.61	0.06	-2.88
220	4.01	17.83	6.60	0.03	-3.35
310	4.43	13.40	2.17	0.01	-4.47
REMAINING	2.17	11.23	0	0.00	
LOSS.	11.23				

SLOPE : -.00584 INTERCEPT:-.131 VARIANCE: .000606
FRC (slope * 2.303 * 60) : .81 L/MIN

TEST NO: 2 AFR: 6.25L/min WWFR : 3 L/min

TIME (s)	Wc (g)	Wcl (g)	Wcl-Woo	Wcl-Woo / Wo-Woo	Ln(Wcl-Woo) / (Wo-Woo)
10	50.69	149.31	136.63	0.73	-0.32
20	27.41	121.9	109.22	0.58	-0.54
30	24.20	97.7	85.02	0.45	-0.79
40	17.50	80.2	67.52	0.36	-1.02
50	12.15	68.05	55.37	0.30	-1.22
60	9.54	58.51	45.83	0.24	-1.41
70	6.89	51.62	38.94	0.21	-1.57
90	10.89	40.73	28.05	0.15	-1.90
110	7.01	33.72	21.04	0.11	-2.19
130	4.99	28.73	16.05	0.09	-2.46
150	3.47	25.26	12.58	0.07	-2.70
170	2.57	22.69	10.01	0.05	-2.93
190	1.86	20.83	8.15	0.04	-3.13
220	2.26	18.57	5.89	0.03	-3.46
280	3.86	14.71	2.03	0.01	-4.52
340	2.03	12.68	0		
REMAINING	3.55				
LOSS	9.13				

SLOPE : -.006084INTERCEPT:-1959 VARIANCE: .003428
FRC (slope * 2.303 * 60) : 0.84 l/min

TEST NO: 3 AFR: 6.25L/min WWFR:2.75 L/min

TIME (s)	Wc (g)	Wcl (g)	Wcl-Woo	Wcl-Woo / Wo-Woo	Ln(Wcl-Woo) / (Wo-Woo)
10	3.74	196.26	146.59	0.98	-0.03
20	17.14	179.12	129.45	0.86	-0.15
30	16.53	162.59	112.92	0.75	-0.29
40	10.79	151.8	102.13	0.68	-0.39
50	10.20	141.6	91.93	0.61	-0.49
60	8.63	132.97	83.3	0.55	-0.59
80	15.58	117.39	67.72	0.45	-0.80
100	11.47	105.92	56.25	0.37	-0.98
120	9.45	96.47	46.8	0.31	-1.17
140	9.38	87.09	37.42	0.25	-1.39
160	7.05	80.04	30.37	0.20	-1.60
180	6.33	73.71	24.04	0.16	-1.83
200	5.59	68.12	18.45	0.12	-2.10
290	18.45	49.67	0	0.00	
REMAINING	35.00				
LOSS	14.67				

SLOPE : -.00442 INTERCEPT:-.0197 VARIANCE: .003428

FRC (slope * 2.303 * 60) : 0.61 l/min

TEST NO: 4 AFR: 6.25L/min WWFR:3.2 L/min

TIME (s)	Wc (g)	Wcl (g)	Wcl-Woo	Wcl-Woo / Wo-Woo	Ln(Wcl-Woo) / (Wo-Woo)
10	9.93	190.07	145.16	0.94	-0.07
20	9.67	180.4	135.49	0.87	-0.14
30	11.29	169.11	124.2	0.80	-0.22
40	11.32	157.79	112.88	0.73	-0.32
50	10.89	146.9	101.99	0.66	-0.42
60	9.72	137.18	92.27	0.59	-0.52
80	15.06	122.12	77.21	0.50	-0.70
100	12.49	109.63	64.72	0.42	-0.87
120	11.70	97.93	53.02	0.34	-1.07
140	8.83	89.1	44.19	0.28	-1.26
160	7.77	81.33	36.42	0.23	-1.45
180	7.37	73.96	29.05	0.19	-1.67
200	6.05	67.91	23	0.15	-1.91
220	5.24	62.67	17.76	0.11	-2.17
310	17.76	44.91	0		
REMAINING	30.18				
LOSS	14.73				

SLOPE : -.00416 INTERCEPT:-.0318 VARIANCE: .000139

FRC (slope * 2.303 * 60) : 0.57 l/min

TEST NO: 5 AFR: 6.25L/min WWFR:2.35 L/min

TIME (s)	Wc (g)	Wcl (g)	Wcl-Woo	Wcl-Woo / Wo-Woo	Ln(Wcl-Woo) / (Wo-Woo)
10	16.55	183.45	130.5	0.89	-0.12
20	12.56	170.89	117.94	0.80	-0.22
30	10.94	159.95	107	0.73	-0.32
40	9.07	150.88	97.93	0.67	-0.41
50	8.82	142.06	89.11	0.61	-0.50
60	5.93	136.13	83.18	0.57	-0.57
80	13.14	122.99	70.04	0.48	-0.74
100	11.26	111.73	58.78	0.40	-0.92
120	8.60	103.13	50.18	0.34	-1.08
140	8.36	94.77	41.82	0.28	-1.26
160	7.20	87.57	34.62	0.24	-1.45
180	5.37	82.20	29.25	0.20	-1.61
200	5.38	76.82	23.87	0.16	-1.82
220	4.72	72.10	19.15	0.13	-2.04
240	2.28	69.82	16.87	0.11	-2.17
330	16.87	52.95	0		
REMAINING	40.03				
LOSS	12.92				

SLOPE : -.00377 INTERCEPT:-.01875 VARIANCE: .00005

FRC (slope * 2.303 * 60) : 0.52 l/min

TEST NO: 6 AFR: 6.25L/min WWFR:3 L/min

TIME (s)	Wc (g)	Wcl (g)	Wcl-Woo	Wcl-Woo / Wo-Woo	Ln(Wcl-Woo) / (Wo-Woo)
10	8.72	191.28	143.51	0.94	-0.06
20	8.96	182.32	134.55	0.88	-0.12
30	8.92	173.4	125.63	0.83	-0.19
40	7.76	165.64	117.87	0.77	-0.26
50	7.63	158.01	110.24	0.72	-0.32
60	7.49	150.52	102.753	0.67	-0.39
80	14.37	136.15	88.383	0.58	-0.54
100	11.50	124.65	76.883	0.51	-0.68
120	11.33	113.32	65.55	0.43	-0.84
140	10.05	103.27	55.50	0.36	-1.01
160	8.65	94.62	46.85	0.31	-1.18
180	7.70	86.92	39.15	0.26	-1.36
200	7.33	79.59	31.82	0.21	-1.57
220	6.17	73.42	25.65	0.17	-1.78
240	5.61	67.81	20.04	0.13	-2.03
330	20.04	47.77	0		
REMAINING	28.47				
LOSS	19.30				

SLOPE : -.00266 INTERCEPT:-.03 VARIANCE: .00262

FRC (slop * 2.303 * 60) : 0.37 l/min

TEST NO: 7 AFR: 6.25L/min WWFR:2.65 L/min

TIME (s)	Wc (g)	Wcl (g)	Wcl-Woo	Wcl-Woo / Wo-Woo	Ln(Wcl-Woo) / (Wo-Woo)
10	13.83	186.17	78.29	0.85	-0.16
20	7.00	179.17	71.29	0.77	-0.26
30	7.33	171.84	63.96	0.69	-0.36
40	6.15	165.69	57.81	0.63	-0.47
50	5.94	159.75	51.87	0.56	-0.57
60	4.24	155.51	47.63	0.52	-0.66
80	8.13	147.38	39.5	0.43	-0.85
100	7.19	140.19	32.31	0.35	-1.05
120	5.78	134.41	26.53	0.29	-1.24
140	4.62	129.79	21.91	0.24	-1.44
160	4.01	125.78	17.9	0.19	-1.64
180	3.23	122.55	14.67	0.16	-1.84
200	2.76	119.79	11.91	0.13	-2.05
220	2.90	116.89	9.01	0.10	-2.32
240	1.87	115.02	7.14	0.08	-2.56
330	7.14	107.88	0		
REMAINING	91.00				
LOSS	16.88				

SLOPE : -.004246 INTERCEPT: -.0214 VARIANCE: .00008

FRC (slope * 2.303 * 60) : 0.59 l/min

TEST NO: 8 AFR:2.55 L/min WWFR:3 L/min

TIME (s)	Wc (g)	Wcl (g)	Wcl-Woo	Wcl-Woo / Wo-Woo	Ln(Wcl-woo) / (Wo-Woo)
10	19.10	480.90	357.66	0.95	-0.05
20	31.32	449.58	326.34	0.87	-0.14
30	27.06	422.52	299.28	0.79	-0.23
40	25.58	396.94	273.70	0.73	-0.32
50	21.25	375.69	252.45	0.67	-0.40
60	19.54	356.15	232.91	0.62	-0.48
80	33.01	323.14	199.90	0.53	-0.63
100	32.52	290.62	167.38	0.44	-0.81
120	25.04	265.58	142.34	0.38	-0.97
140	21.46	244.12	120.88	0.32	-1.14
160	20.21	223.91	100.67	0.27	-1.32
180	17.22	206.69	83.45	0.22	-1.51
200	14.29	192.40	69.16	0.18	-1.70
220	14.47	177.93	54.69	0.15	-1.93
240	11.56	166.37	43.13	0.11	-2.17
330	43.13	123.24	0		
REMAINING	107.05				
LOSS	16.19				

SLOPE : -.003857 INTERCEPT: .0245 VARIANCE: .00026

FRC (slop * 2.303 * 60) : 0.53 l/min

TEST NO: 10 AFR:3.75 L/min WWFR:3 L/min

TIME (s)	Wc (g)	Wcl (g)	Wcl-Woo	Wcl-Woo / Wo-Woo	Ln(Wcl-Woo) / (Wo-Woo)
10	55.20	444.8	398.43	0.88	-0.13
20	37.67	407.13	360.76	0.80	-0.23
30	32.64	374.49	328.12	0.72	-0.32
40	28.94	345.55	299.18	0.66	-0.42
50	24.13	321.42	275.05	0.61	-0.50
60	24.02	297.40	251.03	0.55	-0.59
70	24.52	272.88	226.51	0.50	-0.69
90	35.45	237.43	191.06	0.42	-0.86
110	29.88	207.55	161.18	0.36	-1.03
130	26.23	181.32	134.95	0.30	-1.21
150	22.92	158.40	112.03	0.25	-1.40
170	17.29	141.11	94.74	0.21	-1.57
190	17.08	124.03	77.66	0.17	-1.76
220	20.25	103.78	57.41	0.13	-2.07
280	29.90	73.88	27.51	0.06	-2.80
340	27.51	46.37	0		
REMAINING	35.02				
LOSS	11.35				

SLOPE : -.00409 INTERCEPT:-.00843 VARIANCE: .000335

FRC (slope * 2.303 * 60) : 0.57 1/min

TEST NO: 11 AFR:9.45 L/min WWFR:3 L/min

TIME (s)	Wc (g)	Wcl (g)	Wcl-Woo	Wcl-Woo / Wo-Woo	Ln(Wcl-Woo) / (Wo-Woo)
10	29.52	470.48	416.53	0.93	-0.07
20	34.75	435.73	381.78	0.86	-0.16
30	37.59	398.14	344.19	0.77	-0.26
40	36.37	361.77	307.82	0.69	-0.37
50	28.80	332.97	279.02	0.63	-0.47
60	26.46	306.51	252.56	0.57	-0.57
70	21.96	284.55	230.6	0.52	-0.66
90	41.70	242.85	188.9	0.42	-0.86
110	36.60	206.25	152.3	0.34	-1.07
130	28.65	177.6	123.65	0.28	-1.28
150	23.42	154.18	100.23	0.22	-1.49
170	20.90	133.28	79.33	0.18	-1.73
190	16.05	117.23	63.28	0.14	-1.95
220	20.20	97.03	43.08	0.10	-2.34
280	21.64	75.39	21.44	0.05	-3.04
340	21.44	53.95	0		
REMAINING	-35.44				
LOSS	18.51				

SLOPE : -.00467 INTERCEPT:.0352 VARIANCE: .000195

FRC (slope * 2.303 * 60) : 0.65 1/min

TEST NO: 12 AFR:8.7 L/min WWFR:3 L/min

TIME (s)	Wc (g)	Wcl (g)	Wcl-Woo	Wcl-Woo / Wo-Woo	Ln(Wcl-Woo) / (Wo-Woo)
10	50.10	449.90	411.03	0.89	-0.12
20	42.98	406.92	368.05	0.80	-0.23
30	38.90	368.02	329.15	0.71	-0.34
40	32.28	335.74	296.87	0.64	-0.44
50	27.31	308.43	269.56	0.58	-0.54
60	24.52	283.91	245.04	0.53	-0.63
70	25.45	258.46	219.59	0.48	-0.74
90	42.65	215.81	176.94	0.38	-0.96
110	31.67	184.14	145.27	0.32	-1.16
130	28.26	155.88	117.01	0.25	-1.37
150	22.42	133.46	94.59	0.21	-1.58
170	17.74	115.72	76.85	0.17	-1.79
190	14.78	100.94	62.07	0.13	-2.01
220	19.90	81.04	42.17	0.09	-2.39
280	24.94	56.10	17.23	0.04	-3.29
340	17.23	38.87	0		
REMAINING	25.50				
LOSS	13.37				

SLOPE : -.004865 INTERCEPT: .0263 VARIANCE: .000719

FRC (slope * 2.303 * 60) : 0.67 l/min

TEST NO: 13 AFR: 6.25L/min WWFR:3.05 L/min

TIME (s)	Wc (g)	Wcl (g)	Wcl-Woo	Wcl-Woo / Wo-Woo	Ln(Wcl-Woo) / (Wo-Woo)
10	35.13	164.87	147.9	0.81	-0.21
20	29.30	135.57	118.6	0.65	-0.43
30	21.41	114.16	97.19	0.53	-0.63
40	16.06	98.1	81.13	0.44	-0.81
50	13.03	85.07	68.1	0.37	-0.99
60	10.35	74.72	57.75	0.32	-1.15
70	10.07	64.65	47.68	0.26	-1.35
90	8.51	56.14	39.17	0.21	-1.54
110	9.96	46.18	29.21	0.16	-1.84
130	6.57	39.61	22.64	0.12	-2.09
150	5.95	33.66	16.69	0.09	-2.39
170	3.78	29.88	12.91	0.07	-2.65
190	2.83	27.05	10.08	0.06	-2.90
220	3.47	23.58	6.61	0.04	-3.32
280	4.16	19.42	2.45	0.01	-4.31
340	2.45	16.97	0		
REMAINING	3.97				
LOSS	13.00				

SLOPE : -.00603 INTERCEPT: -.104 VARIANCE: .00087

FRC (slope * 2.303 * 60) : 0.83 l/min

TEST NO: 14 AFR:7.5 L/min WWFR:3 L/min

TIME (s)	Wc (g)	Wcl (g)	Wcl-Woo	Wcl-Woo / Wo-Woo	Ln(Wcl-Woo) / (Wo-Woo)
10	46.40	453.60	413.49	0.90	-0.11
20	44.95	408.65	368.54	0.80	-0.22
30	43.70	364.95	324.84	0.71	-0.35
40	34.48	330.47	290.36	0.63	-0.46
50	28.67	301.8	261.69	0.57	-0.56
60	30.10	271.70	231.59	0.50	-0.69
70	23.32	248.38	208.27	0.45	-0.79
90	46.64	201.74	161.63	0.35	-1.05
110	28.99	172.75	132.64	0.29	-1.24
130	25.14	147.61	107.5	0.23	-1.45
150	22.79	124.82	84.71	0.18	-1.69
170	17.82	107.00	66.89	0.15	-1.93
190	13.65	93.35	53.24	0.12	-2.16
220	17.87	75.48	35.37	0.08	-2.57
280	20.83	54.65	14.54	0.03	-3.45
340	14.54	40.11	0		
REMAINING	33.09				
LOSS	7.02				

SLOPE : -.004984 INTERCEPT: .00316 VARIANCE: .00008
FRC (slope * 2.303 * 60) : 0.69 1/min

TEST NO: 16 AFR:3.75 L/min WWFR:3 L/min

TIME (s)	Wc (g)	Wcl (g)	Wcl-Woo	Wcl-Woo / Wo-Woo	Ln(Wcl-Woo) / (Wo-Woo)
10	42.48	457.52	390.28	0.90	-0.10
20	33.49	424.03	356.79	0.82	-0.19
30	26.19	397.84	330.6	0.76	-0.27
40	24.88	372.96	305.72	0.71	-0.35
50	23.20	349.76	282.52	0.65	-0.43
60	22.23	327.53	260.29	0.60	-0.51
70	20.15	307.38	240.14	0.55	-0.59
90	36.57	270.81	203.57	0.47	-0.75
110	30.16	240.65	173.41	0.40	-0.91
130	28.31	212.34	145.1	0.34	-1.09
150	24.31	188.03	120.79	0.28	-1.28
170	19.20	168.83	101.59	0.23	-1.45
190	18.88	149.95	82.71	0.19	-1.65
220	24.21	125.74	58.5	0.14	-2.00
280	34.70	91.04	23.8	0.05	-2.90
340	23.8	67.24	0		
REMAINING	42.54				
LOSS	24.70				

SLOPE : -.004148 INTERCEPT: .02728 VARIANCE: .001748
FRC (slope * 2.303 * 60) : 0.57 1/min

TEST NO: 22 AFR:7.5 L/min WWFR:3 L/min

TIME (s)	Wc (g)	Wcl (g)	Wcl-Woo	Wcl-Woo / Wo-Woo	Ln(Wcl-Woo) / (Wo-Woo)
10	55.95	444.05	407.8	0.88	-0.13
20	37.89	406.16	369.91	0.80	-0.23
30	34.48	371.68	335.43	0.72	-0.32
40	30.88	340.8	304.55	0.66	-0.42
50	30.07	310.73	274.48	0.59	-0.52
60	28.73	282.00	245.75	0.53	-0.64
70	26.56	255.44	219.19	0.47	-0.75
90	41.17	214.27	178.02	0.38	-0.96
110	39.27	175	138.75	0.30	-1.21
130	25.35	149.65	113.4	0.24	-1.41
150	22.75	126.90	90.65	0.20	-1.63
170	17.90	109.00	72.75	0.16	-1.85
190	15.49	93.51	57.26	0.12	-2.09
220	16.48	77.03	40.78	0.09	-2.43
280	24.17	52.86	16.61	0.04	-3.33
340	16.61	36.25	0		
REMAINING	27.67				
LOSS	8.58				

SLOPE : -.004988INTERCEPT:.02074 VARIANCE: .000539
FRC (slope * 2.303 * 60) : 0.69 l/min

TEST NO: 24 AFR:5 L/min WWFR:3 L/min

TIME (s)	Wc (g)	Wcl (g)	Wcl-Woo	Wcl-Woo / Wo-Woo	Ln(Wcl-Woo) / (Wo-Woo)
10	95.77	404.23	385.71	0.80	-0.22
20	54.56	349.67	331.15	0.69	-0.37
30	48.50	301.17	282.65	0.59	-0.53
40	40.68	260.49	241.97	0.50	-0.69
50	29.97	230.52	212	0.44	-0.82
60	30.03	200.49	181.97	0.38	-0.97
70	24.35	176.14	157.62	0.33	-1.12
90	34.45	141.69	123.17	0.26	-1.36
110	27.80	113.89	95.37	0.20	-1.62
130	22.94	90.95	72.43	0.15	-1.89
150	16.22	74.73	56.21	0.12	-2.15
170	12.56	62.17	43.65	0.09	-2.40
190	10.29	51.88	33.36	0.07	-2.67
220	11.19	40.69	22.17	0.05	-3.08
280	13.95	26.74	8.22	0.02	-4.07
340	8.22	18.52	0		
REMAINING	14.38				
LOSS	4.14				

SLOPE : -.005885INTERCEPT:-.0655 VARIANCE: .0000718
FRC (slope * 2.303 * 60) : 0.81 l/min

TEST NO: 26 AFR:6.25 L/min WWFR:3 L/min

TIME (s)	Wc (g)	Wcl (g)	Wcl-Woo	Wcl-Woo / Wo-Woo	Ln(Wcl-Woo) / (Wo-Woo)
10	80.66	419.34	404.71	0.83	-0.18
20	57.67	361.67	347.04	0.72	-0.34
30	46.87	314.8	300.17	0.62	-0.48
40	35.79	279.01	264.38	0.54	-0.61
50	29.56	249.45	234.82	0.48	-0.73
60	23.08	226.37	211.74	0.44	-0.83
70	22.58	203.79	189.16	0.39	-0.94
90	37.76	166.03	151.4	0.31	-1.16
110	27.60	138.43	123.8	0.26	-1.37
130	22.74	115.69	101.06	0.21	-1.57
150	19.20	96.49	81.86	0.17	-1.78
170	17.22	79.27	64.64	0.13	-2.02
190	15.85	63.42	48.79	0.10	-2.30
220	13.30	50.12	35.49	0.07	-2.62
280	23.55	26.57	11.94	0.02	-3.71
340	11.94	14.63	0		
REMAINING	13.24				
LOSS	1.39				

SLOPE : -.005179 INTERCEPT: -.03444 VARIANCE: .00124

FRC (slope * 2.303 * 60) : 0.72 1/min

TEST NO: 27 AFR:5 L/min WWFR:3 L/min

TIME (s)	Wc (g)	Wcl (g)	Wcl-WOO	Wcl-Woo / Wo-Woo	Ln(Wcl-Woo) / (Wo-Woo)
10	99.18	400.82	388.48	0.80	-0.23
20	67.36	333.46	321.12	0.66	-0.42
30	49.08	284.38	272.04	0.56	-0.58
40	47.74	236.64	224.30	0.46	-0.78
50	39.85	196.79	184.45	0.38	-0.97
60	24.42	172.37	160.03	0.33	-1.11
70	22.53	149.84	137.50	0.28	-1.27
90	32.28	117.56	105.22	0.22	-1.53
110	27.72	89.84	77.50	0.16	-1.84
130	20.24	69.60	57.26	0.12	-2.14
150	18.45	51.15	38.81	0.08	-2.53
170	10.04	41.11	28.77	0.06	-2.83
190	7.83	33.28	20.94	0.04	-3.15
220	8.78	24.50	12.16	0.02	-3.69
280	8.09	16.41	4.07	0.01	-4.79
340	4.07	12.34	0		
REMAINING	3.24				
LOSS	9.10				

SLOPE : -.00688 INTERCEPT: -.05599 VARIANCE: .000172

FRC (slope * 2.303 * 60) : 0.95 1/min

TEST NO: 28 AFR:8.7 L/min WWFR:3 L/min

TIME (s)	Wc (g)	Wcl (g)	Wcl-Woo	Wcl-Woo / Wo-Woo	Ln(Wcl-Woo) / (Wo-Woo)
10	78.86	421.14	378.85	0.83	-0.19
20	65.43	355.71	313.42	0.68	-0.38
30	46.56	309.15	266.86	0.58	-0.54
40	35.29	273.86	231.57	0.51	-0.68
50	28.74	245.12	202:83	0.44	-0.81
60	26.89	218.23	175.94	0.38	-0.96
70	21.28	196.95	154.66	0.34	-1.09
90	33.26	163.69	121.4	0.27	-1.33
110	20.06	143.63	101.34	0.22	-1.51
130	17.34	126.29	84	0.18	-1.70
150	16.36	109.93	67.64	0.15	-1.91
170	9.54	100.39	58.1	0.13	-2.06
190	10.35	90.04	47.75	0.10	-2.26
220	11.95	78.09	35.8	0.08	-2.55
280	18.46	59.63	17.34	0.04	-3.27
340	17.34	42.29	0		
REMAINING	32.52				
LOSS	9.77				

SLOPE : -.004727 INTERCEPT: -.1023 VARIANCE: .000987

FRC (slope * 2.303 * 60) : 0.65 l/min

TEST NO: 29 AFR: 6.25L/min WWFR:3 L/min

TIME (s)	Wc (g)	Wcl (g)	Wcl-Woo	Wcl-Woo / Wo-Woo	Ln(Wcl-Woo) / (Wo-Woo)
10	57.99	142.01	133.55	0.70	-0.36
20	21.30	120.71	112.25	0.59	-0.53
30	18.20	102.51	94.05	0.49	-0.71
40	13.19	89.32	80.86	0.42	-0.86
50	12.69	76.63	68.17	0.36	-1.03
60	10.15	66.48	58.02	0.30	-1.19
70	7.60	58.88	50.42	0.26	-1.33
90	12.09	46.79	38.33	0.20	-1.61
110	7.38	39.41	30.95	0.16	-1.82
130	7.22	32.19	23.73	0.12	-2.09
150	5.42	26.77	18.31	0.10	-2.35
170	3.82	22.95	14.49	0.08	-2.58
190	3.13	19.82	11.36	0.06	-2.82
220	3.55	16.27	7.81	0.04	-3.20
280	4.44	11.83	3.37	0.02	-4.04
340	3.37	8.46	0		
REMAINING	4.66				
LOSS	3.80				

SLOPE : -.006665 INTERCEPT: -.121 VARIANCE: .00088

FRC (slope * 2.303 * 60) : 0.92 l/min

TEST NO: 20 AFR: 6.25L/min WWFR:2.9 L/min

TIME (s)	Wc (g)	Wcl (g)	Wcl-Woo	Wcl-Woo / Wo-Woo	Ln(Wcl-Woo) / (Wo-Woo)
10	17.44	182.56	159.21	0.90	-0.10
20	13.65	168.91	145.56	0.82	-0.19
30	12.66	156.25	132.9	0.75	-0.28
40	9.88	146.37	123.02	0.70	-0.36
50	9.59	136.78	113.43	0.64	-0.44
60	11.20	125.58	102.23	0.58	-0.55
70	8.88	116.70	93.35	0.53	-0.64
90	15.46	101.24	77.89	0.44	-0.82
110	14.56	86.68	63.33	0.36	-1.03
130	12.78	73.90	50.55	0.29	-1.25
150	9.96	63.94	40.59	0.23	-1.47
170	7.55	56.39	33.04	0.19	-1.68
190	6.15	50.24	26.89	0.15	-1.88
220	7.55	42.69	19.34	0.11	-2.21
280	11.38	31.31	7.96	0.05	-3.10
340	7.96	23.35	0		
REMAINING	20.38				
LOSS	2.97				

SLOPE : -.00456 INTERCEPT:.0331 VARIANCE: -.00071

FRC (slope * 2.303 * 60) : 0.63 1/min

TEST NO: 21 AFR: 6.25L/min WWFR:3.05 L/min

TIME (s)	Wc (g)	Wcl (g)	Wcl-Woo	Wcl-Woo / Wo-Woo	Ln(Wcl-Woo) / (Wo-Woo)
10	42.90	157.1	144.59	0.77	-0.26
20	20.51	136.59	124.08	0.66	-0.41
30	19.20	117.39	104.88	0.56	-0.58
40	12.90	104.49	91.98	0.49	-0.71
50	13.85	90.64	78.13	0.42	-0.88
60	9.57	81.07	68.56	0.37	-1.01
70	9.40	71.67	59.16	0.32	-1.15
90	12.70	58.97	46.46	0.25	-1.40
110	8.74	50.23	37.72	0.20	-1.60
130	6.70	43.53	31.02	0.17	-1.80
150	5.10	38.43	25.92	0.14	-1.98
170	3.75	34.68	22.17	0.12	-2.13
190	4.05	30.63	18.12	0.10	-2.34
220	5.56	25.07	12.56	0.07	-2.70
280	7.63	17.44	4.93	0.03	-3.64
340	4.93	12.51	0		
REMAINING	9.74				
LOSS	2.77				

SLOPE : -.004997INTERCEPT:-.108 VARIANCE: .00119

FRC (slop * 2.303 * 60) : 0.69 1/min

TEST NO: 18 AFR:6.25 L/min WWFR:3 L/min

TIME (s)	Wc (g)	Wcl (g)	Wcl-Woo	Wcl-Woo / Wo-Woo	Ln(Wcl-Woo) / (Wo-Woo)
10	69.10	430.90	409.70	0.86	-0.16
20	44.48	386.42	365.22	0.76	-0.27
30	40.74	345.68	324.48	0.68	-0.39
40	32.99	312.69	291.49	0.61	-0.50
50	30.37	282.32	261.12	0.55	-0.61
60	32.01	250.31	229.11	0.48	-0.74
70	25.94	224.37	203.17	0.42	-0.86
90	40.65	183.72	162.52	0.34	-1.08
110	32.54	151.18	129.98	0.27	-1.30
130	28.96	122.22	101.02	0.21	-1.56
150	19.66	102.56	81.36	0.17	-1.77
170	17.62	84.94	63.74	0.13	-2.02
190	15.37	69.57	48.37	0.10	-2.29
220	22.75	46.82	25.62	0.05	-2.93
280	25.62	21.20	0		
REMAINING	16.54				
LOSS	4.66				

SLOPE : --.005153INTERCEPT:.00603 VARIANCE: .0000512

FRC (slope * 2.303 * 60) : 0.71 1/min

TEST NO: 19 AFR: 6.25L/min WWFR:3 L/min

TIME (s)	Wc (g)	Wcl (g)	Wcl-Woo	Wcl-Woo / Wo-Woo	Ln(Wcl-Woo) / (Wo-Woo)
10	16.16	183.84	157.58	0.91	-0.10
20	20.41	163.43	137.17	0.79	-0.24
30	13.54	149.89	123.63	0.71	-0.34
40	12.87	137.02	110.76	0.64	-0.45
50	10.89	126.13	99.87	0.57	-0.55
60	12.56	113.57	87.31	0.50	-0.69
70	9.27	104.30	78.04	0.45	-0.80
90	14.18	90.12	63.86	0.37	-1.00
110	11.69	78.43	52.17	0.30	-1.20
130	8.47	69.96	43.70	0.25	-1.38
150	8.25	61.71	35.45	0.20	-1.59
170	8.71	53.00	26.74	0.15	-1.87
190	5.94	47.06	20.80	0.12	-2.12
220	7.09	39.97	13.71	0.08	-2.54
280	8.95	31.02	4.76	0.03	-3.60
340	4.76	26.26	0		
REMAINING	8.78				
LOSS	17.48				

SLOPE : -.005066INTERCEPT:.0218 VARIANCE: .0012

FRC (slope * 2.303 * 60) : 0.70 1/min

TEST NO: 32 AFR: 6.25L/min WWFR:3 L/min

TIME (s)	Wc (g)	Wcl (g)	Wcl-Woo	Wcl-Woo / Wo-Woo	Ln(Wcl-Woo) (Wo-Woo)
10	73.67	126.33	120.47	0.62	-0.48
20	28.80	97.53	91.67	0.47	-0.75
30	19.14	78.39	72.53	0.37	-0.98
40	11.92	66.47	60.61	0.31	-1.16
50	10.91	55.56	49.70	0.26	-1.36
60	9.12	46.44	40.58	0.21	-1.57
70	6.11	40.33	34.47	0.18	-1.73
90	8.88	31.45	25.59	0.13	-2.03
110	8.44	23.01	17.15	0.09	-2.43
130	6.02	16.99	11.13	0.06	-2.86
150	3.17	13.82	7.96	0.04	-3.19
170	2.26	11.56	5.70	0.03	-3.53
190	1.62	9.94	4.08	0.02	-3.86
220	1.49	8.45	2.59	0.01	-4.32
280	1.01	7.44	1.58	0.01	-4.81
340	1.58	5.86	0		
REMAINING	3.22				
LOSS	2.64				

SLOPE : -.008045INTERCEPT:-.174 VARIANCE: .000402
FRC (slop * 2.303 * 60) : 1.11 1/min

TEST NO: 34 AFR: 6.25L/min WWFR:3 L/min

TIME (s)	Wc (g)	Wcl (g)	Wcl-Woo	Wcl-Woo / Wo-Woo	Ln(Wcl-Woo) (Wo-Woo)
10	13.19	186.81	153.20	0.92	-0.08
20	11.62	175.19	141.58	0.85	-0.16
30	10.41	164.78	131.17	0.79	-0.24
40	5.36	159.42	125.81	0.76	-0.28
50	10.43	148.99	115.377	0.69	-0.37
60	8.28	140.71	107.1	0.64	-0.44
70	7.81	132.90	99.29	0.60	-0.52
90	13.38	119.52	85.91	0.52	-0.66
110	13.01	106.51	72.9	0.44	-0.83
130	11.23	95.28	61.67	0.37	-0.99
150	9.86	85.42	51.81	0.31	-1.17
170	8.93	76.49	42.88	0.26	-1.36
190	7.82	68.67	35.06	0.21	-1.56
220	9.77	58.90	25.29	0.15	-1.88
280	14.98	43.92	10.31	0.06	-2.78
340	10.31	33.61	0		
REMAINING	26.92				
LOSS	6.69				

SLOPE : -.003748INTERCEPT -.0421 VARIANCE: .0003223
FRC (slop * 2.303 * 60) : 0.52 1/min

TEST NO: 30 AFR:1.3 L/min WWFR:3 L/min

TIME (s)	Wc (g)	Wcl (g)	Wcl-Woo	Wcl-Woo / Wo-Woo	Ln(Wcl-Woo) / (Wo-Woo)
10	54.16	445.84	356.49	0.87	-0.14
20	33.38	412.46	323.11	0.79	-0.24
30	22.13	390.33	300.98	0.73	-0.31
40	18.98	371.35	282.00	0.69	-0.38
50	16.50	354.85	265.5	0.65	-0.44
60	14.72	340.13	250.78	0.61	-0.49
70	15.20	324.93	235.58	0.57	-0.56
90	27.78	297.15	207.8	0.51	-0.68
110	30.16	266.99	177.64	0.43	-0.84
130	23.95	243.04	153.69	0.37	-0.98
150	21.70	221.34	131.99	0.32	-1.14
170	22.06	199.28	109.93	0.27	-1.32
190	18.82	180.46	91.11	0.22	-1.51
220	24.09	156.37	67.02	0.16	-1.81
280	39.93	116.44	27.09	0.07	-2.72
340	27.09	89.35	0		
REMAINING	82.59				
LOSS	6.76				

SLOPE : -.00329 INTERCEPT:-.01904 VARIANCE: .000335

FRC (slope * 2.303 * 60) : 0.45 l/min

TEST NO: 31 AFR:5 L/min WWFR:3 L/min

TIME (s)	Wc (g)	Wcl (g)	Wcl-Woo	Wcl-Woo / Wo-Woo	Ln(Wcl-Woo) / (Wo-Woo)
10	100.61	399.39	378.06	0.79	-0.24
20	88.08	311.31	289.98	0.61	-0.50
30	47.06	264.25	242.92	0.51	-0.68
40	47.43	216.82	195.49	0.41	-0.90
50	27.09	189.73	168.4	0.35	-1.04
60	28.98	160.75	139.42	0.29	-1.23
70	20.36	140.39	119.06	0.25	-1.39
90	25.68	114.71	93.38	0.20	-1.63
110	19.05	95.66	74.33	0.16	-1.86
130	15.77	79.89	58.56	0.12	-2.10
150	12.69	67.20	45.87	0.10	-2.35
170	8.44	58.76	37.43	0.08	-2.55
190	9.17	49.59	28.26	0.06	-2.83
220	8.52	41.07	19.74	0.04	-3.19
280	11.65	29.42	8.09	0.02	-4.08
340	8.09	21.33	0		
REMAINING	17.64				
LOSS	3.69				

SLOPE : -.00581 INTERCEPT:-.1416 VARIANCE: .001426

FRC (slope * 2.303 * 60) : 0.80 l/min

TEST NO: 35 AFR:5 L/min NWFR:3 L/min

TIME (s)	Wc (g)	Wcl (g)	Wcl-Woo	Wcl-Woo / Wo-Woo	Ln(Wcl-Woo) / (Wo-Woo)
10	73.10	926.90	886.88	0.92	-0.08
20	77.56	849.34	809.32	0.84	-0.17
30	79.00	770.34	730.32	0.76	-0.27
40	86.04	684.30	644.28	0.67	-0.40
50	72.95	611.35	571.33	0.60	-0.52
60	64.97	546.38	506.36	0.53	-0.64
70	61.72	484.66	444.64	0.46	-0.77
90	94.46	390.20	350.18	0.36	-1.01
110	75.78	314.42	274.40	0.29	-1.25
130	61.68	252.74	212.72	0.22	-1.51
150	45.78	206.96	166.94	0.17	-1.75
170	36.17	170.79	130.77	0.14	-1.99
190	31.98	138.81	98.79	0.10	-2.27
220	32.70	106.11	66.09	0.07	-2.68
280	41.25	64.86	24.84	0.03	-3.65
340	24.84	40.02	0		
REMAINING	32.90				
LOSS	7.12				

SLOPE : -.005597 INTERCEPT: .0564 VARIANCE: .0006849

FRC (slope * 2.303 * 60) : 0.77 l/min

TEST NO: 36 AFR:5 L/min NWFR:3 L/min

TIME (s)	Wc (g)	Wcl (g)	Wcl-Woo	Wcl-Woo / Wo-Woo	Ln(Wcl-Woo) / (Wo-Woo)
10	70.62	929.38	778.13	0.92	-0.09
20	82.06	847.32	696.07	0.82	-0.20
30	68.42	778.9	627.65	0.74	-0.30
40	58.93	719.97	568.72	0.67	-0.40
50	58.90	661.07	509.82	0.60	-0.51
60	50.28	610.79	459.54	0.54	-0.61
70	48.07	562.72	411.47	0.48	-0.72
90	78.98	483.74	332.49	0.39	-0.94
110	59.94	423.80	272.55	0.32	-1.14
130	51.95	371.85	220.60	0.26	-1.35
150	42.62	329.23	177.98	0.21	-1.56
170	32.26	296.97	145.72	0.17	-1.76
190	28.78	268.19	116.94	0.14	-1.98
220	38.68	229.51	78.26	0.09	-2.38
280	46.89	182.62	31.37	0.04	-3.30
340	31.37	151.25	0		
REMAINING	138.44				
LOSS	12.81				

SLOPE : -.004908 INTERCEPT: .0312 VARIANCE: .0009303

FRC (slope * 2.303 * 60) : 0.68 l/min

TEST NO: 38 AFR:8.7 L/min WWFR:3 L/min

TIME (s)	Wc (g)	Wcl (g)	Wcl-Woo	Wcl-Woo / Wo-Woo	Ln(Wcl-Woo) / (Wo-Woo)
10	95.20	904.80	849.99	0.91	-0.09
20	88.94	815.86	761.05	0.82	-0.20
30	80.07	735.79	680.98	0.73	-0.31
40	76.63	659.16	604.35	0.65	-0.43
50	65.63	593.53	538.72	0.58	-0.55
60	55.32	538.21	483.40	0.52	-0.66
70	60.32	477.89	423.08	0.45	-0.79
90	87.66	390.23	335.42	0.36	-1.02
110	67.81	322.42	267.61	0.29	-1.25
130	58.19	264.23	209.42	0.22	-1.49
150	45.02	219.21	164.40	0.18	-1.73
170	34.16	185.05	130.24	0.14	-1.97
190	28.69	156.36	101.55	0.11	-2.22
220	30.15	126.21	71.40	0.08	-2.57
280	37.04	89.17	34.36	0.04	-3.30
340	20.8	68.37	13.56	0.01	-4.23
400	13.56	54.81	0.00		
REMAINING	50.26				
LOSS	4.55				

SLOPE : -.005118 INTERCEPT: .011 VARIANCE: .000025

FRC (slope * 2.303 * 60) : 0.71 1/min

TEST NO: 39 AFR:6.25 L/min WWFR:3 L/min

TIME (s)	Wc (g)	Wcl (g)	Wcl-Woo	Wcl-Woo / Wo-Woo	Ln(Wcl-Woo) / (Wo-Woo)
10	100.28	899.72	835.81	0.94	-0.10
20	85.48	814.24	750.33	0.82	-0.20
30	71.42	742.82	678.91	0.74	-0.30
40	64.36	678.46	614.55	0.67	-0.40
50	62.78	615.68	551.77	0.60	-0.51
60	65.33	550.35	486.44	0.53	-0.64
70	47.27	503.08	439.17	0.48	-0.74
90	82.71	420.37	356.46	0.39	-0.95
110	67.53	352.84	288.93	0.31	-1.16
130	60.82	292.02	228.11	0.25	-1.39
150	42.67	249.35	185.44	0.20	-1.60
170	36.69	212.66	148.75	0.16	-1.82
190	31.14	181.52	117.61	0.13	-2.06
220	35.20	146.32	82.41	0.09	-2.41
280	38.94	107.38	43.47	0.05	-3.05
340	27.23	80.15	16.24	0.02	-4.04
400	16.24	63.91	0.00		
REMAINING	57.37				
LOSS	6.54				

SLOPE : -.00497 INTERCEPT: .0244 VARIANCE: .000713

FRC (slope * 2.303 * 60) : 0.69 1/min

TEST NO: 40 AFR:3.75 L/min WWFR:3 L/min

TIME (s)	Wc (g)	Wcl (g)	Wcl-Woo	Wcl-Woo / Wo-Woo	Ln(Wcl-woo) / (Wo-Woo)
10	114.12	885.88	826.80	0.90	-0.10
20	79.13	806.75	747.67	0.81	-0.20
30	63.86	742.89	683.81	0.75	-0.29
40	62.03	680.86	621.78	0.68	-0.39
50	53.70	627.16	568.08	0.62	-0.48
60	53.91	573.25	514.17	0.56	-0.58
70	42.65	530.60	471.52	0.51	-0.67
90	79.41	451.19	392.11	0.43	-0.85
110	73.28	377.91	318.83	0.35	-1.06
130	51.23	326.68	267.60	0.29	-1.23
150	43.99	282.69	223.61	0.24	-1.41
170	39.06	243.63	184.55	0.20	-1.60
190	34.91	208.72	149.64	0.16	-1.81
220	35.26	173.46	114.38	0.12	-2.08
280	55.38	118.08	59.00	0.06	-2.74
340	35.68	82.40	23.32	0.03	-3.67
400	23.32	59.08	0.00		
REMAINING	48.48				
LOSS	10.60				

SLOPE : -.004158 INTERCEPT: -.011 VARIANCE: .00008

FRC (slope * 2.303 * 60) : 0.57 l/min

TEST NO: 41 AFR:8.7 L/min WWFR:3 L/min

TIME (s)	Wc (g)	Wcl (g)	Wcl-Woo	Wcl-Woo / Wo-Woo	Ln(Wcl-woo) / (Wo-Woo)
10	111.44	888.56	809.88	0.89	-0.11
20	79.31	809.25	730.57	0.81	-0.21
30	72.84	736.41	657.73	0.73	-0.32
40	59.46	676.95	598.27	0.66	-0.41
50	61.52	615.43	536.75	0.59	-0.52
60	68.33	547.10	468.42	0.52	-0.66
70	47.07	500.03	421.35	0.47	-0.76
90	81.29	418.74	340.06	0.38	-0.98
110	57.51	361.23	282.55	0.31	-1.16
130	58.44	302.79	224.11	0.25	-1.40
150	43.69	259.10	180.42	0.20	-1.61
170	36.67	222.43	143.75	0.16	-1.84
190	29.49	192.94	114.26	0.13	-2.07
220	32.38	160.56	81.88	0.09	-2.40
280	40.96	119.60	40.92	0.05	-3.10
340	25.05	94.55	15.87	0.02	-4.04
400	15.87	78.68	0.00		
REMAINING	74.59				
LOSS	4.09				

SLOPE : -.004767 INTERCEPT: .00034 VARIANCE: .00004

FRC (slope * 2.303 * 60) : 0.66 l/min

TEST NO: 42 AFR:1.3 L/min WWFR:3 L/min

TIME (s)	Wc (g)	Wcl (g)	Wcl-Woo	Wcl-Woo / Wo-Woo	Ln(Wcl-Woo) / (Wo-Woo)
10	53.92	946.08	766.50	1.01	0.01
20	25.31	920.77	741.19	0.98	-0.02
30	27.55	893.22	713.64	0.94	-0.06
40	28.52	864.70	685.12	0.91	-0.10
50	26.03	838.67	659.09	0.87	-0.14
60	26.19	812.48	632.90	0.84	-0.18
70	25.53	786.95	607.37	0.80	-0.22
90	51.25	735.70	556.12	0.74	-0.31
110	49.62	686.08	506.50	0.67	-0.40
130	47.57	638.51	458.93	0.61	-0.50
150	49.45	589.06	409.48	0.54	-0.61
170	43.10	545.96	366.38	0.48	-0.73
190	46.07	499.89	320.31	0.42	-0.86
220	69.14	430.75	251.17	0.33	-1.10
280	101.81	328.94	149.36	0.20	-1.62
340	85.51	243.43	63.85	0.08	-2.47
400	63.85	179.58	0.00		
REMAINING	161.60				
LOSS	17.98				

SLOPE : -.002569 INTERCEPT: .0179 VARIANCE: .000284

FRC (slope * 2.303 * 60) : 0.35 1/min

TEST NO: 44 AFR:2.55 L/min WWFR:3 L/min

TIME (s)	Wc (g)	Wcl (g)	Wcl-Woo	Wcl-Woo / Wo-Woo	Ln(Wcl-Woo) / (Wo-Woo)
10	75.26	424.74	369.53	0.83	-0.19
20	28.80	395.94	340.73	0.77	-0.27
30	35.07	360.87	305.66	0.69	-0.38
40	22.58	338.29	283.08	0.64	-0.45
50	20.92	317.37	262.16	0.59	-0.53
60	21.98	295.39	240.18	0.54	-0.62
70	20.43	274.96	219.75	0.49	-0.71
90	40.92	234.04	178.83	0.40	-0.91
110	31.22	202.82	147.61	0.33	-1.10
130	24.65	178.17	122.96	0.28	-1.29
150	24.11	154.06	98.85	0.22	-1.50
170	18.84	135.22	80.01	0.18	-1.72
190	16.07	119.15	63.94	0.14	-1.94
220	20.50	98.65	43.44	0.10	-2.33
280	28.05	70.60	15.39	0.03	-3.36
340	15.39	55.21	0		
REMAINING	45.21				
LOSS	10.00				

SLOPE : -.004549 INTERCEPT: .018 VARIANCE: .000156

FRC (slope * 2.303 * 60) : 0.63 1/min

TEST NO: 33 AFR:5 L/min WWFR:3 L/min

TIME (s)	Wc (g)	Wcl (g)	Wcl-Woo	Wcl-Woo / Wo-Woo	Ln(Wcl-Woo) / (Wo-Woo)
10	97.24	402.76	369.62	0.79	-0.23
20	61.98	340.78	307.64	0.66	-0.42
30	50.04	290.74	257.6	0.55	-0.59
40	26.81	263.93	230.79	0.49	-0.70
50	29.55	234.38	201.24	0.43	-0.84
60	21.84	212.54	179.4	0.38	-0.96
70	23.26	189.28	156.14	0.33	-1.10
90	33.45	155.83	122.69	0.26	-1.34
110	27.87	127.96	94.82	0.20	-1.59
130	19.26	108.70	75.56	0.16	-1.82
150	16.19	92.51	59.37	0.13	-2.06
170	12.01	80.50	47.36	0.10	-2.29
190	11.47	69.03	35.89	0.08	-2.57
220	11.99	57.04	23.9	0.05	-2.97
280	14.95	42.09	8.95	0.02	-3.95
340	8.95	33.14	0		
REMAINING	13.88				
LOSS	19.26				

SLOPE : -.005653 INTERCEPT: -.0702 VARIANCE: .000625

FRC (slope * 2.303 * 60) : 0.78 1/min

TEST NO: 43 AFR:5 L/min WWFR:3 L/min

TIME (s)	Wc (g)	Wcl (g)	Wcl-Woo	Wcl-Woo / Wo-Woo	Ln(Wcl-Woo) / (Wo-Woo)
10	93.02	1406.98	1284.14	0.93	-0.07
20	73.29	1333.69	1210.85	0.88	-0.13
30	78.59	1255.1	1132.26	0.82	-0.20
40	68.12	1186.98	1064.14	0.77	-0.26
50	74.10	1112.88	990.04	0.72	-0.33
60	73.95	1038.93	916.09	0.67	-0.41
70	67.39	971.54	848.70	0.62	-0.48
90	141.34	830.2	707.36	0.51	-0.67
110	121.68	708.52	585.68	0.43	-0.86
130	100.83	607.69	484.85	0.35	-1.04
150	103.46	504.23	381.39	0.28	-1.28
170	81.73	422.50	299.66	0.22	-1.53
190	66.92	355.58	232.74	0.17	-1.78
220	78.42	277.16	154.32	0.11	-2.19
280	107.69	169.51	46.67	0.03	-3.38
340	46.67	122.84	0		
REMAINING	21.12				
LOSS	101.72				

SLOPE : -.005852 INTERCEPT: .2994 VARIANCE: .004935

FRC (slope * 2.303 * 60) : 0.81 1/min

TEST NO: 45 AFR:1.3 L/min WWFR:3 L/min

TIME (s)	Wc (g)	Wcl (g)	Wcl-Woo	Wcl-Woo / Wo-Woo	Ln(Wcl-Woo) / (Wo-Woo)
10	32.11	467.89	383.7	0.92	-0.08
20	22.36	445.53	361.34	0.87	-0.14
30	18.05	427.48	343.29	0.83	-0.19
40	20.48	407.00	322.81	0.78	-0.25
50	19.20	387.80	303.61	0.73	-0.31
60	19.33	368.47	284.28	0.68	-0.38
70	19.77	348.70	264.51	0.64	-0.45
90	33.68	315.02	230.83	0.56	-0.59
110	32.53	282.49	198.30	0.48	-0.74
130	33.04	249.45	165.26	0.40	-0.92
150	24.59	224.86	140.67	0.34	-1.08
170	23.68	201.18	116.99	0.28	-1.27
190	21.73	179.45	95.26	0.23	-1.47
220	28.44	151.01	66.82	0.16	-1.83
280	40.35	110.66	26.47	0.06	-2.75
340	26.47	84.19	0		
REMAINING	77.49				
LOSS	6.70				

SLOPE : -.003503 INTERCEPT: .034 VARIANCE: .0005819

FRC (slope * 2.303 * 60) : 0.48 l/min

TEST NO: 48 AFR:3.75 L/min WWFR:3 L/min

TIME (s)	Wc (g)	Wcl (g)	Wcl-Woo	Wcl-Woo / Wc-Woo	Ln(Wcl-Woo) / (Wo-Woo)
10	74.71	425.29	381.64	0.84	-0.18
20	45.54	379.75	336.1	0.74	-0.31
30	41.34	338.41	294.76	0.65	-0.44
40	34.46	303.95	260.30	0.57	-0.56
50	29.32	274.63	230.98	0.51	-0.68
60	27.01	247.62	203.97	0.45	-0.81
70	21.44	226.18	182.53	0.40	-0.92
90	34.14	192.04	148.39	0.33	-1.12
110	29.94	162.10	118.45	0.26	-1.35
130	24.46	137.64	93.99	0.21	-1.58
150	17.76	119.88	76.23	0.17	-1.79
170	16.34	103.54	59.89	0.13	-2.03
190	13.40	90.14	46.49	0.10	-2.28
220	15.25	74.89	31.24	0.07	-2.68
280	19.50	55.39	11.74	0.03	-3.66
340	11.74	43.65	0		
REMAINING	32.31				
LOSS	11.34				

SLOPE : -.005273 INTERCEPT: .0163 VARIANCE: .000718

FRC (slope * 2.303 * 60) : 0.73 l/min

TEST NO: 50 AFR:1.3 L/min WWFR:3 L/min

TIME (s)	Wc (g)	Wcl (g)	Wcl-Woo	Wcl-Woo / Wo-Woo	Ln(Wcl-Woo) / (Wo-Woo)
20	15.43	484.57	275.77	0.95	-0.05
40	12.04	472.53	263.73	0.91	-0.10
60	12.78	459.75	250.95	0.86	-0.15
80	14.17	445.58	236.78	0.81	-0.21
100	12.86	432.72	223.92	0.77	-0.26
120	16.95	415.77	206.97	0.71	-0.34
140	15.77	400.00	191.20	0.66	-0.42
160	18.08	381.92	173.12	0.59	-0.52
180	17.38	364.54	155.74	0.53	-0.63
210	27.49	337.05	128.25	0.44	-0.82
270	65.11	271.94	63.14	0.22	-1.53
340	63.14	208.80	0		
REMAINING	195.49				
LOSS	13.31				

SLOPE : -.001688 INTERCEPT: .036 VARIANCE: .000337

FRC (slope * 2.303 * 60) : 0.23 l/min

TEST NO: 51 AFR:1.3 L/min WWFR:3 L/min

TIME (s)	Wc (g)	Wcl (g)	Wcl-Woo	Wcl-Woo / Wo-Woo	Ln(Wcl-Woo) / (Wo-Woo)
20	12.22	87.78	66.10	0.84	-0.17
40	9.08	78.70	57.02	0.73	-0.32
60	7.92	70.78	49.10	0.63	-0.47
80	8.56	62.22	40.54	0.52	-0.66
100	5.99	56.23	34.55	0.44	-0.82
120	5.42	50.81	29.13	0.37	-0.99
140	5.50	45.31	23.63	0.30	-1.20
160	4.55	40.76	19.08	0.24	-1.41
180	3.87	36.89	15.21	0.19	-1.64
210	5.05	31.84	10.16	0.13	-2.04
270	5.79	26.05	4.37	0.06	-2.89
340	4.37	21.68	0		
REMAINING	19.06				
LOSS	2.62				

SLOPE : -.004762 INTERCEPT .1465 VARIANCE: .000147

FRC (slope * 2.303 * 60) : 0.66 l/min

APPENDIX 5.2

Air flow rate versus flotation rate constant

(7 % solids)

TEST NO	AFR (L/min)	FRC (1/min)
11	9.45	0.6453
12	8.70	0.6722
28	8.70	0.6532
22	7.50	0.6892
14	7.50	0.6887
26	6.25	0.7160
18	6.25	0.7134
31	5.00	0.8037
27	5.00	0.9507
24	5.00	0.8130
48	3.75	0.7286
16	3.75	0.5730
10	3.75	0.5650
8	2.55	0.5326
44	2.55	0.5835
30	1.30	0.4557
45	1.30	0.4840
50	0.50	0.1430

APPENDIX 5.3

Air flow rate versus flotation rate constant

(14 % solids)

TEST NO	AFR (L/min)	FRC (1/min)
38	8.70	0.707
41	8.70	0.659
36	7.50	0.682
39	6.25	0.687
35	5.00	0.780
40	3.75	0.575
47	2.55	0.442
42	1.30	0.355

APPENDIX 5.4

Size (um)	PRODUCT # 1-2	3-5	6-8	9-11	12-14	15+R	FRC (1/min)
- 74	100.00	100.00	100.00	100.00	100.00	100.00	.8455
-30 + 23	66.72	75.00	79.23	84.50	86.45	85.32	.9671
-23 + 16	41.37	56.57	59.46	67.30	71.60	76.27	.9448
-16 + 10	21.72	32.67	31.69	38.20	43.95	58.67	.8508
-10 + 8	13.12	17.40	13.59	15.70	19.45	37.51	.4813
- 8	11.12	12.90	7.66	7.90	10.65	22.95	.6675

Product #	WEIGHT 30 um	23 um	16 um	10 um	8 um	-8 um
1 - 3	62.77	47.81	37.06	16.22	3.77	20.97
3 - 5	27.89	20.56	26.67	17.04	5.02	14.39
6 - 8	15.58	14.83	20.83	13.58	4.22	4.22
9 - 11	7.36	8.17	13.83	10.69	3.71	3.75
12 - 14	3.53	3.86	7.20	6.38	2.29	2.77
14 - R	5.33	3.38	6.58	6.58	7.90	5.44
TOTAL	122.46	98.41	112.17	70.49	27.01	51.64

Calculation of the FRC of each size class

(Test-31 cyclosizer results).

APPENDIX 5.5

	PRODUCT #						FRC
Size (um)	1-2	3-5	6-8	9-11	12-14	15-R	(l/min)
- 74	100.00	100.00	100.00	100.00	100.00	100.00	.964
-30 + 23	62.00	79.97	78.33	82.67	85.95	89.93	.967
-23 + 16	42.17	50.14	64.33	68.04	73.05	80.00	.791
-16 + 10	21.87	28.02	43.76	46.64	50.20	59.10	.735
-10 + 8	9.49	10.98	23.89	24.44	26.45	31.87	.681
- 8	5.58	3.91	14.22	13.87	14.45	16.40	.803

	WEIGHT					
Product #	30 um	23 um	16 um	10 um	8 um	-8 um
1 - 3	60.11	31.57	32.32	18.99	6.94	8.88
3 - 5	21.31	31.74	23.54	18.12	7.52	4.16
6 - 8	17.02	10.99	16.15	15.61	7.59	11.17
9 - 11	11.01	6.26	13.53	14.03	6.64	8.78
12 - 14	4.98	4.57	8.10	8.42	4.25	5.12
14 - R	3.92	3.75	7.89	10.28	5.84	6.19
TOTAL	118.35	81.88	101.53	85.55	38.78	44.30

Calculation of the FRC of each size classes.

(Test-33 cyclosizer results).

APPENDIX 6.1

Slurry kinetics in continuous flotation

Determination of the FRC:

The slurry phase of individual flotation cells is assumed to be perfectly mixed. This of course implies that concentrations are constant throughout the slurry. As the tailing stream is simply the in discriminate removal of a fraction of the slurry, it will have the same characteristics.

First order kinetics yield a production rate of a given mineral in the concentrate proportional to its mass in the slurry phase or

$$C_c * Q_c = K * C_t * V = Km \qquad 1$$

where Cc: concentration of mineral of interest in the concentrate stream (g/L)

K : FRC (1/min)

Ct: concentration of mineral of interest in the tailing stream (g/L).

V : volume of the slurry (L).

The recovery of any mineral in the concentrate stream is its concentrate flowrate divided by its total flowrate out of cell.

$$R = \frac{Q_c * C_c}{Q_c * C_c + Q_t * C_t} = \frac{K * C_t * V}{K * C_t * V + Q_t * C} \qquad 2$$

Dividing both the numerator and denominator by Qt.Ct

$$R = \frac{K\,(V/Q_t)}{K\,(V/Q_t) \quad 1} = \frac{K * \tau}{K * \tau + 1} \qquad 3$$

where τ is the mean solids residence time.

The FRC is given by;

$$K = \frac{R}{\tau + \tau * R} \qquad 4$$

and τ is calculated from;

$$\tau = \frac{\text{mass of solid in the pulp (g)}}{\text{tails solid mass flowrate (g/min)}} \qquad 5$$

APPENDIX 6-1

AFR (L/min)	FRC (min)	Ln(FRC/Q)	RES.TIME (min)	AV.FRC (min)	AV.RE.TI. (MIN)
8.7	1.53	-1.73806	3.02	1.53	2.94625
7.5	1.73	-1.46678	2.84	1.725	
	1.72	-1.47258	2.97		
	1.74	-1.46102	2.91		
	1.71	-1.47841	2.98		
6.25	1.8	-1.24479	3.02	1.8	
5	1.4	-1.27297	2.84	1.4725	
	1.4	-1.27297	2.97		
	1.57	-1.15836	2.91		
	1.52	-1.19073	2.98		
2.25	.77	-1.07229	3.01	.77	
1.3	.49	-.975714	2.84	.59	
	.5	-.955511	2.97		
	.55	-.860201	2.99		
	.71	-.604853	2.91		
	.7	-.619039	2.98		

Slurry kinetics results

TEST-23

AFR L/MIN		SLURRY	SOLID G/MIN	RECOVERY	RES.TIME MIN.	AVE.R.T. MIN.	FRC MIN	AVE.FRC MIN
7.5	CON.1	1656.2	171.23	.8331955		2.909959	1.716533	1.742300
	TLS.1	1297.5	34.28					
	FEED 1	1753.7	205.51					
	CON.2	1692.6	170.12	.8350677			1.739920	
	TLS.2	1246.3	33.6					
	FEED 2	1738.9	203.72					
	CON.3	1640	163.48	.8374494			1.770447	
	TLS.3	1274.3	32.12					
	FEED 3	1714.3	197.6					
5	CON.1	1562.2	153.08	.8182596			1.547222	1.574376
	TLS.1	1257.5	34					
	FEED 1	1619.7	187.08					
	CON.2	1553.3	165.56	.8367110			1.760087	
	TLS.2	1254.1	32.31					
	FEED 2	1607.4	197.87					
	CON.3	1463.4	140	.8045977			1.415019	
	TLS.3	1259	34					
	FEED 3	1524.4	174					
	CON.4	1483.2	132.78	.8058017			1.429722	
	TLS.4	1259.4	32					
	FEED 4	1544.6	164.78					
1.3	CON.1	1529.9	121.49	.6797024			.7292528	.7162599
	TLS.1	1330.9	57.25		2.020786			
	FEED 1	1660.8	178.74					
	CON.2	1465.5	109.92	.6624480			.6744103	
	TLS.2	1328.6	56.01		2.083235			
	FEED 2	1614.1	165.93					
	CON.3	1328.6	115.72	.6843693			.7451167	
	TLS.3	1538.2	53.37		3.025857			
	FEED 3	1666.8	169.09					
	FROTH		30.01					
	PULP		161.49					
	WATER	1200						

FEED AV.			% SOLID	
FEED 7.5	1735.633	202.2767	0.12	
FEED 5	1583.833	185.935	0.12	
FEED 1.3	1647.233	171.2533	0.10	

TEST-23

AFR L/MIN		SLURRY	SOLID G/MIN	RECOVERY	RES.TIME MIN.	AVE.R.T. MIN.	FRC MIN	AVE.FRC MIN
7.5	CON.1	1689.2	128.84	.8339720		2.975978	1.712553	1.763511
	TLS.1	1346.4	25.28					
	FEED 1	1795.6	154.12					
	CON.2	1742	137.74	.8497224			1.899998	
	TLS.2	1110	24.36					
	FEED 2	1652	162.1					
	CON.3	1650	125.54	.8331564			1.677982	
	TLS.3	1200.4	25.14					
	FEED 3	1730.4	150.68					
5	CON.1	1501.6	138.84	.8292916			1.632585	1.522095
	TLS.1	1390.6	28.58					
	FEED 1	1692.2	167.42					
	CON.2	1539.8	117.84	.8207271			1.538348	
	TLS.2	1250	25.74					
	FEED 2	1589.8	143.58					
	CON.3	1519	115.54	.8059431			1.393551	
	TLS.3	1233.2	27.82					
	FEED 3	1552.2	143.36					
	CON.4	1735	134.2	.8284672			1.622925	
	TLS.4	1345	28.2					
	FEED 4	1880	164.4					
1.3	CON.1	1429.9	86.16	.6699844			.6821826	.7042474
	TLS.1	1330.9	42.44		2.895382			
	FEED 1	1560.8	128.6					
	CON.2	1535.5	87.38	.6784161			.7088793	
	TLS.2	1328.6	41.42		2.966683			
	FEED 2	1664.1	128.8					
	CON.3	1528.6	86.98	.6823082			.7216804	
	TLS.3	1538.2	40.08		3.065868			
	FEED 3	1666.8	126.16					
	FROTH		32.2					
	PULP		122.08					
	WAFR	1200						
	FEED AV.			% SOLID				
	FEED 7.5	1726	155.6333			0.09		
	FEED 5	1611.4	143.47			0.09		
	FEED 1.3	1630.567	127.8533			0.08		

TEST-4

AFR L/MIN		SLURRY G/MIN	SOLID G/MIN	RECOVERY	RES.TIME MIN.	AVE.R.T. MIN.	FRC MIN	AVE.FRC MIN
7.5	CON.1	1703.43	139.85	.8351747		2.836171	1.786574	1.734541
	TLS.1	1329.7	27.6					
	FEED 1	1833.13	167.45					
	CON.2	1571.7	149.5	.8341238			1.773021	
	TLS.2	1334.2	29.73					
	FEED 2	1705.9	179.23					
	CON.3	1591.2	146.55	.8234071			1.644028	
	TLS.3	1320.3	31.43					
	FEED 3	1711.5	177.98					
5	CON.1	1577.7	155.47	.8004840			1.414629	
	TLS.1	1344.9	38.75					
	FEED 1	1724.6	194.22					
	CON.2	1553.2	148.68	.7991400			1.402804	1.399796
	TLS.2	1343.4	37.37					
	FEED 2	1714.6	184.05					
	CON.3	1526.7	153.43	.7984492			1.396788	
	TLS.3	1370.2	38.73					
	FEED 3	1696.9	192.16					
1.3	CON.1	1382.3	99.27	.5818533			.4906283	.4888170
	TLS.1	1560.1	71.34		2.883936			
	FEED 1	1742.4	170.61					
	CON.2	1289.9	98.8	.5835105			.4939833	
	TLS.2	1522.1	70.52		2.917470			
	FEED 2	1612	169.32					
	CON.3	1499.5	103.86	.5774491			.4818395	
	TLS.3	1504.9	76		2.707105			
	FEED 3	1804.4	179.86					
	FROTH		75.44					
	PULP		205.74					
	WWFR	1200						
	FEED 1	1861.6	196.4					
	FEED 2	1699.8	177.02					
	FEED 3	1850.4	192.52					
	FEED 4	1705.4	177.4					
	FEED AV.	1779.3	185.835% SOLID			0.10		
	FEED 7.5	1750.177	174.8867			0.10		
	FEED 5	1712.7	189.105			0.11		
	FEED 1.3	1719.6	173.2633			0.10		

TEST-5

AFR L/MIN		SLURRY	SOLID G/MIN	RECOVERY	RES.TIME MIN.	AVE.R.T. MIN.	FRC MIN	AVE.FRC MIN
7.5	CON.1	1530.7	134.84	.8296014		2.966785	1.641033	1.717511
	TLS.1	1343.9	27.7					
	FEED 1	1674.6	162.54					
	CON.2	1554.3	137.74	.8393662			1.761281	
	TLS.2	1273.6	26.36					
	FEED 2	1427.9	164.1					
	CON.3	1562.4	130.54	.8385149			1.750219	
	TLS.3	1251.8	25.14					
	FEED 3	1614.2	155.68					
5	CON.1	1484.5	142.07	.8236101			1.573845	1.376863
	TLS.1	1475.9	34.71					
	FEED 1	1760.4	196.78					
	CON.2	1457.4	148.51	.7929414			1.290809	
	TLS.2	1476.7	38.78					
	FEED 2	1734.1	187.29					
	CON.3	1439.1	145.51	.7973151			1.325936	
	TLS.3	1489.2	36.99					
	FEED 3	1728.3	182.5					
	CON.4	1474.9	140.09	.7958755			1.314207	
	TLS.4	1477.3	35.93					
	FEED 4	1752.2	176.02					
1.3	CON.1	1376.9	98.38	.6161458			.5410422	.4994518
	TLS.1	1555.5	61.29		3.085822			
	FEED 1	1732.4	159.67					
	CON.2	1363.4	90.88	.5880298			.4811134	
	TLS.2	1578.7	63.67		2.970473			
	FEED 2	1742.1	154.55					
	CON.3	1341.1	93.95	.5855467			.4761997	
	TLS.3	1592.1	64.5		2.844060			
	FEED 3	1733.2	160.45					
	FROTH		21.13					
	PULP		189.13					
	WWFR	1200						
	FEED 1	1627	154.24					
	FEED 2	1518.8	142.08					
	FEED 3	1606.8	150.22					
	FEED 4	1546.4	144					
	FEED AV.	1574.75	147.8351	SOLID	0.09			
	FEED 7.5	1638.9	160.78		0.10			
	FEED 5	1740.933	184.895		0.11			
	FEED 1.3	1733.9	158.2233		0.09			

TEST-28

AFR L/MIN		SLURRY	SOLID G/MIN	RECOVERY	AVE.REC	RES.TIME MIN.	AV.RE.TI. MIN	FRC MIN	AV.FRC MIN
0.7	CON.1	1904.2	165.07	.8262589	.8219088		3.016726	1.576441	
	TLS.1	1269.2	34.71			3.042518			1.531746
	FEED 1	1973.4	199.78						
	CON.2	1007.6	160.51	.8177187				1.487051	
	TLS.2	1181	35.78			2.970933			
	FEED 2	1988.6	196.29						
2.25	CON.1	1724	110.38	.6977073				.7650852	
	TLS.1	1472.4	91.29		.6977131				.7651063
	FEED 1	1996.4	169.67						
	CON.2	1801.8	123.88	.6977190				.7651274	
	TLS.2	1297.6	53.67						
	FEED 2	1850.4	177.55						
6.25	CON.1	1836.6	160.4	.8451001				1.808511	
	TLS.1	1297.2	29.4		.8447481				1.803670
	FEED 1	1933.8	189.8						
	CON.2	1724.4	155.2	.8443961				1.798829	
	TLS.2	1240.2	28.6						
	FEED 2	1764.6	183.8						
	FROTH		41						
	PULP		106.3						
	WWFR	1200							

FEED AV.			% SOLID	
FEED 0.7	1881	198.035		0.11
FEED 2.25	1927.9	173.61		0.09
FEED 6.25	1849.2	186.8		0.10

TEST-12

LIT./MIN		SLURRY G/MIN	SOLID G/MIN	R (%)	RES.TIME MIN.	AVE.R.T. MIN.	FRC MIN	AVE.FRC MIN
AFR:1.3	CON.1	1451.1	125.1	.6415385			.6594623	.5489721
	TLS.1	1295.4	69.9		2.713077	2.984727		
	CON.2	1408.6	100.1	.6244945			.5698471	
	TLS.2	1301.6	65		2.918462			
	CON.3	1403.3	100.4	.6243781			.5292567	
	TLS.3	1325.7	60.4		3.140728			
	CON.4	1368.5	96.4	.6191394			.5081700	
	TLS.4	1333.6	59.3		3.190980			
	CON.5	1353.2	90.7	.5893437			.4781234	
	TLS.5	1332.2	63.2		3.001582			
	FROTH		29.1					
	PULP		189.7					

APPENDIX 6.2

Slurry and froth kinetics in continuous flotation

Derivation of the recovery formula

Flowrate of mineral over the cell lip

$$Q_c * C_c = K_1 * C_c * V_F = K_1 * M_F \qquad 1$$

Flowrate of mineral back to the slurry

$$Q_d * C_c = K_2 * C_c * V_F = K_2 * M_F \qquad 2$$

where K : FTC (1/min)

K : DBC (1/min)

Mf : mass in the froth (g)

Qd : drainage flow rate from the froth back to the slurry (L/min).

The fraction of mineral recovered in the concentrate, having been transferred from the slurry to the froth, is;

$$R_F = \frac{Q_c * C_c}{Q_c * C_c + Q \ * C_c} = \frac{K_1}{K_1 + K_2} \qquad 3$$

Rf is the recovery in the froth phase.

The total recovery can be expressed as:

$$R = \frac{R_F * Q_C * C_C}{R * Q_C * C_C + Q_t * C_t} \qquad 4$$

or

$$R = \frac{R_F * K * T}{R_F * K * T + 1} \qquad 5$$

The ORC can be defined as;

$$R_F K = K \frac{K_1}{K_1 + K_2} = ORC \qquad 6$$

a) Determination of FTC

$$K = \frac{Q_C * C_C}{C_C * V_F} \qquad 7$$

$$K = \frac{\text{Conc. mass flow rate (g/min)}}{\text{mass in the froth (g)}} \qquad 8$$

b) Determination of DBC

Recovery in the froth can be calculated using the following equation.

$$R = \frac{R_F * \tau * K}{R_F * \tau * K + 1} \qquad 9$$

$$R_F = \frac{R}{\tau * K - R * \tau * K} \qquad 10$$

By definition,

$$R_F = \frac{K_1}{K_1 + K_2} \qquad 11$$

The DBC can be found from;

$$K = K \frac{(1-R_F)}{R_F} \qquad 12$$

c) Determination of ORC

By definition,

$$ORC = K \frac{K_1}{K_1 + K_2} \qquad 13$$

APPENDIX 6-2

AFR (l/min)	F.T. (cm)	REC.	FRC (min)	FTC (min)	DBRC (min)	DRC (min)	CONC. (g/min)	SOLID (g)	TLS. (g/min)	SOLID (g)	FROTH (g)	PULP (g)
1.30	1	0.58	0.59	1.51	.41	.46	303.68	93.42	1192.12	67.99	61.99	409.85
	2	0.52		0.70	.43	.36	214.58	73.69	1285.42	68.68	105.42	442.22
	2	0.50		0.70	.53	.33	243.81	73.56	1256.19	47.01	105.60	389.04
	3	0.38		0.31	.59	.21	77.41	52.2	1422.60	86.08	166.91	515.53
	5	0.32		0.32	.65	.16	184.49	44.19	1315.55	93.50	180.15	433.52
3.75	1	0.71	1.35	1.67	0.98	0.85	470.50	114.48	1029.50	46.00	68.53	316.36
	2	0.64		0.95	1.13	0.62	295.22	95.60	1204.78	52.55	100.91	337.74
	2	0.63		0.91	1.24	0.57	311.18	103.04	1188.83	60.98	113.66	405.37
	5	0.48		0.57	1.86	0.32	296.93	72.38	1203.07	76.91	126.37	381.52
5.00	1	0.74	1.47	2.24	1.13	0.98	474.49	118.33	1036.76	40.88	52.82	271.32
	1	0.73		2.11	1.28	0.92	349.88	110.09	1150.12	40.77	52.27	258.15
	3	0.66		1.16	1.37	0.67	211.63	89.76	1288.37	45.43	77.58	330.02
	3	0.63		1.03	1.65	0.57	137.80	96.26	1362.20	58.78	93.40	385.46
	4	0.56		0.81	1.98	0.43	160.01	74.06	1339.99	58.50	91.04	347.10
	5	0.51		0.65	2.03	0.36	96.82	77.56	1403.18	73.81	120.00	325.35
7.50	1	0.76	1.73	1.88	1.18	1.05	701.89	116.25	798.11	36.80	61.98	294.02
	1	0.73		1.95	1.69	0.93	725.16	109.68	773.90	39.97	56.14	227.35
	2	0.74		1.45	1.20	0.94	335.53	137.40	1164.47	48.00	94.53	389.99
	3	0.63		0.89	1.74	0.58	150.25	78.96	943.04	44.89	88.6	325.35
	5	0.57		0.81	2.25	0.46	532.70	91.55	967.30	68.09	112.55	396.44
	5	0.60		0.83	2.02	0.50	187.95	96.17	1312.05	66.11	115.57	463.94

Slurry-Froth kinetics results

Appendix 6.3

TEST-23

AFR: 1.3 l/min F.T.:1 cm FRC: .59 Tover.: 2.94625

CONC.	W.W.F.R.	SOLID F.RFTRC (g/min)	(min)	RECOVERY TOFRC	Ri	DORC (min)	ORC (min)
1	337.24	104.08	1.691653	.6069796 1.738200	.8004589	.2123777	.5241907
2	317.39	95.59	1.541811	.5873065	.8186825	.3414722	.4830227
3	293.2	86.61	1.396969	.5612728	.7359664	.5011742	.4342200
4	266.9	86.61	1.396969	.5562978	.7212637	.5398660	.4255456
AVERAGE	303.6825	93.4225	1.506850	.5779641	.7878253	.4058203	.4648169

TLO.		
1	1182.03	67.91
2	1189.91	67.17
3	1195.4	67.7
4	1196.24	69.08
5	1196.24	68.12
AVERAGE	1192.124	67.996

FEED 1495.007 161.4185 % SOLID: 10.79

FROTH 61.99853

PULP 409.0507 FRO./PULP 0.15

TEST-17

AFR: 1.3 l/min F.T.:2 cm FRC: .59 Tover.: 2.94625

CONC.	W.W.F.R.	SOLID F.RFTRC (g/min)	(min)	RECOVERY TOFRC	Ri	DORC (min)	ORC (min)
1	195.3	67.3	.6383900	.5049099 1.738200	.5868768	.4493913	.3462573
2	219.32	75.77	.7187441	.5279404	.6433703	.3983967	.3795932
3	207.56	71.56	.6700086	.5067989	.5911395	.4694967	.3487723
4	236.15	80.11	.7599127	.5327080	.6560226	.3904509	.3870533
AVERAGE	214.5825	73.605	.6909660	.5181293	.6185659	.4310123	.3649539

TLO.		
1	1279.07	65.97
2	1292.13	67.75
3	1280.25	69.64
4	1287.42	70.75
5	1287.42	69.79
AVERAGE	1285.418	68.68

FEED 1500.001 142.365 % SOLID: 9.49

FROTH 105.42

PULP 442.2194 FRO./PULP 0.24

TEST-13

AFR: 1.3 l/min F.T.:2 cm FRC: .59 Tover.: 2.94625

CONC.	SLU.F.R.	SOLID F.RFTRC (g/min)	(min)	RECOVERY T8FRC		RF	DOAC (min)	OAC (min)
1	233.23	70.79	.6703598	.4841997	1.738288	.5440343	.5709684	.3106203
2	219.74	83.65	.7921402	.5241556		.6336855	.4579124	.3738744
3	240.87	68.84	.6520833	.4841114		.5398433	.5558209	.3185075
4	281.38	70.93	.6716856	.4932202		.5590865	.5279961	.3303330
AVERAGE	243.805	73.5575	.6965672	.4964217		.5671033	.5317225	.3349910

TLS.		
1	1234.06	75.41
2	1241.49	75.94
3	1338.48	73.38
4	1232.86	72.08
5	1234.06	72.42
AVERAGE	1256.19	74.006

FEED 1499.995 147.5435 % SOLID: 9.84

FROTH 105.6

PULP 389.0435 FRO./PULP 0.27

TEST-10

AFR: 1.3 l/min F.T.:3 cm FRC: .59 Tover.: 2.94625

CONC.	SLU.F.R.	SOLID F.RFTRC (g/min)	(min)	RECOVERY T8FRC		RF	DOAC (min)	OAC (min)
1	64.22	43.31	.2594819	.3350093	1.738288	.2098142	.6358569	.1709904
2	75.34	50.28	.3012410	.3743021		.3441406	.5741018	.2038430
3	90.7	60.64	.3633106	.4120021		.4045565	.5347360	.2386083
4	79.35	54.57	.3269436	.3796438		.3520575	.6017218	.2077139
AVERAGE	77.4025	52.2	.3127443	.3754593		.3458443	.5915400	.2040401

TLS.		
1	1442.18	85.97
2	1420.59	84.05
3	1412.67	86.23
4	1439.20	89.17
5	1398.27	85
AVERAGE	1422.590	86.084

FEED 1500.001 138.204 % SOLID: 9.22

FROTH 166.9995

PULP 515.5269 FRO./PULP 0.32

TEST-21

AFR: 1.3 l/min F.T.:5 cm FRC: .59 Tover.: 2.94625

CONC.	SLU.F.R.	SOLID (g/min)	F.RFTRC (min)	RECOVERY	T&FRC	Rf	DOOC (min)	OOC (min)
1	193.12	46.14	.2561199	.3210056	1.738200	.2720722	.6052475	.1605226
2	152.89	43.15	.2395226	.3111255		.2598200	.6823535	.1532943
3	213.57	43.75	.2420532	.3404404		.2969378	.5750053	.1751933
4	178.37	43.72	.2426867	.3147362		.2642209	.6758123	.1550903
AVERAGE	184.4875	44.19	.2452956	.3210469		.2730235	.6531457	.1610839

TLS.		
1	1325.86	97.56
2	1315.55	95.54
3	1309.38	84.76
4	1313.3	95.19
5	1313.65	94.40
AVERAGE	1315.548	93.506

FEED 1500.036 137.696 % SOLID: 9.18

FROTH 100.15

PULP 433.5277 FRO./PULP 0.42

TEST-30

AFR: 3.75 l/mi F.T.:1 cm FRC: 1.35 Tover.: 2.94625

CONC.	SLU.F.R.	SOLID (g/min)	F.RFTRC (min)	RECOVERY	T&FRC	Rf	DOOC (min)	OOC (min)
1	456.96	110.62	1.614228	.7064759	3.977438	.6051322	1.053334	.8169285
2	500.06	120.89	1.764093	.7276831		.6718378	.8616795	.9069810
3	443.06	110.21	1.600245	.7084726		.6109988	1.023912	.8240484
4	481.12	116.18	1.695362	.7153500		.6318356	.9878709	.8529781
AVERAGE	470.5	114.475	1.670082	.7144954		.6291918	.9944829	.8494089

TLS.		
1	1029.817	45.96
2	1043.712	45.20
3	1014.185	45.35
4	1050.975	46.23
5	1000.816	47.22
AVERAGE	1029.501	46

FEED 1500.001 160.475 % SOLID: 10.70

FROTH 68.52812

PULP 316.3583 FRO./PULP 0.22

TEST-32

AFR: 3.75 l/mi F.T.:2 cm FRC: 1.35 Tavor.: 2.94625

CONC.	SLN.F.R.	SOLID F.RFTRC (g/min)	(min)	RECOVERY TOFRC	Rf	DORC (min)	DRC (min)
1	284.85	92.36	.9152941	.6394351 3.977438	.4458714	1.137527	.6019263
2	305.58	95.72	.9485919	.6372836	.4417354	1.190829	.5963420
3	296.79	97.15	.9627633	.6487046	.4602704	1.110948	.6267652
4	293.64	97.18	.9630606	.6523899	.4718582	1.077935	.6370085
AVERAGE	295.215	95,6025	.9474275	.6444533	.4557130	1.131573	.6152126

TLS.		
1	1156.64	52.08
2	1270.78	54.48
3	1179.63	52.61
4	1292.84	51.78
5	1126.62	51.78
AVERAGE	1204.702	52.546

FEED 1499.997 148.1085 % SOLID: 9.88

FROTH 100.9075

PULP 337.7352 FRO./PULP 0.30

TEST-31

AFR: 3.75 l/mi F.T.:2 cm FRC: 1.35 Tavor.: 2.94625

CONC.	SLN.F.R.	SOLID F.RFTRC (g/min)	(min)	RECOVERY TOFRC	Rf	DORC (min)	DRC (min)
1	327.43	111.27	.9789983	.6429191 3.977438	.4526747	1.183699	.6111109
2	299.56	98.33	.8651469	.6150238	.4016563	1.288001	.5422360
3	314.62	104.86	.9226005	.6364409	.4401287	1.173606	.5941737
4	303.09	97.7	.8596039	.6147747	.4012341	1.282796	.5416661
AVERAGE	311.175	103.04	.9065874	.6272896	.4231489	1.235091	.5712510

TLS.		
1	1182.71	61.8
2	1199.37	61.55
3	1148.26	59.9
4	1214.744	61.22
5	1199.84	60.44
AVERAGE	1188.825	60.992

FEED 1500.000 164.022 % SOLID: 10.93

FROTH 113.6570

PULP 405.3684 FRO./PULP 0.28

248

TEST-33

AFR: 3.75 l/m F.T.:5 cm FRC: 1.35 Tavor.: 2.94625

CONC.	SLU.F.R.	SOLID (g/min)	F.OFTRC (min)	RECOVERY	TOFRC	RF	DOAC (min)	OAC (min)
1	317.66	77.40	.6131317	.5023992	3.977438	.2538426	1.002270	.3426875
2	291.98	66.83	.5200530	.4590500		.2140417	1.941944	.2809563
3	301.64	77.93	.6166920	.5044339		.2559171	1.793043	.3454081
4	276.42	67.27	.5323357	.4679001		.2210837	1.075512	.2904629
AVERAGE	296.925	72.3775	.5727535	.4834450		.2354921	1.059402	.3179143

TLB.		
1	1203.4	76.74
2	1207.79	78.5
3	1204.16	76.56
4	1194.94	76.5
5	1205.07	76.23
AVERAGE	1203.072	76.906

FEED 1499.997 149.2835 % SOLID: 9.95

FROTH 126.3676

PULP 383.5197 FRO./PULP 0.33

TEST-19

AFR: 5 L/MIN F.T.:1 cm FRC: 1.472 Tavor.: 2.94625

CONC.	SLU.F.R.	SOLID (g/min)	F.OFTRC (min)	RECOVERY	TOFRC	RF	DOAC (min)	OAC (min)
1	543.51	121.55	2.301211	.7452483	4.33600	.6745382	1.110324	.9929202
2	370.76	109.19	2.067200	.7390186		.6529327	1.090827	.9413170
3	483.17	122.92	2.327140	.7410673		.6426831	1.104558	.9794695
4	500.51	119.64	2.265050	.7431056		.6469087	1.130005	.9818073
AVERAGE	474.4075	118.325	2.240154	.7423100		.6642174	1.132448	.9777200

TLB.		
1	1028.08	41.35
2	1024.97	38.56
3	1049.30	42.77
4	1044.2	41.36
5	1037.17	40.18
AVERAGE	1036.76	40.804

FEED 1511.208 159.209 % SOLID: 10.53

FROTH 52.02002

PULP 271.3105 FRO./PULP 0.19

TEST-6

AFR: 5 L/MIN F.T.: 1 cm FRC: 1.472 Tover.: 2.94625

CONC.	SLU.F.R.	SOLID (g/min)	F.RFTRC (min)	RECOVERY	TOFRC	RF	DOOC (min)	OOC (min)
1	385.73	110.24	2.109049	.7329787	4.33688	.6329481	1.223055	.9316996
2	381.95	101.23	1.936675	.7105054		.5661330	1.484200	.8333478
3	281.77	115.2	2.203941	.7366671		.6458431	1.212794	.9495034
4	350.05	113.7	2.175244	.7376890		.6484542	1.179263	.9545246
AVERAGE	349.875	110.0925	2.106227	.7294001		.6217800	1.281189	.9152601

TLS.		
1	1154.30	40.16
2	1153.57	41.23
3	1154.10	41.10
4	1134.6	40.43
5	1153.67	40.87
AVERAGE	1150.12	40.774

FEED 1499.995 150.8665 % SOLID: 10.06

FROTH 52.27

PULP 258.1455 FRO./PULP 0.20

TEST-9

AFR: 5 l/min F.T.: 3 cm FRC: 1.472 Tover.: 2.94625

CONC.	SLU.F.R.	SOLID (g/min)	F.RFTRC (min)	RECOVERY	TOFRC	RF	DOOC (min)	OOC (min)
1	253.61	97.24	1.253328	.6825277	4.33688	.4957252	1.274944	.7297074
2	203.8	86.72	1.117736	.6668205		.4614003	1.304330	.6792990
3	185.91	84.09	1.094149	.6469288		.4224904	1.495611	.6219058
4	203.19	90.18	1.142332	.6635762		.4540064	1.393331	.6694751
AVERAGE	211.6275	89.7575	1.156806	.6649638		.4576451	1.371025	.6736536

TLS.		
1	1288.51	45.23
2	1296.09	43.33
3	1288.92	44.33
4	1283.29	45.72
5	1285.03	44.55
AVERAGE	1288.368	45.432

FEED 1499.996 135.1895 % SOLID: 9.01

FROTH 77.58543

PULP 330.9199 FRO./PULP 0.24

TEST-11

AFR: 5 l/min F.T.:3 cm FRC: 1.472 Tavor.: 2.94625

CONC.	SLU.F.R.	SOLID (g/min)	F.RFTRC (min)	RECOVERY	T0FRC	R1	DDRC (min)	DRC (min)
1	172.02	100.42	1.075161	.6402295	4.33600	.4103295	1.545076	.6040951
2	160.8	99.34	1.063597	.6354100		.4018573	1.503107	.5915340
3	115.56	94.02	1.015203	.6076258		.3570740	1.027914	.5256130
4	102.82	99.48	.9687366	.6160530		.3712264	1.640021	.5464453
AVERAGE	137.8	96.265	1.030475	.6250296		.3843493	1.650934	.5657622

TLS.		
1	1313.35	56.43
2	1311.75	57
3	1378.7	61.23
4	1370.59	56.2
5	1436.62	63.05
AVERAGE	1362.202	58.782

FEED 1500.002 155.047 % SOLID: 10.34

FROTH 93.4

PULP 385.4596 FRO./PULP 0.24

TEST-8

AFR: 5 l/min F.T.:6 cm FRC: 1.472 Tavor.: 2.94625

CONC.	SLU.F.R.	SOLID (g/min)	F.RFTRC (min)	RECOVERY	T0FRC	R1	DDRC (min)	DRC (min)
1	172.41	77.58	.8520757	.5775329	4.33600	.3152147	1.851004	.4639961
2	147.23	66.95	.7353244	.5382698		.2688032	2.000225	.3956782
3	152.81	71.82	.7888125	.5411800		.2719706	2.111547	.4003408
4	167.59	79.87	.8772272	.5761379		.3134184	1.921674	.4613519
AVERAGE	160.01	74.055	.8133599	.5582802		.2914257	1.977600	.4289787

TLS.		
1	1331.33	56.75
2	1347.09	57.43
3	1348.38	60.09
4	1368.26	58.76
5	1304.93	58.67
AVERAGE	1339.998	58.5

FEED 1500.008 132.555 % SOLID: 8.84

FROTH 91.04825

PULP 347.0959 FRO./PULP 0.26

TEST-7

AFR: 5 l/min F.T.:5 cm FRC: 1.472 Taver.: 2.94625

CONC.	SLU.F.R.	SOLID F.R. (g/min)	F.RFTRC (min)	RECOVERY	T&FRC	Rf	DDRC (min)	ORC (min)
1	99.32	83.44	.697	.3398567	4.33680	.2705254	1.879468	.3982133
2	114.68	82.12	.6843333	.5287149		.2586786	1.961163	.3807749
3	91.96	65.48	.5456667	.4624947		.1984023	2.204638	.2920481
4	81.33	79	.6583333	.5143564		.2442132	2.037399	.3594818
AVERAGE	96.8225	77.56	.6463333	.5113557		.2412975	2.032241	.3551899

TLS.		
1	1403.824	71.29
2	1408.265	73.2
3	1396.24	76.1
4	1404.379	74.59
5	1403.177	73.85
AVERAGE	1403.177	73.806

FEED 1500.000 151.366 % SOLID: 10.09

FROTH 120

PULP 325.3500 FRO./PULP 0.37

TEST-10

AFR: 7.5 l/min F.T.:1 cm FRC: 1.725 Taver.: 2.94625

CONC.	SLU.F.R.	SOLID F.R. (g/min)	F.RFTRC (min)	RECOVERY	T&FRC	Rf	DDRC (min)	ORC (min)
1	598.63	113.41	1.829714	.7371446	5.002201	.5517990	1.406100	.9518546
2	646.50	113.04	1.823744	.7583523		.6174897	1.129737	1.045170
3	768.78	106	1.710164	.7472682		.5817790	1.229378	1.003569
4	793.59	132.57	2.138834	.7855069		.7205730	.8294044	1.202980
AVERAGE	701.895	116.255	1.875614	.7570685		.6131866	1.183184	1.037747

TLS.		
1	800.83	40.44
2	793.76	36.02
3	795.175	35.85
4	806.12	36.2
5	794.65	35.49
AVERAGE	798.107	36.8

FEED 1500.002 153.055 % SOLID: 10.20

FROTH 61.98230

PULP 294.0190 FRO./PULP 0.21

TEST-26

AFR: 7.5 l/min F.T.:1 cm FRC: 1.725 Tavor.: 2.94625

CONC.	SLU.F.R.	SOLID F.R. (g/min)	F.TRC (min)	RECOVERY	T&FRC	Rf	DDRC (min)	DRC (min)
1	702.01	107.79	1.920021	.7252725	5.082281	.5194460	1.776265	.8960443
2	783.54	114.66	2.042394	.7411286		.5633142	1.583280	.9717170
3	495.49	108.12	1.925900	.7288170		.5288071	1.716070	.9121923
4	719.59	108.16	1.926612	.7316512		.5364704	1.664662	.9254115
AVERAGE	725.1575	109.6825	1.953732	.7317173		.5366511	1.686860	.9257231

TLS.

1	756	40.83
2	789.51	40.05
3	771.76	40.23
4	777.37	39.67
5	774.84	39.07
AVERAGE	773.896	39.97

FEED 1499.054 149.6525 % SOLID: 9.98

FROTH 56.14

PULP 227.3529 FRO./PULP 0.25

TEST-16

AFR: 7.5 l/min F.T.:2 cm FRC: 1.725 Tavor.: 2.94625

CONC.	SLU.F.R.	SOLID F.R. (g/min)	F.TRC (min)	RECOVERY	T&FRC	Rf	DDRC (min)	DRC (min)
1	366.75	137.91	1.450857	.7197808	5.082281	.5054098	1.427626	.8718319
2	338.94	137.91	1.450857	.7332128		.5407623	1.238922	.9328150
3	308.98	137.02	1.453674	.7543917		.6043594	.9516396	1.042520
4	327.46	136.35	1.442355	.7355559		.5472971	1.193060	.9440075
AVERAGE	335.5325	137.3975	1.453436	.7357353		.5478022	1.199777	.9449508

TLS.

1	1172.325	53.69
2	1167.66	50.18
3	1127.392	44.74
4	1223.87	49.02
5	1131.09	42.4
AVERAGE	1164.467	48.006

FEED 1500.000 185.4035 % SOLID: 12.36

FROTH 94.53291

PULP 389.9969 FRO./PULP 0.24

TEST 27

AFR: 7.5 l/min F.T.:5 cm FRC: 1.725 Taver.: 2.94625

CONC.	SLU.F.R.	SOLID F.R (g/min)	F.TRC (min)	RECOVERY	T6FRC	Rf	DBRC (min)	DRC (min)
1	547.93	92.28	.8199023	.5742377	5.082281	.2653786	2.269655	.4577780
2	527.09	91.61	.8139494	.5742854		.2654303	2.252579	.4578672
3	577.5	96.7	.8591737	.5878777		.2806740	2.201936	.4841626
4	478.28	85.59	.7604620	.5586815		.2490883	2.292519	.4296774
AVERAGE	532.7	91.545	.8133718	.5737706		.2648720	2.257439	.4569043

TLS.		
1	961.31	68.42
2	959.13	67.91
3	979.37	67.79
4	962.3	67.61
5	974.4	68.7
AVERAGE	967.302	68.084

FEED 1500.002 159.631 % SOLID: 10.64

FROTH 112.55

PULP 396.4404 FRO./PULP 0.28

TEST-14

AFR: 7.5 l/min F.T.:3 cm FRC: 1.725 Taver.: 2.94625

CONC.	SLU.F.R.	SOLID F.R (g/min)	F.TRC (min)	RECOVERY	T6FRC	Rf	DBRC (min)	DRC (min)
1	200.2	97.025	1.095090	.6762974	5.082281	.4110861	1.568005	.7091234
2	134.7	72.4	.8171558	.6046434		.3009204	1.898366	.5190877
3	163.35	82.64	.9327314	.6490732		.3639305	1.630297	.6277001
4	102.75	63.775	.7190001	.5976190		.2922333	1.743320	.5041025
AVERAGE	150.25	78.96	.8911964	.6319084		.3377844	1.747162	.5826701

TLS.		
1	922.7	46.44
2	950.5	47.34
3	946	44.68
4	951	42.94
5	945	43.07
AVERAGE	943.04	44.894

FEED 1093.29 123.854 % SOLID: 11.33

FROTH 88.6

PULP 325.35 FRO./PULP 0.27

TEST-15

AFR: 7.5 l/min F.T.:5 cm FRC: 1.725 Tover.: 2.94625

CONC.	SLU.F.R.	SOLID (g/min)	F.RFTRC (min)	RECOVERY	TIFRC	Rf	BDRC (min)	DRC (min)
1	190.09	98	.8479709	.5894382	5.082281	.2824887	2.153816	.4872930
2	160.32	91.98	.7093536	.5570807		.2474770	2.156988	.4268978
3	201.48	102.21	.8843991	.6508947		.3668560	1.526353	.6328267
4	199.92	102.5	.8869084	.5898262		.2829420	2.247685	.4884750
AVERAGE	187.9525	96.1725	.8321580	.5968100		.2912511	2.025026	.5024082

TLS.		
1	1309.8	68.26
2	1302.81	65.18
3	1310.68	54.82
4	1324.22	71.28
5	1312.72	70.99
AVERAGE	1312.046	66.104

FEED 1499.999 162.2785 % SOLID: 10.82

FROTH 115.57

PULP 463.9367 FRO./PULP 0.25

APPENDIX 7.1

Size-by-size Kinetics in the Continous Slurry Froth Flotation

AFR (l/min)	F.T. (cm)	SIZE (uM)	FRC (min)	FTC (min)	DBRC (min)	ORC (min)
1.3	1	+37	.59	1.57	.27	.5
		-37+28		1.6	.25	.51
		-28+20		1.5	.09	.56
		-20+13		1.47	.02	.58
		-13+9		1.27	.34	.46
		-9		1.57	1.9	.27
	2	+37		.75	.45	.37
		-37+28		.77	.26	.44
		-28+20		.76	.25	.44
		-20+13		.75	.22	.46
		-13+9		.59	.44	.34
		-9		.42	1.84	.11
	5	+37		.32	.6	.21
		-37+28		.34	.48	.25
		-28+20		.27	.43	.22
		-20+13		.23	.55	.17
		-13+9		.18	.48	.16
		-9		.12	.07	.04
5	1	+37	1.425	1.68	.8	.96
		-37+28		2.28	.68	1.1
		-28+20		2.39	.55	1.16
		-20+13		2.08	.93	.98
		-13+9		2.06	1.65	.79
		-9		2.06	1.95	.73
	3	+37		1.21	1.45	.67
		-37+28		1.43	1.53	.71
		-28+20		1.5	1.37	.77
		-20+13		1.03	1.41	.62
		-13+9		.91	1.55	.54
		-9		.98	1.14	.68
	5	+37		.69	1.47	.47
		-37+28		.7	1.91	.39
		-28+20		.9	117	.51
		-20+13		.63	1.99	.35
		-13+9		.61	2.17	.32
		-9		.45	2.47	.23

7.5	1	+37	1.725	1.85	.92	1.15
		-37+28		1.71	.78	1.19
		-28+20		2.21	.61	1.35
		-20+13		1.99	1.22	1.07
		-13+9		2.46	1.7	1.02
		-9		1.48	5.99	.34
	3	+37		1.11	2.68	.51
		-37+28		1.08	1.17	.83
		-28+20		1.15	1.16	.86
		-20+13		.68	1.32	.59
		-13+9		.7	1.73	.5
		-9		.61	2.73	.31
	5	+37		1.1	3.26	.44
		-37+28		.71	2.03	.446
		-28+20		.97	1.75	.62
		-20+13		1.01	2.16	.55
		-13+9		.59	2.31	.35
		-9		.63	1.83	.44

WARMAN CYCLOSIZER CONDITIONS

amount of sample: 30-40 g
specific gravity: 4.1 g/cc
temperature: 22 C
flowrate: 175 (scale).
elutriation time: 30 min

TEST-26

AFR: 7.5 l/min FRC 1.725 FT: 1 cm Taver.: 2.94625

SIZE (uM)	WEIGHT (g)	% WEIGHT	CUM.WEI.	AV.SO.F.R (g/min)	FTC (min)	RECOVERY	T8FRC	Rf	DBRC (min)	ORC (MIN)
CONCENTRE										
+37	5.19	12.975	100	109.68 14.23098	1.853681	.7724223	5.082281	.6678308	.9219936	1.152008
-37+28	5.3	13.25	87.025	14.5326	1.711495	.7775818		.6878871	.7765513	1.186605
-28+20	11.12	27.8	73.775	30.49104	2.210071	.7990883		.7825837	.6139990	1.349957
-20+13	10	25	45.975	27.42	1.999680	.7594415		.6211763	1.219503	1.071529
-13+9	4.2	10.5	20.975	11.5164	2.456732	.7498868		.5899300	1.707715	1.017629
-9	4.19	10.475	10.475	11.48898	1.477608	.5013431		.1978219	5.991776	.3412429
TAILINGS										
+37	3.62	10.49	100	39.97 4.192853						
-37+28	3.59	10.4	89.51	4.15688						
-28+20	6.62	19.18	79.11	7.666246						
-20+13	7.5	21.73	59.93	8.685481						
-13+9	3.32	9.61	38.2	3.841117						
-9	9.87	28.59	28.59	11.42742						
FROTH										
+37	5.47	13.675	100	56.14 7.677145						
-37+28	6.05	15.125	86.325	8.491175						
-28+20	9.83	24.575	71.2	13.79641						
-20+13	9.77	24.425	46.625	13.71220						
-13+9	3.34	8.35	22.2	4.68769						
-9	5.54	13.85	13.85	7.77539						
PULP										
+37	3.56	8.9	100	227.35 20.23415						
-37+28	4.03	10.075	91.1	22.90551						
-28+20	7.29	18.225	81.025	41.43454						
-20+13	9.24	23.1	62.8	52.51785						
-13+9	4	10	39.7	22.735						
-9	11.88	29.7	29.7	67.52295						

TEST-14

AFR: 7.5 l/min FRC 1.725 FT: 3 cm Taver.: 2.94625

SIZE (uM)	WEIGHT (g)	% WEIGHT	CUM.WEI.	AV.SO.F.R (g/min)	FTC (min)	RECOVERY	T%FRC	Rf	DBRC (min)	ORC (MIN)
		CONCENTRE								
+37	5	12.5	100	78.96 9.87	1.113995	.5984769	5.082281	.2932771	2.684445	.5059030
-37+28	6.9	17.25	87.5	13.6206	1.088364	.7098700		.4814238	1.172355	.8304561
-28+20	12.95	32.375	70.25	25.5633	1.154099	.7167726		.4979519	1.163593	.8589670
-20+13	7	17.5	37.875	13.818	.6840323	.6339140		.3407129	1.323618	.5877298
-13+9	3.5	8.75	20.375	6.909	.7041055	.5944315		.2883891	1.737406	.4974713
-9	4.65	11.625	11.625	9.1791	.6094211	.4808467		.1822436	2.734570	.3143703
		TAILINGS								
+37	5.9	14.75	100	44.894 6.621865						
-37+28	4.96	12.4	85.25	5.566856						
-28+20	9	22.5	72.85	10.10115						
-20+13	7.11	17.775	50.35	7.979909						
-13+9	4.2	10.5	32.575	4.71387						
-9	8.83	22.075	22.075	9.910351						
		FROTH								
+37	4	10	100	88.6 8.86						
-37+28	5.65	14.125	90	12.51475						
-28+20	10	25	75.875	22.15						
-20+13	9.12	22.8	50.875	20.2008						
-13+9	4.43	11.075	28.075	9.81245						
-9	6.8	17	17	15.062						
		PULP								
+37	5.5	13.75	100	325.35 44.73563						
-37+28	4.5	11.25	86.25	36.60188						
-28+20	8.07	20.175	75	65.63936						
-20+13	5.85	14.625	54.825	47.58244						
-13+9	2.89	7.225	40.2	23.50654						
-9	13.19	32.975	32.975	107.2842						

TEST-7

AFR: 5 l/min FRC 1.472 FT: 5 cm Taver.: 2.94625

SIZE (uM)	WEIGHT (g)	% WEIGHT	CUM.WEI.	AV.SO.F.R (g/min)	FTC (min)	RECOVERY	T%FRC	Rf	DBRC (min)	ORC (MIN)
		CONCENTRE								
+37	4.29	10.725	100	77.65	8.327963	.6939969	.5813708	4.33688	.3202184	1.473264	.4713615
-37+28	4.3	10.75	89.275		8.347375	.6956146	.5370345		.2674707	1.905099	.3937169
-28+20	11.43	28.575	78.525		22.18849	.8997765	.6005054		.3466001	1.696231	.5101953
-20+13	9.3	23.25	49.95		18.05363	.6294848	.5100177		.2400090	1.993271	.3532932
-13+9	2.84	7.1	26.7		5.51315	.6065072	.4867964		.2187158	2.166530	.3219497
-9	7.84	19.6	19.6		15.2194	.4533631	.4014111		.1546263	2.478629	.2276099
		TAILINGS								
+37	3.25	8.125	100	73.806	5.996738					
-37+28	3.9	9.75	91.875		7.196085					
-28+20	8	20	82.125		14.7612					
-20+13	9.4	23.5	62.125		17.34441					
-13+9	3.15	7.875	38.625		5.812223					
-9	12.3	30.75	30.75		22.69535					
		FROTH								
+37	4	10	100	120	12					
-37+28	4	10	90		12					
-28+20	8.22	20.55	80		24.66					
-20+13	9.56	23.9	59.45		28.68					
-13+9	3.03	7.575	35.55		9.09					
-9	11.19	27.975	27.975		33.57					
		PULP								
+37	2.06	5.15	100	325.35	16.75553					
-37+28	2.8	7	94.85		22.7745					
-28+20	6.88	17.2	87.85		55.9602					
-20+13	8.2	20.5	70.65		66.69675					
-13+9	3.2	8	50.15		26.028					
-9	16.86	42.15	42.15		137.1350					

TEST-6

AFR: 5 l/min FRC 1.425 FT: 1 cm Taver.: 2.94625

SIZE (uM)	WEIGHT (g)	% WEIGHT	CUM.WEI.	AV.SO.F.R (g/min)	FTC (min)	RECOVERY	T*FRC	Rf	DBRC (min)	ORC (MIN)
CONCENTRE										
+37	4	10	100	110.09	11.009	1.684944	.7397453	4.198406	.6770163	.8038350	.9647482
-37+28	3.9	9.75	90		10.73378	2.281694	.7636148		.7694310	.6837362	1.096439
-28+20	9.2	23	80.25		25.3207	2.392204	.7736083		.8139095	.5469483	1.159821
-20+13	8.4	21	57.25		23.1189	2.081401	.7436256		.6908682	.9313311	.9844873
-13+9	3.1	7.75	36.25		8.531975	2.059671	.6992691		.5538369	1.659241	.7892176
-9	11.4	28.5	28.5		31.37565	2.064527	.6835639		.5145324	1.947907	.7332086
TAILINGS										
+37	3.8	9.5	100	40.77	3.87315					
-37+28	3.26	8.15	90.5		3.322755					
-28+20	7.27	18.175	82.35		7.409948					
-20+13	7.82	19.55	64.175		7.970535					
-13+9	3.6	9	44.625		3.6693					
-9	14.25	35.625	35.625		14.52431					
FROTH										
+37	5	12.5	100	52.27	6.53375					
-37+28	3.6	9	87.5		4.7043					
-28+20	8.1	20.25	78.5		10.58468					
-20+13	8.5	21.25	58.25		11.10738					
-13+9	3.17	7.925	37		4.142398					
-9	11.63	29.075	29.075		15.19750					
PULP										
+37	3.14	7.85	100	258.15	20.26478					
-37+28	2.88	7.2	92.15		18.5868					
-28+20	7.23	18.075	84.95		46.66061					
-20+13	7.8	19.5	66.875		50.33925					
-13+9	3.6	9	47.375		23.2335					
-9	15.35	38.375	38.375		99.06506					

TEST-9

AFR: 5 l/min FRC 1.472 FT: 3 CM Taver.: 2.94625

SIZE (uM)	WEIGHT (g)	% WEIGHT	CUM.WEI.	AV.SO.F.R (g/min)	FTC (min)	RECOVERY	T%FRC	Rf	DBRC (min)	ORC (MIN)
		CONCENTRE								
+37	4.2	10.5	100	89.76	9.4248	1.214693	.6639544	4.33688	.4555780	1.451575	.6706108
-37+28	5.3	13.25	89.5		11.8932	1.432548	.6768287		.4829126	1.533927	.7108474
-28+20	10.4	26	76.25		23.3376	1.503905	.6942380		.5235371	1.368680	.7706466
-20+13	7.4	18.5	50.25		16.6056	1.025232	.6460579		.4208835	1.410673	.6195405
-13+9	5.11	12.775	31.75		11.46684	.9094622	.6157663		.3695243	1.551708	.5439398
-9	7.59	18.975	18.975		17.03196	.9899089	.6683934		.4647630	1.140013	.6841311
		TAILINGS								
+37	4.2	10.5	100	45.43	4.77015					
-37+28	5	12.5	89.5		5.67875					
-28+20	9.05	22.625	77		10.27854					
-20+13	8.01	20.025	54.375		9.097358					
-13+9	6.3	15.75	34.35		7.155225					
-9	7.44	18.6	18.6		8.44998					
		FROTH								
+37	4	10	100	77.59	7.759					
-37+28	4.28	10.7	90		8.30213					
-28+20	8	20	79.3		15.518					
-20+13	8.35	20.875	59.3		16.19691					
-13+9	6.5	16.25	38.425		12.60838					
-9	8.87	22.175	22.175		17.20558					
		PULP								
+37	2.89	7.225	100	330.02	23.84395					
-37+28	2.91	7.275	92.775		24.00896					
-28+20	7.05	17.625	85.5		58.16603					
-20+13	6.5	16.25	67.875		53.62825					
-13+9	5.2	13	51.625		42.9026					
-9	15.45	38.625	38.625		127.4702					

TEST-22

AFR: 1.3 l/min FRC .59 FT.: 1 cm Taver.: 12.94625

SIZE (uM)	WEIGHT (g)	% WEIGHT	CUM.WEI.	AV.SO.F.R (g/min)	FTC (min)	RECOVERY	T1FRC	R1	DBRC (min)	ORC (MIN)
		CONCENTRE								
+37	5.77	14.425	100	93.42	13.47584	1.566755	.5970817	1.738288	.8525017	.2710771 .5029760
-37+28	6.58	16.45	85.575		15.36759	1.599383	.6010927		.8668578	.2456520 .5114463
-28+20	9.78	24.45	69.125		22.84119	1.500879	.6216111		.9450587	.0872541 .5575846
-20+13	9.01	22.525	44.675		21.04286	1.467916	.6319545		.9877857	.0181513 .5827936
-13+9	2.99	7.475	22.15		6.983145	1.272876	.5779603		.7878130	.3429523 .4648097
-9	5.87	14.675	14.675		13.70939	1.568474	.4401253		.4522348	1.899799 .2668185
		TAILINGS								
+37	5.35	13.375	100	67.99	9.093663					
-37+28	6	15	86.625		10.1985					
-28+20	8.18	20.45	71.625		13.90396					
-20+13	7.21	18.025	51.175		12.25520					
-13+9	3	7.5	33.15		5.09925					
-9	10.26	25.65	25.65		17.43944					
		FROTH								
+37	5.55	13.875	100	61.99	8.601113					
-37+28	6.2	15.5	86.125		9.60845					
-28+20	9.82	24.55	70.625		15.21855					
-20+13	9.25	23.125	46.075		14.33519					
-13+9	3.54	8.85	22.95		5.486115					
-9	5.64	14.1	14.1		8.74059					
		PULP								
+37	4.62	11.55	100	409.85	47.33768					
-37+28	4.8	12	88.45		49.182					
-28+20	9.58	23.95	76.45		98.15908					
-20+13	9.18	22.95	52.5		94.06058					
-13+9	3.8	9.5	29.55		38.93575					
-9	8.02	20.05	20.05		82.17493					

TEST-15

AFR: 7.5 l/min FRC 1.725 FT: 5 cm Taver.: 2.94625

SIZE (uM)	WEIGHT (g)	% WEIGHT	CUM.WEI.	AV.SO.F.R (g/min)	FTC (min)	RECOVERY	T&FRC	Rf	DBRC (min)	ORC (MIN)
CONCENTRE										
+37	5.3	13.25	100	96.18 12.74385	1.102695	.5624003	5.082281	.2528773	3.257899	.4362133
-37+28	5	12.5	86.75	12.0225	.7052736	.5667987		.2574426	2.034264	.4440885
-28+20	11	27.5	74.25	26.4495	.9738779	.6452227		.3578452	1.747628	.6172830
-20+13	8.3	20.75	46.75	19.95735	1.015801	.6194085		.3202281	2.156317	.5523934
-13+9	2.2	5.5	26	5.2899	.5906098	.5088111		.2038212	2.307076	.3515916
-9	8.2	20.5	20.5	19.7169	.6318729	.5664865		.2571155	1.825672	.4435243
TAILINGS										
+37	6	15	100	66.106 9.9159						
-37+28	5.56	13.9	85	9.188734						
-28+20	8.8	22	71.1	14.54332						
-20+13	7.42	18.55	49.1	12.26266						
-13+9	3.09	7.725	30.55	5.106689						
-9	9.13	22.825	22.825	15.08869						
FROTH										
+37	4	10	100	115.57 11.557						
-37+28	5.9	14.75	90	17.04658						
-28+20	9.4	23.5	75.25	27.15895						
-20+13	6.8	17	51.75	19.6469						
-13+9	3.1	7.75	34.75	8.956675						
-9	10.8	27	27	31.2039						
PULP										
+37	6.2	15.5	100	463.94 71.9107						
-37+28	5	12.5	84.5	57.9925						
-28+20	7.8	19.5	72	90.4683						
-20+13	5.25	13.125	52.5	60.89213						
-13+9	1.99	4.975	39.375	23.08102						
-9	13.19	32.975	34.4	152.9842						

TEST-13

AFR: 1.3 l/min FRC .59 FT: 2 cm Taver.: 2.94625

SIZE (uM)	WEIGHT (g)	% WEIGHT	CUM.WEI.	AV.SO.F.R (g/min)	FTC (min)	RECOVERY	T&FRC	Rf	DBRC (min)	ORC (MIN)
		CONCENTRE								
+37	6	15	100	73.55	11.0325	.7529689	.5206509	1.738288	.6248461	.4520781	.3686592
-37+28	6.88	17.2	85		12.6506	.7728861	.5656709		.7492440	.2586685	.4420540
-28+20	10.78	26.95	67.8		19.82173	.7645855	.5670486		.7534589	.2501818	.4445408
-20+13	9.8	24.5	40.85		18.01975	.7550512	.5746216		.7771144	.2165576	.4584975
-13+9	2.99	7.475	16.35		5.497863	.5882835	.4976201		.5698284	.4441037	.3361987
-9	3.55	8.875	8.875		6.527563	.4226601	.2450406		.1867209	1.840933	.1101653
		TAILINGS								
+37	5.49	13.725	100	74.006	10.15732					
-37+28	5.25	13.125	86.275		9.713288					
-28+20	8.18	20.45	73.15		15.13423					
-20+13	7.21	18.025	52.7		13.33958					
-13+9	3	7.5	34.675		5.55045					
-9	10.87	27.175	27.175		20.11113					
		FROTH								
+37	5.55	13.875	100	105.6	14.652					
-37+28	6.2	15.5	86.125		16.368					
-28+20	9.82	24.55	70.625		25.9248					
-20+13	9.04	22.6	46.075		23.8656					
-13+9	3.54	8.85	23.475		9.3456					
-9	5.85	14.625	14.625		15.444					
		PULP								
+37	4.3	10.75	100	389.04	41.8218					
-37+28	4.6	11.5	89.25		44.7396					
-28+20	9.58	23.95	77.75		93.17508					
-20+13	9.18	22.95	53.8		89.28468					
-13+9	3.8	9.5	30.85		36.9588					
-9	8.54	21.35	21.35		83.06004					

TEST-21

AFR: 1.3 l/min FRC .59 FT: 5 cm Taver.: 2.94625

SIZE (uM)	WEIGHT (g)	% WEIGHT	CUM.WEI.	AV.SO.F.R (g/min)	FTC (min)	RECOVERY	T*FRC	Rf	DBRC (min)	DRC (MIN)
		CONCENTRE								
+37	7.19	17.975	100	44.19 7.943153	.3224269	.3768116	1.738288	.3478431	.6045052	.2052274
-37+28	7.11	17.775	82.025	7.854773	.3446742	.4194996		.4157262	.4844152	.2452785
-28+20	10.68	26.7	64.25	11.79873	.2665063	.3984647		.3810720	.4328531	.2248325
-20+13	9.06	22.65	37.55	10.00904	.2274696	.3349992		.2898011	.5574466	.1709827
-13+9	3.24	8.1	14.9	3.57939	.1758313	.3156459		.2653369	.4868406	.1565488
-9	2.72	6.8	6.8	3.00492	.1247110	.1110556		.0718694	1.610533	.0424030
		TAILINGS								
+37	5.62	14.05	100	93.5 13.13675						
-37+28	4.65	11.625	85.95	10.86938						
-28+20	7.62	19.05	74.325	17.81175						
-20+13	8.5	21.25	55.275	19.86875						
-13+9	3.32	8.3	34.025	7.7605						
-9	10.29	25.725	25.725	24.05288						
		FROTH								
+37	5.47	13.675	100	180.15 24.63551						
-37+28	5.06	12.65	86.325	22.78898						
-28+20	9.83	24.575	73.675	44.27186						
-20+13	9.77	24.425	49.1	44.00164						
-13+9	4.52	11.3	24.675	20.35695						
-9	5.35	13.375	13.375	24.09506						
		PULP								
+37	4.56	11.4	100	433.52 49.42128						
-37+28	5.03	12.575	88.6	54.51514						
-28+20	8.26	20.65	76.025	89.52188						
-20+13	9.24	23.1	55.375	100.1431						
-13+9	4	10	32.275	43.352						
-9	8.91	22.275	22.275	96.56658						

AFR (l/min)	F.T. (cm)	TAILS (g/min)	CONC. (g/min)	TAILS (g/min)	CONC. (g/min)	SOLID RECOVERY	WATER RECOVERY	CONC. RECOVERY	TAILS RECOVERY	SILICA (g/min)	ZINC (g/min)	SILICA (g/min)	ZINC (g/min)	SILICA RECOVERY	ZINC RECOVERY
1.3	1	1463.13	236.87	122.75	13.38	0.10	0.14	.42	.415	5.62	7.76	50.94	71.81	0.10	0.10
	3	1600.02	99.98	183.61	10.35	0.05	0.06	.4	.4	4.14	6.21	73.44	110.17	0.05	0.05
	5	1645.31	54.69	174.5	6.25	0.03	0.03	.3	.385	1.88	4.38	67.18	107.32	0.02	0.04
5	1	1354.59	345.41	168.76	19.72	0.10	0.22	.46	.405	9.07	10.65	68.35	100.41	0.12	0.10
		1376.68	323.32	172.89	20.67	0.11	0.20	.47	.4	9.71	10.95	69.16	103.74	0.12	0.10
	AVE.	1365.64	334.36	170.83	20.19	0.11	0.21	.465	.4025	9.39	10.80	68.76	102.07	0.12	0.10
	3	1447.32	252.68	179.14	15.77	0.08	0.16	.33	.39	5.20	10.56	69.87	109.28	0.07	0.09
		1428.52	271.48	179.69	16.04	0.08	0.17	.32	.4	5.13	10.91	71.88	107.81	0.07	0.09
		1473.05	226.95	139.84	10.66	0.07	0.14	.34	.38	3.62	7.04	53.14	86.70	0.06	0.08
	AVE.	1449.63	250.37	166.23	14.16	0.08	0.16	.33	.39	4.67	9.49	64.83	101.40	0.07	0.09
	5	1621.80	78.20	157.11	6.86	0.04	0.05	.28	.375	1.92	4.94	58.92	98.20	0.03	0.05
7.5	1	1245.39	454.61	112.86	22.52	0.17	0.28	.48	.475	10.81	11.71	53.61	59.25	0.17	0.17
	3	1302.84	397.16	150.31	17.36	0.10	0.25	.35	.4625	6.08	11.28	69.52	80.79	0.08	0.12
		1294.51	405.49	131.93	19.17	0.13	0.25	.345	.46	6.61	12.56	60.69	71.24	0.10	0.15
		1315.35	384.65	139.09	18.74	0.12	0.24	.355	.4675	6.65	12.09	65.03	74.07	0.09	0.14
	AVE.	1304.23	395.77	140.45	18.42	0.12	0.24	.35	.46	6.45	11.98	64.60	75.84	0.09	0.14
	5	1512.55	187.45	183.71	12.84	0.07	0.12	.245	.4125	3.15	9.69	75.78	107.93	0.04	0.08
		1501.97	198.03	122.56	11.14	0.08	0.12	.24	.4	2.67	8.47	49.02	73.54	0.05	0.10
		1500.08	199.92	187.56	10.11	0.05	0.13	.24	.42	2.43	7.68	78.78	108.79	0.03	0.07
	AVE.	1504.87	195.13	164.61	11.36	0.07	0.12	.24	.41	2.73	8.64	67.49	97.12	0.04	0.08

APPENDIX 8.1

Effect of AFR and FT on entrainment

AFR: 7.5 l/min FT: 3 cm

WWFR (cc/min)	TYPE	TAILS (g/min)	CONC. (g/min)	TAILS (g/min)	CONC. (g/min)	SOLID RECOVERY	WATER RECOVERY	CONC. RECOVERY	TAILS RECOVERY	TAILS RECOVERY	SILICA (g/min)	ZINC (g/min)	SILICA (g/min)	ZINC (g/min)	SILICA RECOVERY	ZINC RECOVERY
0		1302.84	397.16	150.31	17.36	0.10	0.28	.48	.475	.475	6.08	11.28	69.52	80.79	0.08	0.12
		1294.51	405.49	131.93	19.17	0.13	0.25	.35	.46	.46	6.61	12.56	60.69	71.24	0.10	0.15
		1315.35	384.65	139.09	18.74	0.12	0.25	.345	.46	.46	6.65	12.09	65.03	74.06	0.09	0.14
	AVE.	1304.23	395.77	140.45	18.42	0.12	0.26	.335	.47	.47	6.45	11.97	64.60	75.85	0.09	0.14
200	BELOW	1419.35	480.65	155.30	20.84	0.12	0.27	.235	.445	.445	4.90	15.94	69.11	86.19	0.07	0.16
		1414.68	485.32	153.45	21.56	0.12	0.27	.235	.445	.445	5.07	16.49	68.29	85.16	0.07	0.16
	AVE.	1417.02	482.99	154.38	21.20	0.12	0.27	.235	.445	.445	4.98	16.22	68.70	85.68	0.07	0.16
400		1629.65	570.35	151.32	18.89	0.11	0.27	.19	.42	.42	3.59	15.30	63.55	87.77	0.05	0.15
		1621.74	578.26	150.74	18.56	0.11	0.28	.19	.42	.42	3.53	15.03	63.31	87.43	0.05	0.15
	AVE.	1625.70	574.31	151.03	18.73	0.11	0.28	.19	.42	.42	3.56	15.17	63.43	87.60	0.05	0.15
200	ABOVE	1400.00	500.00	140.21	20.13	0.13	0.28	.27	.45	.45	5.44	14.69	63.09	77.12	0.08	0.16
400		1610.77	589.23	155.00	18.74	0.11	0.28	.27	.44	.44	5.06	13.68	68.20	86.80	0.07	0.14

Effect of wash water flow rate and addition level in mixture flotation

ENTRAINMENT OF SILICA

AFR 7.5 l/min

FT (cm)	CONC. (g/min)	TAILS (g/min)	FEED (g/min)	CONC. (g/min)	TAILS (g/min)	SILICA RECOVERY	WATER RECOVERY
0	929.00	505.67	1434.67	28.55	27.55	0.51	0.65
.8	628.28	854.34	1482.62	19.23	54.42	0.26	0.43
1.5	383.78	1115.23	1499.01	10.29	73.68	0.12	0.26
2.5	268.35	1269.01	1537.36	7.08	109.97	0.06	0.18
4.5	66.21	1482.92	1549.13	1.36	116.82	0.01	0.05
WWFR (BELOW)			FT: 3 cm				
200	148.45	1733.26	1881.71	3.425	109.72	.0302709	.0820015
400	164.20	1880.85	2045.05	2.585	131.42	.0192903	.0845689
600	195.25	2137.14	2332.39	1.65	135.62	.0120201	.0881956
WWFR (ABOVE)			FT: 3 cm				
200	190.915	1697.54	1888.46	5.50	125.74	.0419080	.1055164
400	271.905	1839.96	2111.87	4.25	130.20	.0316103	.1353560
600	319.50	2001.00	2320.50	2.95	138.54	.0208495	.1452724

PULP: 230 g WATER: 6730 g

Effect of wash water flow rate and addition level in silica flotation

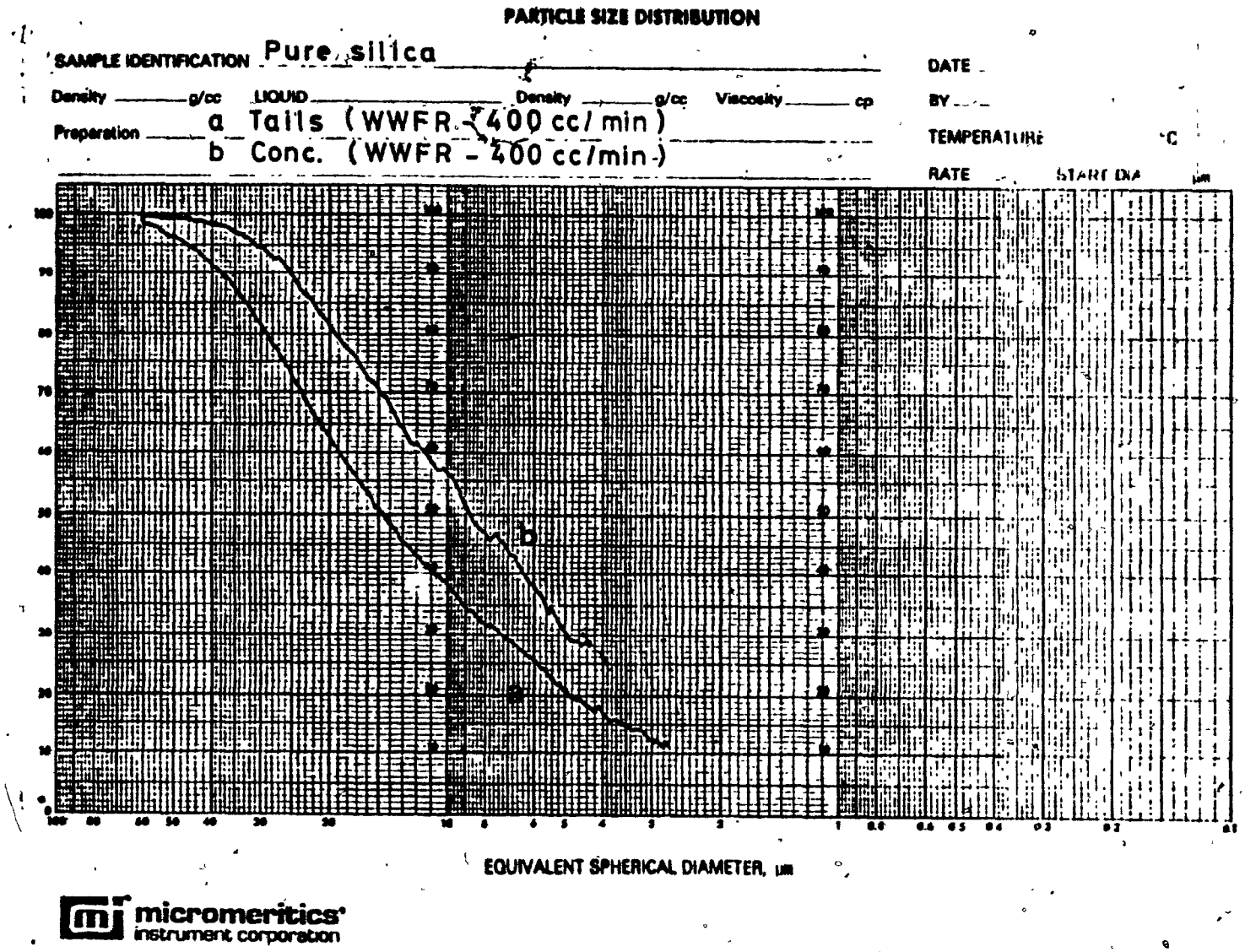

Size distribution of concentrate and tail products in pure silica flotation.

PARTICLE SIZE DISTRIBUTION

SAMPLE IDENTIFICATION Pure silica

DATE

Density LIQUID Density g/cc Viscosity cp

BY

Preparation a WWFR 600 cc/min (under-froth)
b WWFR (over froth)

TEMPERATURE °C

RATE START DIA. µm

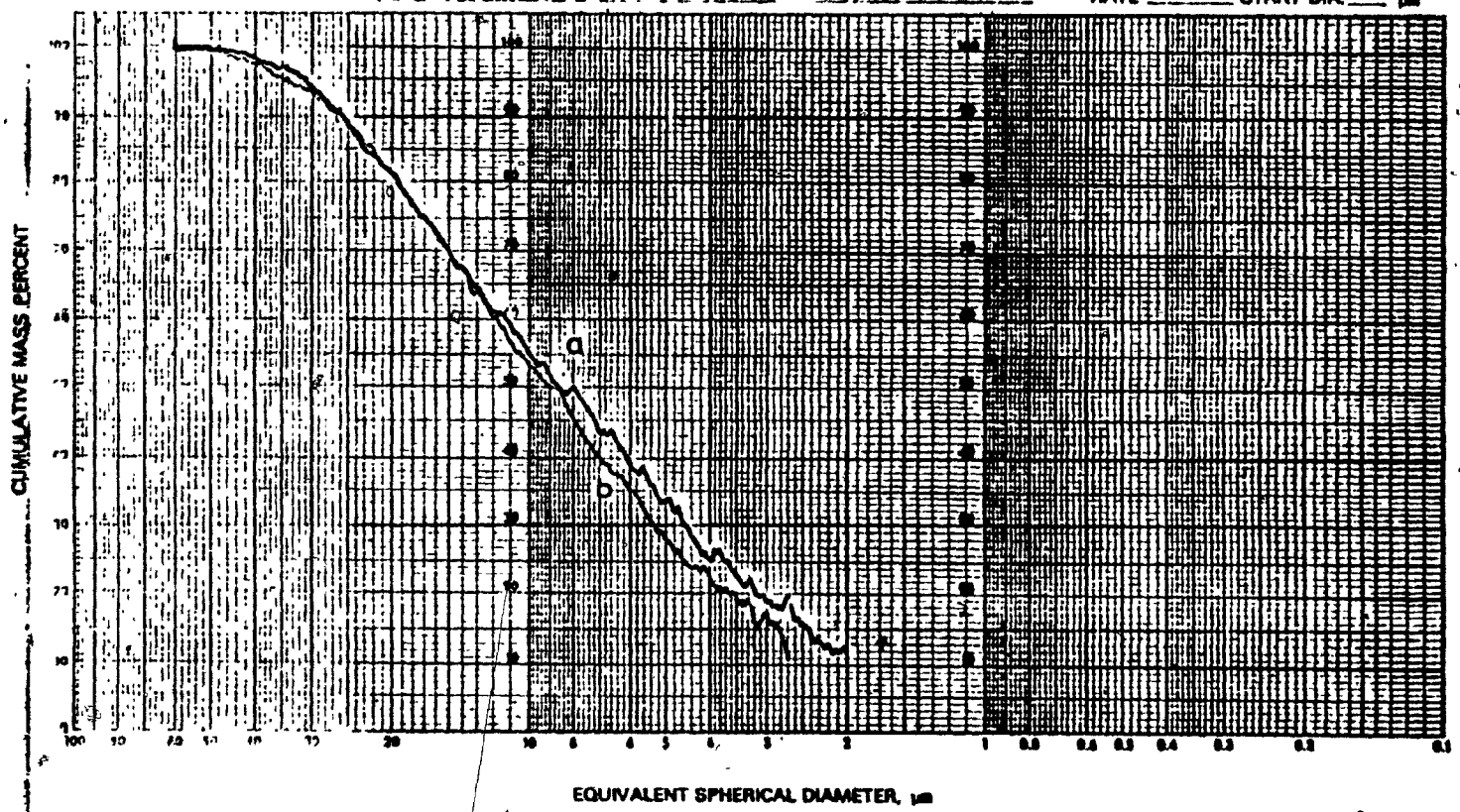

micromeritics
instrument corporation

Form 000A02701

Effect of particle size on entrainment of pure silica at different WWFR

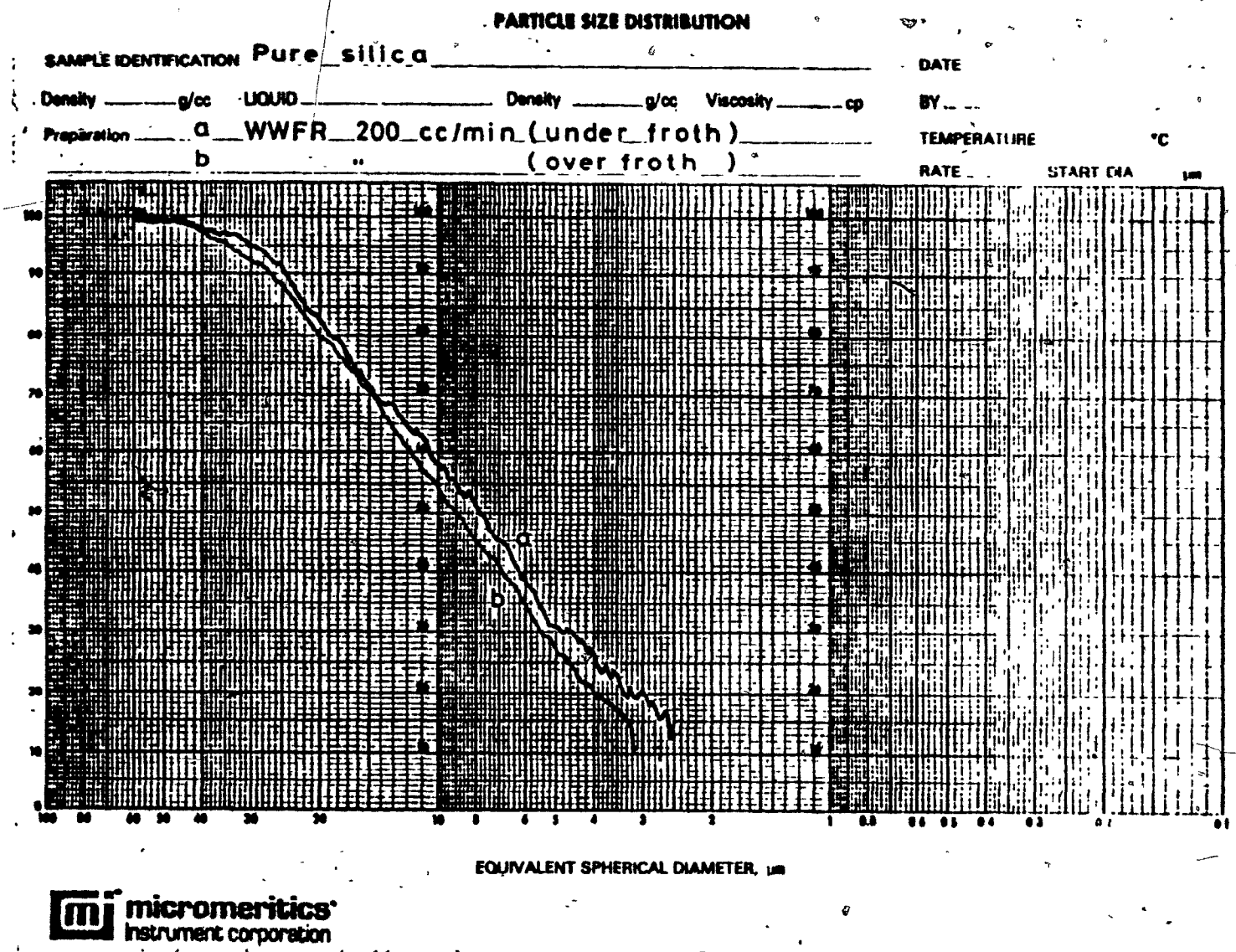

Effect of particle size on entrainment of pure silica at different wash water addition levels

ENTRAINMENT OF SILICA FOR EACH SIZE CLASS (WITHOUT WASH WATER ADDITION)
AFR:7.5

FT (cm)	SIZE (mm)	FEED (g/min)	CONC. (g/min)	(%) FEED	(%) CONC.	SILICA RECOVERY	WATER RECOVERY
4.5	60	118.18	1.36	2	0	0	0.05
	50			5	1	0.23	
	40			10	2	0.23	
	30			22	15	0.78	
	20			51	16	0.36	
	10			64	40	0.72	
	8			69	44	0.73	
	6			75	54	0.82	
	5			78	60	0.88	
	4			83	70	0.96	
2.5	60	117.05	7.08	2	1	2.92	0.18
	50			5	2	2.38	
	40			10	5	2.99	
	30			22	10	2.73	
	20			51	22	2.60	
	10			64	48	4.50	
	8			69	52	4.83	
	6			75	62	4.96	
	5			78	72	5.54	
	4			83	69	4.99	
0	60	56.1	28.55	2	2	33.73	0.65
	50			5	4	28.93	
	40			10	8	28.93	
	30			22	19	30.53	
	20			51	35	25.88	
	10			64	60	32.30	
	8			69	64	32.07	
	6			75	72	32.82	
	5			78	76	33.15	
	4			83	84	34.00	

ENTRAINMENT OF SILICA FOR EACH SIZE CLASS (WITH WASH WATER ADDITION)

AFR:7.5

WWFR (cc/min)	SIZE (mm)	FEED (g/min)	CONC. (g/min)	(%) FEED	(%) CONC.	SILICA RECOVERY	WATER RECOVERY
200	60	113.145	3.425	2	0	0	0.08
	50			5	1	0.60	
	40			10	2	0.60	
	30			22	5	0.69	
	20			51	17	1.01	
UNDER	10			64	42	1.97	
	8			69	50	2.18	
	6			75	62	2.48	
	5			78	69	2.66	
	4			83	75	2.71	
200	60	131.24	5.5	2	0	0.00	0.11
	50			5	1	0.83	
	40			10	2	0.83	
	30			22	8	1.52	
	20			51	20	1.64	
OVER	10			64	45	2.93	
	8			69	55	3.32	
	6			75	65	3.61	
	5			78	74	3.95	
	4			83	80	4.01	
600	60	137.27	1.65	2	0	0.00	0.08
	50			5	1	0.24	
	40			10	2	0.24	
	30			22	6	0.33	
	20			51	19	0.45	
UNDER	10			64	45	0.84	
	8			69	50	0.86	
	6			75	62	0.98	
	5			78	67	1.02	
	4			83	76	1.09	
600	60	141.49	2.95	2	0	0.00	.15
	50			5	1	0.42	
	40			10	2	0.42	
	30			22	7	0.66	
	20			51	19	0.77	
	10			64	47	1.51	
OVER	8			69	55	1.63	
	6			75	65	1.77	
	5			78	62	1.63	
	4			83	78	1.92	

CLASSIFICATION MATRIX FOR SILICA

AFR: 7.5 (L/MIN)
FT: 3 (CM)

PULP SOL. 230 (G)
PULP WAT. 6730 (G)
CONC SOL. 7.08 (g/min)
CONC.F.R. 261.27 (g/min)

SIZE (um)	CONC. (%)	PULP (%)	CLASS. MATRICS
50	2	3	0.53
40	4	6	0.53
30	10	14	0.57
20	22	30	0.58
10	47	57	0.65
8	52	62	0.67
6	62	70	0.70
4	72	80	0.71
3	79	85	0.74

APPENDIX 9.1

Liquid residence time results

RESIDENCE TIME DISTRIBUTION OF LIQUID IN SILICA FLOTATION . (CONC.)

TRACER: LITHIUM CLORIDE . ANALYSIS: ATOMIC ABSORPTION

FT: 3 cm . AFR: 7.5 l/min WAFR: 400 cc/min
ADDITION: WASH WATER

TIME (min)	ABSORBANCE 1	2	3	AVERAGE ABSOR.	Li(CON)	C(t)&T	Ln(CON) PPM
.5	.141	.136	.144	0.14	0.65	0.33	-1.42
1	.118	.122	.116	0.12	0.55	0.28	-1.59
1.5	.1	.102	.098	0.10	0.46	0.23	-1.76
2	.099	.098	.1	0.10	0.46	0.23	-1.77
2.5	.092	.093	.093	0.09	0.43	0.22	-1.84
3	.084	.082	.083	0.08	0.38	0.19	-1.96
3.5	.071	.074	.072	0.07	0.33	0.17	-2.10
4	.066	.067	.066	0.07	0.30	0.15	-2.19
4.5	.052	.054	.054	0.05	0.24	0.12	-2.41
5	.05	.05	.048	0.05	0.22	0.11	-2.50
5.5	.039	.04	.038	0.04	0.17	0.09	-2.74
6	.038	.036	.036	0.04	0.16	0.08	-2.81
6.5	.029	.027	.028	0.03	0.12	0.06	-3.10
7	.024	.023	.023	0.02	0.10	0.05	-3.30
7.5	.021	.023	.022	0.02	0.09	0.05	-3.37
8	.02	.019	.017	0.02	0.08	0.04	-3.55
8.5	.02	.019	.02	0.02	0.08	0.04	-3.50
9	.018	.017	.016	0.02	0.07	0.03	-3.66
9.5	.017	.017	.017	0.02	0.07	0.03	-3.66
10.5	.016	.016	.015	0.02	0.06	0.06	-3.76
11.5	.012	.013	.012	0.01	0.05	0.05	-4.05
12.5	.01	.011	.011	0.01	0.04	0.04	-4.23
13.5	.009	.008	.009	0.01	0.03	0.03	-4.51
14.5	.006	.006	.006	0.01	0.02	0.02	-5.06
15.5	.005	.005	.005	0.01	0.01	0.01	-5.38
					TOTAL	2.70	

RESIDENCE TIME DISTRIBUTION OF LIQUID IN SILICA FLOTATION (TAILS)

TRACER: LITHIUM CLORIDE. ANALYSIS: ABSORPTION

FT: 3 cm AFR: 7.5 l/min WWFR: 400 cc/min
ADDITION: WASH WATER

TIME (min)	ABSORPTION 1	2	3	AVERAGE ABSOR.	Li(CON)	C(t)δT	Ln(CON) PPM
.25	.135	.145	.147	0.14	0.67	0.17	-1.26
.5	.122	.117	.115	0.12	0.55	0.14	-1.45
.75	.115	.113	.111	0.11	0.53	0.13	-1.50
1	.105	.101	.107	0.10	0.49	0.12	-1.58
1.25	.096	.1	.091	0.10	0.44	0.11	-1.67
1.5	.094	.089	.091	0.09	0.42	0.11	-1.71
1.75	.091	.087	.088	0.09	0.41	0.10	-1.74
2	.083	.084	.086	0.08	0.39	0.10	-1.80
2.5	.083	.083	.083	0.08	0.38	0.19	-1.81
3	.075	.074	.076	0.08	0.35	0.17	-1.92
3.5	.064	.065	.063	0.06	0.29	0.15	-2.08
4	.054	.055	.056	0.06	0.25	0.13	-2.24
4.5	.048	.052	.046	0.05	0.22	0.11	-2.37
5	.044	.042	.042	0.04	0.19	0.10	-2.51
5.5	.034	.036	.034	0.03	0.15	0.08	-2.73
6	.034	.033	.033	0.03	0.15	0.07	-2.77
6.5	.029	.027	.027	0.03	0.12	0.06	-2.97
7	.026	.027	.026	0.03	0.11	0.06	-3.03
7.5	.025	.023	.024	0.02	0.10	0.05	-3.13
8	.019	.018	.019	0.02	0.08	0.04	-3.41
8.5	.015	.014	.015	0.01	0.06	0.03	-3.69
9	.014	.013	.013	0.01	0.05	0.03	-3.81
10	.013	.013	.012	0.01	0.05	0.02	-3.87
11	.009	.01	.01	0.01	0.03	0.02	-4.22
12	.008	.008	.009	0.01	0.03	0.03	-4.42
13	.007	.007	.007	0.01	0.02	0.02	-4.67
14	.006	.006	.005	0.01	0.02	0.02	-5.01
15	.005	.005	.005	0.01	0.01	0.01	-5.24
					TOTAL	2.35	

RESIDENCE TIME DISTRIBUTION OF LIQUID IN SPHALERITE FLOTATION (TAILS)

TRACER:LITHIUM CLORIDE(1 g) ANAYLSIS:ATOMIC ABSORPTION

F.T: 3 cm AFR: 5 l/min 10 % SOLIDS NWFR : 1200 cc/min

TIME (min)	ABSORB. 1	ABSORB. 2	ABSORB. 3	AVERAGE ABSORB.	Li(CON) PPM	C(t)*T	Ln(CON) PPM
.5	.368	.372	.361	0.37	1.74	0.87	-1.34
1	.325	.331	.342	0.33	1.57	0.79	-1.44
1.5	.294	.275	.299	0.29	1.37	0.68	-1.58
2	.262	.258	.272	0.26	1.25	0.62	-1.67
2.5	.221	.217	.218	0.22	1.03	0.51	-1.86
3	.214	.212	.209	0.21	1.00	0.50	-1.89
3.5	.163	.164	.161	0.16	0.76	0.38	-2.16
4	.136	.131	.133	0.13	0.62	0.31	-2.36
4.5	.107	.108	.112	0.11	0.51	0.25	-2.57
5	.096	.097	.092	0.10	0.44	0.22	-2.71
5.5	.078	.082	.076	0.08	0.36	0.18	-2.90
6	.073	.067	.068	0.07	0.32	0.16	-3.03
6.5	.069	.068	.067	0.07	0.31	0.16	-3.05
7	.066	.063	.064	0.06	0.30	0.15	-3.11
7.5	.057	.056	.054	0.06	0.25	0.13	-3.26
8	.047	.049	.048	0.05	0.22	0.11	-3.42
8.5	.041	.039	.04	0.04	0.18	0.09	-3.61
9	.035	.036	.037	0.04	0.16	0.16	-3.72
9.5	.033	.03	.031	0.03	0.14	0.14	-3.87
10	.028	.028	.029	0.03	0.12	0.12	-3.98
11	.019	.017	.02	0.02	0.08	0.08	-4.44
					TOTAL	6.61	

RESIDENCE TIME DISTRIBUTION OF LIQUID IN SILICA FLOTATATION (TAILS)

TRACER: LITHIUM CLORITE (1g) ANALYSIS:ATOMIC ABSORPTION

FT:3 cm AFR: 7.5 l/min WWFR : 400 cc/min

TIME (sec)	ABSORBANCE 1	2	3	AVERAGE ABSORB.	Li PPM	C(t)*T	Ln(CON) PPM
.25	.228	.232	.226	0.23	1.08	0.27	-1.25
.5	.187	.185	.183	0.19	0.87	0.22	-1.46
.75	.168	.171	.171	0.17	0.80	0.20	-1.55
1	.167	.168	.165	0.17	0.78	0.20	-1.57
1.25	.155	.16	.164	0.16	0.75	0.19	-1.61
1.5	.166	.155	.162	0.16	0.76	0.19	-1.60
1.75	.145	.147	.146	0.15	0.68	0.17	-1.70
2	.128	.126	.125	0.13	0.59	0.15	-1.85
2.5	.12	.119	.123	0.12	0.56	0.28	-1.90
3	.107	.108	.111	0.11	0.51	0.25	-2.00
3.5	.089	.09	.094	0.09	0.42	0.21	-2.18
4	.081	.086	.084	0.08	0.39	0.19	-2.27
4.5	.07	.067	.068	0.07	0.31	0.16	-2.48
5	.057	.059	.056	0.06	0.26	0.13	-2.60
5.5	.055	.056	.055	0.06	0.25	0.13	-2.70
6	.048	.049	.05	0.05	0.22	0.11	-2.83
6.5	.045	.043	.044	0.04	0.20	0.10	-2.94
7	.04	.041	.039	0.04	0.18	0.09	-3.04
7.5	.03	.031	.032	0.03	0.14	0.07	-3.31
8	.028	.029	.028	0.03	0.12	0.06	-3.41
8.5	.029	.028	.028	0.03	0.12	0.06	-3.41
9	.027	.027	.026	0.03	0.12	0.06	-3.48
9.5	.023	.022	.023	0.02	0.10	0.05	-3.66
10.5	.016	.017	.016	0.02	0.07	0.07	-4.03
11.5	.013	.012	.011	0.01	0.05	0.05	-4.40
12.5	.012	.011	.011	0.01	0.04	0.04	-4.47
13.5	.01	.009	.008	0.01	0.03	0.03	-4.77
14.5	.01	.01	.009	0.01	0.03	0.03	-4.68
					TOTAL	3.75	

RESIDENCE TIME DISTRIBUTION OF LIQUID IN SILICA FLOTATATION (CONC.)

TRACER: LITHIUM CLORIDE (1g) ANALYSIS:ATOMIC ABSORPTION

FT: 3 cm AFR: 7.5 l/min WWFR:400 cc/min

TIME (sec)	ADSORBTION 1	2	3	AVERAGE ADSORB.	Li PPM	C(t)*T ppm	LN(CON) PPM
.5	.209	.213	.207	0.21	0.99	0.49	-1.44
1	.195	.193	.202	0.20	0.92	0.46	-1.50
1.5	.17	.168	.174	0.17	0.80	0.40	-1.64
2	.151	.147	.146	0.15	0.69	0.35	-1.79
2.5	.137	.144	.138	0.14	0.65	0.33	-1.85
3	.12	.123	.124	0.12	0.57	0.29	-1.98
3.5	.103	.109	.109	0.11	0.50	0.25	-2.12
4	.101	.099	.098	0.10	0.46	0.23	-2.20
4.5	.082	.085	.086	0.08	0.39	0.20	-2.36
5	.082	.083	.08	0.08	0.38	0.19	-2.40
5.5	.065	.064	.066	0.07	0.30	0.15	-2.63
6	.056	.057	.058	0.06	0.26	0.13	-2.77
6.5	.048	.051	.05	0.05	0.23	0.11	-2.91
7	.041	.042	.043	0.04	0.19	0.09	-3.09
7.5	.038	.039	.039	0.04	0.17	0.09	-3.18
8	.036	.034	.039	0.04	0.16	0.08	-3.24
8.5	.034	.034	.035	0.03	0.15	0.08	-3.30
9	.026	.025	.026	0.03	0.11	0.06	-3.62
10	.024	.024	.025	0.02	0.10	0.05	-3.68
11	.021	.02	.021	0.02	0.09	0.04	-3.86
12	.015	.016	.016	0.02	0.06	0.03	-4.18
13	.012	.013	.012	0.01	0.05	0.02	-4.47
14	.009	.01	.009	0.01	0.03	0.02	-4.83
15	.009	.008	.008	0.01	0.03	0.01	-4.98
					TOTAL	4.15	

RESIDENCE TIME DISTRIBUTION OF LIQUID IN SPHALERITE FLOTATION (TAILS)

TRACER:LITHIUM CLORIDE(1 g) ANALYSIS:ATOMIC ABSORPTION

F.T: 3 cm AFR: 5 l/min 10 % SOLIDS WWFR:0 l/min

TIME (S)	ABSORB. 1	2	3	AVERAGE ABSORB.	Li(CON) PPM	C(t)*T	Ln(CON) PPM
.25	.332	.327	.325	0.33	1.55	0.39	-1.26
.5	.32	.316	.319	0.32	1.50	0.38	-1.29
.75	.307	.3	.304	0.30	1.43	0.36	-1.34
1	.295	.283	.287	0.29	1.36	0.34	-1.39
1.25	.269	.278	.271	0.27	1.29	0.32	-1.45
1.5	.261	.26	.255	0.26	1.22	0.31	-1.50
2	.228	.226	.22	0.22	1.06	0.26	-1.64
2.5	.195	.198	.201	0.20	0.93	0.23	-1.77
3	.173	.174	.17	0.17	0.81	0.40	-1.91
3.5	.149	.156	.152	0.15	0.71	0.36	-2.04
4	.139	.134	.135	0.14	0.64	0.32	-2.15
4.5	.114	.111	.116	0.11	0.53	0.26	-2.34
5	.105	.1	.102	0.10	0.48	0.24	-2.44
5.5	.093	.094	.095	0.09	0.44	0.22	-2.53
6	.083	.082	.081	0.08	0.38	0.19	-2.67
6.5	.071	.074	.073	0.07	0.33	0.17	-2.79
7	.065	.068	.066	0.07	0.30	0.15	-2.89
7.5	.056	.053	.053	0.05	0.25	0.12	-3.10
8	.047	.048	.049	0.05	0.22	0.11	-3.23
8.5	.025	.024	.026	0.03	0.11	0.05	-3.93
9.5	.018	.019	.02	0.02	0.08	0.08	-4.24
10.5	.014	.016	.016	0.02	0.06	0.06	-4.48
11.5	.011	.012	.013	0.01	0.05	0.05	-4.78
12.5	.008	.01	.009	0.01	0.03	0.03	-5.15
13.5	.006	.007	.008	0.01	0.02	0.02	-5.51
14.5	.006	.007	.006	0.01	0.02	0.02	-5.67
15.5	.005	.006	.005	0.01	0.01	0.01	-5.96
16.5	.004	.004	.004	0.00	0.01	0.01	-6.55
17.5	.004	.004	.004	0.00	0.01	0.01	-6.55
18.5	.003	.003	.003	0.00	0.00	0.00	-7.48
19.5	.003	.002	.002	0.00	0.00	0.00	
					TOTAL	5.47	

RESIDENCE TIME DISTRIBUTION OF LIQUID IN SPHALERITE FLOTATION (CONCENTRATE STREAM)

TRACER: LITHIUM CLORIDE (1g) ANALYSIS:ATOMIC ABSORPTION ADDITION:FEED

FT: 3 cm AFR: 5 l/min 10 % SOLIDS WWFR: 0 l/MIN

TIME (min)	ABSORBANCE 1	2	3	4	5	6	AVERAGE ABSORB.	Li(CON) PPM	C(t)*T	Ln(CON) PPM
.5	.056	.055	.054	.069	.07	.071	0.06	0.29	0.14	-2.58
1	.102	.107	.105	.143	.141	.142	0.12	0.58	0.29	-1.88
1.5	.127	.133	.133	.196	.193	.191	0.16	0.76	0.38	-1.60
2	.111	.109	.114	.134	.152	.138	0.13	0.59	0.30	-1.86
2.5	.1	.098	.112	.134	.141	.156	0.12	0.58	0.29	-1.88
3	.082	.085	.086	.111	.114	.113	0.10	0.46	0.23	-2.11
3.5	.094	.096	.095	.122	.152	.123	0.11	0.53	0.26	-1.97
4	.079	.081	.08	.099	.114	.103	0.09	0.43	0.21	-2.17
4.5	.067	.073	.071	.094	.12	.093	0.09	0.40	0.20	-2.25
5	.062	.065	.066	.083	.107	.08	0.08	0.36	0.18	-2.36
5.5	.058	.057	.059	.073	.095	.072	0.07	0.32	0.16	-2.48
6	.052	.051	.052	.062	.082	.067	0.06	0.28	0.14	-2.61
6.5	.046	.048	.047	.057	.075	.058	0.06	0.25	0.13	-2.71
7	.039	.041	.042	.055	.066	.055	0.05	0.23	0.11	-2.82
7.5	.035	.038	.036	.044	.059	.048	0.04	0.20	0.10	-2.96
8	.033	.034	.035	.036	.056	.035	0.04	0.17	0.09	-3.10
8.5	.033	.033	.034	.037	.047	.036	0.04	0.16	0.08	-3.14
9.5	.027	.028	.027	.03	.035	.031	0.03	0.13	0.13	-3.37
10.5	.021	.02	.021	.021	.036	.024	0.02	0.10	0.10	-3.61
11.5	.015	.016	.015	.016	.028	.017	0.02	0.07	0.07	-3.94
12.5	.013	.014	.012	.014	.024	.015	0.02	0.06	0.06	-4.11
13.5	.009	.009	.008	.01	.018	.01	0.01	0.04	0.04	-4.56
14.5	.008	.008	.008	.009	.014	.009	0.01	0.03	0.03	-4.73
15.5	.006	.006	.008	.005	.009	.007	0.01	0.02	0.02	-5.18
16.5	.004	.004	.007	.004	.008	.005	0.01	0.01	0.01	-5.59
17.5	.005	.006	.006	.007	.005	.005	0.01	0.02	0.02	-5.48
18.5	.004	.004	.004	.004	.005	.004	0.00	0.01	0.01	-6.08
								TOTAL	3.78	

RESIDENCE TIME DISTRIBUTION OF LIQUID IN SILICA FLOTATION (TAILS)

TRACER: LITHIUM CLORIDE (1g) ANALYSIS:ATOMIC ABSORPTION

FT: 3 cm AFR: 7.5 l/min WWFR: 0 CC/min

TIME (SEC)	ADSORBTION 1	2	3	AVERAGE ADSORB.	Li(CON) PPM	C(t)*T	Ln(CON) PPM
.25	.179	.181	.178	0.18	0.84	0.21	-1.34
.5	.177	.18	.177	0.18	0.84	0.21	-1.35
.75	.158	.163	.157	0.16	0.75	0.19	-1.46
1	.14	.138	.143	0.14	0.66	0.16	-1.59
1.25	.14	.141	.143	0.14	0.66	0.17	-1.59
1.5	.136	.131	.133	0.13	0.62	0.16	-1.64
1.75	.133	.131	.129	0.13	0.61	0.15	-1.66
2	.12	.117	.111	0.12	0.54	0.14	-1.79
2.5	.099	.1	.101	0.10	0.46	0.23	-1.94
3	.077	.076	.085	0.08	0.37	0.18	-2.18
3.5	.077	.078	.078	0.08	0.36	0.18	-2.20
4	.068	.071	.069	0.07	0.32	0.16	-2.32
4.5	.062	.06	.063	0.06	0.28	0.14	-2.44
5	.056	.057	.055	0.06	0.26	0.13	-2.54
5.5	.049	.054	.053	0.05	0.24	0.12	-2.61
6	.045	.05	.051	0.05	0.22	0.11	-2.68
6.5	.043	.041	.04	0.04	0.19	0.09	-2.86
7	.033	.036	.036	0.04	0.16	0.08	-3.03
7.5	.032	.031	.032	0.03	0.14	0.07	-3.14
8	.028	.03	.031	0.03	0.13	0.07	-3.21
8.5	.026	.027	.026	0.03	0.11	0.06	-3.34
9	.022	.022	.021	0.02	0.09	0.05	-3.56
9.5	.019	.018	.017	0.02	0.07	0.04	-3.77
10.5	.015	.015	.016	0.02	0.06	0.06	-3.96
11.5	.013	.014	.014	0.01	0.05	0.05	-4.09
12.5	.011	.012	.012	0.01	0.04	0.04	-4.29
					TOTAL	3.23	

Solid residence time results

TAIL STREAM

AFR: 5 L/min FT: 0 CM WWFR: 1200 cc/min

INITIAL ACTIVITY: 11026000 DPS COUNTING EFFICIENCY: .000104 INITIAL COUNT: 1146.70

TAIL FLOWRATE: 1963.4 cc/min CONC. FLOW RATE: 1548 L/min

SAMPLING TIME INTERVAL (MIN)	TIME ELAPSED (min)	DECAY FACTOR (%)	TOTAL COUNT RATE (cps)	MEASURED COUNT RATE (cps)	DECAY CORREC.	CORREC. COUNT RATE (cps)	Ln(count rate)	MASS OF TRACER (g)	Ln(MASS FLOW RATE)
0.25	43	0.82	945.91	769.60	0.00	769.60	-0.21	.0023547	-1.88
0.50	45	0.82	937.48	689.15	8.43	680.72	-0.31	.0020827	-1.83
0.75	47	0.81	929.12	647.75	8.36	639.39	-0.36	.0019563	-1.93
1.00	48	0.81	924.97	706.28	4.15	702.12	-0.27	.0021482	-2.03
1.25	50	0.80	916.73	643.43	8.24	635.18	-0.35	.0019434	-2.10
1.50	52	0.79	908.56	677.78	8.17	669.60	-0.29	.0020487	-2.15
1.75	53	0.79	904.50	554.93	4.06	550.87	-0.49	.0016854	-2.10
2.00	54	0.79	900.46	436.70	4.04	432.66	-0.72	.0013238	-2.43
2.50	55	0.78	896.44	424.66	4.02	420.65	-0.75	.0012870	-2.49
3.00	56	0.78	892.43	376.00	4.00	372.00	-0.86	.0011382	-2.71
3.50	58	0.77	884.48	314.05	7.95	306.10	-1.04	9.365E-4	-2.87
4.00	59	0.77	880.53	252.63	3.95	248.67	-1.25	7.608E-4	-3.05
4.50	61	0.76	872.68	219.48	7.85	211.63	-1.38	6.475E-4	-3.19
5.00	63	0.75	864.90	187.48	7.78	179.70	-1.53	5.498E-4	-3.45
5.50	65	0.75	857.19	153.80	7.71	146.09	-1.72	4.470E-4	-3.48
6.00	66	0.74	853.36	136.68	3.83	132.85	-1.83	4.065E-4	-3.65
6.50	68	0.74	845.75	111.50	7.61	103.89	-2.03	3.179E-4	-3.83
7.00	69	0.73	841.98	96.63	3.78	92.86	-2.16	2.841E-4	-4.07
7.50	71	0.73	834.47	72.27	7.50	64.76	-2.45	1.981E-4	-4.41
8.00	75	0.71	819.66	59.37	14.81	44.56	-2.63	1.363E-4	-4.84
8.50	77	0.71	812.36	47.75	7.31	40.44	-2.83	1.237E-4	-4.83
9.00	79	0.70	805.11	44.80	7.24	37.56	-2.89	1.149E-4	-4.97
10.00	81	0.70	797.94	23.92	7.18	16.74	-3.51	5.122E-5	-5.60
11.00	83	0.69	790.83	17.78	7.11	10.67	-3.79	3.265E-5	-6.20
12.00	84	0.69	787.29	15.77	3.53	12.23	-3.91	3.743E-5	-6.00
13.00	87	0.68	776.79	11.63	10.50	1.13	-4.20	3.459E-6	-8.33
14.00	88	0.67	773.32	8.18	3.47	4.71	-4.55	1.442E-5	-7.01
15.00	89	0.67	769.87	5.52	3.45	2.06	-4.94	6.310E-6	-7.72
16.00	91	0.67	763.00	4.02	6.86				
17.00	92	0.66	759.60	4.68	3.41	1.28	-5.09	3.902E-6	-8.31
18.00	94	0.66	752.83	1.55	6.77				
19.00	95	0.65	749.46	3.57	3.36	0.20		6.241E-7	-10.15
								.0230415	

				CONC.	STREAM				
.5	98	0.64	739.66	509.83	10.00	499.84	-0.37	7.557E-5	-5.07
1	99	0.64	736.16	332.63	3.30	329.33	-0.79	4.930E-5	-5.49
1.5	100	0.64	732.87	267.80	3.29	264.51	-1.01	3.969E-5	-5.75
2	103	0.63	723.10	165.05	9.78	155.27	-1.48	2.446E-5	-5.95
2.5	104	0.63	719.87	121.83	3.23	118.60	-1.78	1.806E-5	-6.30
3	106	0.62	713.45	92.47	6.42	86.05	-2.04	1.371E-5	-6.41
3.5	107	0.62	710.26	70.50	3.19	67.31	-2.31	1.045E-5	-6.62
4	109	0.61	703.93	102.35	6.33	96.02	-1.93	1.517E-5	-6.96
4.5	111	0.61	697.66	82.28	6.27	76.01	-2.14	1.220E-5	-6.96
5	112	0.61	694.54	50.72	3.12	47.60	-2.62	7.517E-6	-7.10
5.5	115	0.60	685.28	51.98	9.27	42.72	-2.58	7.705E-6	-7.32
6	117	0.59	679.17	43.12	6.11	37.01	-2.76	6.391E-6	-7.43
6.5	119	0.59	673.11	31.03	6.05	24.98	-3.08	4.600E-6	-7.72
7	120	0.58	670.11	29.45	3.01	26.44	-3.12	4.365E-6	-8.03
7.5	121	0.58	667.11	16.93	2.99	13.94	-3.67	2.510E-6	-8.20
8	123	0.58	661.17	18.43	5.95	12.49	-3.58	2.732E-6	-8.34
8.5	124	0.57	658.21	10.17	2.95	7.21	-4.17	1.507E-6	-8.58
9	126	0.57	652.35	11.28	5.87	5.42	-4.06	1.672E-6	-8.86
10	127	0.57	649.43	10.40	2.91	7.49	-4.13	1.541E-6	-8.96
11	129	0.56	643.64	5.75	5.79		-4.72	8.523E-7	-9.62
12	130	0.56	640.77	5.88	2.87	3.01	-4.69	8.720E-7	-9.77
13	133	0.55	632.22	2.33	8.55	-6.21		3.458E-7	-10.11
14	135	0.55	626.59	3.05	5.64	-2.59	-5.33	4.521E-7	-10.21
15	137	0.54	621.00	3.25	5.59	-2.34		4.817E-7	-10.06
16	139	0.54	615.47	1.80	5.54	-3.74		2.668E-7	-10.73
17	141	0.53	609.98	2.25	5.49	-3.24		3.335E-7	-10.42
18	142	0.53	607.26	1.75	2.72	-0.97		2.594E-7	-10.68
19	146	0.52	596.48	1.38	10.78	-9.40		2.042E-7	-10.83
								3.032E-4	

TAIL STREAM

AFR: 5 L/MIN FT: 5 cm WWFR: 0 L/min

SAMPLING TIME INTERVAL (min)	TIME ELAPSED (min)	DECAY FACTOR (%)	TOTAL MEASURED COUNT RATE (cps)	COUNT RATE (cps)	DECAY CORREC.	CORREC. COUNT RATE (cps)	Ln(COUNT RATE)	TRACER AMOUNT (g)
0.25	52	0.79	908.53	901.90	8.10	893.80	-0.01	.0057805
0.50	54	0.79	900.43	952.27	4.02	948.24	0.06	.0061033
0.75	55	0.78	896.40	845.58	7.99	837.59	-0.06	.0054195
1.00	57	0.77	888.41	918.50	15.77	902.73	0.03	.0058869
1.25	61	0.76	872.64	790.03	3.90	786.13	-0.10	.0050635
1.50	62	0.76	868.74	763.05	3.88	759.17	-0.13	.0050485
1.75	63	0.75	864.86	739.73	11.54	728.19	-0.16	.0048942
2.00	66	0.74	853.32	686.70	3.81	682.89	-0.22	.0045434
2.50	67	0.74	849.51	556.45	3.80	552.65	-0.42	.0036816
3.00	68	0.74	845.72	557.55	11.28	546.27	-0.42	.0036889
3.50	71	0.73	834.43	454.80	7.44	447.36	-0.61	.0030091
4.00	73	0.72	826.99	411.80	3.69	408.11	-0.70	.0028465
4.50	74	0.72	823.30	396.80	10.98	385.82	-0.73	.0027428
5.00	77	0.71	812.31	352.45	3.63	348.82	-0.83	.0024362
5.50	78	0.71	808.69	256.05	7.21	248.84	-1.15	.0017699
6.00	80	0.70	801.48	234.28	7.15	227.14	-1.23	.0016194
6.50	82	0.69	794.33	205.87	7.08	198.79	-1.35	.0014230
7.00	84	0.69	787.25	176.87	10.50	166.36	-1.49	.0012226
7.50	87	0.68	776.75	159.90	10.36	149.54	-1.58	.0011710
8.00	90	0.67	766.38	134.58	3.42	131.16	-1.74	9.856E-4
8.50	91	0.67	762.96	97.33	6.80	90.53	-2.06	7.129E-4
9.00	93	0.66	756.16	90.23	6.74	83.49	-2.13	6.608E-4
10.00	95	0.65	749.42	70.81	10.00	60.81	-2.36	5.186E-4
11.00	98	0.64	739.42	49.25	6.59	42.66	-2.71	3.607E-4
12.00	100	0.64	732.83	34.88	6.53	28.34	-3.05	2.554E-4
13.00	102	0.63	726.29	27.48	9.69	17.78	-3.27	2.012E-4
14.00	105	0.62	716.60	13.81	6.39	7.42	-3.95	1.012E-4
15.00	107	0.62	710.21	13.15	6.33	6.82	-3.99	9.630E-5
16.00	109	0.61	703.88	12.10	15.58	-3.48	-4.06	9.733E-5
17.00	114	0.60	688.30	11.13	6.14	4.99	-4.13	8.948E-5
18.00	116	0.59	682.16	11.99				9.645E-5

.0725266

CONCENTRATE STREAM

.5	123	0.57	652.29	360.06	0.00	360.06	-0.59	.0028961
1	126	0.57	652.29	356.00	5.82	350.18	-0.61	.0028635
1.5	128	0.56	646.48	361.75	8.63	353.12	-0.58	.0029097
2	131	0.56	637.85	283.65	11.32	272.33	-0.81	.0022815
2.5	135	0.55	626.53	220.41	11.12	209.29	-1.04	.0017729
3	139	0.54	615.41	208.89	8.21	200.68	-1.08	.0016802
3.5	141	0.53	607.20	193.25	8.10	185.15	-1.14	.0015544
4	144	0.52	599.10	171.43	5.34	166.09	-1.25	.0013789
4.5	147	0.52	593.76	158.18	5.29	152.89	-1.32	.0012723
5	149	0.51	588.46	145.15	5.25	139.90	-1.40	.0011675
5.5	151	0.51	583.22	143.15	5.20	137.95	-1.40	.0011514
6	153	0.50	578.02	135.88	5.15	130.73	-1.45	.0010929
6.5	157	0.50	572.87	136.20	2.56	133.64	-1.44	.0010955
7	159	0.50	570.31	128.10	2.55	125.55	-1.49	.0010304
7.5	161	0.50	567.76	112.00	5.06	106.94	-1.62	9.009E-4
8	162	0.49	562.70	113.00	2.51	110.49	-1.61	9.089E-4
8.5	163	0.49	560.18	106.33	2.50	103.83	-1.66	8.553E-4
9	164	0.49	557.68	100.90	2.49	98.41	-1.71	8.116E-4
10	165	0.48	555.19	84.19	4.95	79.24	-1.89	6.772E-4
11	167	0.48	550.24	89.50	2.46	87.04	-1.82	7.199E-4
12	169	0.48	547.78	88.38	4.88	83.50	-1.82	7.109E-4
13	170	0.47	542.90	84.68	2.43	82.25	-1.86	6.811E-4
14	172	0.47	540.47	83.38	2.41	80.97	-1.87	6.707E-4
15	173	0.47	538.06	82.48	2.40	80.08	-1.88	6.634E-4
16	174	0.47	535.66	78.20	2.41	75.79	-1.92	6.290E-4
								.0294798

APPENDIX 9.2

a) Activity, Count Rate and Decay factor

As with any radioactive source, the induced activity in an irradiated sample decreases as time passes. The rate of decrease is exponential and varies with the individual isotope. The period of time taken for the activity to decrease by one half is known as the half-life ($T_{1/2}$). The radioactive decay may be expressed mathematically by the equation (Lyon, 1964):

$$A = A_0 * (\exp(0.693t/T_{1/2})) \qquad 1$$

where A: initial activity (dps)

Ao: activity remaining after time t

t: elapsed time

The exponantial term is also known as the decay factor.

Eq.2 may be also expressed in terms of the counting rate R and Ro corresponding to the disintegration rates A and Ao respectively. Since

$$R = A * Y \qquad 2$$

where R: count rate

Y: counting efficiency of the detector

$$R = R_0 * (\exp(0.693t/T_{1/2})) \qquad 3$$

d) Calculation of the tracer amount

Under ideal conditions, the specific activities (disintegration rate/weight of element) of both standard and unknown are the same. Therefore,

$$W_x = \frac{W_s * R_x}{R_s} \qquad 4$$

where Wx: weight of element X in unknown

Ws: weight of element in standard

Rx: count rate of unknown

Rs: count rate of standard

e) Calculation of the Mean Solid Residence Time

$$-\frac{dw(t)}{dt} (C(t) * Q_t + W(t) * K) \qquad 5$$

By definition:

$$C(t) = \frac{W(t)}{V} \qquad \tau = \frac{V}{Q} \qquad 6$$

$$-\frac{dC(t)}{dt} = (1/\tau\ K) * C(t) \qquad 7$$

$$C(t) = C_0 * \exp(-(1/\tau + K)) \qquad 8$$

$$R(t) = R_0 * \exp(-(1/\tau + K)) \qquad 9$$

A plot of Ln(R(t)/Ro(t)) versus time gives rise to a straight line with a slope of $-(1/\tau+K)$

f) Total Recovery of Tracer

Wc: solids recovery rate (g/s)

Wc(t): conc. of Mn in conc. stream (corr. for decay)

Wt: solids recovery rate (g/s)

Ct(t): conc. Mn in tls. stream (corr. for decay).

$$R = \frac{W_C \int C_C(t) * dt}{W_C \int C_C * dt + W_t \int C_t(t) * dt} \qquad 10$$

g) Calculation of Rate Constant of Tracer

$$R = \frac{K * \tau}{1 + \tau * K} \qquad 11$$

BIBLIOGRAPHY

1-.Anfruns J.P. and Kitchener J.A., "The absolute rate of capture of single particles by single bubbles", in Flotation, A. M.Gaudin Memorial, AIME, 1976, pp. 625-637.

2- Anthony R.M., "The effect of particle size on the activation and flotation of sphalerite", Proc. Aust. Inst. Min. Metal., No 254, June 1975.

3- Arbiter N., "Flotation rates and flotation efficiency", AIME Trans., Sep. 1951, pp. 791-796.

4-.Arbiter N.and Harris C.C., "Flotation kinetics", in Flotation, A. M. Gaudin Memorial, AIME, 1976, pp. 215-247.

5- Bhaga D., "Holdup and Pressure Drop in Vertical Two and Three phase Flow", Master Thesis, McGill Uni., 1970.

6- Bascur O.A., "Dynamic modelling of a flotation cell with a view toward automatic control", 16th CIM Int. Min. Proc. Cong., 1982.

7-.Bisshop J.P. and White M. E., "Study of particle entrainment in flotation froths", transactions of Ins. of Min. and Metall., London, Dec. 1976, pp. C191-194.

8- Brown D.J. and Smith H.G., "The flotation of coal as a rate process, AIME Transaction, Vol. 113, 1953, pp. 1001-1036.

9- Bushell C.H.G., "Kinetics of flotation" , AIME Transaction, Vol. 226, 1963, pp. 266-278.

10- Collins G.L. and Jameson G.L., "Experiments on the flotation of fine particles", Chem. Eng. Sci., Vol. 31, 1976, pp.985-991.

11- Copper H.R., "Feedback process control of mineral flotation part 1;Development of a Model for Froth Flotation", AIME Transaction, Dec 1966 pp.439-450.

12- Cutting G.W., Watson D., Whitehead A. and Barber S. P., "Froth structure in continuous flotation cells", Int. Jour. of Min. Proc., 7, 1981, pp. 347-368.

13- Cutting G.W., Barber S. P. and Watson D., "Prediction of flotation plant performance from batch tests using process models", 16th CIM Int. Min. Proc. Cong., 1982.

14- de Bruyn P.L. and Modi H.J.," Particle size and flotation rate of quartz", AIME Transaction , Apr. 1956, pp. 415-419.

15- Dippenaar A., "The destabilization of froth by solids Part 1 and 2", Int. Jour. of Min. Proc., 9, 1982, pp.1-22.

16- Derjaguin B.V. and Dukhin S.S., "Theory of Flotation of Small and Medium Sized Particles", Trans. Inst. Min. Met , 70, 1960, pp. 221-245.

17- Dobby G.S., "A fundamental flotation model and flotation column scale-up", Ph.D thesis, McGill Uni., Canada, 1984.

18- Engelbrecht J.A. and Woodburn E.T., "The effect of froth height, aeration rate, and gas precipitation on flotation", Jour. of Met., Oct. 1975, pp. 125-131.

19- Flint L.R., "Factors influencing design of flotation equipment", Min. Sci. Eng., Vol. 5, No 3, July 1973, pp. 233-241.

20- Flint L.R., "Mechanistic approach to flotation kinetics", AIME Transaction, June 1974.

21- Flint L.R. and Howarth W.J., "The collision efficiency of small particles with spherical air bubbles, Chem. Eng. Sci , 1971, Vol. 26, pp. 1155-1168.

22- Fuerstenau D.W. and Ball B., "On determination of rate constants from semi batch flotation tests", Col. Sch. of Mines Quaterly, Vol. 69, 1974, pp. 27-40.

23- Gaudin A.M., " Flotation ",McGraw-Hill, 1957, pp.347-381.

24- Gaudin A.M., Fuerstenau D.W. and Mao G.W., "Activation and Deactivation Studies with Copper on shpalerite", Min. Eng., Apr. 1959, pp. 439-450.

25- Gardner R.P. and Ely R.L., "Radioisotopes measurement applications in engineering, Reinhold, New York, 1967, pp. 168-221.

26- Gardner R.P., Verghese K. and Rogers R.S.C., "On stream determination of large scale ball mill residence time distribution with short lived radioactive tracer", Min. Eng., Apr. 1980, pp. 422-431.

27- Grainger-Allen T.J.N., "Bubble generation in the froth flotation machines", Trans. of Inst. of Min. and Metall., London, Mar. 1970, pp.15-22.

28- Greaves M. and Allen B.W., "Steady state and dynamic characteristics of flotation in a single cell", Trans. Ins. Chem. Engrs., Vol. 52, 1974, pp. 136-147.

29- Harris C.C., "Multiphase models of flotation machine behaviour", Int. Jour. of Min. Proc., 1978, pp. 107-128.

30- Harris C.C. and Rimmer H.W., "Study of a two phase modal of flotation process", AIME Transaction, 1966, pp. 153-163.

31- Harris C.C., Jowett A. and Ghosh S. K., "Analysis of data from continuous flotation tests, AIME Transaction", Dec. 1963, pp. 444-447."

32- Harris C.C., "Impeller Speed, Air and Power Requirements in Flotation Machine Scale-up", Int. J. of Min. Proc., 1974, pp.51.64.

33- Hemmings C.E., "On the significance of flotation froth liquid lamella thickness", Trans. Inst. M. M., 90, 1981, pp. C96-102.

34- Imaizumi T. and Inoue T., "Kinetic consideration of froth flotation", 4th Int. Cong. of Min. Proc., 1963.

35- Inoue T.and Imaizumi T., "A series of works related to flotation kinetics", 4th Joint Meeting MMIJ-AIME 1980, Tokyo, pp. 85-99.

36- Jameson G.J., McKee D.J. and Young M., "Physical factors affecting recovery rates in flotation", Min. Sci. Eng., Vol.9, No 3, July 1977, pp. 103-118.

37- Johnson D.J., McKee D.J. and Lynch A.J., "Flotation rates of nonsulfate minerals in chalcopyrite flotation processes, AIME Transaction, Vol.256, Sep. 1974, pp.204-209.

38- Jowett A. and Safvi M.M., "Refinement in methods of determining flotation rates", AIME Trasaction, Vol. 217, 1960, pp. 351-357.

39- Jowett A., "Investigation of residence time of fluid in froth flotation cells", British Chem. Eng., pp. 254-258.

40- Jowett A., "Gangue mineral contamination of froth", Chem. Engr., London, Vol. 2, No. 5, May 1966, pp.303-333.

41- Kallioinen J.O., "The control of zinc flotation", in Control 84, Chap. 28, AIME, 1984.

42- King R.P., "Flotation Research Work on the N.I.M. Research group and the Department of Uni. of Natal, J. of South Afr. Inst. of Min. and Metall., Apr. 1972 pp. 135-145.

43- King R.P. and Buchalter E.M., "A pilot- plant investigation of a flotation model", NIM Reasearch report No: 1573, Feb. 1974, 105p.

44- King R.P et al., "A pilot investigation of a kinetics model for flotation", NIM Research report No: 1847, Nov. 1976, 41p.

45- Laplante A., "Effect of air flow rate on the kinetics of flotation", Ph.D.thesis, Univ. of Toronto, 1980.

46- Laplante A.R., Toguri J. M. and Smith H.W., "The effect of AFR on the kinetics of flotation part 1", Int. Jour. of Min. Proc. , 11, 1983, pp. 203-219.

47- Laplante A.R. Toguri J.M. and Smith H.W., "The effect of AFR on the kinetics of flotation part 2 ", Int. Jour. of Min. Proc., 11, 1983, pp. 221-234.

48- Laskowski J., "Particle bubble attachment in flotation", Min.Sci.Eng., Vol. 6, Oct.1974, pp.223-235.

49- Leja J., in Surface Chemistry of Flotaion Froths, Plenum, 1982.

50- Levenspiel O., "Nonideal flow" in Chemical reaction enginering, John-Wiley and Sons Inc., pp. 242-300.

51- Loveday B.K., "Analysis of froth kinetics", AIME Transaction, Sep. 1966, pp. 219-225.

52- Loveday B.K. and Merchant G.R., "Simulation of multicomponent flotation plants", J. of South Afr. Inst. of. M. M., June 1972, pp.288-294.

53- Lynch A. J., Johnson N.W., McKee D.J., and Thorne C.G., "The behaviour of minerals in sulphide flotation processes with referance to simulation and control, J. of Sou. Afr. Inst. of Min. and Met., Apr. 1974, pp. 349-356.

54- Lynch A. J. Johnson N.W., Manlapig E.V., Thorne C.G., "The automatic control of flotation circuits", in Mineral and Coal Flotation circuits, Elsevier, chap. 8, 1981.

55- McGill Uni. manual of radiation safety, Jan. 1984.

56- McKee D.J., Fewings J.H., Manlapig E.V. and Lynch A.J., "Computer Control of Chalcopyrite flotation at Mount Isa Mines limited", in Flotation, Vol.2, 1976, pp.964-994.

57- Mining Chemicals Handbook, American Cyanamid Co., 1984.

58- Morris T.M., "Measurement of equlibrium forces betweden an air bubble and an attached solid in water, AIME Transaction , Vol. 187, 1950, pp. 91-95.

59- Moys M.H., "Study of a plug flow model for flotation

froth behaviour", Int. Min. Proc. Jour., 1978, pp. 21-38.

60- Moys M.H., "The modelling and measurement of residence time distribution in flotation froths", Dept. of Chem. Eng. Uni. of The Witwaterstrand, Johannesburg, 1982.

61- Paakkinen U.E. and Cooper H.R., "Flotation process control", pp. 787-799.

62- Reay D. and Ratcliff G.A., " Experimental testing of the hydrodynamic collision model of fine particle flotation, Can. Jour. of Chem. Eng., Vol. 53, Oct. 1975, pp. 481-486.

63- Reay R.G.A., "Removal of fine particles from water by dispersed air flotation; Effects of bubble size and particle size on collection efficiency", Can. Jour. of Chem. Eng. Vol. 51, Apr. 1973, pp. 178-185.

64- Rey M., "Quelgues problemes partiques et théoriques de la flottation des Minerais 8th Internat. Miner. Proc. cong. Leningrad Paper D-1.

65- Lyon W.S., "Guide to activation analysis", D. Van Nostrand Comp. Inc., chap. 1, 1964.

66- Schuhmann R., "Flotation kinetics 1", Jour. of Phys. Chem., Vol. 46, 1942, pp. 891-901.

67- Schulze H.J., in Physico-chemical Elementary Process in Flotaion, Elsevier Sci. Pub. Com., 1983, pp.234-238.

68- Shah Y.T., Kelkar B.G. and Godbole S.P., " Design parameters estimations for bubble column reactors", AIChE Jour., Vol. 28, No.3, May 1982, pp. 353-379.

69- Smith H.W., "Canadian experience in flotation control", Proc. of 6th IFAC Cong. Section 60.2, 6p, 1975.

70- Steiner L., Hunkel R. and Hardland S., "Behavior of dynamic celluler foams, Trans. IChem. E., Vol. 55, 1977.

71- Suna Atak, "Flotasyon", Istanbul Teknik Universitesi, 1976.

72- Sutherland W., "Principles of flotation", 1948, pp. 369-393.,

73- Sutherland D.N., "An appreciation of galena concentration using a steady-state flotation model, Int. Jour. of Min. Proc., 4, 1977, pp.149-162.

74- Thorne G.C., Manlapig E.V., Hall J.S. and Lynch A.J., "Modelling of industrial sulphide flotation", in

Flotation, Vol. 2, AIME, pp. 725-753.

75- Tomlinson H.S. and Fleming M.G., "Flotation rate studies", 4th Int. Min. Proc. Cong., 1963.

76- Trahar W.J., "The selective flotation of galena from sphalerite with special referance to the effects of particle size", Int. Jour. of Min. Proc. 3, 1976, pp. 151-166

77- Trahar W.J. and Warren L.J., "The flotability of very fine particles, Int. Jour. of Min. Proc., 3, 1976, pp.103-129.

78- Trahar W.J., "A rational interpretation of the particle size in flotation, Int. Jour. of Min. Proc., 1981, pp.289-327.

79- Warren L.J., "Determination of the conribution of true flotation and entrainment in batch flotation tests", Int. Jour. of Min. Proc., 14, , 1985, pp. 33-45.

80- Watson D. and Grainger-Allen T.J.N., " Study of froth flotation using a steady state technique", AIME Transaction, Vol. 256, Sep. 1974, pp. 242-247.

81- Weber M.E., "Collision efficeny for small particles with a spherical collector at intermediate reynolds numbers", J. Separ. Proc., 1980, pp. 29-33.

82- Woodburn E.T. and Loveday B.K., "The effect of variable residence time on the performance of a flotation system", Jour. of Sou. Afr. Ins. of Min. and Met., July 1965 , pp. 612-629.

83- Woodburn E.T. etal., "The effect of particle size distribution on the performance of a phosphate flotation process", Met. Trans., Vol. 2, Nov. 1971, pp. 3163-3174.

84- Yu S., "Particle collection in a flotation column", Master Thesis, McGill Uni., Canada, 1985.